AQUADUCT
Ab Initio Quantum Dynamics Using Coupled Cluster in Time

by

Sebastian Gregorius Winther-Larsen

Thesis

for the degree of

Master of Science

Faculty of Mathematics and Natural Sciences
University of Oslo

August 31, 2019

Contents

Part I

Fundamentals

Chapter 1

Quantum Mechanics

Here we present basic and foundational quantum theory, a theory that seek to describe the nature at the smallest scales of energy. The name "quantum" stems from the need to see energy not as a continuous and unbroken expanse, but rather as a sum of discrete quantities of equal size. Quantum mechanics came to the rescue when classical physics was unable to explain phenomena such as the mysterious sodium line, the ulatraviolet catastrophe, and the bewildering photo-electric effect. With the new theory came new challenges like an axiomatic uncertainty, the wave-particle duality of light and a probabilistic interpretation of nature. In this chapter we will not be so hubristic as to delve into the philosophical particulars, but hope only to revitalise the reader's faculties with the principal ideas on which this thesis is built.

1.1 Classical Mechanics

The formalism used in quantum mechanics largely stems from William Rowan Hamilton's formulation of classical mechanics. Through the process of canonical quantisation any classical model of a physical system is turned into a quantum mechanical model.

In Hamilton's formulation of classical mechanics, a complete description of a system of N particles is described by a set of canonical coordinates $q = (\vec{q}_1, \ldots, \vec{q}_N)$ and corresponding conjugate momenta $p = (\vec{p}_1, \ldots \vec{p}_N)$. Together, each pair of coordinate and momentum form a point $\xi = (q, p)$ in phase space, which is the space of all possible states of the system. Moreover, pairs of generalised coordinates and conjugate momenta are canonical if they satisfy the Poisson brackets so that $\{q_i, p_k\} = \delta_{ij}$. The Poisson bracket of two functions is defined as

$$\{f, g\} = \frac{\partial f}{\partial q}\frac{\partial g}{\partial g} - \frac{\partial f}{\partial p}\frac{\partial g}{\partial q}. \tag{1.1}$$

The governing equations of motion in a classical system is Hamilton's equations,

$$\dot{q} = \frac{\partial}{\partial p}\mathscr{H}(q, p) \tag{1.2}$$

$$\dot{p} = -\frac{\partial}{\partial q}\mathscr{H}(q, p) \tag{1.3}$$

where $\mathscr{H}(q, p)$ is the Hamiltonian, a function for the total energy of the system. Hamilton's equations may also be stated in terms of the Poisson brackets,

$$\frac{dp_i}{dt} = \{p_i, \mathscr{H}\}, \ \frac{dq_i}{dt} = \{q_i, \mathscr{H}\}. \tag{1.4}$$

A system consisting of N of equal mass m, subject to forces caused by an external potential, as well as acting on each other with forces stemming from a central potential $w(q_{ij})$ has the following Hamiltonian,

$$\mathscr{H}(q,p) = \mathscr{T}(q) + \mathscr{V}(p) + \mathscr{W}(p) = \frac{1}{2m}\sum_i |\vec{p}_i|^2 + \sum_i v(\vec{r}_i) + \frac{1}{2}\sum_{i<j} w(\vec{r_{ij}}). \tag{1.5}$$

This Hamiltonian conveniently contains several parts - the kinetic energy, the external potential energy and the interaction energy; denoted by $\mathscr{T}$, $\mathscr{V}$ and $\mathscr{W}$ respectively.

1.2 Canonical Quantisation

In order to transition from a classical system to a quantum system, we move from the classical phase space to the Hilbert space, through the procedure known as canonical, or first[1]-, quantisation. Whilst the state of a classical system is a point in phase space, a quantum state is a complex-valued state vector in discrete, infinite-dimensional, Hilbert space, that is a complete vector space equipped with an inner product. This space is most commonly chosen to be the space of square-integrable functions Ψ, dependent on all coordinates

$$\Psi = \Psi(x_1, x_2, \ldots, x_N). \tag{1.6}$$

These functions are dubbed wavefunctions and are maps from a point $(x_1, \ldots, x_N)$ in configuration space to the complex vector space,

$$\Psi : X^N \to \mathbb{C}. \tag{1.7}$$

It has been widely discussed how such an object can represent the state of a particle. The answer is provided by Max Born's probabilistic interpretation, which says that $|\Psi(x_1, \ldots, x_N)|^2$, gives the probability of finding the particle at a certain position. For a situation with one particle in one dimension we have,

$$\int_a^b |\Psi(x)|^2 dx = \left\{\begin{matrix}\text{probability of finding the} \\ \text{particle between } a \text{ and } b\end{matrix}\right\} \tag{1.8}$$

while $|\Psi(x_1, x_2, \ldots, x_N)|^2$ is the probability density for locating all particles at the point $(x_1, \ldots x_N) \in X^N$. Since the total probability must be 1, we are provided with a normalisation condition for the wavefunction,

$$\int_{X^N} |\Psi(x_1, x_2, \ldots, x_N)|^2 dx_1 dx_2 \ldots dx_N = \mathbb{1}. \tag{1.9}$$

The relation between a classical- and quantum decsription of a mechanical system is most clearly seen when the two descriptions are expressed in terms of the same variables. In fact, we may apply *quantisation* of the classical variables to produce the quantum equivalent of the system. The classical phase space variables are changed into quantum observables,

$$q_i \to \hat{q}_i, \; p_i \to \hat{p}_i. \tag{1.10}$$

The quantum observables are required to satisfy the Heisenberg commutation relation,

$$[\hat{q}_i, \hat{p}_j] = i\hbar\delta_{ij}, \tag{1.11}$$

[1]Second quantisation comes later.

instead of the Poisson bracket (Equation 1.1). Here $\hbar$ is the reduced Planck's constant. For any general variables A and B, this transition can be expressed by substitution between Poisson brackets for the classical variables and commutators for the quantum observables,

$$\{A, B\} \rightarrow \frac{1}{i\hbar}[\hat{A}, \hat{B}]. \tag{1.12}$$

This correspondence between the classical and quantum dynamical equations is directly related to *Ehrenfest's therom*, which states that the classical dynamical equations keep their validity also in the quantum theory, with the classical variables replaced by their corresponding quantum expectation values[15].

1.2.1 The Dirac-von Neumann Postulates

The following postulates, or axioms, provide a precise and concise description of quantum mechanics in terms of operators on the Hilbert space. There are many variations of these postulates, introduced both by their namesakes Paul Adriene Maurice Dirac[14] and John von Neumann[55].

Hilbert Space

A quantum state of an isolated physical system is described by a vector with unit norm in a Hilbert space $\mathcal{H}$, a complex vector space equipped with an inner product. The inner product associates a scalar value, which may be either real or complex, with any pair of state vectors.

The inner product can be defined as

$$\langle\psi_\alpha|\psi_\beta\rangle = \int \psi_\alpha^*(x)\psi_\beta(x)dx, \tag{1.13}$$

where ψ^* is the complex conjugate of ψ. Here we have introduced Dirac notation, which is very common when describing quantum states. For each quantum state $|\psi_\alpha\rangle$ there exists a dual state $\langle\psi_\alpha|$. We refer to these two vectors as *bra* and *ket* vectors, respectively. Some properties of an inner product, written in Dirac's style, read

$$\langle\psi_\alpha|\psi_\beta\rangle = \langle\psi_\beta|\psi_\alpha\rangle^* \tag{1.14}$$

$$\langle\psi_\alpha|\left(z_1|\psi_\beta\rangle + z_2|\psi_\beta\rangle\right) = z_1\langle\psi_\alpha|\psi_\beta\rangle + z_2\langle\psi_\alpha|\psi_\beta\rangle \tag{1.15}$$

$$\langle\psi_\alpha|\psi_\alpha\rangle \geq 0, \tag{1.16}$$

where $z_n = a_n + ib_n$ is some complex number. Notice that in these properties, a superposition of a state wavefunction in the form of linear combination of two other states have appeared. Such superpositions are generally written

$$|\psi_\gamma\rangle = z_1|\psi_\alpha\rangle + z_2|\psi_\beta\rangle, \tag{1.17}$$

where we have produced a new quantum state from two other states. Any two or more states may be superposed to produce a new state. Superposition is of fundamental importance to quantum mechanics, and even though the concept is similar to the classical superposition principle for waves in classical physics, "the superposition that occurs in quantum mechanics is of an essentially different nature from any occuring in the classical theory" according to Dirac[14].

Proceeding with the description of quantum states, a state function ψ is said to be *normal* if its innerproduct with itself is one, $\langle\psi|\psi\rangle = 1$. Two different state functions are *orthogonal* if their inner product is zero. We have orthogonal functions if $\langle\psi_\alpha|\psi_\beta\rangle = \delta_{\alpha\beta}$, where $\delta_{\alpha\beta}$ is the Kronecker delta.

Observables

Each physical observable of a system is accociated with a *hermitian* operator acting on the Hilbert space. The eigenstates of each such operator define a *complete*, *orthonormal* basis set of vectors $\mathcal{B}$ for the d-dimensional Hilbert space,

$$\mathcal{B} = \{|i\rangle\}_{i=1}^{d}. \tag{1.18}$$

Completeness of the basis set $\mathcal{B}$ means,

$$\sum_{i=1}^{d} |i\rangle \langle i| = \mathbb{1}. \tag{1.19}$$

With $\hat{O}$ an operator, *hermiticity* means,

$$\langle \phi | \hat{O}\psi\rangle = \langle \hat{O}\phi | \psi\rangle \equiv \langle \phi | \hat{O} | \psi\rangle . \tag{1.20}$$

This means that the operator $\hat{O}$ is its own Hermitian conjugate,

$$\hat{O}^{\dagger} = \hat{O}. \tag{1.21}$$

Some properties of the Hermitian conjugate reads,

$$(z\hat{O})^{\dagger} = z^{*}\hat{O}^{\dagger} \tag{1.22}$$

$$(\hat{O}_1 + \hat{O}_2)^{\dagger} = \hat{O}_1^{\dagger}\hat{O}_2^{\dagger} \tag{1.23}$$

$$(\hat{O}_1\hat{O}_2)^{\dagger} = \hat{O}_2^{\dagger}\hat{O}_1^{\dagger}. \tag{1.24}$$

Measurements

Physically measurable values, associated with an observable $\hat{O}$ are defined by the eigenvalues o_n of the observable,

$$\hat{O} |n\rangle = o_n |n\rangle . \tag{1.25}$$

The probability for finding a particular eigenvalue in the measurement is

$$p_n = |\langle n|\psi\rangle|^2, \tag{1.26}$$

with the system in state $|\psi\rangle$ before the measurement, and $|n\rangle$ as the eigenstate corresponding to the eigenvalue o_n. If the observable $\hat{O}$ is Hermitian, we can write the operators as a spectral decomposition

$$\hat{O} = \sum_{n=1}^{d} o_n |n\rangle\langle n| , \tag{1.27}$$

where d is the dimensionality of the Hilbert space.

Time Evolution

In the *Schrödinger picture* time evolution of the state vector, $|\psi\rangle = |\psi(t)\rangle$, is given by the Schrödinger equation[2],

$$i\hbar\frac{d}{dt} |\psi(t)\rangle = \hat{H} |\psi(t)\rangle . \tag{1.28}$$

Note that any superposed state, as described by 1.17, will also be a solution to the Schrödinger equation due to its linearity.

[2] In the Schrödinger picture.

The Schrödinger equation is first order in the time derivate, meaning that the time evolution $|\psi\rangle = |\psi(t)\rangle$ is uniquely determined by some initial condition $|\psi_0\rangle = |\psi(t_0)\rangle$. $\hat{H}$ is the Hamiltonian of the system, which is a *linear*, *hermitian* operator. The Hamiltonian gives rise to the time evolution, which is a *unitary* mapping between quantum states in time,

$$|\psi(t)\rangle = \hat{\mathcal{U}}(t, t_0) \, |t_0\rangle \, . \tag{1.29}$$

The time evolution operator $\hat{\mathcal{U}}$ is determined by the Hamiltonian through the equation

$$i\hbar \frac{\partial}{\partial t} \hat{\mathcal{U}}(t, t_0) = \hat{H} \hat{\mathcal{U}}(t, t_0), \tag{1.30}$$

which follows from the Schrödinger equation. For a time-independent Hamiltonian it is given by

$$\hat{\mathcal{U}}(t, t_0) = e^{-i\hat{H}(t - t_0/\hbar)}. \tag{1.31}$$

We see that this time-propagater is Hermitian

$$\hat{\mathcal{U}}\hat{\mathcal{U}}^\dagger = \hat{\mathcal{U}}^\dagger \hat{\mathcal{U}} = 1. \tag{1.32}$$

If however $\hat{H}$ is time-dependent, so that the operator at different times do not commute, we may use a more general integral expression for the time-propagator,

$$\hat{\mathcal{U}}(t, t_0) = \sum_{n=0}^{\infty} (-\frac{i}{\hbar})^n \int_{t_0}^{t} \int_{t_0}^{t_1} dt_1 \int_{t_0}^{t_1} dt_2 \cdots \int_{t_0}^{t_{n-1}} dt_n \hat{H}(t_1) \hat{H}(t_2) \ldots \hat{H}(t_n). \tag{1.33}$$

A unitary transformation of states and observables

$$|\psi\rangle \to |\psi'\rangle = \hat{U} \, |\psi\rangle \, , \; \hat{O} \to \hat{O}' = \hat{U} \hat{O} \hat{U}^\dagger, \; \hat{U}^\dagger \hat{U} = 1. \tag{1.34}$$

leads to a different, but equivalent representation of a quantum system. The transition to the *Heisenberg picture* is defined by a special time-dependent unitary transformation,

$$\hat{U} = \hat{\mathcal{U}}^\dagger(t, t_0), \tag{1.35}$$

which is the inverse of the time-evolution operator. When applied to the time-dependent state vector of the Schrödinger picture it will cancel the time-dependence

$$|\psi\rangle_{\mathrm{H}} = \hat{\mathcal{U}}^\dagger(t, t_0) \, |\psi(t)\rangle_{\mathrm{S}} = |\psi(t_0)\rangle_{\mathrm{S}} \, . \tag{1.36}$$

The time-dependence is now carried by the observables, rather than the state vectors,

$$\hat{O}_{\mathrm{H}} = \hat{\mathcal{U}}^\dagger(t, t_0) \hat{O}_{\mathrm{S}} \hat{\mathcal{U}}(t, t_0), \tag{1.37}$$

and the Schrödinger equation is replaced by the Heisenberg equation

$$\frac{d}{dt} = \frac{i}{\hbar} [\hat{H}, \hat{O}_{\mathrm{H}}] + \frac{\partial}{\partial t} \hat{O}_{\mathrm{H}}. \tag{1.38}$$

There is a third representation called the *interaction picture*, but we will remain firmly rooted in the Schrödinger picture and halt this general introduction to time-development here.

1.3 The Quantum Hamiltonian

The full Hamiltionian for a quantum many-body system can be a large and unwieldy thing. In this study we will constrain ourselves to the study of electronic systems. Purely on a phenomenological basis, one would include nuclear terms in the Hamiltonian as well. In this study however, we will stay within the Born-Oppenheimer approximation and treat the nuclei as stationary particles, thereby refraining from introducing terms that involve the motion of nuclei.

The full molecular electronic Breit-Pauli Hamiltionian, thoroughly described in Helgaker et al.[35], contains the following types of terms

$$\hat{H}^{\mathrm{BP}}_{\mathrm{mol}} = \begin{cases} \hat{H}_{\mathrm{kin}} & \leftarrow \text{kinetic energy} \\ +\hat{H}_{\mathrm{cou}} & \leftarrow \text{Coulomb interactions} \\ +\hat{H}_{\mathrm{ee}} & \leftarrow \text{external electric field interaction} \\ +\hat{H}_{Z} & \leftarrow \text{Zeeman interactions} \\ +\hat{H}_{\mathrm{so}} & \leftarrow \text{spin-orbit interactions} \\ +\hat{H}_{\mathrm{ss}} & \leftarrow \text{spin-spin interactions} \\ +\hat{H}_{\mathrm{oo}} & \leftarrow \text{orbit-orbit interactions} \\ +\hat{H}_{\mathrm{dia}} & \leftarrow \alpha^4 \text{ diamagnetic interactions} \end{cases} \tag{1.39}$$

We will not be working with this enormous Hamiltionian, but we will go into some of the most import terms that an electronic Hamiltonian can constitute.

Kinetic energy The genereal kinetic energy operator is given by

$$\hat{H}_{\mathrm{kin}} = -\frac{\hbar}{2m} \sum_i \nabla_i^2, \tag{1.40}$$

where ∇ is the differential operator and the sum is over all electrons in the system. This term is an example of a one-particle operator as it remains the same for all eletrons and contains no terms that would constitute interaction between particles. For a free particle or a gas of non-interacting particles, Equation 1.40 is sufficient to describe the system.

Potential terms By adding a confining potential to the Hamiltonian in addition to the kinetic energy term Equation 1.40,

$$\hat{H} \supset \hat{H}_{\mathrm{kin}} + \hat{V} \tag{1.41}$$

gives rise to much more interesting systems and are the beginning of an approximation of reality. Perhaps the most common is the harmonic oscillator potential, which in one dimension reads

$$\hat{V}(x) = \frac{1}{2} m\omega^2 x^2. \tag{1.42}$$

This is a very popular confining potential because virtually any oscilaltory motion can be approximated by it, if the amplitude of the oscillations are small. The parabolic potential is the basis of a quantum dot which is a central part of this study. In quantum chemistry we only consider potentials derived from particle-particle interactions, and not such external potentials.

Coulomb interactions Electrostatic interaction between particles in a molecule or atom is modelled by Coulomb terms in the Hamiltonian.

$$\hat{H}_{\mathrm{cou}} = -\sum_{iK} \frac{k_e Z_K e^2}{r_{iK}} + \frac{1}{2} \sum_{i \neq j} \frac{k_e e^2}{r_{ij}} + \frac{1}{2} \sum_{K \neq L} \frac{k_e Z_K Z_L e^2}{R_{KL}}, \tag{1.43}$$

where e is the elementary particle charge and $k_e = 1/4\pi\epsilon_0$ is the Coulomb constant. The first term is the potential between nuclei and electrons, the second term is the potential between electrons and the last term is the potential between nuclei. In the Born-Oppenheimer approximaton we ignore the first and third term.

External electric field interactions This section goes through, in broadest of strokes, a quantisation of an electromagnetic field. For a thorough derivation see for instance Joachain, Kylstra, and PotvliegeJoachain, Kylstra, and Potvliege. Applying an electromagnetic field we need to include terms in the Hamiltonian that model the effects of an externally applied scalar potential $\phi = \phi(\mathbf{r}, t)$ and a vector potential $\mathbf{A} = \mathbf{A}(\mathbf{r}, t)$. This will also affect the kinetic energy of the particles, which we therefore include at first,

$$\hat{H}_{\text{ef}} \subset \frac{1}{2m}(\mathbf{p} + e\mathbf{A})^2 - e\phi = \frac{\hat{\mathbf{p}}}{2m} + \frac{e}{2m}(\mathbf{A} \cdot \hat{\mathbf{p}} + \hat{\mathbf{p}} \cdot \mathbf{A}) + \frac{e^2}{2m}\mathbf{A}^2 - e\phi. \tag{1.44}$$

This Hamiltonian now describes a free particle subject to an external electric field. Since we have already included a term for kinetic energy we now wish to remove it,

$$\hat{H}_{\text{ef}} = -\frac{e}{2m}(\mathbf{A} \cdot \hat{\mathbf{p}} + \hat{\mathbf{p}} \cdot \mathbf{A}) + \frac{e^2}{2m}\mathbf{A}^2 - e\phi. \tag{1.45}$$

We assume that the external field has sufficiently large wavelength compared to the system, making the vector potential uniform in space $\mathbf{A}(\mathbf{r}, t) = \mathbf{A}(t)$. This approximation is very reasonable, because visible light has a wavelength of $\lambda \sim 5000$Å and an atom is around 1Å. In the dipole approximation we can write the vector potential as

$$\mathbf{A}(t) = \mathbf{A}_0 e^{-i\omega_k t} + \mathbf{A}_0^* e^{i\omega_k t} a, \tag{1.46}$$

where $\mathbf{A}_0$ and $\mathbf{A}_0^*$ are photon creation and annihilation operators. These allow for spontaneous emission and absorption of photons without the presence of a field, but we will disregard such phenomena and stick to a semi-classical description. We therefore rewrite the vector potential to

$$\mathbf{A}(t) = \epsilon A_0 \sin(\omega_k t), \tag{1.47}$$

which is the same up to a phase. In the Coulomb gauge we have

$$\mathbf{E} = -\frac{d}{dt}\mathbf{A}, \tag{1.48}$$

which gives us an expression for the E-field

$$\mathbf{E} = \epsilon \mathscr{E}_0 \cos(\omega_k t), \tag{1.49}$$

where $\mathscr{E}_0 = -\omega_k A_0$ and we can approximate the external electric field time-dependent field by

$$\hat{H}_{\text{ef}} = -\hat{\mathbf{d}} \cdot \epsilon \mathscr{E}_0 \cos \omega_k t, \tag{1.50}$$

where $\hat{\mathbf{d}} = q\hat{\mathbf{r}}$, is the dipole operator, dictating the allowed transitions.

1.3.1 Angular Momentum and Intrinsic Spin

In general, modelling of interaction with magnetic fields necessitates the use of operators for intrinsic angular momentum ($\mathbf{S}$) and extrinsic angular momentum ($\mathbf{L}$). These are often referred to as *spin* and *angular momentum*, respectively. We will spend some time here elaborating on such terms.

Angular momentum

In a classical system, the angular momentum of a particle with resepct to the orign is given as

$$\mathbf{L} = \mathbf{r} \times \mathbf{p}, \tag{1.51}$$

which broken down into components becomes,

$$L_x = yp_z - zp_y,\ L_y = yp_x - xp_z,\ L_z = xp_y - yp_x. \tag{1.52}$$

From this we can obtain the quantum mechanical description by promotion to operators, and inserting the representaion for the momentum operator in position space, $p_x \to i\hbar\partial/\partial x$.

The commutators of the angular momentum operators follows a nice cyclic permutation of indices rule:

$$[\hat{L}_x, \hat{L}_y] = i\hbar\hat{L}_z,\ [\hat{L}_y, \hat{L}_z] = i\hbar\hat{L}_x,\ [\hat{L}_z, \hat{L}_x] = i\hbar\hat{L}_y. \tag{1.53}$$

We see that they do not commute with each other, but the square of the total angular momentum, defined by

$$\hat{L}^2 \equiv \hat{L}_x^2 + \hat{L}_y^2 + \hat{L}_z^2, \tag{1.54}$$

does

$$[\hat{L}^2, \hat{L}_x] = 0,\ [\hat{L}^2, \hat{L}_y] = 0,\ [\hat{L}^2, \hat{L}_z] = 0. \tag{1.55}$$

In spherical coordinates, which is better suited for our needs, the angular momentum operator is given by

$$\hat{\mathbf{L}} = -i\hbar\hat{\mathbf{r}} \times \nabla. \tag{1.56}$$

Given the gradient in spherical coordinates,

$$\nabla = e_r\frac{\partial}{\partial} + e_\theta\frac{1}{r}\frac{\partial}{\partial\theta} + e_\phi\frac{1}{r\sin\theta}\frac{\partial}{\partial\phi} \tag{1.57}$$

and $\mathbf{r} = re_r$ we get

$$\begin{aligned}\hat{\mathbf{L}} &= -i\hbar\left[r(e_r \times e_r)\frac{\partial}{\partial r} + (e_r \times e_\theta)\frac{\partial}{\partial\theta} + (e_r \times e_\phi)\frac{1}{\sin\theta}\frac{\partial}{\partial\phi}\right] \\ &= -i\hbar\left(e_\phi\frac{\partial}{\partial\theta} - e_\theta\frac{1}{\sin\theta}\frac{\partial}{\partial\phi}\right).\end{aligned} \tag{1.58}$$

Now, with a bit of algebra we get

$$\hat{L}_x = i\hbar\left(\sin\phi\frac{\partial}{\partial\theta} + \cos\phi\cot\theta\frac{\partial}{\partial\phi}\right) \tag{1.59}$$

$$\hat{L}_y = i\hbar\left(\cos\phi\frac{\partial}{\partial\theta} + \sin\phi\cot\theta\frac{\partial}{\partial\phi}\right) \tag{1.60}$$

$$\hat{L}_z = -i\hbar\frac{\partial}{\partial\phi} \tag{1.61}$$

The squared operator becomes

$$\hat{L}^2 = -\hbar^2\left[\frac{1}{\sin\theta}\frac{\partial}{\partial\theta}\left(\sin\theta\frac{\partial}{\partial\theta}\right) + \frac{1}{\sin^2\theta}\frac{\partial^2}{\partial\phi^2}\right]. \tag{1.62}$$

The eigenvalue equations of $\hat{L}^2$ and $\hat{L}_z$ are

$$\hat{L}^2\psi = \hbar^2 l(l+1)\psi, \quad \hat{L}_z\psi = \hbar m\psi, \tag{1.63}$$

where $\psi = Y_l^m(\theta, \phi)$ are the spherical harmonics,

$$Y_l^m(\theta, \phi) = \epsilon\sqrt{\frac{(2l+1)}{4\pi}\frac{(l-|m|)!}{(1+|m|)!}}e^{im\theta}P_l^m(cos\theta), \tag{1.64}$$

and P_l^m are the associated Legendre polynomials.

Spin

In classical mechanics, intrinsic spin ($\mathbf{S} = I\omega$) is associated with an objects motion about its centre of mass. A similar thing goes on in quantum mechanics, but it has nothing to do with motion in space. In quantum mechanics spin is seen as a property that particles can carry, but i analoguous with its classical counterpart only in name.

Algebraically, *spin* is the same as *angular momentum*, beginning with the commutator relations,

$$[\hat{S}_x, \hat{S}_y] = i\hbar\hat{S}_z, \ [\hat{S}_y, \hat{S}_z] = i\hbar\hat{S}_x, \ [\hat{S}_z, \hat{S}_x] = i\hbar\hat{S}_y, \tag{1.65}$$

while the eigenvectors of $\hat{S}^2$ and S_z satisfy

$$\hat{S}^2 |s\ m_s\rangle = \hbar^2 s(s+1) |s\ m_s\rangle, \quad \hat{S}_z |s\ m_s\rangle = \hbar m |s\ m_s\rangle. \tag{1.66}$$

Because the quantum mechanical spin has nothing to do with motion in space and is independent of any coordinates r, θ or ϕ, there is no reason to exclude half-integer values of s and m_s,

$$s = 0, \frac{1}{2}, 1, \frac{3}{2}, \ldots, \quad m_s \in [-s, s]. \tag{1.67}$$

As it would turn out, every elemental particle as a specific and immutable value of s, and the most important one is $s = \frac{1}{2}$ (!) as it is the spin-value for all leptons, including the electron, all quarks as well as protons and neutrons. Since our particle of scrutiny is the electron our interest lies in spin-half systems, i.e.

$$s = \frac{1}{2}, \quad m_s = \pm\frac{1}{2}. \tag{1.68}$$

In such a system there are only two spin eigenstates,

$$\left|\frac{1}{2}, +\frac{1}{2}\right\rangle = |\uparrow\rangle = |+\rangle, \quad \left|\frac{1}{2}, -\frac{1}{2}\right\rangle = |\downarrow\rangle = |-\rangle. \tag{1.69}$$

This means that the Hilbert space $\mathcal{H}$ for spin-half particles has two dimensions. This means that any state can be expressed as a two-dimensional vectors called spinors,

$$|\chi\rangle = \begin{pmatrix} a \\ b \end{pmatrix} = a|\uparrow\rangle + b|\downarrow\rangle = a\begin{pmatrix} 1 \\ 0 \end{pmatrix} + b\begin{pmatrix} 0 \\ 1 \end{pmatrix}. \tag{1.70}$$

The probability of finding a particle represented by the state vector $|\chi\rangle$ in the spin up or spin down state is $|a|^2$ and $|b|^2$, respectively. This requires a normalisation, $|a|^2 + |b|^2 = 1$.

In the basis of $|\uparrow\rangle$ and $|\downarrow\rangle$ the operators $\hat{S}^2$, $\hat{S}_x$, $\hat{S}_y$ and $\hat{S}_z$ are represented by two-dimensional matrices,

$$\hat{S}^2 = \frac{3}{4}\hbar^2 \begin{pmatrix} 1 & 0 \\ 0 & 1 \end{pmatrix} \tag{1.71}$$

$$\hat{S}_x = \frac{\hbar}{2}\sigma_x, \quad \hat{S}_y = \frac{\hbar}{2}\sigma_y, \quad \hat{S}_z = \frac{\hbar}{2}\sigma_z, \tag{1.72}$$

where the Pauli matricies are given by,

$$\sigma_x = \begin{pmatrix} 0 & 1 \\ 1 & 0 \end{pmatrix} \quad \sigma_y = \begin{pmatrix} 0 & -i \\ i & 0 \end{pmatrix} \quad \sigma_z = \begin{pmatrix} 1 & 0 \\ 0 & -1 \end{pmatrix}. \tag{1.73}$$

Table 1.1: Conversion of atomic units to SI units.

Physical quantity	Conversion factor	Value
Length	a_0	$5.2918 \times 10^{-11} m$
Mass	m_e	$9.1095 \times 10^{-31} kg$
Time	$\hbar/E_a$	$2.4189 \times 10^{-17} s$
Charge	e	$1.6022 \times 10^{-19} C$
Energy	E_a	$4.3598 \times 10^{-18} J$
Velocity	$a_0 E_a/\hbar$	$2.1877 \times 10^{6} ms^{-1}$
Angular momentum	$\hbar$	$1.0546 \times 10^{-34} Js$
Electric dipole moment	ea_0	$8.4784 \times 10^{-30} Cm$
Electric polarizability	$e^2 a_0^2/E_a$	$1.6488 \times 10^{-41} C^2 m^2 J^{-1}$
Electric field	$E_a/(ea_0)$	$5.1423 \times 10^{11} V m^{-1}$
Wave function	$a_0^{-3/2}$	$2.5978 \times 10^{15} m^{-3/2}$

1.3.2 Atomic Units

It is common practice to switch to a set of units that are easier to work with, i.e. setting $\hbar = m_e = e = \cdots = 1$. In this study we use atomic units, a form of such dimensionless units. To see how these units arise, consider the time-independent Schrödinger equation for a Hydrogen atom,

$$\left(-\frac{\hbar^2}{2m_e}\nabla^2 - \frac{e^2}{4\pi\epsilon_0 r}\right)\phi = E\phi, \tag{1.74}$$

where $\hbar$ is the reduced Planck constant, equal to Planck's constant divided by 2π; m_e is the mass of the electron, $-e$ is the charge of the electron and ϵ_0 is the permitivity of free space. We make this equation dimensionless by letting $r \to \lambda r'$,

$$\left(-\frac{\hbar^2}{2m_e\lambda^2}\nabla'^2 - \frac{e^2}{4\pi\epsilon_0 \lambda r'}\right)\phi' = E\phi'. \tag{1.75}$$

We can factor out the constants in front of the operators, if we choose λ so that,

$$\frac{\hbar^2}{m_e\lambda^2} = \frac{e^2}{4\pi\epsilon_0\lambda} = E_a \to \lambda\frac{4\pi\epsilon_0\hbar^2}{m_e e^2} = a_0 \tag{1.76}$$

where E_a is the atomic unit of energy that chemists call Hartree. Incidently, we see that λ is just the Bohr radius, a_0. If we let $E' = E/E_a$, we obtain the dimensionless Schrödinger equation,

$$\left(-\frac{1}{2}\nabla'^2 - \frac{1}{r'}\right)\phi' = E'\phi'. \tag{1.77}$$

Some conversion factors between atomic units and SI units can be found in Table 1.1.

1.4 Indistinguishable Particles

In classical mechanics, although particles are indistinguishable, one typically regards particles as individuals because a permutation of particles is counted as a new arrangement and something different than the initial configuration. This was called "Transcedental Individuality" by Heinz Post[63]. In quantum mechanics, on the other hand, a permutation is not regarded as giving rise to a new arrangement. It follows that quantum objects are very different from anything else we know from everyday life, and must be considered "non-individual". This idea has its origin from the uncertainty principle, stating that no sharply defined particle exist. If we take this idea to its extreme one may postulate that all particles of a given type are one and the same. Here from Richard Feynman's Nobel lecture: Feynman[16], "I received a telephone call one day at the graduate college at Princeton from Professor Wheeler, in which he said, 'Feynman, I know why all electrons have the same charge and the same mass' 'Why?' 'Because, they are all the same electron!' "

Following the brief discussion above one may begin to postulate that, the probability density for the location of particles in a system must be permutation invariant,

$$|\Psi(x_1, x_2, \ldots, x_i, x_j, \ldots, x_N)|^2 = |\Psi(x_1, x_2, \ldots, x_j, x_i, \ldots, x_N)|^2, \tag{1.78}$$

where Ψ represents a wavefunction description of N particles For any arbitrary permutation, this is equivalent to

$$\Psi(x_1, \ldots x_N) = e^{i\alpha(\sigma)}\Psi(x_{\sigma(1)}, x_{\sigma(2)}, \ldots, x_{\sigma(N)}), \tag{1.79}$$

where $\sigma \in S_N$ is some permutation of N indices and α is some real number that may be dependent on σ. The same relation can be written by way of a linear permutation operator,

$$(\hat{P}_\sigma \Psi)(x_1, \ldots, x_N) = \Psi(x_{\sigma(1)}, x_{\sigma(2)}, \ldots, x_{\sigma(N)}). \tag{1.80}$$

The 'indistinguishability postulate" states that if a permutation P is applied to a state representing an assembly of particles, there is no way of distinguishing between the permuted state and the original, by means of an observation at any time.

One can show that the resulting wavefunction that has undergone a permutation operation falls into two categories,

$$\hat{P}_\sigma \Psi = \begin{cases} \Psi \\ (-1)^{|\sigma|}\Psi \end{cases} \quad \forall \sigma \in S_N, \tag{1.81}$$

where $|\sigma|$ is the number of transpositions in σ and the sign will be $(-1)^{|\sigma|} = \pm 1$. In the former case, when the sign is $+$, the wavefunction is "totally symmetric with respect to permutations"; while in the latter case, when the sign is $-$, the wavefunction is "totally anti-symmetric." We show this result with a simple permutation operator $\hat{P}_{ij}$ that exchanges coordinates of particle i and j, i.e.

$$\hat{P}_{ij}\Psi(x_1, x_2, \ldots, x_i, x_j, \ldots, x_N) = \Psi(x_1, x_2, \ldots, x_j, x_i, \ldots, x_N). \tag{1.82}$$

Applying this permutation operator twice will return us to the initial wavefunction,

$$\hat{P}_{ij}\hat{P}_{ij} = 1, \tag{1.83}$$

which implies that the permutation operator is Hermitian and unitary. Morover, the Permutation operator must commute with any operator $\hat{O}$,

$$[\hat{P}_{ij}, \hat{O}] = 0. \tag{1.84}$$

Consider an eigenvalue equation for the permutation operator $\hat{P}_{ij}$,

$$\hat{P}_{ij}\Psi = \lambda_{ij}\Psi, \tag{1.85}$$

from which it follows that

$$\Psi = \hat{P}_{ij}^2\Psi = \lambda_{ij}^2\Psi \;\rightarrow\; \lambda_{ij}^2 = 1. \tag{1.86}$$

This leads us to another postulate in quantum theory, that we have only two types of basic particles. *Bosons* have totally symmetric wavefunctions only, while *fermions* have totally anti-symmetric wavefunctions only. "The physical consequences of this postulate seems to be in good agreement with experimental data" [47]. Moreover, all particles with integer spin are bosons, and all particles with half-integer spin are fermions [18, 58]. This can be proved in relativistic quantum mechanics, but must be accepted as an axiom in nonrelativistic theory[36].Generally, the degeneracy of a state for a given energy ϵ is divided into three categories,

$$n(\epsilon) = \begin{cases} e^{-(\epsilon-\mu)/k_BT} & \text{Maxwell-Boltzmann} \\ \frac{1}{e^{-(\epsilon-\mu)/k_BT}+1} & \text{Fermi-Dirac} \\ \frac{1}{e^{-(\epsilon-\mu)/k_BT}-1} & \text{Bose-Einstein.} \end{cases} \tag{1.87}$$

The Maxwell-Boltzmann distribution is the classical result, for *distinguishable* particles; the Fermi-Dirac distribution applies to *identical fermions*, and the Bose-Einstein distribution is for *identical bosons*. Here, T is the temperature, k_B is Boltzmann's constant and μ is the chemical potential.

To this day, particles with no other spin has been found, but norwegian physicists Jon Magne Leinaas and Jan Myrheim discovered that in one- and two dimensions, more general permutation symmetries are possible. They dubbed this third class of fundamental particles "anyons"[47].

1.5 Density Operators

Density operators will become very useful, especially later when we use them to compute expectation values. A formal introduction to this concept is therefor warranted. Consider a system that is described not by a single state vector, but by an ensemble of state vectors $\{|\psi\rangle_1, |\psi\rangle_2, \dots, |\psi\rangle_n\}$ with a probability distribution $\{p_1, p_2, \dots p_m\}$ defined over the ensemble. We may consider this ensemble to contain *quantum probabilites* carried by the state vectors $\{|\psi\rangle_k\}$ and classical propabilities carried by the distribution $\{p_k\}$. A system described by an ensemble state is said to be in a *mixed* state.

The expectation value of a quantum observable in a state described by an ensemble of state vectors is

$$\left\langle \hat{O} \right\rangle = \sum_{k=1}^{n} p_k \left\langle \hat{O} \right\rangle_k = \sum_{k=1}^{n} p_k \langle \psi_k | \hat{O} | \psi_k \rangle . \tag{1.88}$$

This expression motivates the introduction of the *density operator* associated with the mixed state,

$$\hat{\rho} = \sum_{k=1}^{n} p_k |\psi_k\rangle\langle\psi_k| . \tag{1.89}$$

The corresponding matrix, defined by reference to an orthogonal basis $\{|\phi_i\rangle\}$, is called the *density matrix*,

$$\rho_{ij} = \sum_{i=1}^{n} p_k \langle \phi_i| |\psi_k\rangle\langle\psi_k| |\phi_j\rangle . \tag{1.90}$$

An important note is that all measurable information about the system is contained in its density operator. We can for instance compute expectation values using the density operator,

$$\begin{aligned} \left\langle \hat{O} \right\rangle &= \sum_{k=1}^{n} p_k \sum_{i} \langle \psi_k | \hat{O} | \phi_i \rangle \langle \phi_i | \psi_k \rangle \\ &= \sum_{i} \sum_{k=1}^{n} p_k \langle \phi_i | \psi_k \rangle \langle \psi_k | \hat{O} | \phi_i \rangle = \mathrm{tr}\left\{ \hat{\rho}\hat{O} \right\}. \end{aligned} \tag{1.91}$$

There are certain general properties that any density operator has to satisfy,

$$\begin{aligned}
p_k = p_k^* \;&\rightarrow\; \hat{\rho} = \hat{\rho}^\dagger && \text{Hermiticity} \\
p_k \geq 0 \;&\rightarrow\; \langle\chi|\hat{\rho}|\chi\rangle\,\forall\chi && \text{Positive semi-definite} \\
\sum_k p_k = 1 \;&\rightarrow\; \mathrm{tr}\{\hat{\rho}\} = 1 && \text{Normalisation.}
\end{aligned} \tag{1.92}$$

We also note that

$$\mathrm{tr}\,\hat{\rho}^2 = \sum p_k^2 \;\rightarrow\; \mathrm{tr}\,\hat{\rho}^2 \leq 1, \tag{1.93}$$

because all eigenvalues are $p_k \leq 1$, which means that $\mathrm{tr}\,\hat{\rho}^2 \leq \mathrm{tr}\,\hat{\rho}$. The pure state is a special case where one of the probabilities p_k is equal to one, and the others are 0. In this case, the density operator will ve equivalent to a projection opertor onto this single state. Morover, $\mathrm{tr}\,\hat{\rho}^2 = 1$ for a pure state, while for a mixed state we have $\mathrm{tr}\,\hat{\rho}^2 < 1$.

Chapter 2

Second Quantisation

The second-quantisation formalism is a very useful tool used in the description of many-body systems. Here the particles themselves are discrete quanta created and destroyed by *creation*- and *annihilation* operators. We start by introduction of the Slater determinant, a very useful description of an anti-symmetric wavefunction, in order to build a nomenclature for describing the many-electron systems with which we are concerned.

2.1 Slater Determinants

For some smaller systems it can be satisfactory or even provident to use a single, special function to describe the entire system. Here however, we introduce the Slater determinant which is a way to write a product of wavefunctions. We will only consider many-electron wavefunctions that can be written as a single Slater determinant or as a linear combination of several Slater determinants.

We define an *orbital*[1] which is the wavefunction for a single particle, or more precicely a single electron. The wavefunction a larger group of electrons, for instance those electrons that surround an atom or molecule, we call the *molecular orbital*. We also discriminate between spatial orbitals which are functions of spatial coordinates; and spinorbitals, which are functions of the space and spin coordinates (typically a product of a spatial orbital and a spin function). A very complete description and thorough discussion of all things concerning electronic sructure wavefunctions is given by Szabo and Ostlund[74].

The best description for a multiple-electron wavefunction, given by the independent-particle approximation is the Slater determinant,

$$\Phi = \frac{1}{\sqrt{N!}} \begin{vmatrix} \phi_1(1) & \phi_2(1) & \dots & \phi_N(1) \\ \phi_1(2) & \phi_2(2) & \dots & \phi_N(2) \\ \vdots & \vdots & \ddots & \vdots \\ \phi_1(N) & \phi_2(N) & \dots & \phi_N(N) \end{vmatrix} = \mathcal{A}\phi_1\phi_2\dots\phi_N, \tag{2.1}$$

where $\phi_i(\mu)$ is a spinorbital and $\mathcal{A}$ is the antisymmetriser. The spinorbitals, are single-particle functions in the proper two-dimensional Hilbert space and they are not necessarily orthonormal.

To illustrate why this is a good approximation of the electronic wave function, consider first the two-electron case,

$$\Phi_{N=2} = \frac{1}{\sqrt{2}}(\phi_1(1)\phi_2(2) - \phi_1(2)\phi_2(1)). \tag{2.2}$$

[1]Sometimes also called a single-particle function, a single-particle orbital, a single-electron orbital or similar. There is a chance that these terms will be used interchangably throughout this text without warning.

We see from this relatively simple expression that if the electrons were to occupy the same state the wavefunction would equal zero, in effect forbidding such a state. This ensures that the Pauli exclusion principle for fermions is satisfied[59]. Moreover, if we switch coordinates of any two single-particle functions (spinorbitals), corresponding to the interchange of rows in Equation 2.1, the result is a change of sign. This attribute of a determinant accomodates the total anti-symmetry necessary for a fermionic wavefunction. Conversely, a bosonic wavefunction can be constructed as a *permanent*.

We usually write a Slater determinant in a much more simple way,

$$|\Phi\rangle = |\phi_i \phi_j \phi_k \dots \phi_z\rangle = |ijk \dots z\rangle \,. \tag{2.3}$$

The N single-particle functions $\phi_i \dots \phi_z$, that make up this Slater determinant now form a basis for an N-particle Hilbert space $\mathcal{H}_N$.

2.2 Creation and Annihilation Operators

The introduction of creation- and annihilation operators are what establishes the second quantisation formalism. As we will see, such operators makes the construction of N-particle wavefunctions as symmetrised or anti-symmetrised products redundant, because these symmetry properties are encompassed in the anticommutation properties of the operators. This is a great advantage of the second quantisation framework. Another advantage is the relatively easy management of many-particle systems.

The notation of creation and annihilation operators vary,

$$\begin{aligned} &\text{creation operator for spinorbital } \phi_i,\ \hat{X}_i^\dagger, \hat{a}_i^\dagger, \hat{c}_i^\dagger, \hat{\imath}^\dagger; \\ &\text{annihilation operator for spinorbital } \phi_i,\ \hat{X}_i, \hat{a}_i, \hat{c}_i, \hat{\imath}. \end{aligned}$$

Herein, $\hat{a}_i^\dagger$, $\hat{a}_i$ is used and, if there is no chance of confusion, $\hat{\imath}^\dagger$, $\hat{\imath}$.

The Creation Operator For every single-particle index q, we define the creation operator $a_q^\dagger$ acting on the vacuum state by

$$\hat{a}_i^\dagger |0\rangle = |q\rangle \,. \tag{2.4}$$

For any slater determinant with $N > 0$, the action is defined by

$$\hat{a}_i^\dagger |jk \dots z\rangle = |ijk \dots z\rangle \,, \tag{2.5}$$

$$\hat{a}_i^\dagger |ijk \dots z\rangle = 0. \tag{2.6}$$

We see that this the the same as inserting a column into the matrix-form of the Slater determinant in Equation 2.1.

The Annihilation Operator It i sufficient to state that the annihilation operator a_i is the hermitian adjoint of the creation operator $\hat{a}_i$, but to specify we have

$$\hat{a}_i |0\rangle = 0, \tag{2.7}$$

as there is no particle in the vacuum state to annihilate. For any arbitrary Slater determinant, we have

$$\hat{a}_i |ijk \dots z\rangle = |ij \dots z\rangle \,, \tag{2.8}$$

$$\hat{a}_i |jk \dots z\rangle = 0. \tag{2.9}$$

The creation- and annihilation operators map wavefunctions between Hilbert spaces of different dimensionality, or particle number;

$$\hat{a}_i^\dagger : \quad \mathcal{H}_N \to \mathcal{H}_{N+1} \tag{2.10}$$

$$\hat{a}_i : \quad \mathcal{H}_N \to \mathcal{H}_{N-1}, \tag{2.11}$$

where $\mathcal{H}_N$ is the Hilbert space for N particles. The space comprising all Hilbert spaces of different particles numbers is called the Fock space, defined as a direct sum of all Hilbert spaces

$$\mathscr{F} = \bigoplus_{N=0}^{\infty} \mathcal{H}_N. \tag{2.12}$$

The creation- and annihilation operate on this Fock space.

We can now build a Slater determinant as the result of successive operations of several creation operators $\hat{a}_q^\dagger$ on the vacuum state $|0\rangle$,

$$\hat{a}_i^\dagger \hat{a}_j^\dagger \hat{a}_k^\dagger \ldots \hat{a}_z^\dagger |0\rangle = |ijk\ldots z\rangle . \tag{2.13}$$

It is convenient to arrange the spinorbitals in a Slater determinant in alphabetical order, as in Equation 2.13. This makes it necessary to ascertain the effects a creation or annihilation operator will have on a Slater determinant when the affected orbital is not at the beginning of the string of orbitals in the Slater determinant. Generally we have,

$$\hat{P} |ijk\ldots z\rangle = (-1)^{\sigma(\hat{P})} |ijk\ldots z\rangle , \tag{2.14}$$

where $\hat{P}$ permutes the string of orbitals and $\sigma(\hat{P})$ is the parity of the permutation $\hat{P}$. We have

$$\hat{a}_p^\dagger |ijk\ldots z\rangle = (-1)^{\eta_p} |ijk\ldots p\ldots z\rangle , \tag{2.15}$$

$$\hat{a}_p |ijk\ldots p\ldots z\rangle = (-1)^{\eta_p} |ijk\ldots z\rangle , \tag{2.16}$$

where η_p is the number of orbitals preceeding the orbital ϕ_p, pertaining to the creation (annihilation) operator, in the Slater determinant.

2.3 Anticommutator Relations

To show how the anticommutator relations are built into the creation- and annihilation operators, we start by considering two arbitrary creation operators acting on a Slater determinant,

$$\begin{aligned} \hat{a}_p^\dagger \hat{a}_q^\dagger |ijk\ldots\rangle &= |pqijk\ldots\rangle , \\ \hat{a}_q^\dagger \hat{a}_p^\dagger |ijk\ldots\rangle &= |qpijk\ldots\rangle = - |pqijk\ldots\rangle . \end{aligned} \tag{2.17}$$

We demand that these two operations be equivalent, or that

$$\begin{aligned} \hat{a}_p^\dagger \hat{a}_q^\dagger &= -\hat{a}_q^\dagger \hat{a}_p^\dagger, \\ \{\hat{a}_p^\dagger, \hat{a}_q^\dagger\} &\equiv \hat{a}_p^\dagger \hat{a}_q^\dagger + \hat{a}_q^\dagger \hat{a}_p^\dagger = \hat{0}. \end{aligned} \tag{2.18}$$

Which is the first of three anti-commutator relations we are going to derive.

The logical next step is to perform a similar operation with annihilation operators,

$$\begin{aligned} \hat{a}_p \hat{a}_q |qpijk\ldots\rangle &= \hat{a}_p |pijk\ldots\rangle = |ijk\ldots\rangle , \\ \hat{a}_q \hat{a}_p |qpijk\ldots\rangle &= -\hat{a}_q \hat{a}_p |pqijk\ldots\rangle = -\hat{a}_q |qijk\ldots\rangle = - |ijk\ldots\rangle . \end{aligned} \tag{2.19}$$

We also require these two operations to be equivalent,

$$\begin{aligned}\hat{a}_p\hat{a}_q &= -\hat{a}_q\hat{a}_p,\\ \{\hat{a}_p,\hat{a}_q\} &\equiv \hat{a}_p\hat{a}_q + \hat{a}_q\hat{a}_p = \hat{0}.\end{aligned} \tag{2.20}$$

One case remains, when a creation operator and an annihilation operator is applied together on a Slater determinant,

$$\hat{a}_p^\dagger\hat{a}_q\left|qijk\ldots\right\rangle = \hat{a}_p^\dagger\left|ijk\ldots\right\rangle = \left|pijk\ldots\right\rangle. \tag{2.21}$$

This operation will replace ϕ_q by ϕ_p even if ϕ_p would have been somewhere else in the interior of the Slater determinant. Any sign change as an effect of moving the orbital to the front of the string would be negated when the orbital is moved back to the original position. Exchanging the order of the operators however,

$$\hat{a}_q\hat{a}_p^\dagger\left|qijk\ldots\right\rangle = \hat{a}_q\left|pqijk\ldots\right\rangle = -\hat{a}_q\left|qpijk\ldots\right\rangle = -\left|pijk\ldots\right\rangle. \tag{2.22}$$

We again see a sign change and have,

$$\{\hat{a}_p^\dagger,\hat{a}_q\} = \hat{0} \quad (p \neq q). \tag{2.23}$$

If, on the other hand, $p = q$ we have

$$\begin{aligned}\hat{a}_p^\dagger\hat{a}_p\left|pijk\ldots\right\rangle &= \left|pijk\ldots\right\rangle,\\ \hat{a}_p\hat{a}_p^\dagger\left|pijk\ldots\right\rangle &= 0,\end{aligned} \tag{2.24}$$

and if the orbital ϕ_p in question does not appear in the Slater determinant,

$$\begin{aligned}\hat{a}_p^\dagger\hat{a}_p\left|ijk\ldots\right\rangle &= 0,\\ \hat{a}_p\hat{a}_p^\dagger\left|ijk\ldots\right\rangle &= \hat{a}_p\left|pijk\ldots\right\rangle = \left|ijk\ldots\right\rangle.\end{aligned} \tag{2.25}$$

For all cases we have that,

$$\left(\hat{a}_p^\dagger\hat{a}_p + \hat{a}_p\hat{a}_p^\dagger\right)\left|\ldots\right\rangle = \left|\ldots\right\rangle, \tag{2.26}$$

or

$$\{\hat{a}_p^\dagger,\hat{a}_p\} = \{\hat{a}_p,\hat{a}_p^\dagger\} = \hat{1}. \tag{2.27}$$

In conclusion, the anti-commutator relations of the creation and annihilation operators are,

$$\{\hat{a}_p,\hat{a}_q\} = \hat{0}, \tag{2.28}$$

$$\{\hat{a}_p^\dagger,\hat{a}_q^\dagger\} = \hat{0}, \tag{2.29}$$

$$\{\hat{a}_p^\dagger,\hat{a}_q\} = \{\hat{a}_p,\hat{a}_q^\dagger\} = \delta_{pq}, \tag{2.30}$$

where δ_{pq} is the Kronecker delta.

2.4 Representation of Operators

Here we shall see that it is very useful to express operators in terms of creation- and annihilation operators. We introduce a general one- and two-body operator. It is possible to create operators pertaining to any number of particles, but these are very uncommon to see in quantum chemistry, which is our domain.

A second-quantised one-body operator is written like

$$\hat{h} = \sum_{i=1}^{N} \hat{h}(i) = \sum_{ij} \langle i | \hat{h} | j \rangle \hat{a}_i^\dagger \hat{a}_j, \tag{2.31}$$

where in general, $\langle p | \hat{h} | q \rangle$ is the matrix element of the single-particle operator $\hat{h}$ in a given one-particle basis,

$$h^p_q = \langle p|\hat{h}|q\rangle = \int dx \phi_p(x)^* \hat{h} \phi_q(x). \tag{2.32}$$

More accurately, we see from Equation 2.31, that $\hat{h}$ weighs each occupied orbital of a Slater determinant with the appropriate matrix element.

A second-quantised two-body operator is written like

$$\hat{u} = \sum_{i,j}^{N} \hat{u}(i,j) = \frac{1}{2} \sum_{ijkl} u^{pq}_{rs} \hat{a}_i^\dagger \hat{a}_j^\dagger \hat{a}_l \hat{a}_k, = \frac{1}{4} \sum_{ijkl} \langle ij | \hat{u} | kl \rangle_{\mathrm{AS}} \hat{a}_i^\dagger \hat{a}_j^\dagger \hat{a}_l \hat{a}_k \tag{2.33}$$

where

$$\langle ij|\hat{u}|kl\rangle \equiv \int\int \phi_i^*(x_1)\phi_j^*(x_2) u(x_1,x_2) \phi_k(x_1) \phi_(x_2) dx_1 dx_2. \tag{2.34}$$

Notice the transposed order of indices in 2.33. The interpretation of the expression is that a fermion is removed from state $|k\rangle$ and $|l\rangle$ and created in state $|i\rangle$ and $|j\rangle$, with the probability $\langle ij|\hat{u}|kl\rangle$. The antisymmetric two-eletron integral for $\hat{u}$ is abreviated,

$$\langle ij | \hat{u} | kl \rangle - \langle ij | \hat{u} | kl \rangle = \langle ij | \hat{u} | kl \rangle_{\mathrm{AS}} \tag{2.35}$$

We see that a full second-quantised Hamiltonian can be written,

$$\hat{H} = \hat{h} + \hat{u} = \sum_{ij} \hat{h}_{ij} \hat{a}_i^\dagger \hat{a}_j + \frac{1}{4} \langle ij|\hat{u}|kl\rangle_{\mathrm{AS}} \hat{a}_i^\dagger \hat{a}_j^\dagger \hat{a}_l \hat{a}_k. \tag{2.36}$$

2.5 Normal Order and Wick's Theorem

We have built the foundations necessary to describe wavefunctions in terms of creation- and annihilation operators as well as a simple way of writing a general electronic Hamiltionian in the second-quantised manner. The following is a necessity to be able to compute vacuum expectation values $\langle - | \hat{A}\hat{B} \ldots | - \rangle$ of products of creation- and annihilation operators. Such expectation values are very important for several computational methods, see Harris, Monkhorst, and Freeman[26].

2.5.1 Normal ordering and contractions

The normal-ordered product of a string of operators $\hat{A}_1$, $\hat{A}_2$, $\hat{A}_3$, ..., is defined as the rearranged product of operators such that all the creation operators are to the left of all the annihilation operators, including a phase factor corresponding to the parity of the permutation, producing the rearrangent

$$\begin{aligned} n[\hat{A}_1\hat{A}_2 \ldots \hat{A}_n] &\equiv (-1)^{|\sigma|} \hat{A}_{\sigma(1)} \hat{A}_{\sigma(2)} \ldots \hat{A}_{\sigma(n)} \\ &= (-1)^{\sigma(\hat{P})} \hat{P}(\hat{A}_1\hat{A}_2 \ldots \hat{A}_n) \\ &= (-1)^{|\sigma|} [\text{creation operators}] \cdot [\text{annihilation operators}] \\ &= (-1)^{|\sigma|} \hat{a}^\dagger \hat{b}^\dagger \ldots \hat{u}\hat{v}, \end{aligned} \tag{2.37}$$

where $\hat{P}$ is a permutation operator acting on the product of operators, and σ is the parity of the permutation. One should bear in mind that this definition is by no means unique. Here are some examples,

$$
\begin{gathered}
n[\hat{a}^\dagger \hat{b}] = \hat{a}^\dagger \hat{b} \quad n[\hat{b}\hat{a}^\dagger] = -\hat{a}^\dagger \hat{b} \\
n[\hat{a}\hat{b}] = \hat{a}\hat{b} = -\hat{b}\hat{a} \\
n[\hat{a}^\dagger \hat{b}^\dagger] = \hat{a}^\dagger \hat{b}^\dagger = -\hat{b}^\dagger \hat{a}^\dagger \\
n[\hat{a}^\dagger \hat{b} \hat{c}^\dagger \hat{d}] = -\hat{a}^\dagger \hat{c}^\dagger \hat{b}\hat{d} = \hat{c}^\dagger \hat{a}^\dagger \hat{b}\hat{d} = \hat{a}^\dagger \hat{c}^\dagger \hat{d}\hat{b} = -\hat{c}^\dagger \hat{a}^\dagger \hat{d}\hat{b}.
\end{gathered}
$$

Note that the second quantised Hamiltonian in Equation 2.36 is already on normal-ordered form.

For two arbitrary creation and annihilation operators, we define their contraction as

$$
\wick{\c{\hat{A}}\c{\hat{B}}} \equiv \langle -|\, \hat{A}\hat{B}\, |-\rangle\,, \tag{2.38}
$$

equivalently,

$$
\wick{\c{\hat{A}}\c{\hat{B}}} \equiv \hat{A}\hat{B} - n[\hat{A}\hat{B}]. \tag{2.39}
$$

For a creation- and annihilation operator there are four possible contractions,

$$
\begin{aligned}
\wick{\c{\hat{a}}^\dagger\c{\hat{b}}^\dagger} &= \langle -|\, \hat{a}^\dagger \hat{b}^\dagger \,|-\rangle = \hat{a}^\dagger \hat{b}^\dagger - n[\hat{a}^\dagger \hat{b}^\dagger] = 0 \\
\wick{\c{\hat{a}}\c{\hat{b}}} &= \langle -|\, \hat{a}\hat{b} \,|-\rangle = \hat{a}\hat{b} - n[\hat{a}\hat{b}] = 0 \\
\wick{\c{\hat{a}}^\dagger\c{\hat{b}}} &= \langle -|\, \hat{a}^\dagger \hat{b} \,|-\rangle = \hat{a}^\dagger \hat{b} - n[\hat{a}^\dagger \hat{b}] = 0 \\
\wick{\c{\hat{a}}\c{\hat{b}}^\dagger} &= \langle -|\, \hat{a}\hat{b}^\dagger \,|-\rangle = \hat{a}\hat{b}^\dagger - n[\hat{a}\hat{b}^\dagger] = \hat{a}\hat{b}^\dagger - (-\hat{b}^\dagger \hat{a}) = \{\hat{a}, \hat{b}^\dagger\} = \delta_{ab}.
\end{aligned} \tag{2.40}
$$

We see that all contractions between creation- and annihilation operators are a number, most of them are zero and only those with a annihilation operator to the left and a creation operator to the right can be one.

Contractions inside a normal ordered product is definded as follows,

$$
\wick{n[\hat{A}\hat{B}\hat{C}\dots \c1{\hat{R}}\dots \c2{\hat{S}}\dots \c1{\hat{T}}\dots \c2{\hat{U}}\dots]} = (-1)^\sigma \wick{\c{\hat{R}}\c{\hat{T}}}\wick{\c{\hat{S}}\c{\hat{U}}}\dots n[\hat{A}\hat{B}\hat{C}\dots], \tag{2.41}
$$

where all contracted operator pairs are moved to the front of the normal ordered product, and σ is the parity of the permutations required for this relocation. The result will be zero, or plus or minus the normal ordred product without the contracted operator pairs.

2.5.2 Wick's Theorem

Wick's theorem states that every string of creation and annihilation operators can be written as a sum of normal-ordered products with all possible contractions,

$$
\begin{aligned}
\hat{A}\hat{B}\hat{C}\hat{D}\cdots =& n[\hat{A}\hat{B}\hat{C}\hat{D}\dots] + n[\wick{\c{\hat{A}}\c{\hat{B}}}\hat{C}\hat{D}\dots] + n[\wick{\c{\hat{A}}\hat{B}\c{\hat{C}}}\hat{D}\dots] + n[\wick{\c{\hat{A}}\hat{B}\hat{C}\c{\hat{D}}}\dots] \\
&+ \cdots + n[\hat{A}\wick{\c{\hat{B}}\c{\hat{C}}}\hat{D}\dots] + n[\hat{A}\wick{\c{\hat{B}}\hat{C}\c{\hat{D}}}\dots] + \cdots + n[\hat{A}\hat{B}\wick{\c{\hat{C}}\c{\hat{D}}}\dots] + \cdots + \\
&+ n[\wick{\c1{\hat{A}}\c1{\hat{B}}\c2{\hat{C}}\c2{\hat{D}}}\dots] + n[\wick{\c1{\hat{A}}\c2{\hat{B}}\c1{\hat{C}}\c2{\hat{D}}}\dots] + n[\wick{\c1{\hat{A}}\c2{\hat{B}}\c2{\hat{C}}\c1{\hat{D}}}\dots] + \dots,
\end{aligned} \tag{2.42}
$$

where eventually all possible contractions of one, two pairs etc, are included.

Especially when computing vacuum expectation values of normal-ordred products Wick's theorem becomes very important. The reason for this is that each contraction will not contribute to the result, unless it is a fully contracted operator string,

$$\langle|\,\hat{A}\ldots\hat{B}\ldots\hat{C}\ldots\hat{D}\ldots|\rangle = \sum_{\substack{\text{all possible}\\ \text{contractions}}} \langle|\,n[\hat{A}\ldots\hat{B}\ldots\hat{C}\ldots\hat{D}\ldots]\,|\rangle\,. \tag{2.43}$$

Most vacuum expectation values contain operator strings that already have substrings that are on normal-ordered form. This warrants a very useful generalisation of Wick's theorem for such strings,

$$\begin{aligned} n[\hat{A}_1\hat{A}_2\ldots]n[\hat{B}_1\hat{B}_2\ldots]\ldots n[\hat{Z}_1\hat{Z}_2\ldots] &= n[\hat{A}_1\hat{A}_2\cdots:\hat{B}_1\hat{B}_2\cdots:\cdots:\hat{Z}_1\hat{Z}_2\ldots] \\ +\sum_{(1)} n[\hat{A}_1\hat{A}_2\cdots:\hat{B}_1\hat{B}_2\cdots:\cdots:\hat{Z}_1\hat{Z}_2\ldots] &+\cdots+\sum_{(n)} n[\hat{A}_1\ldots\ldots\ldots\ldots\hat{Z}_N], \end{aligned} \tag{2.44}$$

where we sum over all combinations of contractions that each involve operators from different substrings, starting with one contractions and up to when all operators, or as many as possible, are contracted.

2.5.3 Particle-Hole Formalism

We see that a Slater determinant can be built recursively with creation operators,

$$\Phi = \hat{\imath}_1\hat{\imath}_2\ldots\hat{\imath}_N = \hat{\imath}_1^\dagger\hat{\imath}_2^\dagger\ldots\hat{\imath}_N^\dagger\,|\rangle\,. \tag{2.45}$$

Instead of rewriting Slater determinants with operators applied to the vacuum state in this manner we will introduce the reference state, or Fermi vacuum,

$$|0\rangle = |\Phi_0\rangle = |ijk\ldots n\rangle\,. \tag{2.46}$$

We will define other Slater determinants relative to this reference state. For instance,

$$|\Phi_i^a\rangle \equiv \hat{a}^\dagger\hat{\imath}\,|\Phi_0\rangle = |ajk\ldots n\rangle \tag{2.47}$$

$$\left|\Phi_{ij}^{ab}\right\rangle \equiv \hat{a}^\dagger\hat{b}^\dagger\hat{\jmath}\hat{\imath}\,|\Phi_0\rangle = |abk\ldots n\rangle \tag{2.48}$$

$$|\Phi_i\rangle \equiv \hat{\imath}\,|\Phi_0\rangle = |jk\ldots n\rangle \tag{2.49}$$

$$|\Phi^a\rangle \equiv \hat{a}^\dagger\,|\Phi_0\rangle = |aijk\ldots n\rangle \tag{2.50}$$

where equations 2.47, 2.48 2.49 and 2.50 constitues a single excitation, a double excitation, an electorn removal and an electron attachment, respectively. Note that these reference relative Slater determinants have the following properties,

$$\left|\Phi_{ij}^{ab}\right\rangle = \left|\Phi_{ji}^{ba}\right\rangle = -\left|\Phi_{ij}^{ba}\right\rangle = -\left|\Phi_{ji}^{ab}\right\rangle. \tag{2.51}$$

Take note of the specific letters used for creating and annihilating electrons in the example above. $i, j, k, l, \ldots$ are letters restricted to indices of *hole* states, and $a, b, c, d, \ldots$ are letters restriced to indices of *particle* states, while $p, q, r, \ldots$ are for general use, indicating any state. Notice that

$$\begin{aligned} \hat{\imath}^\dagger\,|0\rangle = 0 \quad \hat{a}\,|0\rangle = 0, \\ \langle 0|\,\hat{\imath} = 0 \quad \langle 0|\,\hat{a}^\dagger = 0. \end{aligned} \tag{2.52}$$

Whenever we try to insert an electron where there already is one, or when we try to remove an electron that is not there, we get zero as result.

2.5.4 Wick's theorem relative to the Fermi vacuum

Now we will modify the concepts of normal-ordering, contractions and Wick's theoreom so that the work better in conjunction with the freshly defined Fermi vacuum, instead of the physical vacuum. First we introduce pseudo-operators,

$$\begin{aligned} \hat{b}_i &= \hat{i}^\dagger, \quad \hat{b}_i^\dagger = \hat{i} \\ \hat{b}_a &= \hat{a}, \quad \hat{b}_a^\dagger = \hat{a}^\dagger, \end{aligned} \tag{2.53}$$

where $\hat{b}_i^\dagger$ is a hole creation operator and $\hat{b}_i$ is a particle creation operator, but only for vacant spaces below the fermi level. The reason for introducing such operators is to be able to work with the fermi vacuum in the same manner as regular operators work with the physical vacuum. Excited Slater determinants can easily be written using pseudo-operators,

$$|\Phi_i^a\rangle \equiv \hat{b}_a^\dagger \hat{b}_i^\dagger |\Phi_0\rangle \tag{2.54}$$

$$\left|\Phi_{ij}^{ab}\right\rangle \equiv \hat{b}_b^\dagger \hat{b}_j^\dagger \hat{b}_a^\dagger \hat{b}_i^\dagger |\Phi_0\rangle . \tag{2.55}$$

We introduce a new type of normal ordering for the pseudo-operators and for the actual operators that they represent,

$$\{\hat{A}\hat{B}\hat{C}\} = (-1)\hat{b}_p^\dagger \hat{b}_q^\dagger \dots \hat{b}_u \hat{b}_v. \tag{2.56}$$

We write a contraction in the same manner,

$$\overbracket{\hat{A}\hat{B}} = \hat{A}\hat{B} - \{\hat{A}\hat{B}\}. \tag{2.57}$$

A normal-ordered product with contractions inside is also defined in the same way. We see that the only non-zero contractions are

$$\overbracket{\hat{b}_i \hat{b}_j^\dagger} = \overbracket{\hat{i}^\dagger \hat{j}} = \delta_{ij}, \quad \overbracket{\hat{b}_a \hat{b}_b^\dagger} = \overbracket{\hat{a}\hat{b}^\dagger} = \delta_{ab}. \tag{2.58}$$

Here we are also made aware the benefit of pseudo-operators, as we now have only have non-zero contributions from contractions that have a creation operator to the right, and an annihilation operator to the left. More generally we have the anticommutator relations

$$\{\hat{b}_p, \hat{b}_q^\dagger\} = \delta_{pq}, \quad \{\hat{b}_p, \hat{b}_q\} = 0. \tag{2.59}$$

Part II

Quantum Many-Body Approximations

Chapter 3

Hartree-Fock Theory

In 1927, soon after the discovery of the Schrödinger equation in 1926, Douglas R. Hartree introduced a procedure which he called the self-consistent field method[27]. Hartree sought to do without empirical parameters and to solve the many-body time-independent Schrödinger equation from fundamental principles, *ab initio.* A year later John C. Slater and John A. Gaunt provided a sounder theoretical basis for the Hartree method by applying the variational principle to a trial wave function as a product of single-particle functions[72][22]. Slater later pointed out, with support from Vladimir A. Fock, that the method merely applied the Pauli exclusion principle in its older, incorrect formulation; forbidding presence of two electrons in the same state, but neglecting quantum statistics[71][21]. It was shown that a Slater determinant satisfies the antisymmetric property of the exact solution and would be a suitable ansatz for applying the variational principle. Later, Hartree reformulated the method for calculation[28].

The Hartree-Fock methods makes the following simplications to the multi-electron atomic (molecular) problem,

- The full molecular wavefunction is constrained to a function of the coordinates of only the electrons in the molecule. In not so many words, the Born-Oppernheimer approximation is inherent in the method.

- Any relativistic effects are completely ignored, i.e. the momentum operator is assumed to be completely non-relativistic.

- A variational solution is assumed to be a linear combination of a basis set, which is assumed to be approximately complete. This set of basis functions is usually non-orthogonal.

- Some electron correlation effects are ignored, as the methods implies a mean-field approximation. Coulomb correlation is fully incorporated in the Hartree-Fock method, but it ignores Fermi Correlation and is therefore inable to describe some effects, like London dispersion[1].

- The ground state is assumed to be describable by a single Slater determinant.

Relaxation of the last two simplifications give rise to the large group of many-body methods commonly referred to as post-Hartree-Fock methods.

[1]Named after Fritz London; London dispersion forces (LDF) are a type of force between atoms and molecules[30]

3.1 Deriving the Hartree-Fock Equations

Consider a Hamiltonian for some system

$$\hat{H} = \hat{h} + \hat{u} \tag{3.1}$$

where the ground state of $\hat{h}$ is a Slater determinant consisting of N single-particle functions,

$$\Phi = \mathscr{A}\phi_1\phi_2\ldots\phi_N, \quad \langle\phi_i|\phi_j\rangle = \delta_{ij}. \tag{3.2}$$

If $\hat{u}$ is only a limited perturbation to the system, it is reasonable to assume that the actual ground state of the full system can also be represented by a Slater determinant. Because the Hartree-Fock theory includes a mean-field approximation, each particle moves independently of the others interacting with the remainding electrons only indirectly through an average potential $\hat{v}^{\mathrm{HF}}$.

The expectation value of the Hamiltonian in Equation 3.1 is

$$\begin{aligned}\langle\Phi|\,\hat{H}\,|\Phi\rangle &= \sum_i \langle\phi_i|\,\hat{h}\,|\phi_i\rangle + \frac{1}{2}\sum_{ij}\langle\phi_i\phi_k|\,\hat{u}\,|\phi_i\phi_j - \phi_j\phi_i\rangle \\ &= \sum_i \langle\phi_i|\,\hat{h}\,|\phi_i\rangle + \frac{1}{2}\sum_{ij}\langle\phi_i\phi_k|\,\hat{u}\,|\phi_i\phi_j\rangle_{\mathrm{AS}}\end{aligned} \tag{3.3}$$

where

$$\langle\phi_i\phi_j|\,\hat{u}\,|\phi_k\phi_l\rangle = \int\int \bar{\phi}_i(x_1)\bar{\phi}_j(x_2)\hat{u}(x_1,x_2)\phi_k(x_1)\phi_l(x_2)dx_1dx_2$$

Now we want to minimise the energy (Equation 3.1) under the contraint of orthonormal single-particle functions, id est $\langle\phi_i|\phi_k\rangle = \delta_{ij}$. The minimum solution is called the Hatree-Fock state, $|\Phi_{\mathrm{HF}}\rangle$. An optimisation problem with a constraint begs the formualtion of a Lagrangian functional with a Lagrange multiplier for each constraint,

$$\begin{aligned}\mathscr{L}(\phi_1,\ldots,\phi_n,\lambda) &= \langle\Phi|\,\hat{H}\,|\Phi\rangle - \sum_{ij}\lambda_{ij}(\langle\phi_i|\phi_j\rangle - \delta_{ij}) \\ &= \sum_i \langle\phi_i|\,\hat{h}\,|\phi_i\rangle + \frac{1}{2}\sum_{ij}\langle\phi_i\phi_j|\,\hat{u}\,|\phi_i\phi_j - \phi_j\phi_i\rangle - \sum_{ij}\lambda_{ij}(\langle\phi_i|\phi_j - \delta_{ij}\rangle).\end{aligned} \tag{3.4}$$

The constraints can always be treated separately, $\partial\mathscr{L}/\partial\lambda_{ij}\,\langle\phi_i|\phi_j\rangle - \delta_{ij}$, as this demand will be fullfilled by finding that the solutions ϕ_i are orthonormal.

In order to find the optimum of the Lagrangian in (Equation 3.4), we choose a $k \in \{1,\ldots,N\}$ and compute the directional derivative of ϕ_k^*, by varying this single particle function and leaving all others fixed,

$$\delta\phi_k = \epsilon\eta, \quad \delta\phi_l = 0, k \neq l, \tag{3.5}$$

where ϵ is some small number, and η is a normalized single-particle function. We define a function representing this variation,

$$f(\epsilon) = \mathscr{L}(\phi_1,\ldots,\phi_k + \epsilon\eta,\ldots,\phi_N,\lambda), \tag{3.6}$$

expanded to first order in ϵ,

$$f(\epsilon) = f(0) + \epsilon f'(0) + \mathscr{O}(\epsilon^2). \tag{3.7}$$

For an optimum we must have

$$f'(0) = 0, \quad \forall\eta, \tag{3.8}$$

which means that the directional derivative of $\mathscr{L}$ at $\{\phi_i\}_{i=1}^N$, in the direction η vanishes.

We compute the Taylor expansion of the varied Lagrangian (Equation 3.6),

$$\begin{aligned} f(\epsilon) = \sum_i \langle \phi_i + \delta_{ki}\epsilon\eta | \hat{h} | \phi_i \rangle + \frac{1}{2}\sum_{ij} \langle (\phi_i + \delta_{ki}\epsilon\eta)(\phi_j + \delta_{kj}\epsilon\eta) | \hat{u} | \phi_i\phi_j - \phi_j\phi_i \rangle \\ - \sum_{ij} \lambda_{ij}(\langle \phi_i + \delta_{ik}\epsilon\eta | \phi_j \rangle - \delta_{ij}) + \mathscr{O}(\epsilon^2) \end{aligned} \tag{3.9}$$

$$\begin{aligned} = \sum_i \langle \phi_i | \hat{h} | \phi_i \rangle + \frac{1}{2}\sum_i j \langle \phi_i\phi_j | \hat{u} | \phi_i\phi_j - \phi_j\phi_i \rangle + \epsilon \langle \eta | \hat{h} | \phi_k \rangle \\ + \frac{1}{2}\sum_{ij} \langle \phi_i \delta_{kj}\epsilon\eta | \hat{u} | \phi_i\phi_j - \phi_j\phi_i \rangle \\ + \frac{1}{2}\sum_{ij} \langle \delta_{ki}\epsilon\eta\phi_j | \hat{u} | \phi_i\phi_j - \phi_j\phi_i \rangle \\ - \sum_{ij} \lambda_{ij}(\langle \phi_i | \phi_j \rangle - \delta_{ij}) - \sum_{ij} \lambda_{ij}(\langle \delta_{ik}\epsilon\eta | \phi_j \rangle - \delta_{ij}) + \mathscr{O}(\epsilon^2) \end{aligned} \tag{3.10}$$

$$\begin{aligned} = \sum_i \langle \phi_i | \hat{h} | \phi_i \rangle + \frac{1}{2}\sum_i j \langle \phi_i\phi_j | \hat{u} | \phi_i\phi_j - \phi_j\phi_i \rangle + \epsilon \langle \eta | \hat{h} | \phi_k \rangle - \sum_{ij} \lambda_{ij}(\langle \phi_i | \phi_j \rangle - \delta_{ij}) \\ + \frac{1}{2}\epsilon \sum_i \langle \phi_i\eta | \hat{u} | \phi_i\phi_k \rangle - \frac{1}{2}\epsilon \sum_i \langle \phi_i\eta | \hat{u} | \phi_k\phi_i \rangle \\ + \frac{1}{2}\epsilon \sum_j \langle \eta\phi_j | \hat{u} | \phi_k\phi_j \rangle - \frac{1}{2}\epsilon \sum_j \langle \eta\phi_j | \hat{u} | \phi_j\phi_k \rangle \\ - \epsilon \sum_j \lambda_{jk} \langle \eta | \phi_j \rangle + \mathscr{O}(\epsilon^2) \end{aligned} \tag{3.11}$$

$$\begin{aligned} = \sum_i \langle \phi_i | \hat{h} | \phi_i \rangle + \frac{1}{2}\sum_i j \langle \phi_i\phi_j | \hat{u} | \phi_i\phi_j - \phi_j\phi_i \rangle - \sum_{ij} \lambda_{ij}(\langle \phi_i | \phi_j \rangle - \delta_{ij}) \\ + \epsilon \langle \eta | \hat{h} | \phi_k \rangle + \epsilon \sum_i \langle \eta\phi_i | \hat{u} | \phi_k\phi_i \rangle - \epsilon \sum_i \langle \eta\phi_i | \hat{u} | \phi_i\phi_k \rangle \\ - \epsilon \sum_j \lambda_{jk} \langle \eta | \phi_j \rangle + \mathscr{O}(\epsilon^2) \end{aligned} \tag{3.12}$$

Notice that the zeroth term, represented by the first line in Equation 3.12, is simply the original Lagrangian in Equation 3.4. We equate all the first-order terms to zero,

$$\langle \eta | \hat{h} | \phi_k \rangle + \sum_i \langle \eta\phi_i | \hat{u} | \phi_k\phi_i \rangle - \sum_i \langle \eta\phi_i | \hat{u} | \phi_i\phi_k \rangle - \sum_i \lambda_{ik} \langle \eta | \phi_i \rangle = 0. \tag{3.13}$$

This must be valid for any choice η, meaning

$$\hat{h} | \phi_k \rangle + \sum_i \langle \cdot\ \phi_i | \hat{u} | \phi_k\phi_i \rangle - \sum_i \langle \cdot\ \phi_i | \hat{u} | \phi_i\phi_k \rangle - \sum_i \lambda_{ik} | \phi_i \rangle = 0, \tag{3.14}$$

where $\langle \cdot\ \phi_1 | \hat{u} | \phi_2\phi_3 \rangle \in L_1^2$ is interpreted as an integral over only the second particle in the matrix element. We define,

$$\hat{v}_{\text{HF}} = \hat{v}_{\text{direct}} + \hat{v}_{\text{exchange}} = \sum_i \langle \cdot\ \phi_i | \hat{u} | \phi_k\phi_i \rangle - \sum_i \langle \cdot\ \phi_i | \hat{u} | \phi_i\phi_k \rangle \tag{3.15}$$

$$\hat{f} = \hat{h} + \hat{v}_{\text{HF}}, \tag{3.16}$$

and can then rewrite Equation 3.14 to

$$\hat{f}\left|\phi_i\right\rangle = \sum_j \lambda_{ij}\left|\phi_j\right\rangle, \tag{3.17}$$

which are the non-canonical Hartree-Fock equations.

It so happens that the Slater determinant $|\Phi\rangle$ is invariant under unitary transformation of the single particle functions. Consider

$$\tilde{\phi}_k = \sum_j C_k^j \phi_j, \tag{3.18}$$

where C is a unitary matrix. This implies that $\left|\tilde{\Phi}\right\rangle = \det(C)\left|\Phi\right\rangle$, is the same state and the energy must be the same as well. We choose a particular unitary transformation C, rotating the single particle functions in a certain manner so that $\lambda = CEC^H$, where $E_{jk} = \delta_{jk}\epsilon_k$ are the elements of a diagonal matrix (the eigenvalues of λ). This provides us with a new set of eigenvalue equations,

$$\hat{f}(\tilde{\phi}_1, \ldots, \tilde{\phi}_N)\left|\tilde{\phi}_i\right\rangle = \epsilon_i\left|\tilde{\phi}_i\right\rangle, \tag{3.19}$$

which are the canonical Hartree-Fock equations. From now on we will stick with these equations and suppress the tilde notations.

3.2 The Roothan-Hall Equations

In order to solve the Hartree-Fock equations (Equation 3.19) we render the equations in a finite, fixed basis $\{\chi_p\}_{p=1}^L$ of a finite size L. It is not a necessity for this basis to be orthonormal, and we therefore define the overlap matrix,

$$S^\alpha_\beta \equiv \left\langle\chi_\alpha|\chi_\beta\right\rangle. \tag{3.20}$$

The Hartree-Fock single-particle functions are expanded in this basis,

$$\left|\phi_p\right\rangle = \sum_\alpha U_p^\alpha\left|\chi_\alpha\right\rangle, \tag{3.21}$$

where C is not necessarily unitary, because the basis is not necessarily orthongonal. However, we do have $C^H SC = 1$.

We insert the expansion from Equation 3.21 into the expression for the canonical Hartree-Fock equations from Equation 3.19,

$$\hat{f}\sum_\alpha C_p^\alpha\left|\chi_\alpha\right\rangle = \epsilon_p\sum_\alpha C_p^\alpha\left|\chi_\alpha\right\rangle \tag{3.22}$$

Then we left project with an arbitrary function from our new basis,

$$\begin{aligned}\left\langle\chi_\beta\right|\hat{f}\sum_\alpha U_p^\alpha\left|\chi_\alpha\right\rangle &= \epsilon_\alpha\left\langle\chi_\beta|\chi_\alpha\right\rangle\sum_r C_p^\alpha \\ \sum_\alpha f^\beta_\alpha C_p^\alpha &= \epsilon_p\sum_\alpha S^\beta_\alpha C_p^\alpha \\ F(D)C &= SC\epsilon.\end{aligned} \tag{3.23}$$

where the last line is the Roothan-Hall equations.

Elaborating on the computation of the Fock matrix element,

$$f^\alpha_\beta = \left\langle\chi_\alpha\right|\hat{f}\left|\chi_\beta\right\rangle = \left\langle\chi_\alpha\right|\hat{h}\left|\chi_\beta\right\rangle + \left\langle\chi_\alpha\right|\hat{v}_{\text{direct}}\left|\chi_\beta\right\rangle - \left\langle\chi_\alpha\right|\hat{v}_{\text{exchange}}\left|\chi_\beta\right\rangle, \tag{3.24}$$

where

$$\begin{aligned}\langle\chi_\alpha|\,\hat{v}_{\text{direct}}\,|\chi_p\rangle &= \sum_j \langle\chi_\alpha\phi_j|\,\hat{u}\,|\chi_p\phi_j\rangle = \sum_{\beta'\alpha' j} U_j^{\alpha'}(U_{\beta'}^{j})^*\,\langle\chi_\alpha\chi_{\alpha'}|\,\hat{u}\,|\chi_p\chi_{\beta'}\rangle \\ &= \sum_{\beta'\alpha'} D_{\beta'}^{\alpha'}\,\langle\chi_\alpha\chi_{\alpha'}|\,\hat{u}\,|\chi_p\chi_{\beta'}\rangle\end{aligned} \tag{3.25}$$

$$\begin{aligned}\langle\chi_\alpha|\,\hat{v}_{\text{exchange}}\,|\chi_p\rangle &= \sum_j \langle\chi_\alpha\phi_j|\,\hat{u}\,|\phi_j\chi_p\rangle = \sum_{\beta'\alpha' j} U_j^{\alpha'}(U_{\beta'}^{j})^*\,\langle\chi_\alpha\chi_{\alpha'}|\,\hat{u}\,|\chi_{\beta'}\chi_p\rangle \\ &= \sum_{\beta'\alpha'} D_{\beta'}^{\alpha'}\,\langle\chi_\alpha\chi_{\alpha'}|\,\hat{u}\,|\chi_{\beta'}\chi_p\rangle\,,\end{aligned} \tag{3.26}$$

giving us,

$$f_\beta^\alpha = \langle\chi_\alpha|\,\hat{h}\,|\chi_\beta\rangle + \sum_{\beta'\alpha'} D_{\beta'}^{\alpha'}(\langle\chi_\alpha\chi_{\alpha'}|\,\hat{u}\,|\chi_\beta\chi_{\beta'}\rangle - \langle\chi_\alpha\chi_{\alpha'}|\,\hat{u}\,|\chi_{p'}\chi_\beta\rangle), \tag{3.27}$$

where $D = CC^H$, is the density matrix.

The benefit of the Roothan-Hall equations (Equation 3.21), is that they are represented by matrices, and therefore easy to implement on a computer. The Roothan-Hall equations are solved iteratively, starting from an initial guess for C. This guess can be used to compute the density matrix, $D^{(k)} = C^{(k)}(C^{(k)})^H$, where k denotes the kth iteration. The density matrix is used to compute the Fock matrix. This provides us with a general eigenvalue problem, from which a new C and ϵ can be found. This formula is then repeated until the the iterations converge. At this point we say that we have self-consitency in the mean field, and this method is usually called the method of self-constistent field (SCF) iterations.

3.3 Restricted Hartree-Fock Theory

Consider N electrons confined in a potential. To begin with we will assume that these are non-interacting, and can therefore be described by the one-body part of the Hamiltionian, only

$$\hat{h}(\mathbf{r}) = \hat{t}(\mathbf{r}) + \hat{v}(\mathbf{r}), \tag{3.28}$$

where $\hat{v}$ is potential set up by an atomic nucleus, or some other confining force. The one-body operators $\hat{h}$ does noe coupled to electron spin, so the spin-orbitals or single-particle eigenfunctions of $\hat{h}$ separate,

$$\phi_P(\mathbf{r},\sigma) = \varphi_p(\mathbf{r})\chi_\alpha(\sigma), \tag{3.29}$$

where $P = (p,\alpha)$ si the combined spin- and spatial index, $\alpha = \pm 1/2$ is the value of the projection of the electron spin along the z-axis. The spin index/coordinate can only take values $\sigma \pm 1$, and we have orthonormal spinorbitals, $\langle\chi_\alpha|\chi_\beta\rangle = \delta_{\alpha\beta}$.

We restrict the orbitals to have the same spatial wavefunction for spin up and spin down, and we consider only closed-shell configurations. This means that our molecular wavefunctions, in the form of a Slater determinant, can only have an even number of N electrons, with all electrons paired in such a manner that there are two spin values for each of the $n = N/2$ spatial orbitals. The N-electron ground state of $\hat{h}$ is given by the first N eigenfunctions $\phi_{(p,\sigma)}$ occupied,

$$|\Phi\rangle = \left|\phi_{1,+}\phi_{1,-}\dots\phi_{\frac{N}{2},+}\phi_{\frac{N}{2},-}\right\rangle, \tag{3.30}$$

commonly also written as

$$|\Phi\rangle_{\text{RHF}} = |\varphi_1\bar{\varphi}_1\dots\varphi_{N/2}\bar{\varphi}_{N/2}\rangle\,. \tag{3.31}$$

The reasoning behind this restriction is that one would assume, for many systems, that the exact wavefunctions has the same kind of structure. This is true for almost all electronic systems in nature. We therefore do not optimise all the N single-particle functions freely, but asume that they form sets of doubly occupied spatial orbitals. Matrix elements can now be computed more easily on the restricted form,

$$\langle\phi_{(p,\alpha)}|\hat{h}|\phi_{(q,\beta)}\rangle = \langle\chi_\alpha|\chi_\beta\rangle \int d\mathbf{r}\varphi_p(\mathbf{r})^*\hat{h}\varphi_q(\mathbf{r}). \tag{3.32}$$

And similarly for two-body operators,

$$\langle\phi_{p\alpha}\phi_{q\beta}|\hat{u}|\phi_{r\gamma}\phi_{s\delta}\rangle = \langle\chi_\alpha|\chi_\gamma\rangle\langle\chi_\beta|\chi_\delta\rangle \int\int d\mathbf{r}_1 d\mathbf{r}_2\varphi_p(\mathbf{r}_1)\varphi_q(\mathbf{r}_2)\hat{u}(\mathbf{r}_1\mathbf{r}_2)\varphi_r(\mathbf{r}_1)\varphi_s(\mathbf{r}_2). \tag{3.33}$$

Now we will find the special form of the Fock operator in restricted Hartree-Fock theory. First we insert the wavefunction restriction into the Hartree-Fock equation

$$\begin{aligned} \hat{f}\phi_I(\mathbf{r},\sigma) &= \epsilon_i\phi_I(\mathbf{r},\sigma) \\ \hat{f}\varphi_i(\mathbf{r})\chi_\alpha(\sigma) &= \epsilon_i\varphi_i(\mathbf{r})\chi_\alpha(\sigma). \end{aligned} \tag{3.34}$$

Here we have joined the spatial- and spin index with a capital letter $I = (i,\alpha)$. We left multipy with χ_α^*, suppress indices for brevity and integrate over spin,

$$\langle\chi_\alpha|\hat{f}|\varphi_i\chi_\alpha\rangle = \left\langle\chi_\alpha\middle|\hat{f}\middle|\phi_{I=(i,\alpha)}\right\rangle = \epsilon_i\varphi_i. \tag{3.35}$$

Next we insert the Fock operator,

$$\hat{f} = \hat{h} + \sum_i \langle\cdot\varphi_i|\hat{u}|\cdot\varphi_i\rangle_{\text{AS}}$$

This special notation is means that we integrate over the second orbital in the bra and ket only. After insertion we get

$$\begin{aligned} \langle\chi_\alpha|\hat{h}|\chi_\alpha\rangle\varphi_i + \sum_J \langle\chi_\alpha\phi_J|\hat{u}|\phi_I\phi_J\rangle_{\text{AS}} &= \epsilon_i\varphi_i \\ \to \hat{h}\varphi_i + \sum_J \langle\chi_\alpha\phi_J|\hat{u}|\phi_I\phi_J\rangle - \sum_J \langle\chi_\alpha\phi_J|\hat{u}|\phi_J\phi_I\rangle &= \epsilon_i\varphi_i. \end{aligned} \tag{3.36}$$

Because we have a closed-shell system, the sum over occupied spinorbitals include an equal sum over spin up and spin down functions so that

$$\sum_J^n = \sum_\beta \sum_j^{n/2}.$$

We next insert this into our eigenvalue equation and split the single-particle functions into separate spin- and spatial orbitals,

$$\begin{aligned} \hat{h}\varphi_i + \sum_\beta\sum_j^{n/2} \langle\chi_\alpha\varphi_j\chi_\beta|\hat{u}|\varphi_i\chi_\alpha\varphi_j\chi_\beta\rangle - \sum_\beta\sum_j^{n/2} \langle\chi_\alpha\varphi_j\chi_\beta|\hat{u}|\varphi_j\chi_\beta\varphi_i\chi_\alpha\rangle \\ = \hat{h}\varphi_i + 2\sum_j^{n/2} \langle\cdot\varphi_j|\hat{u}|\varphi_i\varphi_j\rangle + \sum_j^{n/2} \langle\cdot\varphi_j|\hat{u}|\varphi_j\varphi_i\rangle = \epsilon_i\varphi_i. \end{aligned} \tag{3.37}$$

We now have the form of the Fock operator within the restricted Hartree-Fock theory,

$$\begin{aligned}\hat{f} &= \hat{h} + \sum_{i}^{n/2} \langle \cdot\varphi_i | (2\hat{u} - \hat{P}_{12}) | \cdot\varphi_i \rangle \\ &= \hat{h} + 2\sum_{i}^{n/2} \int d\mathbf{r}_2 \varphi_i^*(\mathbf{r}_2)\hat{u}\varphi_i(\mathbf{r}_2) - \sum_{i}^{n/2} \int d\mathbf{r}_2 \varphi_i^*(\mathbf{r}_2)\hat{u}\varphi_j(\mathbf{r}_2)\end{aligned} \tag{3.38}$$

The Hartree-Fock energy also has a special form in the restricted Hartree-Fock domain,

$$\begin{aligned}\langle \Phi | \hat{H} | \Phi \rangle =& \sum_P \langle \phi_P | \hat{h} | \phi_P \rangle + \frac{1}{2} \sum_P \sum_Q \langle \phi_P \phi_Q | \hat{u} | \phi_P \phi_Q \rangle_{\mathrm{AS}} \\ =& \sum_\alpha \sum_p^{n/2} \left\langle \phi_{(p,\alpha)} \right| \hat{h} \left| \phi_{(p,\alpha)} \right\rangle \\ &+ \sum_\alpha \sum_p^{n/2} \sum_\beta \sum_q^{n/2} \left\langle \phi_{(p,\alpha)} \phi_{(q,\beta)} \right| \hat{u} \left(\left| \phi_{(p,\alpha)} \phi_{(q,\beta)} \right\rangle - \left| \phi_{(q,\beta)} \phi_{(p,\alpha)} \right\rangle \right) \\ =& 2\sum_p^{n/2} \langle \varphi_p | \hat{h} | \varphi_q \rangle + 2\sum_{pq}^{n/2} \langle \varphi_p \varphi_q | \hat{u} | \varphi_p \varphi_q \rangle - \sum_{pq}^{n/2} \langle \varphi_p \varphi_q | \hat{u} | \varphi_p \varphi_q \rangle\end{aligned} \tag{3.39}$$

3.4 Unrestricted Hartree-Fock Theory

The restricted Hartree-Fock model i often a good enough approximation, but under some circumstances it will fail to provide a good result. The unrestricted Hartree-Fock model is an intermediate between the general Hartree-Fock model and the restricted Hatree-Fock model. Compared with the restricted Hartre-Fock single-particle wavefunction form, what we do in unrestricted form is somewhat obvious - we now allow the spins to be different,

$$\phi_P(\mathbf{r}, \sigma) = \varphi_p^\alpha(\mathbf{r})\chi_\alpha(\sigma), \tag{3.40}$$

where we have given the spatial orbitals a spin-index as well. As before, a capital index is the combined spatial- and spin index $P = (p, \alpha)$, where $P \in [1, L]$, $p \in [1, L/2]$ and $\alpha = \pm 1/2$. Like before, we require the states to be orthonormal

$$\langle \phi_P | \phi_Q \rangle = \left\langle \varphi_p^\alpha \middle| \varphi_q^\beta \right\rangle \langle \chi_\alpha | \chi_\beta \rangle = \delta_{PQ}. \tag{3.41}$$

We can write a general unrestricted Hartree-Fock state as

$$|\Phi\rangle_{\mathrm{UHF}} = |\varphi_1^{1/2}\varphi_1^{-1/2}\varphi_2^{1/2}\varphi_2^{-1/2} \dots \varphi_{L/2}^{1/2}\varphi_{L/2}^{-1/2}\rangle = |\phi_1\phi_2\phi_3\phi_4 \dots \phi_{L-1}\phi_L\rangle\,. \tag{3.42}$$

In order to find an expression for the Fock operator we insert the wavefunction into the canonical Hartree-Fock equation,

$$\hat{f}\phi_P = \epsilon_p\phi_P, \;\rightarrow\; \hat{f}\varphi_p^\alpha\chi_\alpha = \epsilon_p\varphi_p^\alpha\chi_\alpha. \tag{3.43}$$

Now we left multiply by χ_α^* and itegrate over spin,

$$\left\langle \chi_\alpha \middle| \hat{f} \middle| \varphi_p^\alpha \chi_\alpha \right\rangle = \left\langle \chi_\alpha \middle| \epsilon_p \middle| \varphi_p^\alpha \chi_\alpha \right\rangle \tag{3.44}$$

$$\hat{f}^\alpha \varphi_p^\alpha = \left[\int d\sigma_1 \chi_\alpha(\sigma_1)^* \hat{f}(\mathbf{r}, \sigma_1)\chi_\alpha(\sigma_1) \right] \varphi_p^\alpha = \epsilon_p \varphi_p^\alpha. \tag{3.45}$$

We now have what is called the spatial unrestricted Hartree-Fock equations. Inserting for the canonical Fock operator yields the following left-hand side

$$
\begin{aligned}
\hat{f}^{\alpha}\varphi_p^{\alpha} =& \hat{h}\varphi_p^{\alpha} + \sum_{Q}^{L} \left\langle \chi_\alpha \phi_Q \middle| \hat{u} \middle| \varphi_p^{\alpha}\chi_\alpha\phi_Q \right\rangle q - \sum_{Q}^{L} \left\langle \chi_\alpha \phi_Q \middle| \hat{u} \middle| \phi_Q \varphi_p^{\alpha}\chi_\alpha \right\rangle \\
=& \hat{h}\varphi_p^{\alpha} + \sum_{\beta}\sum_{q}^{L/2} \left\langle \chi_\alpha \varphi_q^{\beta}\chi_\beta \middle| \hat{u} \middle| \varphi_p^{\alpha}\chi_\alpha\varphi_q^{\beta}\chi_\beta \right\rangle \\
& - \sum_{\beta}\sum_{q}^{L/2} \left\langle \chi_\alpha \varphi_q^{\beta}\chi_\beta \middle| \hat{u} \middle| \varphi_q^{\beta}\chi_\beta\varphi_p^{\alpha}\chi_\alpha \right\rangle \\
=& \hat{h}\varphi_p^{\alpha} + \sum_{\beta}\sum_{q}^{L/2} \left\langle \cdot\varphi_q^{\beta} \middle| \hat{u} \middle| \cdot\varphi_q^{\beta} \right\rangle \varphi_p^{\alpha} - \sum_{q}^{L/2} \left\langle \cdot\varphi_q^{\alpha} \middle| \hat{u} \middle| \cdot\varphi_p^{\alpha} \right\rangle \varphi_q^{\beta}
\end{aligned}
\tag{3.46}
$$

This means that we get the following form for the spatial Fock operators in unrestricted Hartree-Fock

$$
\hat{f}^{\uparrow} = \hat{h} + \sum_{p}^{L/2}[\hat{v}^{\uparrow}_{\text{Coulomb}} - \hat{v}^{\uparrow}_{\text{exchange}}] + \sum_{p}^{L/2}\hat{v}^{\downarrow}_{\text{Coulomb}} \tag{3.47}
$$

$$
\hat{f}^{\downarrow} = \hat{h} + \sum_{p}^{L/2}[\hat{v}^{\downarrow}_{\text{Coulomb}} - \hat{v}^{\downarrow}_{\text{exchange}}] + \sum_{p}^{L/2}\hat{v}^{\uparrow}_{\text{Coulomb}} \tag{3.48}
$$

From the definition of the two spatial Fock operators in Equation 3.47 and Equation 3.48, we see that the two integro-differential eigenvalue equations that arises from inserting $\hat{f}^{\uparrow}$ and $\hat{f}^{\downarrow}$ into the canonical Hartree-Fock equation,

$$
\hat{f}^{\uparrow}\varphi_p^{\uparrow} = \epsilon_p^{\uparrow}\varphi_p^{\uparrow} \tag{3.49}
$$

$$
\hat{f}^{\downarrow}\varphi_p^{\downarrow} = \epsilon_p^{\downarrow}\varphi_p^{\downarrow}, \tag{3.50}
$$

are coupled and cannot be solved independently. The spin-up orbitals depend on the occupied spin-down orbitals and vice versa. This means that the two equations must be solved by a simultaneous iterative process.

We can also derive an equation for the unrestricted Hartree-Fock energy,

$$
\begin{aligned}
E_{UHF} =& \langle \Phi_{\text{UHF}} | \hat{H} | \Phi_{\text{UHF}} \rangle \\
=& \sum_{\alpha}\sum_{p}^{L/2} \left\langle \varphi_p^{\alpha}\chi_\alpha \middle| \hat{h} \middle| \varphi_p^{\alpha}\chi_\alpha \right\rangle + \sum_{\alpha}\sum_{p}^{L/2}\sum_{\beta}\sum_{q}^{L/2} \left\langle \varphi_p^{\alpha}\chi_\alpha\varphi_q^{\beta}\chi_\beta \middle| \hat{u} \middle| \varphi_p^{\alpha}\chi_\alpha\varphi_q^{\beta}\chi_\beta \right\rangle_{\text{AS}} \\
=& \sum_{\alpha}\sum_{pq}^{L/2} \left\langle \varphi_p^{\alpha} \middle| \hat{h} \middle| \varphi_p^{\alpha} \right\rangle + \sum_{\alpha\beta}\sum_{q}^{L/2} \left\langle \varphi_p^{\alpha}\varphi_q^{\beta} \middle| \hat{u} \middle| \varphi_p^{\alpha}\varphi_q^{\beta} \right\rangle - \sum_{\alpha}\sum_{pq}^{L/2} \left\langle \varphi_p^{\alpha}\varphi_q^{\alpha} \middle| \hat{u} \middle| \varphi_q^{\alpha}\varphi_p^{\alpha} \right\rangle
\end{aligned}
\tag{3.51}
$$

If we were to expand the unrestricted Hartree-Fock equations, Equation 3.49 and Equation 3.50, in a basis like we did in section 3.2, we would get the Pople-Nesbet-Bethier equations[6, 62].

3.5 Time-Dependent Hartree-Fock

This section follows closely the narrative of Hochstuhl, Hinz, and Bonitz[37]. Deriving the time-dependent Hartree-Fock equations start, of course, with the time-dependent Schrödinger equation,

$$i\hbar\frac{\partial}{\partial t}\left|\Phi(t)\right\rangle = \hat{H}(t)\left|\Phi(t)\right\rangle, \tag{3.52}$$

where the Hamiltonian is

$$\hat{H}(t) = \hat{h}(t) + \hat{u}(t). \tag{3.53}$$

This is the same Hamiltonian that we started with in this chapter (Equation 3.1), except for the introduction of a time-dependence. We start by multiplying from the left with the reference Slater determinant $\langle\Phi|$. The right-hand side of the Schrödinger equation becomes the familiar Hartree-Fock energy,

$$\langle\Phi|\hat{H}|\Phi\rangle = \sum_p \langle\phi_p|\hat{h}|\phi_p\rangle + \frac{1}{2}\sum_{pq}\langle\phi_p\phi_q|\hat{u}|\phi_p\phi_q\rangle_{\text{AS}}. \tag{3.54}$$

The left-hand side, is more interesting,

$$\langle\Phi|\frac{\partial}{\partial t}|\Phi\rangle = \sum_p \langle\phi_p|\frac{\partial}{\partial t}|\phi_p\rangle, \tag{3.55}$$

which we will deal with in due time, but before doing so we need to introduce functional derivatives and the functional derivatives of various matrix elements. First, the one-body matrix elements,

$$\frac{\delta}{\delta\phi_r^*}\sum_p\langle\phi_p|\hat{h}|\phi_p\rangle = \sum_p\frac{\delta}{\delta\phi_r^*}\int dr\phi_p^*\hat{h}\phi_p = \sum_p \delta_{pr}\hat{\phi} = \hat{h}\left|\phi_r\right\rangle. \tag{3.56}$$

Second, the matrix elements of the time-derivative,

$$\frac{\delta}{\delta\phi_r^*}\sum_p\langle\phi_p|\frac{\partial}{\partial t}|\phi_p\rangle = \frac{\partial}{\partial t}\left|\phi_q\right\rangle, \tag{3.57}$$

which is so similar to the one-body computation that the result is simply written down, instead of computing the result explicitly. Lastly, we have the two-body matrix elements,

$$\begin{aligned}
&\frac{\delta}{\delta\phi_r^*}\sum_{pq}\langle\phi_p\phi_q|\hat{u}|\phi_p\phi_q\rangle_{\text{AS}} \\
&\quad= \frac{\delta}{\delta\phi_r^*(r_1)}\sum_{pq}\int dr_1dr_2\phi_p^*(r_1)\phi_q^*(r_2)\hat{u}[\phi_p(r_1)\phi_q(r_2) - \phi_q(r_1)\phi_p(r_2)] \\
&\quad= \sum_{pq}\delta_{pq}\int dr_2\phi_q^*(r_2)\hat{u}[\phi_p(r_1)\phi_q(r_2) - \phi_q(r_1)\phi_p(r_2)] = \sum_q\langle\cdot\phi_q|\hat{u}|\phi_r\phi_q\rangle_{\text{AS}}.
\end{aligned} \tag{3.58}$$

Now we want to vary the reference state to find the optimal one, applying the so-called time-dependent variational principle[14],

$$\langle\delta\Phi|(\hat{H} - i\hbar\frac{\partial}{\partial t})|\Phi\rangle = 0, \tag{3.59}$$

which we want to minimise under the requirement of orthonormal single-particle functions in time,

$$\langle\phi_p(t)|\phi_q(t)\rangle = \delta_{pq}. \tag{3.60}$$

Such an optimization problem under a constraint begs the formulation of a Lagrangian, which we will allow to manifest,

$$\mathscr{L}(\Phi,\lambda_{pq}) = \langle\Phi|(\hat{H} - i\hbar\frac{\partial}{\partial t})|\Phi\rangle - \sum_{pq}\lambda_{pq}(\langle\phi_p|\phi_q\rangle - \delta_{pq}). \tag{3.61}$$

We find a stationary point of this Lagrangian functional, by variation of the single-particle functions so that

$$\frac{\delta \mathscr{L}}{\delta \phi_r^*} = 0, \quad \forall r. \tag{3.62}$$

This is where we will make use of the functional derivatives we computed before,

$$\frac{\delta \mathscr{L}}{\delta \phi_r^*} = \hat{h} \left| \phi_r \right\rangle + \sum_q \left\langle \cdot \phi_q \right| \hat{u} \left| \phi_r \phi_q \right\rangle_{\text{AS}} - i\hbar \frac{\partial}{\partial t} \left| \phi_r \right\rangle - \sum_q \lambda_{rq} \left| \phi_r \right\rangle = 0. \tag{3.63}$$

Now we want to solve for the Langrange mulitplier, we do this by left-projection of the functional derivative above with $\langle \phi_s |$ and move the resulting multiplier λ_{sq} to the left, and all other terms to the right. We get the following expression for the Lagrange multiplier,

$$\lambda_{sq} = \left\langle \phi_s \right| \hat{h} \left| \phi_r \right\rangle + \left\langle \phi_s \phi_q \right| \hat{u} \left| \phi_r \phi_q \right\rangle_{\text{AS}} - i\hbar \left\langle \phi_s \right| \frac{\partial}{\partial t} \left| \phi_r \right\rangle \tag{3.64}$$

We insert this expression for the Lagrange multiplier into Equation 3.63 which results in,

$$\hat{P} \left[\hat{h} \left| \phi_r \right\rangle + \sum_q \left\langle \cdot \phi_q \right| \hat{u} \left| \phi_r \phi_q \right\rangle_{\text{AS}} - i\hbar \frac{\partial}{\partial t} \left| \phi_k \right\rangle \right] = 0, \tag{3.65}$$

where we have introduced the projection operator $\hat{P}$,

$$\hat{P} = \hat{1} - \sum_p \left| \phi_p \right\rangle\!\left\langle \phi_p \right| . \tag{3.66}$$

Rearranging Equation 3.65 yields

$$i\hbar \hat{P} \frac{\partial}{\partial t} \left| \phi_r \right\rangle = \hat{P} \left[\hat{h} \left| \phi_r \right\rangle + \left\langle \cdot \phi_q \right| \hat{u} \left| \cdot \phi_q \right\rangle \right] \left| \phi_r \right\rangle_{\text{AS}} = \hat{P} \hat{f} \left| \phi_r \right\rangle , \tag{3.67}$$

where we see that Fock operator has appeared. This equation is an integro-differential equation, as the projection operator $\hat{P}$ appear on both sides of the equality sign, and a solution can be difficult to find. Because the time-dependent Hartree-Fock wavefunction is invariant under unitary transformation, we can obtain equations that are numerically more apporiate, by applying a unitary transformation $\hat{Q}(t)$ which satisfies

$$i\hbar \left\langle \phi_p \right| \frac{\partial}{\partial t} \left| \phi_q \right\rangle \equiv \left\langle \phi_p \right| \hat{Q}(t) \left| \phi_q \right\rangle . \tag{3.68}$$

It turns out that a reasonable choice for $\hat{Q}(t)$ is $\hat{f}(t)$, in which case Equation 3.67 becomes

$$i\hbar \frac{\partial}{\partial t} \left| \phi_p(t) \right\rangle = \hat{f}(t) \left| \phi_p(t) \right\rangle , \tag{3.69}$$

where we have explicitly written out the time-dependence. This is the time-dependent Hartree-Fock equation.

Now we pick a specific, finite and static basis $\{\chi_p\}_{p=1}^{L}$ and expand the Hartree-Fock single-particle functions in this basis,

$$\left| \phi_p(t) \right\rangle = \sum_\alpha C_p^\alpha(t) \left| \chi_\alpha \right\rangle . \tag{3.70}$$

Notice that the basis set is indeed static, with no time-dependence, only the coefficients of the expansions $U_p^\alpha(t)$ evolve in time. We insert the expansion into Equation 3.69,

$$i\hbar \frac{\partial}{\partial} \sum_\alpha C_p^\alpha \left| \chi_\alpha \right\rangle = \hat{f}(t) \sum_\alpha C_p^\alpha \left| \chi_\alpha \right\rangle . \tag{3.71}$$

We left-project this equation with $\langle \chi_\beta |$,

$$\begin{aligned} i\hbar \frac{\partial}{\partial t} \sum_\alpha C_p^\alpha(t) \langle \chi_\beta | \chi_\alpha \rangle &= \sum_\alpha C_p^\alpha(t) \langle \chi_\beta | \hat{f}(t) | \chi_\alpha \rangle \\ \rightarrow i\hbar \sum_\alpha \dot{C}_p^\alpha S_\alpha^\beta &= \sum_\alpha C_p^\alpha \hat{f}_\alpha^\beta(t), \end{aligned} \tag{3.72}$$

which can be written as a matrix equation,

$$i\hbar \mathbf{S}\dot{\mathbf{C}}(t) = \mathbf{F}(t)\mathbf{C}(t). \tag{3.73}$$

Chapter 4

Perturbation Theory

Perturbation theory is a very powerful method and a generic method applicable to all matrix problems. Additionally, perturbation theory is relatively cheap in terms of computing time, especially compared with coupled cluster theory. The method provides a different route to the solution of the Schrödinger equation, by approaching the exact solution systematically, based on an order-by-order expansion of the energy and wavefunction. Therefore, perturbation theory is often used to improve the results from other computational schemes. What is more, the exponential form of the wavefunction in coupled cluster theory stems from the non-degenerate Rayleigh-Schrödinger perturbation theory (RSPT) expansion.

4.1 Formal perturbation theory

We split the Hamiltonian into a known part and a perturbed part,

$$\hat{H} = \hat{H}_0 + \hat{V}. \tag{4.1}$$

Sometimes it is convenient to write

$$\hat{H} = \hat{H}_0 + \lambda\hat{V}, \tag{4.2}$$

where we have included an "order parameter" λ. This parameter is used to categorise the contributions of different order. The exact solution is given by

$$\begin{aligned} \hat{H}\Psi_n &= E_n\Psi_n \\ (\hat{H}_0 + \hat{V})\Psi_n &= E_n\Psi_n, \quad \Psi_n = \Phi_n + \chi_n, \end{aligned} \tag{4.3}$$

while the solvable and simple zero order problem is given by

$$\hat{H}_0\Phi_n = E_n^{(0)}\Phi_n. \tag{4.4}$$

The set $\{\Phi_n\}$ is assumed to be an orthonormal basis for the Hilbert space. The excat wavefunction Ψ_n is split into a zero-order part Φ_n and the perturbative part χ_n.

By projecting Equation 4.3 with $\langle\Phi_0|$ we get

$$\begin{aligned} \langle\Phi_n|\hat{H}_0|\Psi_n\rangle + \langle\Phi_n|\hat{V}|\Psi_n\rangle &= E_n\langle\Phi_n|\Psi_n\rangle \\ \rightarrow E_n &= \langle\Phi_n|\hat{H}|\Psi_n\rangle \\ \rightarrow \Delta E_n = E_n - E_n^0 &= \langle\Phi_n|\hat{V}|\Psi_n\rangle \end{aligned} \tag{4.5}$$

where we have used that

$$\langle \Phi_m | \Phi_n \rangle = \delta_{mn}, \tag{4.6}$$
$$\langle \Psi_n | \Phi_n \rangle = \langle \Phi_n + \chi_n | \Phi_n \rangle = 1, \tag{4.7}$$
$$\langle \Psi_n | \Psi_n \rangle = 1 + \langle \chi_n | \chi_n \rangle . \tag{4.8}$$

This is called the intermediate normalisation assumption.

4.1.1 Energy- and Wavefunction Expansion

We now have need for the order parameter from λ Equation 4.2 as we expand the wavefunction and energy,

$$\begin{aligned} \Psi_n &= \Phi_n + \chi_n = \Psi_n^{(0)} + \lambda \Psi_n^{(1)} + \lambda^2 \Psi_n^{(2)} + \dots \quad (\Psi_n^{(0)} \equiv \Phi_n) \\ E_n &= E_n^{(0)} + \Delta E_n = E_n^{(0)} + \lambda E_n^{(1)} + \lambda^2 E_n^{(2)} + \dots \end{aligned} \tag{4.9}$$

We insert these expansions into the Schrödinger equation,

$$\begin{aligned} (\hat{H} - E_n)\Psi_n &= 0 \\ (\hat{H}_0 + \lambda \hat{V})\Psi_n &= 0, \end{aligned} \tag{4.10}$$

resulting in

$$(\hat{H}_0 + \lambda \hat{V} - E_n^{(0)} - \lambda E_n^{(1)} - \lambda^2 E_n^{(2)} - \dots)(\Psi_n^{(0)} + \lambda \Psi_n^{(1)} + \lambda \Psi_n^{(2)} + \dots) = 0. \tag{4.11}$$

Now we gather the coefficients of different powers of λ,

$$(\hat{H}_0 - E_n^{(0)})\Psi_n^{(0)} = 0 \tag{4.12}$$
$$(\hat{H}_0 - E_n^{(0)})\Psi_n^{(1)} = (E_n^{(1)} - \hat{V})\Psi_n^{(0)} \tag{4.13}$$
$$(\hat{H}_0 - E_n^{(0)})\Psi_n^{(2)} = (E_n^{(1)} - \hat{V})\Psi_n^{(1)} + E_n^{(2)}\Psi_n^{(0)} \tag{4.14}$$
$$\dots$$
$$(\hat{H}_0 - E_n^{(0)})\Psi_n^{(m)} = (E_n^{(1)} - \hat{V})\Psi_n^{(m-1)} + \sum_{l=0}^{m-2} E_n^{(m-l)}\Psi_n^{(l)}. \tag{4.15}$$

Where the last line gives a general mth-order equation. This equation can be simplified somewhat,

$$(E_n^{(0)} - \hat{H}_0)\Psi_n^{(m)} = \hat{V}\Psi_n^{(m-1)} - \sum_{l=0}^{m-1} E_n^{(m-l)}\Psi_n^{(l)}. \tag{4.16}$$

By applying $\langle \Phi_n |$ to each of the equations, we get expressions for $E_n^{(m)}$. For λ^1 (Equation 4.13) we get,

$$\begin{aligned} \langle \Phi_n | \hat{H}_0 - E_n^{(0)} \left| \Psi_n^{(1)} \right\rangle &= \langle \Phi_n | E_n^{(1)} - \hat{V} | \Phi_n \rangle \\ \left\langle (\hat{H}_0 - E_n^{(0)})\Phi_n \middle| \Psi_n^{(1)} \right\rangle &= \langle \Phi_n | E_n^{(1)} - \hat{V} | \Phi_n \rangle \\ \rightarrow E_n^{(1)} &= \langle \Phi_n | \hat{V} | \Phi_n \rangle = \hat{V}_{nn}. \end{aligned} \tag{4.17}$$

Since we have an expression for $E_n^{(1)}$, we can solve the inhomogeneous differential equation for $\Psi_n^{(1)}$, by also requiring the intermediate normalisation condition $\left\langle \Phi_n \middle| \Psi_n^{(1)} \right\rangle = 0$. For the general mth-order expression (Equation 4.15),

$$\begin{aligned} \langle \Phi_n | E_n^0 - \hat{H}_0 \left| \Psi_n^{(m)} \right\rangle &= \langle \Phi_n | \hat{V} \left| \Psi_n^{(m-1)} \right\rangle - \sum_{l=0}^{m-1} E_n^{(m-l)} \left\langle \Phi_n \middle| \Psi_n^{(l)} \right\rangle \\ E_n^{(m)} = \left\langle \Phi_n^{(m)} \right| &= \langle \Phi_n | \hat{V} \left| \Psi_n^{(m-1)} \right\rangle . \end{aligned} \tag{4.18}$$

In principle, we can obtain every next-order energy contribution $E_n^{(m)}$ from the previous-order wavefunctions $\Psi_n^{(m-1)}$ and then solve for $\Psi_n^{(m)}$.

4.1.2 Projection Operators

We define the projection operators, $\hat{P}$ and $\hat{Q}$, in terms of the zero-order wavefunctions,

$$\begin{aligned} \hat{P} &= |\Phi_0\rangle\langle\Phi_0| \\ \hat{Q} &= \hat{1} - \hat{P} = \sum_{i=1}^{N} |\Phi_i\rangle\langle\Phi_i| . \end{aligned} \tag{4.19}$$

The projecton operators have the following convenient properties,

$$\begin{gathered} \hat{P}^2 = |\Phi_0\rangle\langle\Phi_0|\Phi_0\rangle\langle\Phi_0| = |\Phi_0\rangle\langle\Phi_0| = \hat{P} \\ \hat{Q}^2 = (1-\hat{P})^2 = \hat{1} - \hat{P} - \hat{P} + \hat{P} = \hat{1} - \hat{P} = \hat{Q} \\ \hat{P}\hat{Q} = \hat{Q}\hat{P} = 0 \\ [\hat{P}, \hat{H}_0] = [\hat{Q}, \hat{H}_0] = 0 \end{gathered} \tag{4.20}$$

If we write the wavefunction as a linear expansion in terms of Φ_i,

$$\Phi = \sum_i a_i \Phi_i, \tag{4.21}$$

acting on it with the projection operators yields

$$\hat{P}\Psi = \sum_i a_i |\Phi_0\rangle\langle\Phi_0|\Phi_i\rangle = \sum_i a_i |\Phi_0\rangle \delta_{0i} = a_0\Phi_0. \tag{4.22}$$

For sake of specificity, the operator $\hat{P}$ will extract Φ_0 from Ψ, while $\hat{Q}$ annihilates Φ_0,

$$\hat{Q}\Psi = (\hat{1} - \hat{P})\Psi = \Psi - a_0\Phi_0 = \sum_{i=1}^{N} a_i\Phi_i, \tag{4.23}$$

meaning we can write

$$\Psi = \hat{P}\Psi + \hat{Q}\Psi. \tag{4.24}$$

4.1.3 The Resolvent

Now follows what some considers a more elegant derivation of the perturbation equations, including the introduction of the *resolvent* of the unperturbed part of the Hamiltonian $\hat{H}_0$.

Starting from a rearrangment of the Schrödinger equation,

$$\begin{aligned} (\hat{H}_0 + \hat{V})\Psi &= E\Psi, \\ \to -\hat{H}_0\Phi &= (\hat{V} - E)\Psi, \end{aligned} \tag{4.25}$$

we introduce a seemingly arbitrary parameter ζ, the purpose of which will be apperent later. This parameter is introduced by adding $\zeta\Phi$ to both sides,

$$(\zeta - \hat{H}_0)\Phi = (\hat{V} - E + \zeta)\Phi. \tag{4.26}$$

Next, we apply $\hat{Q}$ to both sides,

$$\hat{Q}(\zeta - \hat{H}_0)\Psi = \hat{Q}(\hat{V} - E + \zeta)\Psi. \tag{4.27}$$

The right-hand side of this expression can be rewritten as,

$$\begin{aligned}\hat{Q}(\zeta-\hat{H}_0)\Psi &= \hat{Q}^2(\zeta-\hat{H}_0) = \hat{Q}(\zeta-\hat{H}_0)\hat{Q}\Psi \\ &= \sum_{i\neq 0}\sum_{j\neq 0} |\Phi_i\rangle \langle\Phi_i| \zeta - \hat{H}_0 |\Phi_j\rangle \langle\Phi_j| ,\end{aligned} \tag{4.28}$$

Equation 4.27 is now

$$\hat{Q}(\zeta-\hat{H}_0)\hat{Q}\Psi = \hat{Q}(\hat{V}-E+\zeta)\Psi. \tag{4.29}$$

By restricting to choice of ζ, so they do not coincide with the eigenvalues of $\hat{H}_0$ in $\hat{Q}$-space, i.e. $\{\Phi_i|i\neq 0\}$, we ensure that the inverse of $\hat{Q}(\zeta-\hat{H}_0)\hat{Q}$ exists. This inverse is the *resolvent* of $\hat{H}_0$,

$$\hat{R}_0(\zeta) = \frac{\hat{Q}}{\zeta-\hat{H}_0} \equiv \sum_{i\neq 0}\sum_{j\neq 0} |\Phi_i\rangle \langle\Phi_i| (\zeta-\hat{H}_0)^{-1} |\Phi_j\rangle \langle\Phi_j| . \tag{4.30}$$

The resolvent simplifies in the diagonal case to

$$\hat{R}_0(\zeta) = \sum_{i\neq 0} |\Phi_i\rangle \langle\Phi_i| (\zeta-E_j^{(0)})^{-1} |\Phi_j\rangle \langle\Phi_j| = \sum_{i\neq 0} \frac{|\Phi_i\rangle \langle\Phi_i|}{(\zeta-E_i^{(0)})}. \tag{4.31}$$

We can prove that $\hat{R}_0(\zeta)$ is the inverse of $\hat{Q}(\zeta-\hat{H}_0)\hat{Q}$ in $\hat{Q}$-space,

$$\begin{aligned}&\frac{\hat{Q}}{\zeta-\hat{H}_0}\hat{Q}(\zeta-\hat{H}_0)\hat{Q} \\ &\quad= \left(\sum_{i,j\neq 0} |\Phi_i\rangle \langle\Phi_i| (\zeta-\hat{H}_0)^{-1} |\Phi_j\rangle \langle\Phi_j|\right) \left(\sum_{k,l\neq 0} |\Phi_k\rangle \langle\Phi_k| (\zeta-\hat{H}_0) |\Phi_l\rangle \langle\Phi_l|\right) \\ &\quad= \sum_{i,l\neq 0} |\Phi_i\rangle \langle\Phi_i| (\zeta-\hat{H}_0)^{-1} \left(\sum_{j\neq 0} |\Phi_j\rangle \langle\Phi_j|\right) (\zeta-\hat{H}_0) |\Phi_l\rangle \langle\Phi_l| \\ &\quad= \sum_{i,l\neq 0} |\Phi_i\rangle \langle\Phi_i| (\zeta-\hat{H}_0)^{-1}(1-|\Phi_0\rangle \langle\Phi_0|)(\zeta-\hat{H}_0) |\Phi_l\rangle \langle\Phi_l| \\ &\quad= \sum_{i\neq 0} |\Phi_i\rangle \langle\Phi_i| = \hat{Q}.\end{aligned} \tag{4.32}$$

Applying the resolvent to both sides of Equation 4.29,

$$\begin{aligned}\hat{Q}\Psi &= \hat{R}_0(\zeta)(\hat{V}-E++\zeta)\Psi \\ \rightarrow \Psi &= \Phi_0 + \hat{R}_0(\zeta)(\hat{V}-E+\zeta)\Psi,\end{aligned} \tag{4.33}$$

which can be interpreted as a recursive relation for Ψ. Inserting the expression for Ψ into itself repeatedly, yields

$$\Psi = \sum_{m=0}^{\infty} [\hat{R}_0(\zeta)(\hat{V})-E+\zeta]^m \Phi_0. \tag{4.34}$$

We can find an expression for the perturbative energy correction by left-projecting this expression with $\langle\Phi_0| \hat{V}$,

$$\Delta E = \langle\Phi_0|\hat{V}|\Psi\rangle = \sum_{m=0}^{\infty} \langle\Phi_0|\Big[\hat{R}_0(\zeta)(\hat{V}-E+\zeta)\Big]^m |\Phi_0\rangle . \tag{4.35}$$

The problem with these equations is that E, which is unknown, appears on the right-hand side. One would also wonder what to do with ζ. There are two common choices for ζ that give rise to two important theories,

$$\zeta = E \leftarrow \text{Brillouin-Wigner Perturbation}$$
$$\zeta = E_0^{(0)} \rightarrow -E+\zeta = -\Delta E \leftarrow \text{Rayleigh-Schrödinger Perturbation.}$$

4.2 Brillouin-Wigner Perturbation Theory

By setting $\zeta = E$ in Equation 4.34 and Equation 4.35 we get Brilloun-Wigner perturbation theory[8, 76]. The wavefunction- and energy expression becomes the following,

$$\Psi = \sum_{m=0}^{\infty} [\hat{R}_0(E)\hat{V}]^m \Phi_0 \tag{4.36}$$
$$\Delta E = \sum_{m=0}^{\infty} \langle \Phi_0|\hat{V}[\hat{R}_0(E)\hat{V}]^m|\Phi_0\rangle . \tag{4.37}$$

Moreover, the resolvent is given by

$$\hat{R}_0 = \sum_i \frac{|\Phi_i\rangle\langle\Phi_i|}{E-E_i^{(0)}}. \tag{4.38}$$

As we can see, these equations are still implicit, i.e. E appears on the right-hand side. In order to compute corrections in the energy and wavefunctions estimates, we need an estimate for E. A common estimate for the first-order energy is $E_0^{(0)} + \langle\Phi_0|\hat{V}|\Phi_0\rangle$. From this we can continue computing the second-order energy,

$$\begin{aligned} E^{(2)} &= \langle\Phi_0|\hat{V}\hat{R}_0(E)\hat{V}|\Phi_0\rangle \\ &= \sum_i \frac{\langle\Phi_0|\hat{V}|\Phi_i\rangle\ \langle\Phi_i|\hat{V}|\Phi_0\rangle}{E-E_i^{(0)}} \\ &= \sum_i \frac{V_{0i}V_i0}{E-E_i^{(0)}}. \end{aligned} \tag{4.39}$$

Similiarly for the third-order energy,

$$E^{(3)} = \sum_{ij} \frac{V_{0i}V_{ij}V_{j0}}{(E-E_i^{(0)})(E-E_j^{(0)})}. \tag{4.40}$$

These expressions are somewhat simple, but Brilloun-Wigner is plagued by a fundamental problem as it does not provide a true order-by-order expansion of the energy. This is due to the systematically prevalent presence of the infinite-order E-term in the right-hand sides of the equations. Related to this problem, is the lack of extensivity if the perturbation is truncated at any finite order. See Shavitt and Bartlett[69] for a derivation of this non-extensivity of finite-order Brilloun-Wigner perturbation theory. For this reason, we move on to Rayleigh-Schrödinger perturbation theory.

4.3 Rayleigh-Schrödinger Perturbation Theory

By setting $\zeta = E_0^{(0)}$ in Equation 4.34 and Equation 4.35 we get Rayleigh-Schrödinger perturbation theory[66, 68]. This parametrisation means that $\zeta - E = -\Delta E$, which gives us

$$\Psi = \sum_{m=0}^{\infty} \left[\hat{R}_0(E_0^{(0)})(\hat{V} - \Delta E)\right]^m \Phi_0 \tag{4.41}$$

$$\Delta E = \sum_{m=0}^{\infty} \langle\Phi_0|\hat{V} \left[\hat{R}_0(E_0^{(0)})(\hat{V} - \Delta E)\right]^m |\Phi_0\rangle\,, \tag{4.42}$$

where the resolvent becomes

$$\hat{R}_0(E_0^{(0)}) = \sum_i \frac{|\Phi_i\rangle\langle\Phi_i|}{E^{(0)} - E_i^{(0)}}. \tag{4.43}$$

The keen reader will have noticed that these expressions are lacking the unknown E, but we still have an expression for ΔE in the right-hand side of the expressions.

The first-order correction in energy is simply

$$E^{(1)} = \langle\Phi_0|\hat{V}|\Phi_0\rangle\,. \tag{4.44}$$

For the second order energy correction, $E^{(2)}$ we need the first-order wavefunction correction,

$$\Psi^{(1)} = \hat{R}_0\hat{V}\Phi_0. \tag{4.45}$$

Notice that the ΔE-term to the right disappears as $\hat{R}_0\Delta_E|\Phi_0\rangle = \Delta_E\hat{R}_0|\Phi_0\rangle = 0$. This gives us

$$E^{(2)} = \langle\Phi_0|\hat{V}\hat{R}_0\hat{V}|\Phi_0\rangle = \sum_i \frac{|\langle\Phi_0|\hat{V}|\Phi_i\rangle|^2}{E^{(0)} - E_i^{(0)}}. \tag{4.46}$$

For the third-order energy correction we need the second-order wavefunction correction,

$$\Psi^{(2)} = \hat{R}_0(\hat{V} - \Delta E)\hat{R}\hat{V}\Phi_0 = \hat{R}_0(\hat{V} - \langle\Phi_0|\hat{V}|\Phi_0\rangle)\hat{R}\hat{V}\Phi_0, \tag{4.47}$$

where we have started to treat the stepwise expansions as a recursive relation, by inserting the first-order energy corrections for ΔE. Generally, we can write this recursive relation as

$$E^{(n)} = \left\langle\Psi_k\middle|\hat{V}\middle|\Psi_k^{(n-1)}\right\rangle, \tag{4.48}$$

$$\Psi^n = \hat{R}_0\hat{V}\Psi^{(n-1)} - \sum_{j=1}^{n-1} E^{(n-j)}\Psi^{(j)}. \tag{4.49}$$

The third order-energy correction becomes

$$\begin{aligned} E^{(3)} &= \langle\Phi_0|\hat{V}\hat{R}_0[\hat{V} - \langle\Phi_0|\hat{V}|\Phi_0\rangle]|\Phi_0\rangle \\ &= \langle\Phi_0|\hat{V}\hat{R}\hat{V}\hat{R}\hat{V}|\Phi\rangle - \langle\Phi_0|\hat{V}\hat{R}^2\hat{V}|\Phi_0\rangle \end{aligned} \tag{4.50}$$

We should now notice that a pattern has arisen in the energy terms, albeit a bit complicated one. There will always be a leading term,

$$E^{(n)} = \langle\Phi_0|\hat{V}\hat{R}\hat{V}\hat{R}\ldots\hat{V}|\Phi_0\rangle\,, \tag{4.51}$$

with n factors $\hat{V}$ and $n-1$ factors $\hat{R}$. But then we will have terms that are on the form

$$E^{(j)}\left\langle\Psi^{(n-1)}\middle|\Psi^{(n-j)}\right\rangle = E^{(j)}\langle\Phi_0|\hat{V}\mathcal{M}(\hat{R},\hat{V})\hat{V}|\Phi_0\rangle\,, \tag{4.52}$$

where $\mathcal{M}(\hat{R}, \hat{V})$ is the *monomial* of in total $n - j - 2$ operators $\hat{V}$ and $\hat{R}$'s, in some order. The terms can be systematically generated from the leading energy term by a procedure called *bracketing*.

The bracketing procedure can be quickly summarised as follows. The nth order energy $E^{(n)}$ can be written as the leading term plus terms generated by inserting some brackets $\langle\ \rangle$ around one or more $\hat{V}$s, except for the outer ones, in *any* possible way, in *any* number. These terms may also be nested. The bracket represents an expectation value with Ψ. The sign of each term is $(-1)^j$, where j is the number of brackets in the term. For example, for $n = 4$ we have four possibilities,

$$\langle\Phi_0|\hat{V}\hat{R}_0 \langle\hat{V}\rangle \hat{R}_0\hat{V}\hat{R}_0\hat{V}|\Phi_0\rangle = - \langle\Phi_0|\hat{V}|\Phi_0\rangle \langle\Phi_0|\hat{V}\hat{R}_0^2\hat{V}\hat{R}_0\hat{V}|\Phi_0\rangle \tag{4.53}$$

$$\langle\Phi_0|\hat{V}\hat{R}_0\hat{V}\hat{R}_0 \langle\hat{V}\rangle \hat{R}_0\hat{V}|\Phi_0\rangle = - \langle\Phi_0|\hat{V}|\Phi_0\rangle \langle\Phi_0|\hat{V}\hat{R}_0\hat{V}\hat{R}_0^2\hat{V}|\Phi_0\rangle \tag{4.54}$$

$$\langle\Phi_0|\hat{V}\hat{R}_0 \langle\hat{V}\rangle \hat{R}_0 \langle\hat{V}\rangle \hat{R}_0\hat{V}|\Phi_0\rangle = \langle\Phi_0|\hat{V}|\Phi_0\rangle^2 \langle\Phi_0|\hat{V}\hat{R}_0^3\hat{V}|\Phi_0\rangle \tag{4.55}$$

$$\langle\Phi_0|\hat{V}\hat{R}_0 \langle\hat{V}\hat{R}_0\hat{V}\rangle \hat{R}_0\hat{V}|\Phi_0\rangle = - \langle\Phi_0|\hat{V}\hat{R}_0\hat{V}|\Phi_0\rangle \langle\Phi_0|\hat{V}\hat{R}_0^2\hat{V}|\Phi_0\rangle\,. \tag{4.56}$$

For higher order energies, we would see brackets within brackets, leading to an increasing growth rate in the number of terms.

We will end our discussion of many-body perturbation theory presently. In closing, one should take notice of the special form the second term in $E^{(3)}$ (Equation 4.50) takes. These kinds of terms, called *unlinked* terms, becomes more and more prevalent as the series expansion continues. This is apparent from the fourth-order energy term derived from the bracketing technique above. A very powerful theorem called the *linked-diagram theorem*, derived by Goldstone[23], states that the energy and the wavefunctions can be expressed as a sum of *linked* terms only (!), because all the unlinked diagrams in a Rayleigh-Schrödinger perturbation series cancels against the renormalisation terms[1]. Proving the linked-diagram theorem requires a herculean effort, and we will refrain from doing so. The entirety of chapter 6 in Shavitt and Bartlett[69] is devoted to a proof of the linked-diagram theorem. What we will take with us is that the linked-diagram theorem forms the foundation for the coupled cluster "ansatz" wavefunction, which we will introduce at the very beginning of the next chapter.

[1]Additional sums in the wavefunction expression involving lower-order energies in RSPT, see Equation 4.49

Chapter 5

Coupled Cluster

In the late 1950s Fritz Coester constructed a rigorous formal solution of the bound state Schrödinger equation as a set of single particle wave functions[11]. He wanted to find an expression for the wave operator Ω, which transforms a zero-order wavefunction to the exact wave function,

$$\Psi = \Omega\Phi_0. \tag{5.1}$$

From Coester's solutions it would become apparent that the Rayleigh-Schrödinger perturbation expansions of the energy does not contain matrix elements representing the products of so-called unlinked diagram. In other words, one form of Ω is given a "linked-diagram expansion",

$$\Omega\left|\Phi_0\right\rangle = \left|\Phi_0\right\rangle = \sum_{k=1}^{\infty}\left((\hat{R}_0\hat{V})^k\left|\Phi_0\right\rangle\right)_L. \tag{5.2}$$

This is further underlined in discussions by John Hubbard[38] and Nicolaas Marinus Hugenholtz[39].

Conveniently, Ω may be written quite generally as

$$\Omega = e^{\hat{T}}, \quad \Psi = e^{\hat{T}}\Phi_0. \tag{5.3}$$

This exponential form has been come to be known as the Coupled Cluster ansatz, even though it is much more than a simple guess for the form of the exact wavefunction. To underline this point we quote Herman Kümmel: "Strange as it may be, in spite of the many successes of the coupled cluster method there is still a widspread belief that the underlying exponential structure is something artificial, accidental or an approximation only. This is why I want to make it clear that this feature is extremely natural - even necessary - on a very fundamental level, not necessarily connected with many-body theory"[44].

Throughout the 1950s and early 1960s, Coester and Kümmel developed the coupled cluster method together and proposed using the exponential-form wave operator as coupling between the shell-model state and the correct state vector for nuclear matter[12]. At the time, the method proved too computationally intensive. Specifically, the hard core potenatials of nuclear physics leaves no freedom in truncating the set of coupled cluster equations. However, the method was picked up by Jiří Čížek who in 1966 reformulated the method for modelling of electron correlation in atoms and molecules[10]. Further development with Josef Paldus made the coupled cluster method one of the most succesfull[1] methods in quantum chemistry. Together with Isaiah Shavitt, Čížek and Paldus did the first *ab initio* comutations with the method, which they called the coupled-pair many-electron-theory (MET)[56], as it can be intepreted as the perturbative variant of the many-electron-theory of Oktay Sinanoğlu[70].

[1] At least one of the most prevalent

5.1 The Cluster Operator

Having established the form of the coupled cluster wavefunction as

$$|\Psi\rangle = e^{\hat{T}} |\Phi_0\rangle, \tag{5.4}$$

we now take a closer look at the cluster operator, which is divided into sub-operators

$$\hat{T} = \hat{T}_1 + \hat{T}_2 + \hat{T}_2 + \hat{T}_3 + \ldots, \tag{5.5}$$

where the one-, two- and three-body operators are defined thusly,

$$\hat{T}_1 = \sum_{ai} t_i^a \{\hat{a}^\dagger \hat{i}\} \tag{5.6}$$

$$\hat{T}_2 = \frac{1}{(2!)^2} \sum_{ijab} t_{ij}^{ab} \{\hat{a}^\dagger \hat{i} \hat{b}^\dagger \hat{j}\} \tag{5.7}$$

$$\hat{T}_3 = \frac{1}{(3!)^2} \sum_{ijkabc} \{\hat{a}^\dagger \hat{i} \hat{b}^\dagger \hat{j} \hat{c}^\dagger \hat{k}\}, \tag{5.8}$$

where the coefficients $t_{ijk\ldots}^{abc\ldots}$ are commonly referred to as the coupled cluster *amplitudes*, and are coefficients to be determined. The strings of operators are automatically normal-ordered. The general m-body cluster operator is given by

$$\hat{T}_m = \frac{1}{(m!)^2} \sum_{\substack{ij\ldots \\ ab\ldots}} t_{ij\ldots}^{ab\ldots} \{\hat{a}^\dagger \hat{i} \hat{b}^\dagger \hat{j} \ldots\}, \tag{5.9}$$

which produces an m-fold excitation. It is not necessary to include cluster-operators up to a infinite-fold excitation. Logically, the maximum excitation order is dictated by the number of electrons in the system n, such that $n \geq m$. Any higher-order excitation operator would eventually annihilate an unoccupied orbital, resulting in a zero-contribution. The prefactor $1/(m!)^2$ accounts for the redundancy created by unrestricted summations, as a permutation of any of the m hole or m particle indices will not produce a distinct contributions. Indeed, we have for example that

$$\hat{a}^\dagger \hat{i} \hat{b}^\dagger \hat{j} = -\hat{a}^\dagger \hat{j} \hat{b}^\dagger \hat{i} = -\hat{b}^\dagger \hat{i} \hat{a}^\dagger \hat{j} = \hat{b}^\dagger \hat{j} \hat{a}^\dagger \hat{j}, \tag{5.10}$$

and therefore we must also have that

$$t_{ij}^{ab} = -t_{ji}^{ab} = -t_{ij}^{ba} = t_{ji}^{ba}. \tag{5.11}$$

Hence, the $(2!)^2 = 4$ contributions of two hole indices, ab, and two particle indices, ij, will produce four equal terms, which is offset by the prefactor $1/4$.

The exponential wave operator $e^{\hat{T}}$ may be expanded as a Taylor series,

$$e^{\hat{T}} = 1 + \hat{T} + \frac{1}{2!}\hat{T}^2 + \frac{1}{3!}\hat{T}^3 + \ldots. \tag{5.12}$$

By including only single- and double excitations, $\hat{T}_{\mathrm{CCSD}} = \hat{T}_1 + \hat{T}_2$, this expressions becomes

$$e^{\hat{T}_{\mathrm{CCSD}}} = 1 + \hat{T}_1 + \hat{T}_2 + \frac{1}{2}\hat{T}_1^2 + \hat{T}_1\hat{T}_2 + \frac{1}{2}\hat{T}_2^2 + \frac{1}{3!}\hat{T}_1^3 + \frac{1}{2}\hat{T}_1^2\hat{T}_2 + \frac{1}{2}\hat{T}_1\hat{T}_2^2 + \frac{1}{3!}\hat{T}_2^3 + \ldots \tag{5.13}$$

Contributions to the wave function containing only a single cluster operator, $\hat{T}_m$, are called connected cluster contributions, while those containing products of cluster operators, $\hat{T}_{m_1}^\alpha \hat{T}_{m_2}^\beta$, are called disconnected cluster contributions.

This inclusion of only single- and double excitations is called "Coupled Cluster Singles Doubles", elucidating the subscript CCSD[65]. The most common approximation in coupled cluster theory is the CCSD model. Here, the operator $\hat{T}_2$ describes the important electron-pair interaction and the $\hat{T}_1$ operator carries out the orbital relaxations induced by the field set up by electron-pair interactions.

Importance of different parts of the cluster operator

The most important contribution to the wave-function in quantum chemistry is undoubtedlty $\hat{T}_2$, because of the two-electron nature of the Hamiltonian. It describes the most important interaction of quantum chemistry, the electron-pair interaction. The inclusion of $\hat{T}_1$ and its products are relatively insensitive to the choice of basis set, as the operators $e^{\hat{T}_1}$ has the effect of transforming the reference state $|\Phi_0\rangle$ to another Slater determinant. This is known as Thouless theorem[75]. With very high electron-density, the three-particle operator $\hat{T}_3$ becomes important. Higher-order terms are usually of less and decreasing importance, but they can be of concern in special situations. For instance, the four-particle operator $\hat{T}_4$ is very important in nuclear physics. See for instance Helgaker, Jorgensen, and Olsen[34] or Shavitt and Bartlett[69] for further discussion on this topic.

5.2 Coupled-Cluster Doubles (CCD)

As a good starting point for understanding the coupled cluster scheme and especially where the coupled-cluster equations come from, we now constrain the cluster operator to

$$\hat{T}_{\text{CCD}} = \hat{T}_2, \tag{5.14}$$

and completely derive the coupled cluster equations for this case. The CCD wave function includes all connected and disconnected clusters involving $\hat{T}_2$ only,

$$\Psi_{\text{CCD}} = e^{\hat{T}_2} = \Phi_0 + \hat{T}_2\Phi_0 + \frac{1}{2}\hat{T}_2^2\Phi_0 + \frac{1}{3!}\hat{T}_2^3\Phi_0 + \dots \tag{5.15}$$

There are several methods with which to arrive at the coupled-cluster equations and here we employ two of them for the coupled cluster doubles truncation. First, we use configuration-interaction techniques and the Slater-Condon rules (Appendix B) and second, we use the "algebraic method", employing second quantisation and Wick's theorem. A third way is with the aid of diagrams. Instead of deriving coupled cluster equations by hand it is often prudent to do so with the aid of a symbolic calculater. For higher-order schemes we have used pythons `SymPy` library.

5.2.1 Configuration space derivation

We start from the CCD-constrained time-independent Schrödinger equation,

$$\hat{H}\Psi_{\text{CCD}} = E_{\text{CCD}}\Psi_{\text{CCD}}, \tag{5.16}$$

which we left project with the reference state,

$$\begin{aligned} \langle\Phi_0|\,\hat{H}\,|\Psi_{\text{CCD}}\rangle &= \langle\Phi_0|\,E_{\text{CCD}}\,|\Psi_{\text{CCD}}\rangle \\ \rightarrow E_{\text{CCD}} &= \langle\Phi_0|\,\hat{H}\,|\Psi_{\text{CCD}}\rangle\,, \end{aligned}$$

where we have taken advandage of the intermediate normalisation, $\langle \Phi_0 | \Psi_{\mathrm{CCD}} \rangle = 1$. We then insert the exponential expansion from the coupled cluster ansatz,

$$\begin{aligned} E_{\mathrm{CCD}} &= \langle \Phi_0 | \hat{H}(1+\hat{T}_2) | \Phi_0 \rangle \\ &= E_{\mathrm{ref}} + \sum_{\substack{i>j \\ a>b}} \langle \Phi_0 | \hat{H} \left| \Phi_{ij}^{ab} \right\rangle t_{ij}^{ab} \\ &= E_{\mathrm{ref}} + \sum_{\substack{i>j \\ a>b}} \langle ij | ab \rangle \, t_{ij}^{ab}. \end{aligned} \tag{5.17}$$

The energy expression will truncate here because no higher order terms will contribute. It is common to substract E_{ref} to get,

$$\hat{H}_N \Psi_{\mathrm{CCD}} = \Delta E_{\mathrm{CCD}} \Psi_{\mathrm{CCD}}, \tag{5.18}$$

where $\hat{H}_N = \hat{H} - E_{\mathrm{ref}}$. Now follows a series of expressions intended to show the correspondence between coupled cluster- and perturbation theory, HOPEFULLY THIS WILL BE CLEARER WHEN THE CHAPTER ON PERTURBATION THEORY IS COMPLETE

$$\hat{H}_N = \hat{F} - \hat{U} + \hat{H}_2 - E_{\mathrm{ref}} = \hat{H}_0 + \hat{F}^0 - \hat{U} + \hat{H}_2 - E_{\mathrm{ref}}, \tag{5.19}$$

where,

$$\hat{H}_0 = \hat{F}^d = \sum_{\mu} \hat{f}_{\mu}^d, \quad \langle p | \hat{f}_{\mu}^d | q \rangle = \epsilon_p \delta_{pq} \tag{5.20}$$

$$\hat{F}^0 = \sum_{\mu} \hat{f}_{\mu}^0, \quad \langle p | \hat{f}^0 | q \rangle = (1 - \delta_{pq}) \langle p | \hat{f} | q \rangle \tag{5.21}$$

$$\hat{U} = \sum_{\mu} \hat{u}_{\mu}, \quad \langle p | \hat{u}_{\mu} | q \rangle = \sum_i \langle pi | qi \rangle \tag{5.22}$$

$$\hat{H}_2 = \sum_{\mu>\nu} \frac{1}{r_{\mu\nu}}, \quad E_{\mathrm{ref}} = E_0 + E^{(1)}, \tag{5.23}$$

$$E_0 = \sum_i \epsilon_i, \quad E^{(1)} = -\frac{1}{2} \sum_{ij} \langle ij | ij \rangle \,. \tag{5.24}$$

In the canonical HF case we have $\hat{F}^0 = 0$ and $\hat{F}^d = \hat{F}$.

In order to compute the energy of the system we need the amplitudes t_{ij}^{ab}. Starting from the modified Schrödinger equation,

$$\hat{H}_N \Psi_{\mathrm{CCD}} = \Delta E_{\mathrm{CCD}} \Psi_{\mathrm{CCD}}. \tag{5.25}$$

We left project with a doubly-excited Slater determinant, and insert for the CC ansatz,

$$\left\langle \Phi_{ij}^{ab} \right| \hat{H}_N e^{\hat{T}_2} | \Phi_0 \rangle = \Delta E_{\mathrm{CCD}} \left\langle \Phi_{ij}^{ab} \right| e^{\hat{T}_2} | \Phi_0 \rangle \tag{5.26}$$

$$\left\langle \Phi_{ij}^{ab} \right| \hat{H}_N \left(1 + \hat{T}_2 + \frac{1}{2} \hat{T}_2^2 \right) | \Phi_0 \rangle = \Delta E_{\mathrm{CCD}} t_{ij}^{ab}. \tag{5.27}$$

Here we have only expanded the exponential function up to the quadratic term. The next term in the series will triple-excite the bra Slater determinant, which will give a zero-contribution according to the Slater-Condon rules, because of two noncoincidences. Next we apply the Slater-Condon rules to the rest of the terms on the right-hand side, starting with just the normal-ordered Hamiltonian,

$$\left\langle \phi_{ij}^{ab} \right| \hat{H}_N | \Phi_0 \rangle = \langle ab | ij \rangle \,, \tag{5.28}$$

where only $\hat{H}_2$ contributes.

Next we look at the linear term,

$$\begin{aligned}\left\langle \Phi_{ij}^{ab} \middle| \hat{H}_N \hat{T}_2 \middle| \Phi_0 \right\rangle &= \sum_{klcd} \left\langle \phi_{ij}^{ab} \middle| \hat{H}_N \middle| \phi_{kl}^{cd} \right\rangle \\ &= \left\langle \Phi_{ij}^{ab} \middle| \hat{H}_0 - E_{\mathrm{ref}} \middle| \Phi_{ij}^{ab} \right\rangle t_{ij}^{ab} + \sum_{\substack{k>l \\ c>d}} \left\langle \Phi_{ij}^{ab} \middle| \hat{F}^0 - \hat{U} \middle| \Phi_{kl}^{cd} \right\rangle t_{kl}^{cd} \\ &+ \sum_{\substack{k>l \\ c>l}} \left\langle \Phi_{ij}^{ab} \middle| \hat{H}_2 \middle| \Phi_{kl}^{cd} \right\rangle t_{kl}^{cd} = L_0 + L_1 + L_2.\end{aligned} \tag{5.29}$$

We are going to evaluate these terms one-by-one, starting with L_0,

$$\begin{aligned}L_0 = \left\langle \Phi_{ij}^{ab} \middle| \hat{H}_0 - E_{\mathrm{ref}} \middle| \Phi_{ij}^{ab} \right\rangle &= \left\langle \Phi_{ij}^{ab} \middle| \hat{H}_0 - E_0 - E^{(1)} \middle| \Phi_{ij}^{ab} \right\rangle \\ &= \left(-\varepsilon_{ij}^{ab} + \frac{1}{2} \sum_{kl} \langle kl|kl \rangle \right) t_{ij}^{ab}.,\end{aligned} \tag{5.30}$$

where $\varepsilon_{ij}^{ab} = \varepsilon_i + \varepsilon_j - \varepsilon_a - \varepsilon_b$.

The next term,

$$L_1 = \sum_{\substack{k>l \\ c>d}} \left\langle \Phi_{ij}^{ab} \middle| \hat{F}^0 - \hat{U} \middle| \Phi_{kl}^{cd} \right\rangle t_{kl}^{cd}, \tag{5.31}$$

yields contributions if at least three of the indices k, l, c, d are equal to the indices i, j, a, b (we want one or zero noncoincidences). All the possible terms are,

$$L_1 = \begin{cases} -\sum_k u_{kk} t_{ij}^{ab} & \text{all indices equal} \\ -\sum_k (f_{jk}^0 - u_{jk}) t_{ik}^{ab} & \text{one hole index unequal} \\ +\sum_k (f_{ik}^0 - u_{ik}) t_{jk}^{ab} & \text{the other hole index unequal} \\ -\sum_c (f_{ac}^0 - u_{ac}) t_{ij}^{bc} & \text{one particle index unequal} \\ +\sum_c (f_{bc}^0 - u_{bc}) t_{ij}^{zc} & \text{the other particle index unequal.} \end{cases} \tag{5.32}$$

For the last linear term,

$$L_2 = \sum_{\substack{k>l \\ c>d}} \left\langle \Phi_{ij}^{ab} \middle| \hat{H}_2 \middle| \Phi_{kl}^{cd} \right\rangle t_{kl}^{cd}, \tag{5.33}$$

we require that at least two of the indices k, l, c, d are equal to the indices i, j, a, b, as we can do with at most two noncoincidences in the bra and the ket. For equality in both the hole indices or both the particle indices we have

$$cd = ab \quad \to \quad \sum_{k>l} \langle ij|kl \rangle t_{kl}^{ab} \tag{5.34}$$

$$kl = ij \quad \to \quad \sum_{c>d} \langle ab|cd \rangle t_{ij}^{cd}. \tag{5.35}$$

For one equality in both hole and particle index we have

$$-\sum_{kl} \left(\langle bk|cj \rangle t_{ik}^{ac} - \langle bk|ci \rangle t_{jk}^{ac} - \langle ak|cj \rangle t_{ik}^{bc} - \langle bk|ci \rangle t_{jk}^{ac} \right), \tag{5.36}$$

where the sign stems from the maximum coincidence permutations as dictated by the Slater-Condon rules. Most of the three- and four equal index terms are accounted for by the expression above, the remaining three-index equality terms are

$$-\sum_{kl}\big(\langle jl|kl\rangle\, t_{ik}^{ab} - \langle il|kl\rangle\, t_{jk}^{ab}\big) \tag{5.37}$$

$$+\sum_{cl}\big(\langle bl|cl\rangle\, t_{ij}^{ac} - \langle al|cl\rangle\, t_{ij}^{bc}\big), \tag{5.38}$$

and there is one term for the case where all indices are equal,

$$\sum_{k>l}\langle kl|kl\rangle\, t_{ij}^{ab} = \frac{1}{2}\sum_{kl}\langle kl|kl\rangle\, t_{ij}^{ab}. \tag{5.39}$$

Difference between Coupled Cluster and Configuration Interaction

THIS BOX MAY BELONG SOMEWHERE ELSE (or may not be in a box)
Monkhorst[53] gives a general formuala for transferring back and forth between CC operators $\hat{T}_m$ and CI operators $\hat{C}_m$,

$$\hat{C}_m = \sum_{k}^{m}\frac{1}{k!}\sum_{|m_\mu|}\delta(m_1+m_2+\cdots+m_k, m)\prod_{\mu=1}^{k}\hat{T}_{m_\mu}, \tag{5.40}$$

where the second sum is over all sets of k m_μ-values that sum up to m. The first four of the terms are,

$$\hat{C}_1 = \hat{T}_1 \tag{5.41}$$

$$\hat{C}_2 = \hat{T}_2 + \frac{1}{2}\hat{T}_1^2 \tag{5.42}$$

$$\hat{C}_3 = \hat{T}_3 + \hat{T}_1\hat{T}_2 + \frac{1}{3!}T_1^3 \tag{5.43}$$

$$\hat{C}_4 = \hat{T}_4 + \frac{1}{2}\hat{T}_2 + \frac{1}{2}\hat{T}_2\hat{T}_1^2 + \frac{1}{4!}\hat{T}_1^4. \tag{5.44}$$

For the CCSD and CISDTQ wavfunctions we have,

$$|\Psi_{\text{CCSD}}\rangle = \left(1+\hat{T}_1+\frac{1}{2}\hat{T}_1^2+\frac{1}{3!}\hat{T}_1^3+\hat{T}_2+\frac{1}{2}\hat{T}_2^2+\frac{1}{4!}\hat{T}_1^4+\hat{T}_1\hat{T}_2\right)|\Phi_0\rangle \tag{5.45}$$

$$|\Psi_{\text{CISDTQ}}\rangle = \left(1+\hat{C}_1+\hat{C}_2+\hat{C}_3+\hat{C}_4\right)|\Phi_0\rangle \tag{5.46}$$

which provides us with a relation between the two,

$$|\Psi_{\text{CCSD}}\rangle = |\Psi_{\text{CISDTQ}}\rangle - (\hat{T}_3+\hat{T}_4)\,|\Phi_0\rangle\,. \tag{5.47}$$

Moreover, we see that for a system of $n=2$ particles, that

$$|\Psi_{\text{CCSD}}\rangle = |\Psi_{\text{CISD}}\rangle\,. \tag{5.48}$$

These last three- and four-index equality terms are expressible in terms of $\hat{u}$, and will cancel the first term in L_1 together with the $\hat{u}$ term from L_0. All terms so far are the same as in a configuration interaction with doubles excitations (CID) computation. The difference between coupled cluster with doubles (CCD) and CID is the following extra quadratic terms,

$$Q = \frac{1}{2} \langle \Phi_{ij}^{ab} | \hat{H}_N \hat{T}_2^2 | \Phi_0 \rangle = \frac{1}{2} \sum_{\substack{k>l \\ c>d}} \sum_{\substack{m>n \\ e>f}} \langle \phi_{ij}^{ab} | \hat{H}_N \left| \Phi_{klmn}^{cdef} \right\rangle t_{kl}^{cd} t_{mn}^{ef}. \tag{5.49}$$

From this expression we will have a contrition only when four of the indices k, l, m, n, c, d, e, f are equal to i, j, a, b, and only $\hat{H}_2$ can contribute. After some algebraic acrobatics we'll find that this becomes

$$\begin{aligned} Q = \sum_{\substack{k>l \\ c>d}} \langle kl|cd \rangle \big[&(t_{ij}^{ab} t_{kl}^{cd} + t_{ij}^{cd} t_{kl}^{ab}) - 2(t_{ik}^{ac} t_{jl}^{cd} + t_{ij}^{bd} t_{ij}^{bd}) \\ &-2(t_{ik}^{ab} t_{jl}^{cd} + t_{ik}^{cd} t_{jl}^{ab}) + 4(t_{ik}^{ac} t_{jl}^{bd} + t_{ik}^{bd} t_{jl}^{ac}) \big]. \end{aligned} \tag{5.50}$$

From Equation 5.17 we see that

$$\Delta E_{\mathrm{CCD}} = \sum_{\substack{i>j \\ a>b}} \langle ij|ab \rangle t_{ij}^{ab}, \tag{5.51}$$

and because the indices in Equation 5.50 are dummy variables we see that the first term here cancels with the right-hand side of Equation 5.27. Some algebraic massage after the initial acrobatic exercises leads to,

$$\begin{aligned} \varepsilon_{ij}^{ab} t_{ij}^{ab} = &\langle ab|ij \rangle + \frac{1}{2} \sum_{cd} \langle ab|cd \rangle t_{ij}^{cd} + \frac{1}{2} \sum_{kl} \langle ij|kl \rangle t_{kl}^{ab} \\ &- \sum_{kl} \big(\langle bk|cj \rangle t_{ik}^{ac} - \langle bk|ci \rangle t_{jk}^{ac} - \langle ak|cj \rangle t_{ik}^{bc} + \langle ak|ci \rangle t_{jk}^{bc} \big) \\ &- \sum_{k} \hat{f}_{jk}^{0} t_{ik}^{ab} + \sum_{k} \hat{f}_{ik}^{0} t_{jk}^{ab} + \sum_{c} \hat{f}_{bc}^{0} t_{ij}^{ac} - \sum_{c} \hat{f}_{ac}^{0} t_{ij}^{bc} \\ &+ \sum_{klcd} \langle kl|cd \rangle \Big[\frac{1}{4} t_{ij}^{cd} t_{kl}^{ab} - \frac{1}{2} (t_{ij}^{ac} t_{kl}^{bd} + t_{ij}^{bd} t_{kl}^{ac}) \\ &\quad - \frac{1}{2} (t_{ik}^{ab} t_{jl}^{cd} + t_{ik}^{cd} t_{jl}^{ab}) + (t_{ik}^{ac} t_{jl}^{bd} + t_{ik}^{bd} t_{jl}^{ac}) \Big], \end{aligned} \tag{5.52}$$

which is the CCD amplitude equations. This equation contains simultaneous algebraic expressions, contrary to CI. The equations must be solved iteratively, substituting t_{ij}^{ab} obtained in each iteration, into the quadratic terms for the next iteration.

5.2.2 Algebraic Derivation

In this derivation we make great use of second quantisation formalism and Wick's theorem. We start with the normal-ordered Hamiltonian,

$$\begin{aligned} \hat{H}_N &= (\hat{H}_0)_N + \hat{F}_N^0 + \hat{W} \\ &= \sum_p \varepsilon_p \{\hat{p}^\dagger \hat{p}\} + \sum_{p \neq q} f_{pq} \{\hat{p}^\dagger \hat{q}\} + \frac{1}{4} \sum_{pqrs} \langle pq|rs \rangle \{\hat{p}^\dagger \hat{q}^\dagger \hat{s} \hat{r}\}. \end{aligned} \tag{5.53}$$

The one-particle terms $(\hat{H}_0)_N$ and $\hat{F}_N^0$ can be combined by setting $\varepsilon_p = f_{pp}$, reducing the normal-ordered Hamilionian to

$$\begin{aligned} \hat{H}_N &= \hat{F}_N + \hat{W} \\ &= \sum_{pq} f_{pq} \{\hat{p}^\dagger \hat{q}\} + \frac{1}{4} \sum_{pqrs} \langle pq|rs \rangle \{\hat{p}^\dagger \hat{q}^\dagger \hat{s} \hat{r}\}. \end{aligned} \tag{5.54}$$

First we want to find an expression for the energy,

$$\Delta E_{\mathrm{CCD}} = \langle 0| \hat{H}_N(1+\hat{T}^2)|0\rangle = \langle 0|\hat{H}_N\hat{T}_2|0\rangle\,, \tag{5.55}$$

where only the vacuum expectation value of the product of the Hamiltonian and the doubles cluster operators gives a contributions, because the vacuum expectation value of just the Hamiltonian is zero. Inserting for the operators,

$$\Delta E_{\mathrm{CCD}} = \sum_{\substack{i>j\\a>b}} \langle 0| \left[\sum_{pq} f_{pq}\{\hat{p}^\dagger\hat{q}\} + \frac{1}{4}\sum_{pqrs}\langle pq|rs\rangle\{\hat{p}^\dagger\hat{q}^\dagger\hat{s}\hat{r}\}\right]\{\hat{a}^\dagger\hat{b}^\dagger\hat{j}\hat{i}\}|0\rangle\, t_{ij}^{ab}. \tag{5.56}$$

Here the one-particle part will vanish as there is no manner one can contract all the operators in this term without using an internal contraction in the normal-ordered product. It is also useful to convert the first sum to an unrestricted sum,

$$\Delta E_{\mathrm{CCD}} = \frac{1}{16}\sum_{ijab}\sum_{pqrs}\langle pq|rs\rangle\langle 0|\{\hat{p}^\dagger\hat{q}^\dagger\hat{s}\hat{r}\}\{\hat{a}^\dagger\hat{b}^\dagger\hat{j}\hat{i}\}|0\rangle\, t_{ij}^{ab}. \tag{5.57}$$

We contract the operators in the normal-ordered products,

$$\begin{aligned}
&\langle 0|\{\hat{p}^\dagger\hat{q}^\dagger\hat{s}\hat{r}\}\{\hat{a}^\dagger\hat{b}^\dagger\hat{j}\hat{i}\} + \{\hat{p}^\dagger\hat{q}^\dagger\hat{s}\hat{r}\}\{\hat{a}^\dagger\hat{b}^\dagger\hat{j}\hat{i}\} \\
&+\{\hat{p}^\dagger\hat{q}^\dagger\hat{s}\hat{r}\}\{\hat{a}^\dagger\hat{b}^\dagger\hat{j}\hat{i}\} + \{\hat{p}^\dagger\hat{q}^\dagger\hat{s}\hat{r}\}\{\hat{a}^\dagger\hat{b}^\dagger\hat{j}\hat{i}\}|0\rangle
\end{aligned} \tag{5.58}$$

$$\begin{aligned}
&=\delta_{pi}\delta_{qj}\delta_{sb}\delta_{ra} - \delta_{pi}\delta_{qj}\delta_{sa}\delta_{rb} \\
&-\delta_{pj}\delta_{qi}\delta_{sb}\delta_{ra} + \delta_{pj}\delta_{qi}\delta_{sa}\delta_{rn}.
\end{aligned} \tag{5.59}$$

All these products of delta functions give us a reduction in the sums and the CCD energy becomes,

$$\Delta E_{\mathrm{CCD}} = \frac{1}{4}\sum_{ijab}\langle ij|ab\rangle\, t_{ij}^{ab}. \tag{5.60}$$

The natural next step is to find the amplitude equations,

$$\langle \Phi_{ij}^{ab}|\,\hat{H}_N\left(1+\hat{T}_2+\frac{1}{2}\hat{T}^2\right)|0\rangle = \Delta E_{\mathrm{CCD}} t_{ij}^{ab}. \tag{5.61}$$

We compute this expression in steps, starting with the lone normal-ordred Hamiltonian,

$$\langle \Phi_{ij}^{ab}|\,\hat{H}_N|0\rangle = \frac{1}{4}\sum_{pqrs}\langle 0|\{\hat{a}\hat{b}\hat{j}^\dagger\hat{i}^\dagger\}\{\hat{p}^\dagger\hat{q}^\dagger\hat{s}\hat{r}\}|0\rangle\langle pq|rs\rangle\,, \tag{5.62}$$

here we also have to compute a few contractions,

$$\begin{aligned}
&\langle 0|\{\hat{i}^\dagger\hat{j}^\dagger\hat{b}\hat{a}\}\{\hat{p}^\dagger\hat{q}^\dagger\hat{s}\hat{r}\} + \{\hat{i}^\dagger\hat{j}^\dagger\hat{b}\hat{a}\}\{\hat{p}^\dagger\hat{q}^\dagger\hat{s}\hat{r}\} \\
&+\{\hat{i}^\dagger\hat{j}^\dagger\hat{b}\hat{a}\}\{\hat{p}^\dagger\hat{q}^\dagger\hat{s}\hat{r}\} + \{\hat{i}^\dagger\hat{j}^\dagger\hat{b}\hat{a}\}\{\hat{p}^\dagger\hat{q}^\dagger\hat{s}\hat{r}\}|0\rangle
\end{aligned} \tag{5.63}$$

$$\begin{aligned}
&=\delta_{ir}\delta_{js}\delta_{bq}\delta_{ap} - \delta_{ir}\delta_{js}\delta_{bp}\delta_{aq} \\
&-\delta_{is}\delta_{jr}\delta_{bq}\delta_{ap} + \delta_{is}\delta_{jr}\delta_{bp}\delta_{aq}.
\end{aligned} \tag{5.64}$$

This will leave us with a similar expression as the one in the energy equation,

$$\langle \Phi_{ij}^{ab} | \hat{H}_N |0\rangle = \langle ab|ij\rangle . \tag{5.65}$$

Now for the linear terms,

$$\begin{aligned} \langle \phi_{ij}^{ab} | \hat{H}_N \hat{T}_2 |0\rangle &= \sum_{\substack{k>l \\ c>d}} \langle \phi_{ij}^{an} | \hat{H}_n \{\hat{c}^\dagger \hat{d}^\dagger \hat{l}\hat{k}\} |0\rangle t_{kl}^{cd} \\ &= \frac{1}{4} \sum_{klcd} \langle \Phi_{ij}^{ab} | \hat{F}_N + \hat{W} |\Phi_{kl}^{cd}\rangle t_{kl}^{cd} \end{aligned} \tag{5.66}$$

Starting with the first term,

$$\begin{aligned} L_1 &= \frac{1}{4} \sum_{klcd} \langle \phi_{ij}^{ab} | \hat{F}_N |\phi_{kl}^{cd}\rangle t_{kl}^{cd} \\ &= \frac{1}{4} \sum_{klcd} \sum pq f_{pq} \langle \phi_{ij}^{ab} | \{\hat{p}^\dagger \hat{q}\} |\phi_{kl}^{cd}\rangle t_{kl}^{cd} \\ &= \frac{1}{4} \sum_{klcd} \sum_{pq} f_{pq} \langle 0| \{\hat{i}^\dagger \hat{j}^\dagger \hat{b}\hat{a}\}\{\hat{p}^\dagger \hat{q}\}\{\hat{c}^\dagger \hat{d}^\dagger \hat{l}\hat{k}\} |0\rangle t_{kl}^{cd} \end{aligned} \tag{5.67}$$

The product of normal-ordered operators must be contracted in such a way that three and three operators in the first and last operator strings are contracted with one another, and the two operators in the middle string is contracted with one operator in the last and first one. This provides us with $3 \times 3 \times 2 = 16$ possible contractions. Here are the first four contractions,

$$\begin{aligned} &\{\hat{i}^\dagger \hat{j}^\dagger \hat{b}\hat{a}\}\{\hat{p}^\dagger \hat{q}\}\{\hat{c}^\dagger \hat{d}^\dagger \hat{l}\hat{k}\} + \{\hat{i}^\dagger \hat{j}^\dagger \hat{b}\hat{a}\}\{\hat{p}^\dagger \hat{q}\}\{\hat{c}^\dagger \hat{d}^\dagger \hat{l}\hat{k}\} \\ &+ \{\hat{i}^\dagger \hat{j}^\dagger \hat{b}\hat{a}\}\{\hat{p}^\dagger \hat{q}\}\{\hat{c}^\dagger \hat{d}^\dagger \hat{l}\hat{k}\} + \{\hat{i}^\dagger \hat{j}^\dagger \hat{b}\hat{a}\}\{\hat{p}^\dagger \hat{q}\}\{\hat{c}^\dagger \hat{d}^\dagger \hat{l}\hat{k}\} \end{aligned} \tag{5.68}$$

$$\begin{aligned} &= \delta_{ik}\delta_{jl}\delta_{bd}\delta_{ap}\delta_{cq} + \delta_{ik}\delta_{jl}\delta_{ac}\delta_{bp}\delta_{dq} \\ &- \delta_{ik}\delta_{jq}\delta_{bd}\delta_{ac}\delta_{pl} - \delta_{iq}\delta_{pk}\delta_{jl}\delta_{bd}\delta_{ac}. \end{aligned} \tag{5.69}$$

The last 12 contractions will be equivalent to these four, and thus we rid ourselves of the $\frac{1}{4}$-prefactor, yielding

$$L_1 = \sum_c (f_{bc} t_{ij}^{ac} - f_{ac} t_{ij}^{bc}) + \sum_k (f_{ik} t_{jk}^{ab} - f_{jk} t_{ik}^{ab}). \tag{5.70}$$

Proceeding to the second linear term,

$$\begin{aligned} L_2 &= \frac{1}{4} \sum_{klcd} \langle \Phi_{ij}^{ab} | \hat{W} |\Phi_{kl}^{cd}\rangle t_{kl}^{cd} \\ &= \frac{1}{16} \sum_{pqrs} \sum_{klcd} \langle pq|rs\rangle \langle 0| \{\hat{j}^\dagger \hat{b}\hat{i}^\dagger \hat{a}\}\{\hat{p}^\dagger \hat{q}^\dagger \hat{s}\hat{r}\}\{\hat{c}^\dagger \hat{d}^\dagger \hat{k}\hat{l}\} |0\rangle t_{kl}^{cd} \end{aligned} \tag{5.71}$$

Here there are many possible ways to contract the operator strings, so it is convenient to label the different kinds of contractions. Subscript a-terms consist of two hole-hole contractions, subscript b-terms consist of two particle-particle contractions and subscript c-terms consist of one particle-hole and one hole-particle contractions,

$$
\begin{aligned}
L_{2a} &= \frac{1}{8}\sum_{pqrs}\sum_{klcd} \langle pq|rs\rangle \, \langle 0|\, \{\hat{i}^\dagger \hat{j}^\dagger \hat{b}\hat{a}\}\{\hat{p}^\dagger \hat{q}^\dagger \hat{s}\hat{r}\}\{\hat{c}^\dagger \hat{d}^\dagger \hat{k}\hat{l}\}\, |0\rangle \, t_{kl}^{cd} \\
&= \frac{1}{8}\sum_{pqrs}\sum_{cd} \langle pq|rs\rangle \, \langle 0|\, \{\hat{b}\hat{a}\}\{\hat{p}^\dagger \hat{q}^\dagger \hat{s}\hat{r}\}\{\hat{c}^\dagger \hat{d}^\dagger\}\, |0\rangle \, t_{kl}^{cd}
\end{aligned} \tag{5.72}
$$

$$
\begin{aligned}
L_{2b} &= \frac{1}{8}\sum_{pqrs}\sum_{klcd} \langle pq|rs\rangle \, \langle 0|\, \{\hat{i}^\dagger \hat{j}^\dagger \hat{b}\hat{a}\}\{\hat{p}^\dagger \hat{q}^\dagger \hat{s}\hat{r}\}\{\hat{c}^\dagger \hat{d}^\dagger \hat{l}\hat{k}\}\, |0\rangle \, t_{kl}^{cd} \\
&= \frac{1}{8}\sum_{pqrs}\sum_{kl} \langle pq|rs\rangle \, \langle 0|\, \{\hat{i}^\dagger \hat{j}^\dagger\}\{\hat{p}^\dagger \hat{q}^\dagger \hat{s}\hat{r}\}\{\hat{l}\hat{k}\}\, |0\rangle \, t_{kl}^{cd}
\end{aligned} \tag{5.73}
$$

$$
\begin{aligned}
L_{2c} = \frac{1}{4}\sum_{pqrs}\sum_{klcd} \langle pq|rs\rangle \, \langle 0|\{\hat{i}^\dagger \hat{j}^\dagger \hat{b}\hat{a}\}\{\hat{p}^\dagger \hat{q}^\dagger \hat{s}\hat{r}\}\{\hat{c}^\dagger \hat{d}^\dagger \hat{l}\hat{k}\} \\
+\{\hat{i}^\dagger \hat{j}^\dagger \hat{b}\hat{a}\}\{\hat{p}^\dagger \hat{q}^\dagger \hat{s}\hat{r}\}\{\hat{c}^\dagger \hat{d}^\dagger \hat{l}\hat{k}\} \\
+\{\hat{i}^\dagger \hat{j}^\dagger \hat{b}\hat{a}\}\{\hat{p}^\dagger \hat{q}^\dagger \hat{s}\hat{r}\}\{\hat{c}^\dagger \hat{d}^\dagger \hat{l}\hat{k}\} \\
+\{\hat{i}^\dagger \hat{j}^\dagger \hat{b}\hat{a}\}\{\hat{p}^\dagger \hat{q}^\dagger \hat{s}\hat{r}\}\{\hat{c}^\dagger \hat{d}^\dagger \hat{l}\hat{k}\}\, |0\rangle \, t_{kl}^{cd} \\
= \frac{1}{4}\sum_{pqrs}\sum_{kc} \langle pq|rs\rangle \, \langle 0|\{\hat{i}^\dagger \hat{a}\}\{\hat{p}^\dagger \hat{q}^\dagger \hat{s}\hat{r}\}\{\hat{c}^\dagger \hat{k}\} \\
-\{\hat{j}^\dagger \hat{a}\}\{\hat{p}^\dagger \hat{q}^\dagger \hat{s}\hat{r}\}\{\hat{c}^\dagger \hat{k}\} \\
-\{\hat{i}^\dagger \hat{b}\}\{\hat{p}^\dagger \hat{q}^\dagger \hat{s}\hat{r}\}\{\hat{c}^\dagger \hat{k}\} \\
+\{\hat{j}^\dagger \hat{b}\}\{\hat{p}^\dagger \hat{q}^\dagger \hat{s}\hat{r}\}\{\hat{c}^\dagger \hat{k}\}\, |0\rangle \, .
\end{aligned} \tag{5.74}
$$

The vacuum expectation value in L_{2a} can be evaluated as,

$$
\begin{aligned}
\langle 0|\{\hat{b}\hat{a}\}\{\hat{p}^\dagger \hat{q}^\dagger \hat{s}\hat{r}\}\{\hat{c}^\dagger \hat{d}^\dagger\} + \{\hat{b}\hat{a}\}\{\hat{p}^\dagger \hat{q}^\dagger \hat{s}\hat{r}\}\{\hat{c}^\dagger \hat{d}^\dagger\} \\
+\{\hat{b}\hat{a}\}\{\hat{p}^\dagger \hat{q}^\dagger \hat{s}\hat{r}\}\{\hat{c}^\dagger \hat{d}^\dagger\} + \{\hat{b}\hat{a}\}\{\hat{p}^\dagger \hat{q}^\dagger \hat{s}\hat{r}\}\{\hat{c}^\dagger \hat{d}^\dagger\}\, |0\rangle
\end{aligned} \tag{5.75}
$$

$$
\begin{aligned}
=&\delta_{bq}\delta_{ap}\delta_{sd}\delta_{rc} - \delta_{bq}\delta_{ap}\delta_{sc}\delta_{rd} \\
-&\delta_{aq}\delta_{bp}\delta_{sd}\delta_{rc} + \delta_{aq}\delta_{bp}\delta_{sc}\delta_{rd}
\end{aligned} \tag{5.76}
$$

Inserting this result into the original expression and substituting to similar indicies will yield,

$$
L_{2a} = \frac{1}{2}\sum_{cd} \langle ab|cd\rangle \, t_{ij}^{cd}. \tag{5.77}
$$

A very similar computation will yield the following result for the next linear term,

$$
L_{2b} = \frac{1}{2}\sum_{kl} \langle kl|ij\rangle \, t_{kl}^{ab}. \tag{5.78}
$$

The last linear term is somewhat different, however,

$$
L_{2c} = -\sum_{k} c\left(\langle bk|cj\rangle \, t_{ik}^{ac} - \langle bk|ci\rangle \, t_{jk}^{ac} - \langle ak|cj\rangle \, t_{ik}^{bc} + \langle ak|ci\rangle \, t_{jk}^{bc}.\right) \tag{5.79}
$$

After long last, we have only the quadratic term to deal with,

$$Q = \frac{1}{8} \sum_{pqrs} \sum_{\substack{k>l \\ c>d}} \sum_{\substack{m>n \\ e>f}} \langle pq|rs \rangle \langle 0| \{\hat{i}^\dagger \hat{j}^\dagger \hat{b}\hat{a}\}\{\hat{p}^\dagger \hat{q}^\dagger \hat{s}\hat{r}\}\{\hat{c}^\dagger \hat{d}^\dagger \hat{l}\hat{k}\}\{\hat{e}^\dagger \hat{f}^\dagger \hat{n}\hat{m}\} |0\rangle \, t_{kl}^{dc} t_{mn}^{ef}. \tag{5.80}$$

In this expression there are no non-zero contractions between the third and fourth normal ordered operator string. We therefore need to contract operators in the first normal-ordered string with operators either in the third or four string, and the operator in the second string with the rest.

We start by contracting all operators in the first normal-ordered string with all the operators in the fourth normal-ordered string,

$$\begin{aligned} &\frac{1}{8} \sum_{pqrs} \sum_{\substack{k>l \\ c>d}} \sum_{\substack{m>n \\ e>f}} \langle pq|rs \rangle \langle 0| \{\hat{i}^\dagger \hat{j}^\dagger \hat{b}\hat{a}\}\{\hat{p}^\dagger \hat{q}^\dagger \hat{s}\hat{r}\}\{\hat{c}^\dagger \hat{d}^\dagger \hat{l}\hat{k}\}\{\hat{e}^\dagger \hat{f}^\dagger \hat{n}\hat{m}\} |0\rangle \, t_{kl}^{cd} t_{mn}^{ef} \\ &\qquad = \frac{1}{8} \sum_{pqrs} \sum_{\substack{k>l \\ c>d}} \langle pq|rs \rangle \langle 0| \{\hat{p}^\dagger \hat{q}^\dagger \hat{s}\hat{r}\}\{\hat{c}^\dagger \hat{d}^\dagger \hat{l}\hat{k}\} |0\rangle \, t_{kl}^{cd} t_{ij}^{ab}. \end{aligned} \tag{5.81}$$

There are four possible ways to contract this last term, resulting in

$$\frac{1}{2} \sum_{\substack{k>l \\ c>d}} \langle kl|cd \rangle \, t_{kl}^{cd} t_{ij}^{ab}. \tag{5.82}$$

We get the same result by contracting the four operators in the first string with the four operators in the third string, cancelling the factor $\frac{1}{2}$, eventually yielding a result equal to $\Delta E_{\mathrm{CCD}} t_{ij}^{ab}$, which we see by comparing this result to Equation 5.51.

There are four remaining reasonable classes in which to sort the permutations of contractions that remain;

a the two hole operators in the first string are contracted with the third or fourth operator string, yielding equal results;

b one hole and one particle operators in the first string are contracted with operators in the third string, the rest of the operators in the first string are contracted with operators in the fourth string;

c two particle operators and one hole operator from the first string are contracted with operators in the third string, the last hole operator is contracted with an operator in the fourth string;

d one particle operator and two hole operators are contracted with operators in the third string and the last particle operator with an operator in the fourth string.

The results for class a and class b are agruably the least complicated to compute, yielding the following,

$$\begin{aligned} Q_a &= \frac{1}{16} \sum_{pqrs} \sum_{klcd} \langle pq|rs \rangle \langle 0| \{\hat{p}^\dagger \hat{q}^\dagger \hat{s}\hat{r}\}\{\hat{l}\hat{k}\}\{\hat{c}^\dagger \hat{d}^\dagger\} |0\rangle \, t_{ij}^{cd} t_{kl}^{ab} \\ &= \frac{1}{4} \sum_{klcd} \langle kl|rs \rangle \, t_{ij}^{cd} t_{kl}^{ab} \end{aligned} \tag{5.83}$$

$$
\begin{aligned}
Q_b &= \frac{1}{4} \sum_{pqrs} \sum_{klcd} \langle pq|rs \rangle \langle 0| \{\hat{p}^\dagger \hat{q}^\dagger \hat{s}\hat{r}\}\{\hat{c}^\dagger \hat{k}\}\{\hat{d}^\dagger \hat{l}\} |0\rangle \, (t_{ik}^{ac} t_{jl}^{bd} - t_{ik}^{bc} t_{jl}^{ad}) \\
&= \sum_{klcd} \langle kl|cd \rangle \, (t_{ik}^{ac} t_{jl}^{bd} - t_{ik}^{bc} t_{jl}^{ad}) = \sum_{klcd} \langle kl|cd \rangle \, (t_{ik}^{ac} t_{jl}^{bd} - t_{ik}^{bd} t_{jl}^{ac})
\end{aligned} \tag{5.84}
$$

The sets of terms for class c and d can each be generated in two distinct ways, dependent on the choice of the tree operators from the first operator string ($\hat{i}^\dagger \hat{a}\hat{b}$ or $\hat{j}^\dagger \hat{a}\hat{b}$ for c and $\hat{i}^\dagger \hat{j}^\dagger \hat{a}$ or $\hat{i}^\dagger \hat{j}^\dagger \hat{b}$ for d). In each case there are 16 possibilities; the three operators from the first string can be contracted with operators in both the third or fourth string in four ways and the remaining operators can then be contracted in two ways. All these possibilities lead to equivalent results. For example, here is the first Q_c term,

$$
\begin{aligned}
&\frac{1}{8} \sum_{pqrs} \sum_{klcd} \sum_{mnef} \langle pq|rs \rangle \langle 0| \{\hat{i}^\dagger \hat{j}^\dagger \hat{b}\hat{a}\}\{\hat{c}^\dagger \hat{d}^\dagger \hat{l}\hat{k}\}\{\hat{c}^\dagger \hat{d}^\dagger \hat{l}\hat{k}\}\{\hat{e}^\dagger \hat{f}^\dagger \hat{n}\hat{m}\} |0\rangle \, t_{kl}^{cd} t_{mn}^{ef} \\
&\qquad = -\frac{1}{8} \sum_{pqrs} \sum_{klcd} \langle pq|rs \rangle \langle 0| \{\hat{p}^\dagger \hat{q}^\dagger \hat{s}\hat{r}\}\{\hat{c}^\dagger \hat{d}^\dagger \hat{k}\}\{\hat{l}\} |0\rangle \, t_{kj}^{cd} t_{li}^{ab} |0\rangle
\end{aligned} \tag{5.85}
$$

The remaining operators in this expression can be contracted in four ways,

$$
\begin{aligned}
&\langle 0| \{\hat{p}^\dagger \hat{q}^\dagger \hat{s}\hat{r}\}\{\hat{c}^\dagger \hat{d}^\dagger \hat{k}\}\{\hat{l}\} + \{\hat{p}^\dagger \hat{q}^\dagger \hat{s}\hat{r}\}\{\hat{c}^\dagger \hat{d}^\dagger \hat{k}\}\{\hat{l}\} \\
&\quad + \{\hat{p}^\dagger \hat{q}^\dagger \hat{s}\hat{r}\}\{\hat{c}^\dagger \hat{d}^\dagger \hat{k}\}\{\hat{l}\} + \{\hat{p}^\dagger \hat{q}^\dagger \hat{s}\hat{r}\}\{\hat{c}^\dagger \hat{d}^\dagger \hat{k}\}\{\hat{l}\} |0\rangle
\end{aligned} \tag{5.86}
$$

$$
= \delta_{pl}\delta_{qk}\delta_{rd}\delta_{sc} - \delta_{pk}\delta_{ql}\delta_{rd}\delta_{sc} - \delta_{pl}\delta_{qk}\delta_{rc}\delta_{sd} + \delta_{pk}\delta_{ql}\delta_{rc}\delta_{sd} \tag{5.87}
$$

Some algebraic extertion will eventually lead to,

$$
-\frac{1}{2} \sum_{klcd} \langle kl|cd \rangle \, t_{ik}^{ab} t_{jl}^{cd}. \tag{5.88}
$$

A similar computation provides the second Q_c term,

$$
-\frac{1}{2} \sum_{klcd} \langle kl|cd \rangle \, t_{ik}^{cd} t_{jl}^{ab}. \tag{5.89}
$$

These two terms give us,

$$
Q_c = -\frac{1}{2} \sum_{klcd} \langle kl|cd \rangle \, (t_{ik}^{ab} t_{jl}^{cd} - t_{ik}^{cd} t_{jl}^{ab}) \tag{5.90}
$$

Treating the class d terms gives,

$$
Q_d - \frac{1}{2} \sum_{klcd} \langle kl|cd \rangle \, (t_{ij}^{ac} t_{kl}^{bd} - t_{ij}^{bd} t_{kl}^{ac}). \tag{5.91}
$$

Combining all the quadratic terms will now yield the same as in Equation 5.50, and we can conclude that an algebraic derivation of the coupled cluster method is equivalent to the configuration space derivation.

5.3 The Coupled Cluster Equations

In general there is a more useful and compact approach that can be used to derive the coupled cluster equations, compared to the lengthy derivation of the CCD equations above. We start by inserting the coupled cluster wavefunctions into the time-independent Schrödinger equation,

$$\hat{H}_N e^{\hat{T}} |\Phi_0\rangle = \Delta E e^{\hat{T}} |\Phi_0\rangle . \tag{5.92}$$

In order to find an expression for the energy and amplitude equations one could try to left-project with $\langle\Phi_0|$. This would propel us in the same direction as in the previous section, i.e. Equation 5.17 and onwards. Instead, we multipy from the left with $e^{-\hat{T}}$ first, and then left-project with $\langle\Phi_0|$,

$$\begin{aligned} \langle\Phi_0| e^{-\hat{T}} \hat{H}_N e^{\hat{T}} |\Phi_0\rangle &= \langle\Phi_0| e^{-\hat{T}} \Delta E e^{\hat{T}} |\Phi_0\rangle \\ \rightarrow \langle\Phi_0| e^{-\hat{T}} \hat{H}_N e^{\hat{T}} |\Phi_0\rangle &= \Delta E. \end{aligned} \tag{5.93}$$

Left-projecting with an excited state, $\left\langle\Phi_{ij\dots}^{ab\dots}\right|$ will give us an expression for the corresponding amplitude $t_{ij\dots}^{ab\dots}$,

$$\left\langle\Phi_{ij\dots}^{ab\dots}\right| e^{-\hat{T}} \hat{H}_N e^{\hat{T}} |\Phi_0\rangle = 0. \tag{5.94}$$

Now we have obtained a *non-Hermitian*[2], similarity-transformed Hamiltonian,

$$\mathscr{H} = e^{-\hat{T}} \hat{H}_N e^{\hat{T}}, \tag{5.95}$$

which has $|\Phi_0\rangle$ as right eigenfunction and E as the corresponding eigenvalue. Importantly, a similarity-transformation will not change the eigenvalue spectrum of the operator. This holds for any operator or matrix.

Proving this is not an exercise in perseverance and toil. Consider some matrix A, and the matrix C which is a square, non-singular matrix of the same order as A. We say that the matrices A and $C^{-1}AC$ are *similar*, and $C^{-1}AC$ is the *similarity transformation* of A. If $(\lambda, \mathbf{x})$ is an eigenvalue-eigenvector pair of A, then $(\lambda, C^{-1}\mathbf{x})$ is the eigenvalue-eigenvector pair for $C^{-1}AC$,

$$(C^{-1}AC)C^{-1}\mathbf{x} = C^{-1}A\mathbf{x} = \lambda C^{-1}\mathbf{x}. \tag{5.96}$$

A benefit of the similarity-transformed Hamiltionians that we will take advantage of, is that we can write the operators more expicitly by applying the Baker-Campbell-Haussdorff expansion[9, 4, 29],

$$\begin{aligned} e^{-\hat{B}} \hat{A} e^{\hat{B}} =& (1 - \hat{B} + \frac{1}{2}\hat{B}^2 - \frac{1}{3!} + \dots)\hat{A}(1 + \hat{B} + \frac{1}{2} + \frac{1}{3!}\hat{B}^3 + \dots) \\ =& \hat{A} + (\hat{A}\hat{B} - \hat{B}\hat{A}) + \frac{1}{2}(\hat{A}\hat{B}^2 + 2\hat{B}\hat{A}\hat{B} + \hat{B}^2\hat{A}) \\ &+ \frac{1}{3!}(\hat{A}\hat{B}^3 - 3\hat{B}\hat{A}\hat{B}^2 + 3\hat{B}^2\hat{A}\hat{B} - \hat{B}^3\hat{A}) + \dots \\ =& \hat{A} + [\hat{A}, \hat{B}] + \frac{1}{2}\{(\hat{A}\hat{B} - \hat{B}\hat{A})\hat{B} - \hat{B}(\hat{A}\hat{B} - \hat{B}\hat{A})\} \\ &+ \frac{1}{3!}\{[(\hat{A}\hat{B} - \hat{B}\hat{A})\hat{B} - \hat{B}(\hat{A}\hat{B} - \hat{B}\hat{A})]\hat{B} \\ &- \hat{B}[(\hat{A}\hat{B} - \hat{B}\hat{A})\hat{B} - \hat{B}(\hat{A}\hat{B} - \hat{B}\hat{A})]\} + \dots \\ =& \hat{A} + [\hat{A}, \hat{B}] + \frac{1}{2}[[\hat{A}, \hat{B}], \hat{B}] + \frac{1}{3!}[[[\hat{A}, \hat{B}], \hat{B}], \hat{B}] + \dots . \end{aligned} \tag{5.97}$$

[2]We will show later that this non-Hermiticity is somewhat problematic.

Applying the Baker-Campbell-Haussdorff expansion to the similarity-transformed Hamiltonians yields

$$\begin{aligned}\mathscr{H} = e^{-\hat{T}}\hat{H}_N e^{\hat{T}} = \hat{H}_N + [\hat{H}_N, \hat{T}] + \frac{1}{2}[[\hat{H}_N, \hat{T}], \hat{T}] + \frac{1}{3!}[[[\hat{H}_N, \hat{T}], \hat{T}], \hat{T}] \\ + \frac{1}{4!}[[[[\hat{H}_N, \hat{T}], \hat{T}], \hat{T}], \hat{T}].\end{aligned} \tag{5.98}$$

Notice the absence of an "and so on"-operator $(\dots)$ in this expression. The Baker-Campbell-Hausdorff expansion for the electronic Hamiltionian, containing at most two-particle interactions, will terminate with the four-fold commutator. We will show this shortly.

By applying the generalised Wick's theorem to the Baker-Campbell-Hausdorff expansion of the Hamiltonian in Equation 5.98, we will be confronted with a vast simplification. Applying the generalised Wick's theorm to a commutator gives the following

$$[\hat{A}, \hat{B}] = \hat{A}\hat{B} - \hat{B}\hat{A} = \{\hat{A}\hat{B}\} + \{\overbracket{\hat{A}\hat{B}}\} - \{\hat{B}\hat{A}\} - \{\overbracket{\hat{B}\hat{A}}\}, \tag{5.99}$$

where $\hat{A}$ and $\hat{B}$ are normal-ordered operators, each with an even number of creation- and annihilation operators[3]. In this expression $\{\}$ denotes a normal-ordering of the operators inside the braces and $\{\overbracket{\hat{A}\hat{B}}\}$ represents a sum of all normal-ordered products of operators in which there are one or more contractions between creation or annihilation operators in $\hat{A}$ and those in $\hat{B}$. We must also have that

$$\{\hat{A}\hat{B}\} = \{\hat{B}\ \hat{A}\}, \tag{5.100}$$

since the two operators both contain an even number of creation- and annihilation operators. This means that what remains of Equation 5.99 is simply

$$[\hat{A}, \hat{B}] = \{\overbracket{\hat{A}\hat{B}}\} - \{\overbracket{\hat{B}\hat{A}}\}. \tag{5.101}$$

The general m-fold cluster operator T_m contains some number of creation operators $\hat{a}^\dagger, \hat{b}^\dagger \dots$ and hole operators $\hat{i}, \hat{j}, \dots$, and the only possible non-zero contractions are $\overbracket{\hat{a}\hat{b}^\dagger} = \delta_{ab}$ and $\overbracket{\hat{i}^\dagger\hat{j}} = \delta_{ij}$. Moreover, since the different cluster operators commute, no nonzero conatractions exist between different $\hat{T}_m$ operators. Ergo, in the nested commutators from Equation 5.98, we only see surviving terms between the Hamiltonian $\hat{H}_N$ and one or more of the cluster operators $\hat{T}_m$. This accounts for the natural truncation at the four-fold commutator. In fact, we can rewrite the Baker-Campbell-Haussdorff-expanded similarity-transformed Hamiltonian as

$$\mathscr{H} = e^{-\hat{T}}\hat{H}_N e^{\hat{T}} = \hat{H}_N + \overbracket{\hat{H}_N\hat{T}} + \frac{1}{2}\overbracket{\hat{H}_N\overline{\hat{T}\hat{T}}} + \frac{1}{3!}\overbracket{\hat{H}_N\overline{\hat{T}\hat{T}\hat{T}}} + \frac{1}{4!}\overbracket{\hat{H}_N\overline{\hat{T}\hat{T}\hat{T}\hat{T}}}, \tag{5.102}$$

where the notation combining a contraction line and a horizontal bar indicates a sum over all terms in which the Hamiltonian $\hat{H}_N$ is connected by at least one contraction with each of the following cluster operators $\hat{T}$.

Disconnected clusters on the form $\hat{T}_m\hat{T}_n$, which can be found in the coupled cluster wavefunction are not present in the Baker-Campbell-Hausdorff expansion of the similarity-transformed Hamiltonian. This is true also for the coupled cluster amplitude equations, which may be written

$$\langle\Phi_0| e^{-\hat{T}}\hat{H}_N e^{\hat{T}} |\Phi_0\rangle = \langle\Phi_0| \hat{H}_N e^{\hat{T}} |\Phi_0\rangle_C = \Delta E \tag{5.103}$$

$$\langle\Phi_{ij\dots}^{ab\dots}| e^{-\hat{T}}\hat{H}_N e^{\hat{T}} |\Phi_0\rangle = \langle\Phi_{ij\dots}^{ab\dots}| \hat{H}_N e^{\hat{T}} |\Phi_0\rangle_C = 0, \tag{5.104}$$

[3]It is not a coincidence that both the normal-ordred Hamiltonian $\hat{H}_N$ and the cluster operator $\hat{T}$ satisfy these condtions

where the inclusion of only connected terms is underlined.

The CCSD equations take the form

$$\langle\Phi_0|\,\hat{H}_N\Big(\hat{T}_1+\frac{1}{2}\hat{T}_1^2+\hat{T}_2\Big)\,|\Phi_0\rangle_C=\Delta E \tag{5.105}$$

$$\langle\Phi_i^a|\,\hat{H}_N\Big(1+\hat{T}_1+\frac{1}{2}\hat{T}_1^2+\frac{1}{3!}\hat{T}_1^3+\hat{T}_1\hat{T}_2+\hat{T}_2\Big)\,|\Phi_0\rangle_C=0 \tag{5.106}$$

$$\big\langle\Phi_{ij}^{ab}\big|\,\hat{H}_N\Big(1+\hat{T}_1+\frac{1}{2}\hat{T}_1^2+\frac{1}{3!}\hat{T}_1^3+\frac{1}{4!}\hat{T}_1^4+\hat{T}_2+\frac{1}{2}\hat{T}_2^2+\hat{T}_1\hat{T}_2+\frac{1}{2}\hat{T}_1^2\hat{T}_2\Big)\,|\Phi_0\rangle_C=0. \tag{5.107}$$

For CCSDT, the energy expression is the same, while the amplitude equations take the form

$$\langle\Phi_i^a|\,\hat{H}_N\Big(1+\hat{T}_1+\frac{1}{2}\hat{T}_1^2+\frac{1}{3!}\hat{T}_1^3+\hat{T}_1\hat{T}_2+\hat{T}_2+\hat{T}_3\Big)\,|\Phi_0\rangle_C=0 \tag{5.108}$$

$$\begin{aligned}\big\langle\Phi_{ij}^{ab}\big|\,\hat{H}_N\Big(&1+\hat{T}_1+\frac{1}{2}\hat{T}_1^2+\frac{1}{3!}\hat{T}_1^3+\frac{1}{4!}\hat{T}_1^4+\hat{T}_2\\&+\frac{1}{2}\hat{T}_2^2+\hat{T}_1\hat{T}_2+\frac{1}{2}\hat{T}_1^2\hat{T}_2+\hat{T}_3+\hat{T}_1\hat{T}_3\Big)\,|\Phi_0\rangle_C=0\end{aligned} \tag{5.109}$$

$$\begin{aligned}\big\langle\Phi_{ij}^{ab}\big|\,\hat{H}_N\Big(&\hat{T}_2+\hat{T}_3+\frac{1}{2}\hat{T}_2^2+\hat{T}_1\hat{T}_2+\hat{T}_2\hat{T}_3+\hat{T}_1\hat{T}_3\\&+\frac{1}{2}\hat{T}_1^2\hat{T}_2+\frac{1}{2}\hat{T}_1\hat{T}_2^2+\frac{1}{2}\hat{T}_1^2\hat{T}_3+\frac{1}{3!}\hat{T}_1^3\hat{T}_2)\,|\Phi_0\rangle_C=0\end{aligned} \tag{5.110}$$

The coupled cluster with singles and doubles equations are provided in Appendix D.

5.4 A Variational Formulation of Coupled Cluster

In the following section we follow the narrative of Kvaal[46] closely.

The Coupled Cluster method is very successful in computing energies, but computing other expectations values has been a problem. For instance we see that the way we compute the coupled cluster energy,

$$E_{\mathrm{CC}}=\langle\Phi|e^{-\hat{T}}\hat{H}e^{\hat{T}}|\Phi\rangle\,, \tag{5.111}$$

is not the same as one would compute the energy of the system variationally,

$$\langle\hat{H}\rangle_{\mathrm{var}}=\frac{\langle\Psi|\hat{H}|\Psi\rangle}{\langle\Psi|\Psi\rangle}=\frac{\langle\Phi|e^{\hat{T}^\dagger}\hat{H}e^{\hat{T}}|\Phi\rangle}{\langle\Phi|e^{\hat{T}^\dagger}e^{\hat{T}}|\Phi\rangle}. \tag{5.112}$$

Moreover, the similarity transformed operators are not Hermitian. This can be showed by inference

$$\hat{T}_1^\dagger=\Big(\sum_{ia}t_i^a\hat{a}^\dagger\hat{i}\Big)^\dagger\sum_{ia}(t_i^a)^*\hat{i}^\dagger\hat{a}\neq\hat{T}_1, \tag{5.113}$$

from which it follows that

$$\Big(e^{-\hat{T}}\hat{H}e^{\hat{T}}\Big)^\dagger=(e^{\hat{T}})^\dagger\hat{H}(e^{-\hat{T}})^\dagger=e^{\hat{T}^\dagger}\hat{H}e^{-\hat{T}^\dagger}\neq e^{-\hat{T}}\hat{H}e^{\hat{T}}. \tag{5.114}$$

Variational computations as in Equation 5.112 has been attempted by Cizek[10] and Fink[19]. Regrettably, the coupled cluster exponential wavefunction is not a variationally optimal wavefunction, as it give rise to series expansions in the numerator and denominator in the expression for the variational expectation value. For a general operator $\hat{O}$, we have

$$\begin{aligned}\langle\hat{O}\rangle_{\mathrm{var}}&=\frac{\langle\Psi|\hat{O}|\Psi\rangle}{\langle\Psi|\Psi\rangle}=\frac{\langle\Phi|e^{\hat{T}^\dagger}\hat{O}e^{\hat{T}}|\Phi\rangle}{\langle\Phi|e^{\hat{T}^\dagger}e^{\hat{T}}|\Phi\rangle}\\&=\frac{\langle\Phi|[1+\hat{T}^\dagger+\frac{1}{2!}(\hat{T}^\dagger)^2+\frac{1}{3!}(\hat{T}^\dagger)^3+\ldots]\hat{O}[1+\hat{T}+\frac{1}{2!}\hat{T}2+\frac{1}{3!}\hat{T}^3+\ldots]|\Phi\rangle}{\langle\Phi|[1+\hat{T}^\dagger+\frac{1}{2!}(\hat{T}^\dagger)^2+\frac{1}{3!}(\hat{T}^\dagger)^3+\ldots][1+\hat{T}+\frac{1}{2!}\hat{T}^2+\frac{1}{3!}\hat{T}^3+\ldots]|\Phi\rangle}.\end{aligned} \tag{5.115}$$

In contrast with the expansions of the coupled cluster amplitude equations, which truncates naturally after products of four $\hat{T}$ operators, the expansions for $e^{\hat{T}^\dagger}$ and $e^{\hat{T}}$ terminates only if the total excitation level represented by a product of $\hat{T}$ operators exceed the number of electrons in the wavefunctions. This means that the number of terms and the computational effort required to compute expectation values in this way is usually very high.

An idea is to simply use a similar expression to the coupled cluster energy expression

$$\langle O \rangle_{\text{Goldstone}} = \langle \Phi | e^{-\hat{T}} \hat{O} e^{\hat{T}} | \Phi \rangle \, . \tag{5.116}$$

The problem with this expression, as well as with Equation 5.115, is that none of them conform with the Hellmann-Feynman theorem and the problem remains, the coupled cluster energy is arrived at non-variationally, and is therefore non-stationary.

5.4.1 The Hellmann-Feynman Theorem

The Hellmann-Feynmann[17] theorem relates the first order change of total energy with respect to a parameter to the first order change of the Hamiltonian with respect to the same parameters,

$$\left.\frac{dE}{d\alpha}\right|_{\alpha=0} = \frac{\partial}{\partial t} \langle \Psi_\alpha | \hat{H} | \Psi_\alpha \rangle \, , \tag{5.117}$$

where Ψ is the exact state, variationally determined from the Hamiltonian of the system, and $\Psi_\alpha = N(\Psi + \alpha\delta\Psi)$ is a variation of this state, implicitly dependent on the parameter α.

Proof of the Hellmann-Feynman theorem

Using the following conditions,

$$\hat{H}_\lambda \left|\psi_\lambda\right\rangle = E_\lambda \left|\psi_\lambda\right\rangle \tag{5.118}$$

$$\langle \psi_\lambda | \psi_\lambda \rangle = 1, \tag{5.119}$$

we prove

$$\frac{\partial E_\lambda}{\partial \lambda} = \langle \psi_\lambda | \frac{\partial \hat{H}}{\partial \lambda} \left|\psi_\lambda\right\rangle . \tag{5.120}$$

Now,

$$E_\lambda = \langle \psi_\lambda | \, \hat{H} \left|\psi_\lambda\right\rangle = \int \psi_\lambda \hat{H} \psi_\lambda^* dr \tag{5.121}$$

whence,

$$\begin{aligned} \frac{\partial E_\lambda}{\partial \lambda} &= \int \psi_\lambda \frac{\hat{H}}{\partial \lambda} \psi_\lambda^* dr + \int \frac{\psi_\lambda}{\partial \lambda} \hat{H} \psi_\lambda^* dr + \int \psi_\lambda \hat{H} \frac{\psi_\lambda^*}{\partial \lambda} dr \\ &= \int \psi_\lambda \frac{\hat{H}}{\partial \lambda} \psi_\lambda^* dr + E_\lambda \int \frac{\psi_\lambda}{\partial \lambda} \psi_\lambda^* dr + E_\lambda \int \psi_\lambda \frac{\psi_\lambda^*}{\partial \lambda} dr \\ &= \int \psi_\lambda \frac{\hat{H}}{\partial \lambda} \psi_\lambda^* dr + E_\lambda \frac{\partial}{\partial \lambda} \langle \psi_\lambda | \psi_\lambda \rangle = \langle \psi_\lambda | \frac{\partial \hat{H}}{\partial \lambda} \left|\psi_\lambda\right\rangle . \end{aligned} \tag{5.122}$$

By treating an observable of the system as a perturbation of the Hamiltonian,

$$\hat{H}'(\alpha) = \hat{H} + \alpha \hat{V},$$

the Hellman-Feynman theorem provides us with a way to evaluate the expected value of this observable if we have the exact wavefunction and energy,

$$\left.\frac{dE}{d\alpha}\right|_{\alpha=0} = \frac{\partial}{\partial \alpha} \langle \Psi_\alpha | \hat{H} + \alpha \hat{O} | \Psi_\alpha \rangle = \langle \hat{O} \rangle \, . \tag{5.123}$$

The problem with some computational techniques, like the coupled cluster method, is that the final energy is not variationally determined (non-stationary), and we cannot invoke the Hellmann-Feynman theorem to simplify computation of molecular properties. At first, it would appear that one would have to resort to a more cumbersome computation, like the expansion of clustes operators above (Equation 5.115). But fortunately, there exists a way to reformulate the energy function of a non-variational wavefunction in such a way that the energy is stationary with respect to the variables of the new formulation.

Consider an energy that depends on two sets of parameters. The parameter α which describes a perturbation and the parameters α which describe the wavefunction. The optimal energy $E(\alpha)$ is obtained by an optimised set of parameters λ^*, which are inserted into the energy function

$$E(\alpha) = E(\alpha, \lambda^*), \tag{5.124}$$

the values for α and λ^* are obtained as the solution to some set of equations

$$\mathbf{f}(\alpha, \lambda^*) = 0 \quad \forall \alpha, \tag{5.125}$$

For *variational* wavefunctions, this condition corresponds to the stationarity requirement,

$$\frac{\partial E_{\mathrm{var}}(\alpha, \lambda)}{\partial \lambda}\bigg|_{(\lambda=\lambda^*)} = 0 \quad \forall \alpha, \tag{5.126}$$

but not for *non-variational* wavefunctions. Writing out this derivative yields,

$$\frac{dE(\alpha)}{d\alpha} = \frac{dE(\alpha, \lambda)}{d\alpha}\bigg|_{(\lambda=\lambda^*)} = \frac{\partial E(\alpha, \lambda)}{\partial \alpha}\bigg|_{(\lambda=\lambda^*)} + \frac{\partial E(\alpha, \lambda)}{\partial \lambda}\bigg|_{(\lambda=\lambda^*)} \cdot \frac{\partial \lambda}{\partial}\alpha\bigg|_{(\lambda=\lambda^*)}. \tag{5.127}$$

For a variational wavefunction, the last term will vanish due to the stationarity condition in Equation 5.126. This would leave us with

$$\frac{dE_{\mathrm{var}}(\alpha)}{d\alpha} = \frac{\partial E(\alpha, \lambda)}{\partial \alpha}\bigg|_{(\lambda=\lambda^*)}, \tag{5.128}$$

i.e. that the total derivative corresponds to the partial derivative. This means that if the variational energy corresponds to an expectation value $E_{\mathrm{var}}(\alpha, \lambda) = \langle \lambda | \hat{H}(\alpha) | \lambda \rangle$, and the perturbed system is described by the Hamiltonian $\hat{H}(\alpha) = \hat{H} + \alpha \hat{V}$, we recover the presumed expression

$$\frac{dE(\alpha, \lambda)}{d\alpha}\bigg|_{(\alpha=0)}, \tag{5.129}$$

in accordance with first-order perturbation theory and the Hellmann-Feynmann theorem.

But if we look at nonvariational energies, Equation 5.127, will not simplify to just the partial derivative, since the stationarity condition does not hold. What we do is replace the now nonvariational function $E(\alpha, \lambda)$ by a new function $L(\alpha, \lambda, \bar{\lambda})$ with a stationary point $(\lambda^*, \bar{\lambda}^*)$ that satisfies the nonvariational condition Equation 5.125 , and whose values at this point correspond to the optimal energy. Indeed, we apply Langrange's method of undetermined multipliers, by regarding the energy $E(\alpha, \lambda)$ a an *unconstrained* optimisation problem, but subject to the constraints of the variational parameters λ, which satisfy Equation 3.17;

$$L(\alpha, \lambda, \bar{\lambda}) = E(\alpha, \lambda) + \bar{\lambda} \cdot \mathbf{f}(\alpha, \lambda). \tag{5.130}$$

A necessary condition for the optimum Lagrange multipliers $\bar{\lambda}^*$ to be unique is that the the Jacobian of $\mathbf{f}$, $\mathscr{J} \equiv \partial \mathbf{f}(\alpha, \lambda)/\partial \lambda$ is non-singular and invertible.

5.4.2 The Lagrangian Formulation of Coupled Cluster

As we outlined in the previous section, the solution to making the coupled cluster theory into a variational theory is to find a set of equations which are zero for a set of parameters (Equation 5.125). These parameters should in turn provide the optimal energy by insertion into the expression for energy. Luckily, Helgaker and Jørgensen[32, 33] had the insight to realise that we are already given such a set of parameters and equations in the formulation of coupled cluster, namely the amplitudes and the amplitude equations respectively. The Hellmann-Feynman theorem will be baked into the very definition of such a expectation value functional,

$$\langle \hat{O} \rangle_{\text{H-F}} = \mathscr{L}_{\text{O}}(\alpha^*, \lambda^*, \bar{\lambda}^*) = E(\alpha^*, \lambda^*, \bar{\lambda}^*) + \bar{\lambda}^* \cdot \mathbf{f}(\alpha^*, \lambda^*). \tag{5.131}$$

This equation is essentially a restatement of Equation 5.130, with the optimal parameters.

More specifically, we simplify the notation in some measure and state the coupled cluster energy Lagrangian,

$$\mathscr{L}_{\hat{H}}(t, \lambda) = \langle \Phi | e^{-\hat{T}} \hat{H} e^{\hat{T}} | \Phi \rangle + \sum_{\mu} \lambda_\mu \langle \Phi | X_\mu^\dagger e^{-\hat{T}} \hat{H} e^{\hat{T}} | \Phi \rangle = \langle \Phi | (1 + \Lambda) e^{-\hat{T}} \hat{H} e^{\hat{T}} | \Phi \rangle , \tag{5.132}$$

where we have introduced $\Lambda = \sum_\mu X_\mu^\dagger$. Here, $X_\mu^\dagger$ is a general relaxation operator, for instance $\hat{X}_1^\dagger = \{\hat{i}\hat{a}^\dagger\}$. So Λ written out is

$$\Lambda = \sum_{ia} \lambda_a^i \hat{i}^\dagger \hat{a} + \frac{1}{2!^2} \sum_{ijab} \lambda_{ab}^{ij} \hat{i}^\dagger \hat{a} \hat{j}^\dagger \hat{a} + \dots \tag{5.133}$$

The coupled cluster Lagrangian in Equation 5.132 can be rewritten with the use of density operators,

$$\mathscr{L}_{\hat{H}}(t, \lambda) = \text{tr}\{\hat{H}\hat{\rho}\}, \quad \hat{\rho} = e^{\hat{T}} |\Phi\rangle\langle\Phi| (1 + \Lambda) e^{-\hat{T}}, \tag{5.134}$$

in a pure state description. We check to see if the attributes of the density operator endures,

$$\begin{aligned}
\hat{\rho}^2 &= e^{\hat{T}} |\Phi\rangle\langle\Phi| (1 + \Lambda) e^{-\hat{T}} e^{\hat{T}} |\Phi\rangle\langle\Phi| (1 + \Lambda) e^{-\hat{T}} \\
&= e^{\hat{T}} |\Phi\rangle\langle\Phi| (1 + \Lambda) e^{-\hat{T}} + e^{\hat{T}} |\Phi\rangle \cancelto{0}{\langle\Phi|\Lambda|\Phi\rangle} \langle\Phi| e^{-\hat{T}} = \hat{\rho} \\
\text{Tr}\{\hat{\rho}\} &= \sum_p \langle \phi_p | e^{\hat{T}} |\Phi\rangle\langle\Phi| (1 + \Lambda) e^{-\hat{T}} | \phi_p \rangle = 1 \\
(\hat{\rho})^\dagger &= e^{-\hat{T}^\dagger} (1 + \Lambda^\dagger) |\Phi\rangle\langle\Phi| e^{\hat{T}^\dagger} \neq \hat{\rho}.
\end{aligned}$$

We see that another problem has presented itself, as the density operator is non-Hermitian. This leads us to the *bivariational*, Hellmann-Feynman conforming framework developed by Arponen[2].

5.4.3 The Bivariational Principle

Arponen approached the coupled cluster problem by employing a very general form of the variational principle called the bivariational principle. Letting $\hat{H}$, be a (possibly non-Hermitian) operator over Hilbert space $\mathcal{H}$, the bivariational expectation functional is defined by

$$\mathscr{E}_{\hat{H}} : \mathcal{H}' \times \mathcal{H} \to \mathbb{C}, \quad \mathscr{E}_{\hat{H}}(\tilde{\Psi}, \Psi) = \frac{\langle \tilde{\Psi} | \hat{H} | \Psi \rangle}{\langle \tilde{\Psi} | \Psi \rangle} = \frac{\text{tr}\left\{\hat{H}\hat{\rho}\right\}}{\text{tr}\{\rho\}}. \tag{5.135}$$

The main difference from the traditional and usual variational principle is that $\langle\tilde{\Psi}|$ and $|\Psi\rangle$ are treated as independent elements of the Hilbert space, and $\hat{\rho} = |\Psi\rangle\langle\tilde{\Psi}|$. Since the Hamiltonian

$\hat{H}$ is Hermitian, $\langle\tilde{\Psi}|$ and $|\Psi\rangle$ can be treated independently in the derivations of stationary conditions. However, we must have that $\langle\tilde{\Psi}|$ and $|\Psi\rangle$ are left- and right eigenvalues of the Hamiltonian, with the same eigenvalue

$$\hat{H}|\Psi\rangle = E|\Psi\rangle, \quad \langle\tilde{\Psi}|\hat{H} = \langle\tilde{\Psi}|E. \tag{5.136}$$

We alos have that $E = \mathcal{E}_{\hat{H}}(\tilde{\Psi}, \Psi)$ is the value at the stationary point.

We transition to coupled cluster theory by inserting the coupled cluster exponential wave functions, $|\Psi\rangle = e^{\hat{T}}|\Phi\rangle$ and $\langle\tilde{\Psi}| = \langle\Phi|e^{\tilde{T}}$, where $\tilde{T} = \tilde{t}X^{\dagger}$ are some general relaxation operator. The bivariational functional becomes

$$\mathscr{E}_{\hat{H}} = \frac{\langle\Phi|e^{\tilde{T}}\hat{H}e^{\hat{T}}|\Phi\rangle}{\langle\Phi|e^{\tilde{T}}e^{\hat{T}}|\Phi\rangle} \tag{5.137}$$

Varying this functional over all untruncated excitation and relaxation operators, $\hat{T}$ and $\tilde{T}$, is the foundation of variational coupled cluster theory[5], which is equivalent to full configuration interaction within the given single-particle basis set.

Now we wish to show that Arponen's framework corresponds to that of Helgaker and Jørgensen. We simplify the expression by performing a variable change $(\hat{T}, \tilde{T}) \to (\hat{T}, \hat{S})$, where S is a new relaxation operator. We start by introducing

$$\langle\omega| = \frac{\langle\tilde{\Psi}|e^{\hat{T}}}{\langle\tilde{\Psi}|\Psi\rangle}, \tag{5.138}$$

which satisfies $\langle\omega|\Phi\rangle = 1$, implying that there must exist an operator $\hat{S} = sX^{\dagger}$, such that $\langle\omega| = \langle\Phi|e^{\hat{S}}$. Then we can write,

$$\frac{\langle\tilde{\Psi}|e^{\hat{T}}}{\langle\tilde{\Psi}|\Psi\rangle} = \langle\Psi|e^{\hat{S}}, \to \langle\tilde{\Psi}| = \langle\tilde{\Psi}|\Psi\rangle\langle\Phi|e^{\hat{S}}e^{-\hat{T}}. \tag{5.139}$$

This enables us to rewrite the bivariational principle (Equation 5.137) to

$$\mathscr{E}_{\hat{H}} = \langle\Phi|e^{\hat{S}}e^{-\hat{T}}\hat{H}e^{\hat{T}}|\Phi\rangle, \tag{5.140}$$

which is an exact functional if $\hat{T}$ and $\hat{S}$ are not truncated. Comparing this expression to the coupled cluster Lagrangian in Equation 5.132, we can only conlude that our seemingly serendipitous algebra acrobatics has revealed that $e^{\hat{S}} = 1 + \Lambda$. Truthfully, we have strong indication the coupled cluster bivariational functional (Equation 5.137) is the same as the the coupled cluster Lagrangian (Equation 5.132)[4].

First order conditions of the coupled cluster energy Lagrangian in Equation 5.132 gives us a new set of amplitude equations,

$$\frac{\partial}{\partial\lambda_{\mu}}\mathscr{L}(t,\lambda) = \left\langle\Phi_{X_{\mu}}\middle|e^{-\hat{T}}\hat{H}e^{\hat{T}}\middle|\Phi\right\rangle = 0 \tag{5.141}$$

$$\frac{\partial}{\partial t_{\mu}}\mathscr{L}(t,\lambda) = \langle\Phi|(1+\Lambda)e^{-\hat{T}}[\hat{H}, X_{\mu}]e^{\hat{T}}|\Phi\rangle = 0. \tag{5.142}$$

Under constrained optimisation all partial derivatives vanish at the same point,

$$\left.\frac{\partial\mathscr{L}}{\partial\lambda_{\mu}}\right|_{t=t^*} = 0, \quad \left.\frac{\partial\mathscr{L}}{\partial t_{\mu}}\right|_{(t,\lambda)=(t^*,\lambda^*)} = 0, \quad \forall X_{\mu}. \tag{5.143}$$

[4]Pruning the expression in Equation 5.140 to only include single and double excitations will yield Arponen's *extended coupled cluster* (ECC) method[3]. This method has seen little use due to it's complexity.

What we have arrived at are amplitude equations both for the "bra part" and the "ket part" of the problem, which we refer to as the λ amplitude equations (Equation 5.142) and the τ amplitude equations (Equation 5.142), respectively. Notice that the τ amplitude equations only depend on τ, whilst the λ equations depend both on τ and λ. This means that the τ amplitude equations are solved iteratively first, and then the λ amplitudes are solved similarly. The full equations are given in Appendix D.

The benefit of going through the exercise of reformulating the coupled cluster framework entirely is that it is now possible to define operators,

$$\rho_p^q = \langle\tilde{\Psi}|c_p^\dagger c_q|\Psi\rangle \tag{5.144}$$

$$\rho_{pr}^{qs} = \langle\tilde{\Psi}|c_p^\dagger c_q^\dagger c_s c_r|\Psi\rangle\,, \tag{5.145}$$

which we can use to compute expectation values of operators, $\langle\hat{A}\rangle = \operatorname{tr}\left\{\rho\hat{A}\right\}$. Here, $\hat{A}$ is a general one- and two-body operator,

$$\hat{A} = a_q^p c_p^\dagger c_q + \frac{1}{4} a_{qs}^{pr} c_p^\dagger c_q^\dagger c_s c_r. \tag{5.146}$$

Then we have,

$$\langle\hat{A}\rangle = \langle\tilde{\Psi}|\hat{A}|\Psi\rangle = a_q^p \langle\tilde{\Psi}|c_p^\dagger|\Psi\rangle + \frac{1}{4} a_{qs}^{pr} \langle\tilde{\Psi}|c_p^\dagger c_q^\dagger c_s c_r|\Psi\rangle = a_q^p \rho_p^q + \frac{1}{4} a_{qs}^{pr} \rho_{pr}^{qs}. \tag{5.147}$$

5.5 Generalisation in Time

Here, we will outline a derivation of the orbital-adaptive time-dependent coupled cluster method, a generalisation in time for the coupled cluster method put forth by Kvaal[45]. The method inherits both size-extensivity and size-consistency from the coupled cluster method and is a hierarchy of approximations to the multi-configurational time-dependent Hartree method for fermions.

We now define a time-dependent generalisation of the bivariational principle (Equation 5.135). This is similar to the usual time-dependent action functional and the time-dependent Schrödinger equation can be recovered from it,

$$\mathcal{S}[\Psi'(\cdot), \Psi(\cdot)] = \int_0^T dt \frac{\langle\Psi'(t)|\left(i\hbar\frac{\partial}{\partial t} - \hat{H}\right)|\Psi(t)\rangle}{\langle\Psi'(t)|\Psi(t)\rangle}. \tag{5.148}$$

Functionals like these are quite common throughout the historical literature on quantum mechanics, appearing as early as in Dirac[14]. The integral of the functional depends on all history for the system in question. By applying the principle of least action, requiring that the functional is stationary, $\delta\mathcal{S} = 0$, under all variations of $\langle\Psi'|$ and $|\Psi\rangle$ and vanishing in the endpoints $t = 0$ and $t = T$, gives us the following conditions

$$i\hbar\frac{\partial}{\partial t}|\Psi(t)\rangle = \hat{H}|\Psi(t)\rangle \quad -i\hbar\frac{\partial}{\partial t}\langle\Psi'| = \langle\Psi'|\hat{H}.$$

By a specific parametrisation of $\langle\Psi'|$, such that $\langle\Psi'|\Psi\rangle = 1$ we have indeed recovered the familiar time-dependent Schrödinger euqation.

Instead of venturing down this path, we will presuppose that it is possible that $\langle\Psi'|\Psi\rangle \neq 1$. Indeed, that $\langle\Psi'|$ and $|\Psi\rangle$ are independent. This means we must enact Arponen's[2] Hellmann-Feynman conforming bivariational principle, where the energy expectation functial is given by

$$\mathscr{E}_{\hat{H}}(\tau', \tau, \Phi', \Phi) = \frac{\langle\Phi'|e^{\hat{T}'}\hat{H}e^{\hat{H}}|\Phi\rangle}{\langle\Phi'|e^{\hat{T}'}e^{\hat{T}}|\Phi\rangle}. \tag{5.149}$$

We perform a variable change $(T', T) \to (\lambda, T)$, similarly to the section above, and introduce

$$\langle\tilde{\Psi}| = \frac{\langle\Psi'|}{\langle\Psi'|\Psi\rangle} = \langle\tilde{\Phi}|\,(1+\Lambda)e^{\hat{T}}, \tag{5.150}$$

Where Λ is the same as in Equation 5.133. The bivariational energy expectation functional in Equation 5.149 now becomes

$$\mathscr{E}_{\hat{H}}(\lambda, \tau, \tilde{\Phi}, \Phi) = \langle\tilde{\Phi}|(\hat{1}+\lambda)e^{-\hat{T}}\hat{H}e^{\hat{T}}|\Phi\rangle\,. \tag{5.151}$$

Disregarding the differene in $\tilde{\Phi}$ and Φ, this expression is the same as the coupled cluster expectation functional in Equation 5.140, where the interpretation is that the λs are Lagrange multipliers for a constrained energy minimisation problem. This is not the interpretation here, as the λ-part of the problem is seen as equally important.

We are now assuming biorthogonality in orbitals, $\langle\tilde{\phi}_p|\phi_q\rangle = \delta_{pq}$, but independence of bra and ket states otherwise. For a full Slater determinant state consisting of these orbitals, we have

$$\langle\tilde{\phi}_{p_1}\ldots\tilde{\phi}_{p_n}|\phi_{q_1}\ldots\phi_{q_n}\rangle = \delta_{p_q q_1}\ldots\delta_{p_N q_N}. \tag{5.152}$$

The second quantised operators associated with these Slater determinants are defined through

$$|\phi_{q_1}\ldots\phi_{q_n}\rangle \equiv c^\dagger_{p_1}\ldots c^\dagger_{p_N}\,|\rangle \qquad \langle\tilde{\phi}_{p_1}\ldots\tilde{\phi}_{p_n}| = \langle|\,\tilde{c}_{q_N}\ldots\tilde{c}_{q_1}. \tag{5.153}$$

These creation- and annihilation operators can furtermore be defined by,

$$c^\dagger_p = \int \phi_p(\mathbf{x})\Psi^\dagger(\mathbf{x})d\mathbf{x} \quad \tilde{c}_p = \int \tilde{\phi}_p(\mathbf{x})\Psi(\mathbf{x})d\mathbf{x}, \tag{5.154}$$

where $\Psi^\dagger$ and Ψ are field creation- and annihilation operators. This particular definition may seem like an unecessary and stringent tangent, but its purpose is to underline the dependence of the cluster operator $\hat{T}$ not only on the amplitudes τ, but also on the orbitals. This is an important point to emphasise, in "ordinary" coupled cluster theory, one thinks of the amplitudes as the only unknowns while keeping the orbitals fixed and the dependence on τ are 1-1. This becomes very important when one computes derivatives with respect to time of the cluster operators $\hat{T}$. Furthermore, the second quantised operators are subject to the anticommutator relation,

$$\{\tilde{c}_p, c^\dagger_q\} \equiv \tilde{c}_p c^\dagger_q + c^\dagger_q \tilde{c}_p \overset{!}{\equiv} \langle\tilde{\phi}_p|\phi_q\rangle = \delta_{pq}. \tag{5.155}$$

The time-dependent action(-like) functional (Equation 5.148) defining the Schrödinger dynamics becomes,

$$\begin{aligned}\mathcal{S}[\lambda, \tau, \tilde{\Phi}, \Phi] &= \int_0^T \left\langle\tilde{\Phi}\middle|(1+\Lambda)e^{-\hat{T}}\left(\frac{\partial}{\partial t} - \hat{H}\right)e^{\hat{T}}\middle|\Phi\right\rangle dt \\ &= \int_0^T i\hbar\left\langle\tilde{\Phi}\middle|(1+\Lambda)e^{-\hat{T}}\frac{\partial}{\partial t}e^{\hat{T}}\middle|\Phi\right\rangle dt - \mathscr{E}_{\hat{H}}(\lambda, \tau, \tilde{\Phi}, \Phi).\end{aligned} \tag{5.156}$$

Herein, it is necessary to compute $\frac{\partial}{\partial t}|\Psi\rangle = \frac{\partial}{\partial t}e^{\hat{T}}|\Phi\rangle$. In order to accomplish this we indroduce the expansion,

$$|\Psi\rangle = \Pi\,|\Psi\rangle = |\Phi\rangle + \sum_\mu A^\mu\,|\Phi_\mu\rangle\,, \quad A^\mu = A^\mu(\tau) = \langle\tilde{\Phi}^\mu|e^{\hat{T}}|\Phi\rangle \tag{5.157}$$

Here we write Φ as the reference Slater determinant and Φ_μ are all the other excited Slater determinant. The coefficients A^μ do not depend explicitly on the orbitals, only on the the amplitudes τ. It is important to note that this summation is not truncated, regardless of the truncation of the cluster amplitudes at some excitation level τ^μ. To further the matter, we have introduced a projection operator,

$$\Pi \equiv |\Phi\rangle\langle\tilde{\Phi}| + \sum_\mu |\Phi_\mu\rangle\langle\tilde{\Phi}^\mu| \,. \tag{5.158}$$

The projection operator has the following properties,

$$\begin{aligned} \Pi\,|\Psi\rangle = |\Psi\rangle\,, \quad \langle\Psi'|\,\Phi = \langle\Psi'|\,, \\ \langle\Psi'|\hat{H}|\Psi\rangle = \langle\Psi'|\Pi\hat{H}\Pi|\Psi\rangle\,, \quad \Pi^\dagger \neq \Pi \end{aligned} \tag{5.159}$$

and unless orbitals are complete we have $\Pi\hat{H}\Pi \neq \hat{H}$.

Now we compute the time derivative of a Slater determinant,

$$\begin{aligned} \frac{\partial}{\partial t} c^\dagger_{p_1} c^\dagger_{p_2} \ldots c^\dagger_{p_N}\,|\rangle &= \dot{c}^\dagger_{p_1} c^\dagger_{p_2} \ldots c^\dagger_{p_N}\,|\rangle + c^\dagger_{p_1} \dot{c}^\dagger_{p_2} \ldots c^\dagger_{p_N}\,|\rangle + \ldots \\ &= \left(\sum_q \dot{c}^\dagger_q \tilde{c}_q\right) c^\dagger_{p_1} c^\dagger_{p_2} \ldots c^\dagger_{p_N}\,|\rangle = \hat{D} c^\dagger_{p_1} c^\dagger_{p_2} \ldots c^\dagger_{p_N}\,|\rangle\,, \end{aligned}$$

where we have defined the operator $\hat{D}$ by

$$\hat{D} = \sum_q \dot{c}^\dagger_q \tilde{c}_q, \tag{5.160}$$

which depends explicitly on orbitals, unlike $\hat{H}$. The derivative of the exact wavefunction becomes,

$$\begin{aligned} \frac{\partial}{\partial t}\,|\Psi\rangle &= \sum_\mu \left(\frac{\partial}{\partial t} A^\mu(\tau)\right) |\Phi_\mu\rangle + \hat{D}\,|\Phi\rangle + \sum_\mu A^\mu(\tau)\hat{D}\,|\Phi_\mu\rangle \\ &= \left(\sum_\nu \dot{\tau}^\nu \frac{\partial}{\partial \tau^\nu} + \hat{D}\right) |\Psi\rangle = \left(\sum_\nu \dot{\tau}^\nu X_\nu + \hat{D}\right) |\Psi\rangle\,. \end{aligned} \tag{5.161}$$

The time-derivative part of the functional (Equation 5.156) integrand becomes,

$$\begin{aligned} & i\hbar \left\langle \tilde{\Phi} \middle| (1+\Lambda) e^{-\hat{T}} \frac{\partial}{\partial t} e^{\hat{T}} \middle| \Phi \right\rangle \\ &= i\hbar \left\langle \tilde{\Phi} \middle| \left(1 + \sum_\mu \lambda_\mu \tilde{X}^\mu\right) e^{-\hat{T}} \left(\sum_\nu \dot{\tau}^\nu X_\nu + \hat{D}\right) e^{\hat{T}} \middle| \Phi \right\rangle \\ &= i\hbar \sum_\mu \lambda_\mu \dot{\tau}^\mu + i\hbar \left\langle \tilde{\Phi} \middle| (1+\Lambda) e^{-\hat{T}} \Pi \hat{D} \Pi e^{\hat{T}} \middle| \Phi \right\rangle, \end{aligned} \tag{5.162}$$

where the projected operator $\Pi\hat{D}\Pi$ is given by

$$\Pi\hat{D}\Pi = \hat{D}_0 \equiv \sum_{pq} \langle\tilde{\phi}_p|\dot{\phi}_q\rangle\, c^\dagger_p \tilde{c}_q. \tag{5.163}$$

Finally we obtain a new expression for the functional in Equation 5.156

$$\mathcal{S}[\lambda, \tau, \tilde{\Phi}, \Phi] = \sum_0^T i\hbar \sum_\mu \lambda_\mu \dot{\tau}^\mu - \mathcal{E}_{\hat{H} - i\hbar\hat{D}_0}[\lambda, \tau, \tilde{\Phi}, \Phi] dt \tag{5.164}$$

$$= \int_0^T i\hbar\lambda_\mu \dot{\tau}^\mu + \rho_p^q (h_q^p - i\hbar\eta_q^p) + \frac{1}{4}\rho_{pr}^{qs} u_{qs}^{pr} dt, \tag{5.165}$$

where

$$\rho_p^q = \rho_p^q(\lambda,\tau) \equiv \left\langle \tilde{\Phi} \middle| (1+\Lambda) e^{-\hat{T}} c_p^\dagger \tilde{c}_q e^{\hat{T}} \middle| \Phi \right\rangle, \tag{5.166}$$

$$\rho_{pr}^{qs} = \rho_{pr}^{qs}(\lambda,\tau) \equiv \left\langle \tilde{\Phi} \middle| (1+\Lambda) e^{-\hat{T}} c_p^\dagger c_r^\dagger \tilde{c}_s \tilde{c}_q e^{\hat{T}} \middle| \Phi \right\rangle, \tag{5.167}$$

$$h_q^p = h_q^p(\tilde{\Phi},\Phi) \equiv \left\langle \tilde{\phi}_p \middle| \hat{h} \middle| \varphi_q \right\rangle, \tag{5.168}$$

$$\eta_q^p = \eta_q^p(\tilde{\Phi},\Phi) \equiv \langle \tilde{\phi}_p | \dot{\varphi}_q \rangle, \tag{5.169}$$

$$u_{qs}^{pr} = u_{qs}^{pr}(\tilde{\Phi},\Phi) \equiv \left\langle \tilde{\phi}_p \tilde{\varphi}_r \middle| (\hat{u} - \hat{P}_{12}) \middle| \phi_q \varphi_s \right\rangle. \tag{5.170}$$

We introduced Einstein summation convention over repeated indices of opposite vertical placement in Equation 5.165.

5.5.1 Equations of Motion

The time has now come to apply the principle of least action to the orbital-adaptive coupled cluster functional from Equation 5.164 in order to find the equations of motion. First we keep τ^ν constant and vary λ_μ,

$$\delta\mathcal{S}[\lambda,\tau] = \int_0^T i\hbar\delta\lambda_\mu \dot{\tau}^\nu - \frac{\partial \mathscr{E}_{\hat{H}-i\hbar\hat{D}_0}}{\partial\lambda_\mu}\delta\lambda_\mu dt = 0. \tag{5.171}$$

We see that the stationary condition is

$$\boxed{i\hbar\dot{\tau}^\mu = \frac{\partial}{\partial\lambda_\mu}\mathscr{E}_{\hat{H}-i\hbar\hat{D}_0}[\lambda,\tau,\tilde{\Phi},\Phi] = \langle \tilde{\Phi}_\mu | e^{-\hat{T}} (\hat{H} - i\hbar\hat{D}_0) e^{\hat{T}} | \Phi \rangle,} \tag{5.172}$$

which is also the eqution of motion, dictating the time-development of τ. Next, we hold λ_μ fixed and vary τ^ν,

$$\delta\mathcal{S}[\lambda,\tau] = \int_0^T i\hbar\lambda_\nu \delta\dot{\tau}^\nu - \frac{\partial \mathscr{E}_{\hat{H}-i\hbar\hat{D}_0}}{\partial\lambda^\nu} dt. \tag{5.173}$$

through integration by parts we see that the first term becomes,

$$i\hbar \int_0^T \lambda_\nu \delta\dot{\tau}^\nu = i\hbar\cancelto{0}{\lambda_\nu\delta\tau^\nu} - i\hbar\int_0^T \dot{\lambda}_\nu \delta\tau^\nu dt,$$

yielding

$$\delta\mathcal{S}[\lambda,\tau] = \int_0^T \delta\tau^\nu \left(-i\hbar\dot{\lambda}_\nu - \frac{\partial \mathscr{E}_{\hat{H}-i\hbar\hat{D}_0}}{\partial\tau^\nu} \right). \tag{5.174}$$

Here the stationary condition is

$$\boxed{-i\hbar\dot{\lambda}_\nu = \frac{\partial}{\partial\tau^\nu}\mathscr{E}_{\hat{H}-i\hbar\hat{D}_0}[\lambda,\tau,\tilde{\Phi},\Phi] = \langle \tilde{\Phi} | (1+\Lambda) e^{-\hat{T}} [\hat{H} - i\hbar\hat{D}_0, X_\mu] e^{\hat{T}} | \Phi \rangle.} \tag{5.175}$$

Equation 5.172 and Equation 5.175 together make up the orbital-adaptive coupled cluster (OACC) amplitude equations of motion.

We will return to the OACC equations of motion shortly, but first we consider a special situation where the operator $\hat{D}_0 \equiv \sum_{pq} \langle\tilde{\phi}_p|\dot{\phi}_q\rangle\, c_p^\dagger \tilde{c}_q$, equates to zero. This is the same as keeping the orbitals static over time. The resulting equations of motions are

$$i\hbar\dot{\tau}^\mu = \frac{\partial}{\partial\lambda_\mu}\mathscr{E}_{\hat{H}}[\lambda,\tau,\tilde{\Phi},\Phi] = \langle\tilde{\Phi}_\mu|e^{-\hat{T}}\hat{H}e^{\hat{T}}|\Phi\rangle \tag{5.176}$$

$$-i\hbar\dot{\lambda}_\nu = \frac{\partial}{\partial\tau^\nu}\mathscr{E}_{\hat{H}}[\lambda,\tau,\tilde{\Phi},\Phi] = \langle\tilde{\Phi}|(1+\Lambda)e^{-\hat{T}}[\hat{H},X_\mu]e^{\hat{T}}|\Phi\rangle\,. \tag{5.177}$$

We call these equations the time-dependent coupled cluster (TDCC) amplitude equations. Setting the left-hand side of Equation 5.176 and Equation 5.177 to zero will give a set of non-linar equations that can be solved in order to find initial amplitudes ($\lambda^{(0)}$, $\tau^{(0)}$). These equations are the same as Equation 5.141 and Equation 5.142.

Returning to the orbital-adaptive scheme, the OATDCC equations (Equation 5.172 and Equation 5.175) have parametric redundancies that we need to address briefly[5]. The parametric redundancies exist in the sense that when one derives equations of motion for $(\tau,\lambda,\tilde{\Phi},\Phi) = (\tau^\mu,\lambda_\mu,\tilde{\phi}_p,\phi_q)$, under the stationary condition $\delta\mathcal{S} = 0$, for a given pair of coupled cluster wavefunctions $(\langle\tilde{\Psi}|\,,|\Psi\rangle) \in \mathcal{M}$, there are many choices for the amplitudes and orbitals that would give this same wavefunction pair. It is therefore necessary to define a transformation as a many-to-one mapping from this collection of points $(\lambda,\tau,\tilde{\Phi},\Phi) \in \mathcal{N}$ to the wavefunction pair on $(\langle\tilde{\Psi}|\,,|\Psi\rangle) \in \mathcal{M}$,

$$f : \mathcal{N} \to \mathcal{M}. \tag{5.178}$$

As circumstances would have it, the simplest of such transformations corresponds to a rotation that eliminates the singles amplitudes τ_i^a. This is the same ansatz employed in orbital-optimised- or Bruecker coupled cluster theory (see box). Additionally, including λ_a^i after this rotation would leave the equations of motions overdetermined. The presence of $\hat{T}_1$ is compensated by the freely varying orbitals, but this does not hold for Λ_1, which gives more parameters in the $\langle\tilde{\Psi}|$ than in $|\Psi\rangle$. As such, we set all single amplitudes, τ_i^a and λ_a^i equal to zero.

Orbital-optimised and Bruecker coupled cluster theories [43, 60]

In standard coupled cluster theory including single excitations,

$$e^{\hat{T}_1} = \exp\left\{\sum_{ai}\tau_i^a c_a^\dagger c_i\right\}, \tag{5.179}$$

we determine a set of non-zero single-excitation amplitudes τ_i^a together with any higher-excitation amplitudes. An alternative parametrisation of the singles manifold in Equation 5.179 is the orthogonal orbital-rotation operator

$$e^{-\kappa} = \exp\left\{-\sum_{ai}\kappa_a i(c_a^\dagger c_i - c_i^\dagger c_a)\right\} \tag{5.180}$$

This is a rephrasing of Thouless theorem[75]. We may therefore use

$$|\Psi_{\mathrm{OCC}}\rangle = e^{-\kappa}e^{\hat{T}_{\mathrm{O}}}\,|\Phi\rangle \tag{5.181}$$

as a wavefunction ansatz instead. Here,

$$\hat{T}_{\mathrm{O}} = \hat{T}_2 + \hat{T}_3 + \ldots \tag{5.182}$$

[5] A thorough decription of this matter can be found in the supplementary to Kvaal's articl on OATDCC[45]

In orbital-adaptive time-dependent coupled cluster theory such a gauge condition corresponds to considering orbital time derivatives of the form

$$\left|\dot{\phi}_q\right\rangle = (P+Q)\left|\dot{\phi}_q\right\rangle = \sum_p |\phi_p\rangle \left\langle \tilde{\phi}_p \middle| \dot{\phi}_q \right\rangle + Q\left|\dot{\phi}_q\right\rangle = \sum_p \eta^p_q + Q\left|\dot{\phi}_q\right\rangle \tag{5.183}$$

$$\langle\dot{\tilde{\phi}}_p| = \left\langle \dot{\tilde{\phi}}_p \right| (P+Q) = \sum_q \left\langle \dot{\tilde{\phi}}_p \middle| \phi_q \right\rangle \left\langle \tilde{\phi}_q \right| + \left\langle \dot{\tilde{\phi}}_p \right| Q = -\sum_q \eta^p_q \left\langle \tilde{\phi}_q \right| + \left\langle \dot{\tilde{\phi}}_p \right| Q, \tag{5.184}$$

with $\eta^i_j = \eta^a_b = 0$, $\eta^p_q = \langle\tilde{\phi}_p|\dot{\phi}_q\rangle = -\langle\dot{\tilde{\phi}}_p|\phi_q\rangle$. Here we have defined the projection operators P and Q, where $P = \Phi\tilde{\Phi} = \sum_p |\phi_p\rangle\langle\phi_p|$ projects onto the single-particle space defined by the orbitals, and $Q = 1 - P$ projects onto everything else.

We can write down equations of motions just for the nonzero P-components η^a_i and η^i_a of the orbital derivatives,

$$i\hbar\sum_{bj} A^{ib}_{aj}\eta^j_b = \sum_p \rho^i_p h^p_a - \sum_q \rho^q_a h^i_q + \frac{1}{2}\left[\sum_{qrs}\rho^{is}_{pr}u^{pr}_{as} - \sum_{rqs}\rho^{qs}_{ar}u^{ir}_{qs}\right] \tag{5.185}$$

$$-i\hbar\sum_{bj} A^{ja}_{bi}\eta^b_j = \sum_p \rho^a_p h^p_i - \sum_q \rho^q_i h^a_q + \frac{1}{2}\left[\sum_{prs}\rho^{as}_{ps}u^{pr}_{is} - \sum_{rqs}\rho^{qs}_{ir}u^{ar}_{qs}\right] + i\hbar\hat{\rho}^a_i, \tag{5.186}$$

where the matrix elements A^{ib}_{aj} are defined by,

$$A^{ib}_{aj} \equiv \left\langle \tilde{\Psi} \middle| [c^\dagger_j\tilde{c}_b, c^\dagger_a\tilde{c}_i] \middle| \Psi \right\rangle = \delta^b_a\rho^i_j - \delta^i_j\rho^b_a. \tag{5.187}$$

The Q-part of the orbital derivatives are,

$$i\hbar\sum_q \rho^q_p Q\frac{\partial}{\partial t}|\phi_q\rangle = \sum_q \rho^q_p Qh|\phi_q\rangle + \sum_{qrs}\rho^{qs}_{pr}QW^r_s|\phi_q\rangle, \ \forall p \tag{5.188}$$

$$-i\hbar\sum_p \rho^q_p\left(\frac{\partial}{\partial t}\left\langle\tilde{\phi}_p\right|\right)Q = \sum_p \rho^q_p\left\langle\tilde{\phi}_p\right|hQ + \sum_{prs}\rho^{qs}_{pr}\left\langle\tilde{\phi}_p\right|W^r_sQ, \ \forall q, \tag{5.189}$$

where mean-field operators W^r_s are defined by

$$W^r_s|\psi\rangle \equiv \langle\cdot\tilde{\phi}_r|u|\psi\phi_s\rangle. \tag{5.190}$$

The logical next step is to write down the equations of motion for the lowest truncated form of OATDCC available too us, namely OATDCCD. In addition to the orbitals Φ and $\tilde{\Phi}$, the only parameters of the exact wavefunction are the amplitudes $\tau = \tau^{ab}_{ij}$ and $\lambda = \lambda^{ij}_{ab}$. The OATDCCD amplitude equations read

$$i\hbar\dot{\tau}^{ab}_{ij} = \frac{\partial}{\partial\lambda^{ij}_{ab}}\mathscr{E}_{\mathrm{H}}[\lambda,\tau,\tilde{\Phi},\Phi] = \left\langle\tilde{\phi}^{ab}_{ij}\middle|e^{-\hat{T}}\hat{H}e^{\hat{T}}\middle|\phi\right\rangle \tag{5.191}$$

$$-i\hbar\dot{\lambda}^{ij}_{ab} = \frac{\partial}{\partial\tau^{ab}_{ij}}\mathscr{E}[\lambda,\tau,\tilde{\Phi},\Phi] = \left\langle\tilde{\phi}\middle|(1+\Lambda)e^{-\hat{T}}[\hat{H},X^{ij}_{ab}]e^{\hat{T}}\middle|\phi\right\rangle. \tag{5.192}$$

The P-space orbitals read

$$i\hbar\sum_{bj} A^{ib}_{aj}\eta^j_b = \sum_j \rho^i_j h^j_a - \sum_b \rho^b_a h^i_b + \frac{1}{2}\left[\sum_{prs}\rho^{is}_{pr}u^{pr}_{as} - \sum_{rqs}\rho^{qs}_{ar}U^{ir}_{qs}\right], \tag{5.193}$$

$$-i\hbar\sum_{bj}A^{ja}_{bi}\eta^b_j=\sum_b\rho^a_b h^b_i-\sum_j\rho^j_i h^a_j+\frac{1}{2}\left[\sum_{prs}\rho^{as}_{pr}u^{pr}_{is}-\sum_{rqs}\rho^{qs}_{ir}U^{ar}_{qs}\right] \tag{5.194}$$

and the Q-space orbitals read

$$i\hbar\sum_q\rho^q_pQ\frac{\partial}{\partial t}\left|\phi_q\right\rangle=\sum_q\rho^p_qQh\left|\phi_q\right\rangle+\sum_{qrs}\rho^{qs}_{pr}QW^r_s\left|\phi_q\right\rangle, \tag{5.195}$$

$$-i\hbar\sum_p\rho^q_p\left(\frac{\partial}{\partial t}\left\langle\tilde{\phi}_q\right|\right)Q=\sum_p\rho^q_p\left|\phi_q\right\rangle Qh+\sum_{prs}\rho^{qs}_{pr}\left\langle\phi_q\right|W^r_sQ. \tag{5.196}$$

Notice that the τ and λ OATDCCD equations (Equation 5.191 and Equation 5.192) are the same equations as the ones used in standard TDCCD (Equation 5.176 and Equation 5.177), because the operator $\hat{D}_0$ is eliminated due to $\rho^a_i=\rho^i_a=0$. Because the operators $\hat{D}_0$ disappears from Equation 5.191 and Equation 5.192, the right-hand sides can be evaluated independently of equations 5.193, 5.194, 5.195, 5.196. In order to compute $\dot{\tilde{\Phi}}$ and $\dot{\Phi}$, η must be solved for in addition to $Q\left|\dot{\phi}_q\right\rangle$ and $\langle\dot{\tilde{\phi}}_p|\,Q$, according to Equation 5.183 and Equation 5.184.

Part III

Implementation

Chapter 6

Quantum Systems

For a quantum system to be studied on the computer it is necessary to make a distinction for what defines the system. One must therefore undergo the mathematical procedure of defining a finite basis sets when dealing with the electronic problem.

Here we present the `quantum_systems` python module, designed to provide basis sets for one- and two-dimensional quantum dots. The two-dimensional quantum dot can also be modelled with a constant, homogeneous magnetic field; and as a double quantum dot. Moreover, the module includes an option for constructing a custom system which can be interfaced with popular quantum chemistry packages `PySCF`[73] and `Psi4`[57]. This allows one to construct basis sets representing all kinds of systems of interest in quantum chemistry, like atoms and molecules.

The `quantum_systems` module also contains an implementation of a plane wave or homogenous electron gas basis set, sometimes called the jellium model. However, this implementation exists mainly as a curiosity at this point. In the future it can be developed into something more useful, as the electron gas can serve as a first approximation to a metal or a semi-conductor.

The `quantum_system` module can be installed from github with `pip` by the following command,

```
pip install git+https://github.com/Schoyen/quantum-systems.git
```

The same task can of course be accomplished by more commands,

```
git clone https://github.com/Schoyen/quantum-systems.git
cd quantum-systems
pip install .
```

It can be useful to install the module to a separate environment. We have made this possible through `conda`,

```
conda environment create -f environment.yml
conda activate quantum-systems
```

6.1 Quantum System Abstract Base Class

Here we present the abstract base class that every system class in the `QuantumSystems` model is built upon. This base class forms the foundation of any quantum system, in order to make a system specification function together with the `coupled_cluster` module presented in the next chapter. The base class is reasonably named `QuantumSystem`.

Many of the methods necessary to set up a quantum system can be abstracted away, which is most of the motivation for constructing a parent class that all other quantum system classes can inherit from. Examples of such functionality is setting up the Fock matrix. The one- and two-body operators are necessary to set up for a specific system, but the Fock matrix computations can be abstracted away to the superclass.

class quantum_systems.**QuantumSystem** (*n*, *l*, *n_up=None*, *np=None*)

Abstract base class defining the common methods used by all different quantum systems.

Parameters:
- **n** (*int*) Number of electrons
- **l** (*int*) Number of spinorbitals
- **n_up** (*int, default=None*) Number of spin-up spinorbitals
- **np** (*module*) Matrix library, i.e. numpy, cupy etc.

Attributes:
- **h** One-body matrix **Type** *np.array*
- **f** Fock matrix **Type** *np.array*
- **u** Two-body matrix **Type** *np.array*
- **s** Overlap matrix of spinorbitals **Type** *np.array*
- **spf** Single-particle functions **Type** *np.array*
- **spf_bra** Conjugated single-particle functions **Type** *np.array*

Methods:
- **setup_system**()
  Method must be implemented by subclasses.
- **change_basis**(*c*, *c_tilde=None*)
  Changes basis of system according to coefficient matrices $\mathbf{C}$ and $\tilde{\mathbf{C}}$.
- **change_to_hf_basis**(**args*, *verbose=False **kwargs*)
  Changes basis of system to Hartree-Fock basis.
- **set_time_evolution_operator**(*time_evolution_operator*)
  Setter for time-evolution operator.
  Parameters:
  - **time_evolution_operator** (*TimeEvolutionOperator*)

In the `QuantumSystem` abstract base class we have included a method that changes the basis of the system according to some coefficient matrix $\mathbf{C}$ and $\tilde{\mathbf{C}}$, the `change_basis(c, c_tilde)` method. This method will be useful later, especially when computing the basis for the double well system. In the time-dependent coupled cluster scheme with adaptive oribtals, this method is also very useful.

A similar method `change_to_hf_basis()` is also implemented in the `QuantumSystems` class. This changes the system basis to a basis based on the coefficient matrix found from the Roothan-Hall equations,

$$FC = SC\epsilon. \tag{6.1}$$

See section 3.2 for further discussion of the Roothan-Hall equations. The basis transformation is performed by multiplication with the coefficient matrix,

$$|\phi_p\rangle = C_p^\alpha |\chi_\alpha\rangle, \tag{6.2}$$

where we go from a (naïve) basis $|\chi_\alpha\rangle$, to the much better Hartree-Fock basis $|\phi_p\rangle$. The basis would be better suited to represent the system because is already consitute an approximate ground state solution. The improvent in ground state energies by using the Hartree-Fock basis is well documented[41, 49].

The principal method that needs to be implemented in a subclass subclass of `QuantumSystem` is `setup_system()`, including special considerations for dipole computations. These factors will be discussed for each specific system we have implemented in the following sections.

6.2 Quantum Dots

In reality, quantum dots are nanometre-sized structures made of semiconductor materials. Theoretically, quantum dots are easy to model by harmonic oscillator potential and in practice they are relatively easy to manufacture in a laboratory. This doubly theoretical-experimental benefit has made quantum dots a popular area of study. Moreover so because of their wide area of apllications.

The possible applications of quantum dots are many. Coupled single-electron quantum dots could potentially be used as hardware elements in quantum computers, i.e. qubits[50]; quantum dots also promise to increase the efficiency of photvoltaic solar cells; and they have already found use in cellular imaging in biology. Reimann and Manninen[67] has written an outstandingly thorough review on quantum dots, covering their varied types of fabrication, theoretical methods common in their study and vast ocean of applications.

The usefulness and relative theoretical ease of modelling warrants the study of quantum dots. Herein, several classes have been implemented in order to construct basis sets modelling quantum dots in both one and two dimensions. These basis sets models *bound* systems as the common harmonic oscillator-type potentials that are used have the characteristics of infinite quantum wells.

6.2.1 One Dimension

This is perhaps one of the simplest of all quantum mechanical models, being studied ad nauseum in everyones introductory quantum mechanics course. The one-body part of the Hamiltonian for the one-dimensional quantum harmonic oscillator is,

$$\hat{h} = \frac{\hat{p}^2}{2m} + \frac{1}{2} m\omega^2 \hat{x}^2. \tag{6.3}$$

The potential, $\hat{v} = \frac{1}{2} m\omega^2 \hat{x}^2$, forms the well known parabolic potential. In a general one-dimensional system, this potential could readily be exchanged for something else. For instance that of the *double well*,

$$\hat{v} = \frac{1}{2} m\omega^2 \left(\hat{x}^2 + \frac{1}{4} l^2 - l|\hat{x}| \right), \tag{6.4}$$

where l is the width of a barrier in the middle of the parabolic potential. We have implemented several other potentials, which we summarise in section 6.2.1.

In atomic units we can set $\hbar = m = 1$. Substituting for the momentum operator, $\hat{p} = -i\hbar(\hat{\partial}/\partial x)$, gives us

$$\hat{h} = -\frac{1}{2} \frac{\partial^2}{\partial x^2} + \hat{v}. \tag{6.5}$$

The second-order derivate can be approximated by the central difference formula for some function $f(x)$, yielding

$$f''(x) = \frac{f(x + dx) - 2f(x) + f(x - dx)}{dx^2}, \tag{6.6}$$

for some small dx. This means that we approximate the Hamilton operator of the system (Equation 6.5) by a matrix,

$$h^p_q = \begin{pmatrix} 1/dx^2 + v_1 & -1/2dx^2 & \ddots & & & \\ -1/2dx^2 & 1/dx^2 + v_2 & -1/2dx^2 & \ddots & & \\ \ddots & -1/2dx^2 & 1/dx^2 + v_3 & -1/2dx^2 & \ddots & \\ & \ddots & \ddots & \ddots & \ddots & \ddots \\ & & \ddots & -1/2dx^2 & 1/dx^2 + v_{n-1} & -1/2dx^2 \\ & & & \ddots & -1/2dx^2 & 1/dx^2 + v_n \end{pmatrix}, \tag{6.7}$$

and we have thus transformed the time-independent Schrödinger equation

$$\hat{h} |n\rangle = \epsilon |n\rangle, \tag{6.8}$$

into a matrix equation which constitutes a better representation on a computer. Here n is the number of points used to numerically represent the wavefunciton and Hamiltonian matrix representation. This is done with some generic eigenvalue solver, for instance `numpy.linalg.eigh`. The eigen functions provide the foundations for the single-particle functions.

Since we would like to model interaction between particles we need something more, than just a numerical representation of the one-body operator. We therefore need to compute coulomb interaction, in the form of an integral. This is done in several steps, starting with an "inner intergral" over all all space and two and two single-particle functions,

$$u^q_s = \int \phi_q(x_1) \frac{\alpha}{(x_1 - x_2)^2 + a^2} \phi_s(x_2) dx, \tag{6.9}$$

where a and α are parameters that are necessary to include for this integral to be calculable. Numerically, this part is divided into two functions in our python implementation,

```python
def _shielded_coulomb(x_1, x_2, alpha, a):
    return alpha / np.sqrt((x_1 - x_2) ** + a ** 2)

def _compute_inner_integral(spf, l, num_grid_points, grid, alpha, a):
    inner_integral = np.zeros((l, l, num_grid_points), dtype=np.complex128)

    for q in range(l):
        for s in range(l):
            for i in range(num_grid_points):
                inner_integral[q, s, i] = _trapz(
                    spf[q]
                    * _shielded_coulomb(grid[i], grid, alpha, a)
                    * spf[s],
                    grid,
                )

    return inner_integral
```

The parameters α and a are called the strength and shielding parameter, respectively. The strength parameter defines the strength of the Coulomb interaction, and the shielding parameter is needed to avoid singularities in the one-dimensional formulation. This inner orbital is subsequently used in the computation in the orbial integral,

$$u_{rs}^{pq} = \int \phi_p u_s^q \phi_r dx, \tag{6.10}$$

which numerically is implemented as follows,

```
def _compute_orbital_integrals(spf, l, inner_integral, grid):
    u = np.zeros((l, l, l, l), dtype=np.complex128)

    for p in range(l):
        for q in range(l):
            for r in range(l):
                for s in range(l):
                    u[p, q, r, s] = _trapz(
                        spf[p] * inner_integral[q, s] * spf[r], grid
                    )

    return u
```

Each integral is solved by the trapezoidal scheme, which approximates the integral by

$$\int_x^{x+\Delta x} f(x)dx \approx \Delta x \frac{f(x+\Delta x) - f(x)}{2}. \tag{6.11}$$

Needless to say, computing the coulomb integrals is one of the more intensive tasks, and we therefore make great use of just-in-time compulation from the `numba` module for python.

class quantum_systems.**ODQD**
(*n*, *l*, *grid_length*, *num_grid_points*, *a*=0.25, *alpha*=1.0)

Create One-Dimensional Quantum Dot basis set.

Parameters

- **n**(*int*) Number of electrons
- **l**(*int*) Number of spinorbitals
- **grid_length**(*int*, *float*) Space over which to construct wavefunction.
- **num_grid_points**(*int*, *float*) Number of points for construction of wavefunction.
- **a**(*float*, *default* 0.25) Coulomb screening parameter.
- **alpha**(*float*, *default* 1.0) Coulomb strength parameter.

Attributes

- **h** One-body matrix **Type** *np.array*
- **f** Fock matrix **Type** *np.array*
- **u** Two-body matrix **Type** np.array

Methods

setup_system(*Potential=None*)
Must be called in order to compute basis functions. The method will revert to regular harmonic oscillator potential with $\omega = 0.25$ if no potential has been provided. Optional potentials include one-dimensional double well potentials.

contruct_dipole_moment()
Constructs dipole moment. This method is called by **setup_system**(). Necessary when constructing custom systems with time development.

Table 6.1: One-dimensional potential classes in `quantum_systems`.

`DWPotential`	$\frac{1}{2}\omega^2\left(x^2 + \frac{1}{4}l^2 - l\lvert x\rvert\right)$
`DWPotentialSmooth`	$\frac{1}{2a^2}\left(x + \frac{a}{2}\right)^2\left(x - \frac{a}{2}\right)^2$
`GaussianPotential`	$Ae^{-\frac{(x-\mu)^2}{2\sigma^2}}$
`AtomicPotential`	$-\frac{Z_a}{\sqrt{x^2+c}}$

One-dimensional potentials

We have provided several one-dimensional potentials that can be passed to the `ODQD` class' `setup_system(Potential)` method. All these potentials have been implemented as subclasses of the abstract base class `OneDimPotential`. The only thing necessary for an inheriting class to implement is the `__call__` method which takes position on the grid x as argument, and must logically return the potential value at that point x.

The parabolic harmonic oscillator potential, which we have made most use of and which is discussed above is implemented as follows,

```python
class HOPotential(OneDimPotential):
    def __init__(self, omega):
        self.omega = omega

    def __call__(self, x):
        return 0.5 * self.omega ** 2 * x ** 2
```

Additionally, we have implemented the potentials defined in Table 6.1.

6.2.2 Two Dimensions

The one-body part of the Hamiltonian for a two-dimensional quantum dots is almost identical to the one-body part for a one-dimensional quantum dot. In cartesian coordinates we merely include a y in the potential as well as an x, but mostly because we have analytical expressions for the Coulomb integrals in polar coordinates[1], we write the one-body operators in polar coordinates as well with $\hat{r}^2 = \hat{x}^2 + \hat{y}^2$,

$$\hat{h} = \frac{\hat{p}^2}{2m} + \frac{1}{2}m\omega^2\hat{r}^2 = -\frac{\hbar^2}{2m}\left(\frac{\partial^2}{\partial r^2} + \frac{1}{r}\frac{\partial}{\partial r} + \frac{1}{r^2}\frac{\partial^2}{\partial \theta^2}\right) + \frac{1}{2}m\omega^2\hat{r}^2. \tag{6.12}$$

The wavefunctions for a two-dimensional harmonic oscillator can be written

$$\phi(r,\theta) = N_{nm}R_{nm}(r)Y_m(\theta) = N_{nm}(ar)^{|m|}L_n^{|m|}(a^2r^2)e^{-a^2r^2/2}e^{im\theta}, \tag{6.13}$$

where $a = \sqrt{m\omega/\hbar}$ si the Bohr radius, $L_n^{|m|}$ is the associated Laguerre polynomials, n and m are the principal and the azimutal quantum numbers respectively[1], and N_{nm} is a normalisation factor given by,

$$N_{nm} = a\sqrt{\frac{n!}{\pi(n+|m|)!}}. \tag{6.14}$$

The energy eigenvalues of a two-dimensional harmonic oscillator is given by

$$\epsilon_{nm} = \hbar\omega(2n + |m| + 1). \tag{6.15}$$

[1] There is usually another quantum number called the magnetic quantum number. Because of our restriction to two dimensions, this quantum number does not appear. In three dimensions we would usually denote the azimuthal quantum number by l and the magnetic quantum number by m or m_l. A fourth quantum number is the spin projection quantum number commonly written m_s.

It is very beneficial that such a nice expression exists, because the one-body matrix elements of a harmonic oscillator is simply,

$$\langle \phi_p | \hat{h} | \phi_q \rangle = \hat{h}^p_q = \epsilon_p \delta^p_q. \tag{6.16}$$

These matrix elements encompass both the kinetic energy operator matrix element and potential energy matrix element. If we were dealing with completely none-interacting particles not much more would be needed. We see, however, that this form of one-body matrix elements necessitates a mapping from the general coordinates p, q, as used above, and the quantum numbers n, m.

This functionality $(n, m) \mapsto p$ is achieved by the following python function

```python
def get_index_p(n, m):
    num_shells = 2 * n + abs(m) + 1

    previous_shell = 0
    for i in range(1, num_shells):
        previous_shell += i

    current_shell = previous_shell + num_shells

    if m == 0:
        if n == 0:
            return 0

        p = previous_shell + (current_shell - previous_shell) // 2

        return p

    elif m < 0:
        return previous_shell + n

    else:
        return current_shell - (n + 1)
```

It will also be necessary to map back $p \mapsto (n, m)$,

```python
def get_indices_nm(p):
    n, m = 0, 0
    previous_shell = 0
    current_shell = 1
    shell_counter = 1

    while current_shell <= p:
        shell_counter += 1
        previous_shell = current_shell
        current_shell = previous_shell + shell_counter

    middle = (current_shell - previous_shell) / 2 + previous_shell

    if (current_shell - previous_shell) & 0x1 == 1 and abs(
        p - math.floor(middle)
    ) < 1e-8:
```

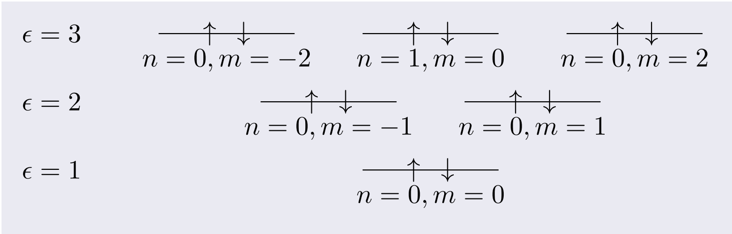

Figure 6.1: The lowest three energy levels in the two-dimensional quantum dot. Each arrow representes a spin up or a spin down state with the quantum numbers n and m as listed below. This pattern goes on indefinitly with the addition of one bar (two oscillators) per level.

```
        n = shell_counter // 2
        m = 0

        return n, m

    if p < middle:
        n = p - previous_shell
        m = -((shell_counter - 1) - 2 * n)

    else:
        n = (current_shell - 1) - p
        m = (shell_counter - 1) - 2 * n

    return n, m
```

An important difference between the one-dimensional quantum dot and a two-dimensional quantum dot is that in the latter we have energy degeneracies of the eigenstates. This is illustrated in Figure 6.1. In this figure we have included a spin-up and a spin-down state for each n, m-state. This spin feature is not in any way included in Equation 6.13, but we may represent the spin condition by including it in the orthonormality conditions of the wavefunctions,

$$\langle n_1 m_1 \sigma_1 | n_2 m_2 \sigma_2 \rangle = \delta_{n_1 n_2} \delta_{m_1 m_2} \delta_{\sigma_1 \sigma_2}, \tag{6.17}$$

where σ is the spin.

Because the electrons we will be studying are interacting, we need two-body matrix elements as well. The analytical formula for the Coulomb interaction integrals, provided by Anisimovas and Matulis[1] is

$$\begin{aligned} \langle \phi_1 \phi_2 | \hat{W} | \phi_3 \phi_4 \rangle =& \delta_{s_1,s_4} \delta_{s_2,s_3} \delta_{m_1+m_2,m_3+m_4} \left[\prod_{i=1}^{4} \frac{n_i!}{(|m_i| + n_i)} \right]^{1/2} \sum_{(4)j=0}^{n} \frac{(-1)^{j_1+j_2+j_3+j_4}}{j_1! j_2! j_3! j_4!} \\ & \times \left[\prod_{i=1}^{n} \binom{n_i + |m_i|}{n_i + j_i} \right] \frac{1}{2^{(G+1)/2}} \sum_{(4)l=0}^{\gamma} (-1)^{\gamma_2+\gamma_3-l_2-l_3} \\ & \times \delta_{l_1+l_2,l_3+l_4} \left[\prod_{i=1}^{4} \binom{\gamma_i}{l_i} \right] \Gamma\left(1 + \frac{L}{2}\right) \Gamma\left(\frac{G-L+1}{2}\right). \end{aligned} \tag{6.18}$$

The symbols j_i are integer summation indices (regular indices) running from 0 to n_i. The symbols γ_i stand for numbers,

$$\gamma_1 = j_1 + j_4 + (|m_1| + m_1)/2 + (|m_4| - m_4)/2$$
$$\gamma_4 = j_1 + j_4 + (|m_1| - m_1)/2 + (|m_4| + m_4)/2$$

γ_2 and γ_3 can be obtained by replacing indices $1 \to 2$ and $4 \to 3$. Moreover,

$$\sum_{(4)j=0}^{n} = \sum_{j_1=0}^{n_1}\sum_{j_2=0}^{n_2}\sum_{j_3=0}^{n_3}\sum_{j_4=0}^{n_4}, \quad G = \sum_i \gamma_i, \quad L = \sum_i l_i$$

For the implementation of this expression for the purpose of computing the two-dimensional quantum dot basis sets, we refer the reader to the appendices (Appendix C).

Dipole Moments

For our implementation of time dependent Hamiltonians, outlined below, we make use of a dipole approximation of an electric field. For this reason it is necessary to compute dipole moments. Moreover, the "transitions rules " of quantum mechanics stems from evalueting matrix elements of this kind,

$$\mathbf{d}_{pq} = \langle\phi_p| \hat{\mathbf{r}} |\phi_q\rangle = \hat{i} \langle\phi_p| \hat{x} |j\rangle + \hat{j} \langle\phi_p| \hat{y} |\phi_q\rangle , \tag{6.19}$$

where ϕ_p, ϕ_q are some typical basis vectors, on the form in Equation 6.13. As we will be representing the two-dimensional quantum dots in polar coordinates, we can rewrite this to,

$$\mathbf{d}_{pq} = \hat{i} \langle\phi_p| \hat{r}\cos\hat{\theta} |\phi_q\rangle = \hat{j} \langle\phi_p| \hat{r}\cos\hat{\theta} |\phi_q\rangle . \tag{6.20}$$

The integrals we need to compute are

$$\langle\phi_p| r\cos\theta |\phi_q\rangle = N^*_{nm}N_{nm}\int_0^\infty r^2 R^*_{nm}(r)R_{nm}(r)dr \int_0^{2\pi} \cos\theta Y^*_m(\theta)Y_m(\theta)d\theta \tag{6.21}$$
$$\langle\phi_p| r\sin\theta |\phi_q\rangle = N^*_{nm}N_{nm}\int_0^\infty r^2 R^*_{nm}(r)R_{nm}(r)dr \int_0^{2\pi} \sin\theta Y^*_m(\theta)Y_m(\theta)d\theta. \tag{6.22}$$

The radially dependent integrals are the most difficult to compute, and we compute this symbolically with `sympy`. For the angular integrals, we can find analytical expressions that can be evaluated quickly,

$$\int_0^{2\pi} \cos\theta e^{i\bar{m}\theta} = \frac{e^{i\bar{m}\theta}}{1-\bar{m}^2}(\sin\theta - i\bar{m}\cos\theta)\Big|_0^{2\pi}, \tag{6.23}$$

where $\bar{m} = (m_q - m_p) \in \mathbb{Z}$. We see that the integral evalues to 0 for all possible values of $\bar{m}$ except for ± 1. This special case warrants further investigation,

$$\int_0^{2\pi} \cos\theta e^{i\theta}d\theta = \int_0^{2\pi} \cos^2\theta + i\cos\theta\sin\theta d\theta = \frac{1}{2}\sin\theta\cos\theta + \frac{\theta}{2} + \frac{i}{2}\sin^2\theta\Big|_0^{2\pi} = \pi. \tag{6.24}$$

Similarly,

$$\begin{aligned} \int_0^{2\pi} \sin\theta\theta e^{i\bar{m}\theta}d\theta &= \frac{e^{i\bar{m}\theta}}{1-\bar{m}^2}(i\bar{m}\sin\theta - \cos\theta)\Big|_0^{2\pi} = 0 \quad \forall \bar{m} \in \mathbb{Z} \neq 1 \\ \int_0^{2\pi} \sin\theta e^{i\theta}d\theta = \int_0^{2\pi} \cos\theta\sin\theta + i\sin^2\theta d\theta &= \frac{1}{2}\sin\theta - \frac{i}{2}\sin\theta\cos\theta + i\frac{\theta}{2}\Big|_0^{2\pi} = i\pi \end{aligned} \tag{6.25}$$

This is a very nice result, as it conforms with the selection rule related to the azimutal quantum number m.

The final specification of the two-dimensional harmonic oscillator basis set class, which is everything the user sees is the following,

class quantum_systems.**TwoDimensionalHarmonicOscillator**
(*n*, *l*, *radius_length*, *num_grid_points*, *omega*=0.25, *mass=1*)

Create Two-Dimensional Quantum Dot basis set.

Parameters
- **n**(*int*) Number of electrons
- **l**(*int*) Number of spinorbitals
- **grid_length**(*int or float*) Space over which to construct wavefunction.
- **num_grid_points**(*int of float*) Number of points for construction of wavefunction.
- **omega**(*float, default* 0.25) Angular frequency of harmonic oscillator potential.
- **mass**(*int or float, default* 1.0) Mass of electrons. Atomic units is used as default.

Attributes
- **h** One-body matrix **Type** np.array
- **f** Fock matrix **Type** np.array
- **u** Two-body matrix **Type** np.array

Methods
- **setup_system**()
  Must be called in order to compute basis functions.
- **contruct_dipole_moment**()
  Constructs dipole moment. This method is called by **setup_system**().

6.2.3 Two-Dimensional Double Well

The extension from a single two-dimensional quantum dot to a double quantum dot is a relatively straight-forward procedure, as it is a mere perturbation of the regular single dot. There are at least two ways to implement the potential of double well in two dimensions. One method is to add a fourth-degree polynomial potential along one cartesian axis, resulting in a smooth "bump" dividing the two potential wells. We have opted for another method, with the an absolute value function resulting in a sharp edge. The potential reads as follows,

$$\hat{h} = \frac{\hat{p}}{2m} + \frac{1}{2}m\omega^2\hat{r}^2 + \frac{1}{2}m\omega^2\left(\frac{1}{4}l^2 - l|\hat{x}|\right), \tag{6.26}$$

where l is the "strength" of the barrier between the wells. We can readily see what makes the barrier so acute, namely the absolute value of the position operator, $|\hat{x}|^2$.

In Equation 6.26, we immediately recognise the first two terms as the normal quantum dot. This is beneficial, as we can reuse single-particle functions from Equation 6.13. This means that the one-body matrix elements are simply,

$$\begin{aligned} h^p_q &= \epsilon_p\delta^p_q + \frac{1}{2}m\omega^2\langle\phi_p|\frac{1}{4}l^2 - l|\hat{x}||\phi_q\rangle \\ &= \epsilon_p\delta^p_q + \frac{1}{8}m\omega^2l^2\delta^p_q - \frac{1}{2}m\omega^2 l\langle\phi_p||\hat{x}||\phi_q\rangle. \end{aligned} \tag{6.27}$$

[2] Here we might as well have used the position operator $\hat{y}$, which would have resulted in an equivalent potential, rotated ninety degrees.

We see from the first two terms a perturbation in the diagonal matrix elements, i.e.

$$\epsilon_p^{\mathrm{DW}} = \epsilon_p + \frac{1}{8}m\omega^2 l^2, \tag{6.28}$$

and that we need only compute the matrix elements of the position operator. Because we are still working with polar coordinates, we make the necessary transformation, and the integral becomes

$$\langle \phi_p || \hat{x} || \phi_q \rangle = \int_0^\infty \int_0^{2\pi} \phi^*_{n_p m_p}(r,\theta) r^2 |\cos\theta| \phi_{n_q m_q}(r,\theta) dr d\theta \tag{6.29}$$

We see that the wavefunctions ϕ_{nm} are the same as for the unperturbed two-dimensional quantum dot, and this directs us to the same kind of interals as for the dipole calculations above. The radial interal is cumbersome, and therefore left for a symbolic solver, but for angular integral we can provide the computer with some help,

$$\begin{aligned}
\int_0^{2\pi} |\cos\theta| e^{i\bar{m}\theta} d\theta &= \int_0^{\pi} \cos\theta e^{-i\bar{m}\theta} d\theta - \int_\phi^{2\pi} \cos\theta e^{-i\bar{m}\theta} d\theta \\
&= \int_0^{\pi} (\cos(\theta\bar{m}) - i\sin(\theta\bar{m}))\cos\theta \\
&\quad - \int_\pi^{2\pi} (\cos(\theta\bar{m}) - i\sin(\theta\bar{m}))\cos\theta \\
&= \left[\frac{e^{-\bar{m}\theta}}{(1-\bar{m}^2)}(\sin\theta - i\bar{m}\cos\theta)\right]_0^{\pi} \\
&\quad - \left[\frac{e^{-\bar{m}\theta}}{(1-\bar{m}^2)}(\sin\theta - i\bar{m}\cos\theta)\right]_\pi^{2\pi} \\
&= \frac{2i\bar{m}}{1-\bar{m}^2}(e^{-i\pi\bar{m}} + 1) = \frac{4i\bar{m}}{1-\bar{m}^2}, \ \bar{m} = 2k, \ \forall k \in \mathbb{Z}.
\end{aligned} \tag{6.30}$$

where $\bar{m} = (m_q - m_p) \in \mathbb{Z}$. We see that this expression is not defined for $\bar{m} = 1$, but inserting for this value in the interegal will yield zero as a result. In fact, we see that the integral will evaluate to zero for each odd value of $\bar{m}$. If the barrier was aligned in the other direction, along the y-axis, a similar computation can be performed for $\sin\theta$ instead of $\cos\theta$.

Since the particles are interacting in the same way as before, there is no need to compute a special version of the Coulomb integral matrix elements for the double well. We do, however, need to transform the single-particle functions and two-body elements from the regular harmonic oscillator basis to an approximate basis for the double-well problem. This can be done via diagonalisation of the one-body Hamiltonian in order to find a matrix of coefficients $\mathbf{C}$, that perform this basis change,

$$|\phi_q\rangle_{\mathrm{DW}} = \sum_p C_p |\phi_p\rangle_{\mathrm{HO}}, \tag{6.31}$$

which can be inserted into an eigenvalue equation for the one-body operator,

$$\begin{aligned}
\hat{h}|\psi_q\rangle_{\mathrm{DW}} &= \epsilon_q |\psi_q\rangle_{\mathrm{DW}} \\
\sum_p \hat{h} C_p |\phi_p\rangle &= \sum_p \epsilon_p C_{pq} |\phi_p\rangle.
\end{aligned} \tag{6.32}$$

Assuming that the eigenvalues ϵ_q are eigenvalues for the double well single-particle functions, we project onto the regular harmonic oscillator basis,

$$\begin{aligned}\sum_p \langle \phi_r|\hat{h}|\phi_p\rangle &= \sum_p C_{pr}\epsilon_p \langle \phi_r|\phi_p\rangle \\ \sum_p h_{pr}C_{pr} &= C_{pr}\epsilon_p \\ \mathbf{hC} &= \mathbf{C}\epsilon\end{aligned} \tag{6.33}$$

This is an eigenvalue equation we can solve in order to obtain the coefficient matrix which transforms from the one basis to the other. This transformation can subsequently be applied to the two-body operator,

$$\langle \psi_\alpha\psi_\beta|\hat{u}|\psi_\gamma\psi_\delta\rangle = C_\alpha^{p*}C_\beta^{p*} \langle \phi_p\phi_q|\hat{u}|\phi_r\phi_s\rangle C_\gamma^r C_\delta^s, \tag{6.34}$$

where summation over same indices is assumed.

class quantum_systems.**TwoDimensionalDoubleWell**
(*n*, *l*, *radius_length*, *num_grid_points*, *barrier_strength*=1.0, *l_ho_factor*=1.0, *omega*=0.25, *mass*=1)

Create Two-Dimensional Quantum Dot with double well potential, i.e. the Double Dot. This class inherits from **TwoDimensionalHarmonicOscillator**.

Parameters
- **n**(*int*) Number of electrons
- **l**(*int*) Number of spinorbitals
- **grid_length**(*int or float*) Space over which to construct wavefunction.
- **num_grid_points**(*int of float*) Number of points for construction of wavefunction.
- **barrier_strength**(*float, default* 1.0) Barrier strength in double well potential.
- **l_ho_factor**(*float, default* 1.0) Normal HO vs double well basis function multiple.
- **omega**(*float, default* 0.25) Angular frequency of harmonic oscillator potential.
- **mass**(*int or float, default* 1.0) Mass of electrons. Atomic units is used as default.

Attributes
- **h** One-body matrix **Type** np.array
- **f** Fock matrix **Type** np.array
- **u** Two-body matrix **Type** np.array

Methods
- **setup_system**(*axis*=0)
  Must be called in order to compute basis functions. Parameter *axis* decices to which axis the well barrier is aligned. $(0, 1) = (x, y)$.

6.2.4 Magnetic field

Extending the two-dimensional quantum dot to be under the influence of a static, transverse magnetic field consitutes not much more than adding constant terms to the one-body operators. We are considering a system with the following one-body hamiltonian, where an angular momentum term is added

$$\hat{h} = \frac{\hat{p}^2}{2m} + \frac{1}{2}m\Omega^2\hat{r}^2 + \frac{\omega_c}{2}\hat{L}_z, \tag{6.35}$$

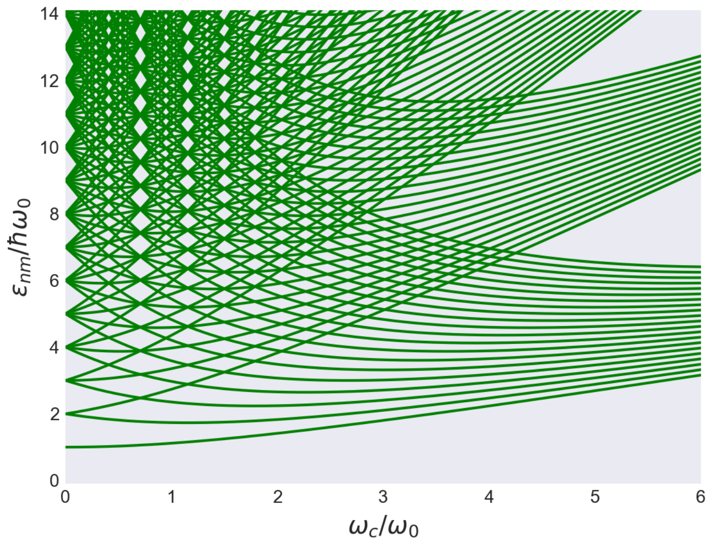

Figure 6.2: A few of the lowest eigenvalues ϵ_{nm} for a two-dimensional quantum dot for transverse magnetic field of increasing strength. This plot of the single-particle energies form the Fock-Darwin spectrum. Some states for very high values of m are omitted to make the formation of Landau bands in strong fields more visible.

where $\Omega = \sqrt{\omega_0^2 + \frac{\omega_c^2}{4}}$ and ω_c is the parameter dictating the strength of the magnetic field. We see that this Hamiltonian is the same as the normal two-dimensional quantum dot one-body Hamiltonian (Equation 6.12) for $\omega_c = 0$ as $\Omega \to \omega_0$, which is the well potential frequency. Conversely, if the magnetic field is infitinely strong we see that $\Omega \to \omega_c/2$ and Equation 6.35 becomes the one-body hamiltonian of a free electron in a transverse magnetic field. The single-particle functions (Equation 6.13) with the adjusted Bohr radius $a = \sqrt{m\Omega/\hbar}$, are also eigenfunctions of the angular momentum L_z and the energy eigenvalues are simply

$$\epsilon_{nm} = \hbar\Omega(2n + |m| + 1) - \frac{\hbar\omega_c}{2}m. \tag{6.36}$$

We see immediately that the energy undergoes a general shift due to the new Ω which is dependent on ω_c, but also that the energy shift of a particular shift is dependent on the sign of the azimuthal quantum number m for the given state. These factors will give different degeneracies, as illustrated in Figure 6.2. Such a plot of single-particle particle energies are sometimes referred to as the Fock-Darwin spectrum[20, 13]. With this comes the challenge of sorting the one-body matrix elements correctly, and ensuring that we keep a closed-shell structure.

Notice in Figure 6.2, that there are lengthy intervals of b-field strength were there is no degeneracy in the eigenenergies. Conversely, for certain specific field strengths there are very interesting shell structures with diverse energies. For $\omega_c/\omega = 1/\sqrt{2}$ we get the interesting shell structure depicted in Figure 6.3. Such accidental bunching also occurs for $\omega_c/\omega = 2/\sqrt{3}, 3/2, 4/\sqrt{5} \ldots$. We also see from figure Figure 6.2 that for an infinitely strong magnetic field as $\omega_c/\omega \to \infty$, in the free particle limit, that the energy levels form a sequence of so-called Landau bands.

As for the computation of the basis set, not much needs to be added in the computation

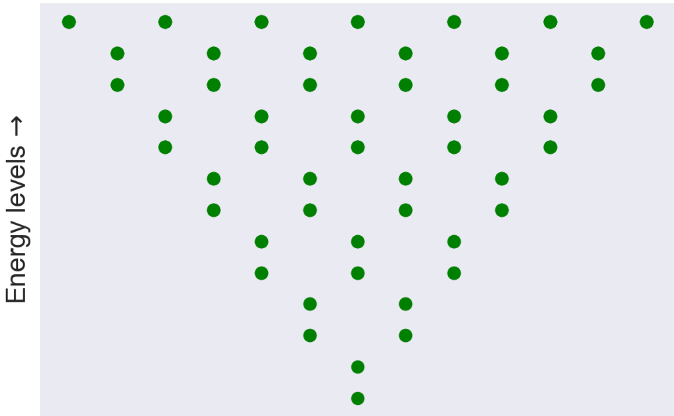

Figure 6.3: Illustration of eigenenergy degeneracies for two-dimensional quantum dot for transverse magnetic field of strength $\omega_c = 1/\sqrt{2}$. Each dot

than the extra energy to the diagonal part of the one-body matrix elements h^p_q, as everything else is the same, including the two-body Coulomb integrals. But, as we have already mentioned and displayed in Figure 6.2, for increasing strength of the magnetic field, the eigenenergies as function of ω_c eventually cross over one another. The magnetic field has the effect of decreasing the energy of a state with $m > 0$ and increasing the energy of a state with $m < 0$. This means that it is necessary to sort the eigenvalues after they have been computed.

The class specification of the two-dimensional quantum dot subjected to a transverse, homogeneous, static magnetic field is below.

class quantum_systems.**TwoDimHarmonicOscB**
(*n*, *l*, *radius_length*, *num_grid_points*, *omega_0*=1.0, *mass*=1, *omega_c*=0)

Create Two-Dimensional Quantum Dot with constant homogenous magnetic field. This class inherits from **TwoDimensionalHarmonicOscillator**.

Parameters
- **n**(*int*) Number of electrons
- **l**(*int*) Number of spinorbitals
- **grid_length**(*int or float*) Space over which to construct wavefunction.
- **num_grid_points**(*int of float*) Number of points for construction of wavefunction.
- **omega_0**(*float, default* 1.0) Part of harmonic osc. not dep. on magnetic field.
- **mass**(*int or float, default* 1.0) Mass of electrons. Atomic units is used as default.
- **omega_c**(*float, default* 0) Frequency corresponding to strenght of magnetic field.

Attributes
- **h** One-body matrix **Type** np.array
- **f** Fock matrix **Type** np.array
- **u** Two-body matrix **Type** np.array

Methods
- **setup_system**()
  Must be called in order to compute basis functions.
- **construct_dipole_moment**()
  Constucts dipole moment. This method is called by setup_system().

6.3 Constructing a Custom System

We have constructed a subclass of the `QuantumSystem` base class called `CustomSystem` with the intent of interfacing with other quantum chemistry libraries. This interfacing allows us to extract basis sets for other systems, like atoms and molecules, that will function with the coupled cluster solvers we have implemented.

The function of the member methods in the `CustomSystem` class should be evident from their names. One can set the one-body matrix elements with `set_h(h, add_spin)`, set dipole matrix with `set_dipole_moment(dipole_moment, add_spin)` and so on. How one would go about getting these structures is somewhat non-trivial, at least for someone not used to using quantum chemistry libraries. We have therefore added functions to the `quantum_systems` module that do just that. The functions
`quantum_systems.custom_system.construct_psi4_system()` and
`quantum_systems.custom_system.construct_pyscf_system()`
extracts the one-body matrix, Coulomb intergrals, dipole moment, overlap matrix and nuclear repulsion from Psi4[57] and PySCF[73], respectively. The functions are provided in full in section E.1 and section E.2. We have picked Psi4 and PySCF to interface with as they seem to be widely used in the quantum chemistry community. Psi4 has 354 stars and 235 forks, while PySCF has 308 stars and 175 forks on GitHub. Arguably this can be considered widely popular considering the specificity of the topic.

class quantum_systems.**CustomSystem**

Constructs custom quantum system, where a uses can add matrix elements for other sources. The purpose of this class is to allow usage of quantum many-body solvers that function with *quantum_systems* module using other sources basis sets.

Methods:

set_h(*h*, *add_spin=False*)
Add one-body matrix elements, i.e. matrix elements from non-interacting part of Hamiltonian.
Parameters:
h (*np.array*) One-body matrix
add_spin (*bool*) Enforces spin orthogonality

set_u (*u*, *add_spin=False*, *anti_symmetrize=False*)
Add two-body matrix elements, i.e. matrix elements from interacting part of Hamiltonian.
Parameters:
u (*np.array*) Two-body matrix
add_spin (*bool*) Enforces spin orthogonality
anti_symmetrize (*bool*) Anti-symmetrises two-body matrix

set_s(*u*, *add_spin=False*)
Add overlap matrix
Parameters:
s (*np.array*) Overlap matrix
add_spin (*bool*) Enforces spin orthogonality

set_dipole_moment(*dipole_moment*, *add_spin=False*)
Add dipole moment, i.e. transition matrix.
Parameters:
dipole_moment (*np.array*) Dipole moment
add_spin (*bool*) Enforces spin orthogonality

set_spf(*spf*, *add_spin=False*)
Add single-particle functions, i.e. eigenfunctions of non-interacting part of Hamiltonian.
Parameters:
spf (*np.array*) Single-particle functions
add_spin (*bool*) Enforces spin orthogonality

set_nuclear_repulsion_energy (*set_nuclear_repulsion_energy*)
Add nuclear repulsion energy. For atoms and molecules.
Parameters:
nuclear_repulsion_energy (*float*) Nuclear reulsion energy

6.4 Time Evolution

In order to compute the time-development of a quantum system, we add a time-dependent term to the Hamiltonian that describes the system. The class `TimeEvolutionOperator` is an abstract base class, which defines components necessary to make such time-dependent operators. A time-dependent operator usually applies solely the one- or two-body part of the Hamiltonian, and more often just the non-interacting one-body operator. For this reason we have implemented abstract attributes in the `TimeEvolutionOperator` which will make it possible for the time-dependent coupled cluster solver to determine what parts of the Hamiltonian is necessary to update for each time step.

class quantum_systems.**TimeEvolutionOperator**

Abstract base class for time evolution operator

Attributes:

is_one_body_operator
Property used to determine if the time-evolution operator only applies to the one-body part of the Hamiltonian.
Type *bool*

is_two_body_operator
Property used to determine if the time-evolution operator only applies to the two-body part of the Hamiltonian.
Type *bool*

Methods:

set_system(*system*)
Internal function used to set callback system. This is done in the *QuantumSystem* class and allows the user to specify the time-evolution operator parameters when setting the operator.
Parameters:
system (*QuantumSystem*) System the time-evolution operator is applied to.

h_t(*current_time*)
Function computing the one-body part of the Hamiltonian for a specified time.
Parameters:
current_time (*float*) One-body operator evaluated at specified time.
Returns: One-body operator.
Return type: np.array

u_t(*current_time*)
Function computing the two-body part of the Hamiltonian for a specified time.
Parameters:
current_time (*float*) Two-body operator evaluated at specified time.
Returns: Two-body operator.
Return type: np.array

A common time evolution operator used in the study is a dipole approximation of a laser field. We have implemented a class `LaserField`, which makes a simulation of such a field possible. This is a relatively simple time evolution operator, as it only affects the one-body part of the Hamiltonian, i.e. the non-interacting part. Consequently, the `LaserField` class only needs to switch the `is_one_body_operator` to `True` and implement the method `h_t(current_time)`. The time-dependent pulse, incorporating the shape and frequency of the laser is passed as a parameter to the class. This can be any callable type. The polarisation of the field is also passed to the class as a simple static vector, meaning that as of now the class only allows for linear polarisation. The electric field in the dipole appriximation typically reads

$$\mathbf{E}(t) = \epsilon \mathscr{E}_0 F(t) \cos{(\omega_k t)}, \tag{6.37}$$

where ϵ is the polarisation vector, $\mathscr{E}_0$ is a parameter for the maximum amplitude (strength) of the field, $F(t)$ defines the time-dependent envelope of the laser pulse, the cosine term is there to make sure it's a waveform and ω_k is the angular frequency of the laser.

class quantum_systems.**LaserField** (*laser_pulse*, *polarization_vector=None*)

Implementation of laser field. Needs time-dependent *callable* to function properly.

Attributes:

is_one_body_operator Always *True* **Type** *Bool*

Methods:

h_t(*current_time*)
Computes one-body operator as a sum of the one-body operator of the system and product of *laser_pulse* parameter at current time, *polarization_vector* parameter and *dipole_moment* attribute of system.

Chapter 7

Coupled Cluster

The main product of this study is manifested in the `coupled_cluster` module for Python. This module is designed to fit together with the `quantum_systems` module described in the previous chapter. We have tried to make this module easy to extend, resulting in a framework where every solver scheme inherits from an abstract parent class that specifies what must be implemented in order to make a supplemental solver or class operational in conjunction with the rest of the framework.

As a beginning to this project, which we hope will continue to grow and be used, we have implemented several different ground state solver classes, and several time-dependent solver classes. In order of increasing sophistication and elegance, we have a ground state- and a time-dependent solver for both the coupled cluster method with double excitations (CCD), the coupled cluster method with singles- and double excitations (CCSD), and for the orbital-adaptive coupled cluster method with double excitations (OACCD). The time-dependent solvers within a particular category are dependent on its ground state counterpart, but the ground state solvers can be used independently.

The `coupled_cluster` module can be install from github via `pip` by the following command,

```
pip install git+https://github.com/Schoyen/coupled-cluster.git
```

If one prefers, the same task can be accomplished by the following commands,

```
git clone https://github.com/Schoyen/coupled-cluster.git
cd coupled-cluster
pip install .
```

We have supplied environment specifications for `conda`, with requirement specifications for the convenience of the user. Assuming the git repository is cloned properly,

```
conda environment create -f environment.yml
```

Activate the environment with,

```
conda activate cc
```

Full documentation of this module, which we hope will be kept up to date with any future revisions can be found at `www.coupled-cluster.com`.

7.1 Ground State Computations

Before any development in time can be performed, we need to derive configurations of systems that we can be pretty certain exist in nature. This makes the implementation of ground state solvers necessary. We have implemented ground state solvers; the `CoupledClusterDoubles` and `CoupledClusterSinglesDoubles` are based on the theoretical framework form of the Lagrangian formulation of coupled cluster, while `OATDCCD` is a ground state version of an orbital-adaptive ground state coupled cluster solver with double excitations. Moreover, we constructed a data structure for the amplitudes in the `AmplitudeContainer` class and we have implemented two "mixer" classes that help with convergences of the ground state solvers, `AlphaMixer` and `DIIS`.

7.1.1 Representation of Amplitudes

The most central structure in any coupled cluster solver are the amplitudes. The amplitudes are what defines the true structure of the wavefunction as a linear combination of single-particle functions contained in the reference Slater determinant. We have found it beneficial to implement a special container class for the amplitudes, aptly called `AmplitudeContainer`.

class coupled_cluster.cc_helper.**AmplitudeContainer** (*t*, *l*, *np*)

Container for amplitude functions.

Parameters:
- **t**(*list*, *tuple*, *set*) τ amplitudes
- **l**(*list*, *tuple*, *set*) λ amplitudes
- **np**(*module*) Matrix library, e.g. numpy, cupy etc

Attributes:
- **t** τ amplitudes
- **l** λ amplitudes

Methods:
- **unpack**()
  - **Returns:** Amplitudes
  - **Return type:** *generator*
- **asarray**()
  - **Returns:** Amplitude vector
  - **Return type:** *np.array*

The `AmplitudeContainer` class is built as a data structure for the amplitude functions, and comprises all methods and attributes to serve this purpose. This includes overloading of primitive methods of the base python `Object` type.: `__add__` and `__radd__` enables adding a scalar or properly shaped vector to the amplitudes, `__mul__` and `__rmul__` allows for multiplication with scalars and vectors, and `__iter__` is implemented to make the class an iterable. In summary, the `AmplitudeContainer` functions as a fully operational data structure for amplitudes of coupled cluster solver, with both τ and λ amplitudes.

7.1.2 Coupled Cluster Base Class

All ground state solvers within the `coupled_cluster` module are built as sub-classes of the abstract base class `CoupledCluter`. The most important method of this class is the `compute_ground_state()` method. This method in turn calls the `iterate_t_amplitudes()` and `iterate_l_amplitudes()` successively.

class coupled_cluster.cc.**CoupledCluster**
(*system*, *mixer=<class'coupled_cluster.mix.DIIS'>*, *verbose=False*, *np=None*)

Abstract base class defining the basic structure of a coupled cluster ground state solver class.

Parameters
- **system**(*QuantumSystem*) A system class from the *quantum_systems* module.
- **mixer**(*AlphaMixer, default AlphaMixer*) Mixer - Subclass of *AlphaMixer* class.
- **verbose**(*bool, default False*) Will print results for each iteration if *True*.

Methods

compute_ground_state (*t_args=[]*, *t_kwargs={}*, *l_argys=[]*, *l_kwargs={}*)
Computes ground state of system given as parameter. Allows for parameters relating the the τ- and λ amplitudes, for use in inheriting classes.

compute_particle_density()
Computes the one-body density of the system.
Returns: Particle density
Return type: *np.array*

compute_reference_energy()
Computes reference energy
Returns: Reference energy
Return type: *np.array*

get_amplitudes(*get_t_0=False*)
Getter for amplitudes.
Parameters:
get_t_0 (*bool, default False*) Returns amplitude at $t = 0$ if `True`.
Returns: Amplitudes
Return type: *AmplitudeContainer*

iterate_l_amplitudes (*max_iterations*=100, *tol*=$1e^{-4}$, ***mixer_kwargs*)
Finds solution to λ amplitudes iteratively.
Parameters:
max_iterations (*int*) The limit of iterations allowed.
tol (*float, default* $1e^{-4}$) The tolerance for convergence.

iterate_t_amplitudes (*max_iterations*=100, *tol*=$1e^{-4}$, ***mixer_kwargs*)
Finds solution to τ amplitudes iteratively.
Parameters:
max_iterations (*int*) The limit of iterations allowed.
tol (*float, default* $1e^{-4}$) The tolerance for convergence.

_get_t_copy Abstract method
_get_l_copy Abstract method
compute_energy Abstract method
compute_one_body_density_matrix Abstract method
compute_t_amplitudes Abstract method
compute_l_amplitudes Abstract method
setup_t_mixer Abstract method
setup_l_mixer Abstract method
compute_t_residuals Abstract method
compute_l_residuals Abstract method

As we have outlined in chapter 5, the τ amplitudes are only dependent on τ, while the λ amplitudes are dependent on both τ and λ. Therefore, the τ amplitude equations iterative solver `iterate_t_amplitudes()` is called first, and the λ amplitude equation solver is called second. For illustration, the most important section of the `compute_l_amplitudes()` method is the following

```
for i in range(max_iterations):
self.compute_l_amplitudes()
residuals = self.compute_l_residuals()

if self.verbose:
    print(f"Iteration: {i}\tResiduals (l): {residuals}")

if all(res < tol for res in residuals):
    break

assert i < (
    max_iterations - 1
), f"The l amplitudes did not converge. Last residual: {residuals}"
```

The equivalent section of code in the `compute_t_amplitudes()` method is nearly identical. The `CoupledCluster` class is supposed to provide a framework for which to implement various coupled cluster ground state solver classes. It therefore has several abstract methods that such subclasses need to implement and overwrite. The most important of these are the methods `compute_t_amplitudes` and `compute_l_amplitudes`, which are supposed to contain the evaluation of amplitude equations for a given coupled cluster truncation and scheme.

With the hope that the functiunality of the rest of the methods in the abstract base class `CoupledCluster` can be inferred from name, and with the goal of brevity we proceed to a study of the simplest ground state coupled cluster solver, namely CCD, implemented in the `CoupledClusterDoubles` class.

7.1.3 Coupled Cluster Doubles

Starting from construction, the `CoupledClusterDoubles` class passes the system, defined through a `QuantumSystem` object to the parent class constructor, along with any keyword arguments, such as turning on verbosity, mixer type and what matrix library to apply. The `QuantumSystem` class will contain all the information necessary to set up the system, i.e. construct a one-body matrix, fock matrix and two-body matrix. These will be used to set up empty arrays for the τ and λ amplitudes. The `compute_initial_guess` is called lastly in the constructor, computing the inital guess of the double-excited amplitudes as

$$\tau^{(0)} = \frac{u_{ij}^{ab}}{D_{ij}^{ab}}, \tag{7.1}$$

where u is the two-body operator and $D_{ij}^{ab} = f_a^a + f_b^b - f_i^i - f_j^j$, where f is the Fock operator.

In the `CoupledClusterDobles` class specification one would notice that it has implementations of all the abstract methods from the `CoupledCluster` abstract class. The reason for the existence of the class, the `compute_ground_state()` method, is inherited from the parent class, and does the same thing as described above - calling `iterate_t_amplitudes()` and `iterate_l_amplitudes()`. These methods also exist as members of `CoupledClusterDoubles`, but are excluded from the class specification for sake of brevity. It is possible to pass arguments to the the two iterator methods; one list for each iteration method, or as keywords. One can also pass arguments to the mixer through the `compute_ground_state_method()`. An overview of mixing applied to iterative solvers is given in the next section.

The important part of the specific coupled cluster scheme solver is contained in the two methods `compute_t_amplitudes()` and `compute_l_amplitudes()`. These functions evaluate the entire coupled cluster doubles amplitude equations. The computation of each term (diagram) in the amplitude equation is done in separate functions, as calls to `numpy.tensordot()`, for a total of ten terms for the τ amplitude equation in the coupled cluster doubles method including permutation operators:

$$\begin{aligned}0 =& u^{ab}_{ij} + f^b_c \tau^{ac}_{ij} P(ab) - f^k_j \tau^{ab}_{ik} P(ij) + \frac{1}{4}\tau^{ac}_{ij}\tau^{ab}_{mn}u^{mn}_{cd} + \frac{1}{2}\tau^{cd}_{ij}u^{ab}_{cd} + \frac{1}{2}\tau^{cd}_{jm}\tau^{ab}_{in}u^{mn}_{cd}P(ij) \\ &- \frac{1}{2}\tau^{ac}_{nm}\tau^{bd}_{ij}u^{nm}_{cd}P(ab) + \tau^{ac}_{im}\tau^{bd}_{jn}u^{mn}_{cd}P(ij) + \tau^{ac}_{im}u^{bm}_{jc}P(ab)P(ij) + \frac{1}{2}\tau^{ab}_{mn}u^{mn}_{ij}.\end{aligned} \tag{7.2}$$

class coupled_cluster.cc.**CoupledClusterDoubles** (*system*, ***kwargs*)

Implementation of coupled cluster with double excitations ground state solver. Inherits from the **CoupledCluster** abstract base class.

Parameters
- **system**(*QuantumSystem*) A system class from the *quantum_systems* module.

Methods
- **compute_ground_state** (*t_args=[], t_kwargs={}, l_args=[], l_kwargs={}*)
  Computes CCD ground state of given system.
- **compute_initial_guess**() Computes initial guess for amplitudes.
- **_get_t_copy**()
  Returns: Copy of τ^{ab}_{ij} amplitudes
  Return type: *AmplitudeContainer*
- **_get_l_copy**()
  Returns: Copy of λ^{ij}_{ab} amplitudes
  Return type: *AmplitudeContainer*
- **compute_t_residuals**()
  Returns: Norm of τ^{ab}_{ij} amplitudes
  Return type: *float*
- **compute_l_residuals**()
  Returns: Norm of λ^{ij}_{ab} amplitudes
  Return type: *float*
- **setup_t_mixer**(***kwargs*) Sets up mixer for τ amplitudes
- **setup_l_mixer**(***kwargs*) Sets up mixer for λ amplitudes
- **compute_energy**()
  Returns: CCD ground state energy
  Return type: *float*
- **compute_t_amplitudes**() Computes τ amplitudes
- **compute_l_amplitudes**() Computes λ amplitudes
- **compute_one_body_density**()
  Returns: One-body density matrix
  Return type: *np.array*
- **compute_two_body_density**()
  Returns: Two-body density matrix
  Return type: *np.array*

The initial guess in equation Equation 7.1 is terms 2 and 3 from Equation 7.2. These terms also form the basis of the iterative scheme, if we move them to the left of the equal sign in

Equation 7.2,

$$D_{ij}^{ab}\tau_{ij}^{ab} = g(u,\tau), \tag{7.3}$$

where $g(u,\tau)$ now consists of the rest of the doubles amplitude equation, our recursion relation can be written

$$t^{(k+1)} = \frac{g(u,\tau^{(k)})}{D_{ij}^{ab}}. \tag{7.4}$$

An example of a computation of one term from Equation 7.2 is,

```
def add_d2e_t(u, t, o, v, out, np):
    term = np.tensordot(t, u[o, v, v, o], axes=((1, 3), (2, 0))).transpose(
        0, 2, 1, 3
    )
    term -= term.swapaxes(0, 1)
    term -= term.swapaxes(2, 3)
    out += term
```

This function particular computes the D_{2e} diagram[1].

7.1.4 Coupled Cluster Singles Doubles

Most of the rest of the methods in the `CoupledClusterDoubles` class are there for the use of other methods, or for extracting observables. Moving to the next logical coupled cluster solver scheme; the coupled cluster method with single- and double excitations is now a matter of taking into account the extra computations needed in this scheme, for each method in the abstract base clase `CoupledCluster`. There are indeed many more computations, but the code will structurally be the same. The class specification for `CoupledClusterSinglesDoubles` is therefore given here without specification of the methods as they are excactly the same. For testing purposes, the `CoupledClusterSingelsDoubles` class have the option to only include double excitation at construction. The amplitude equations for the CCSD scheme is found by constructing the coupled cluster Lagrangian (Equation 5.132) in `sympy` and differentiating it symbolically. The resulting equations can be found in Appendix D.

class coupled_cluster.cc.**CoupledClusterSinglesDoubles**
(*system*, *include_singles=True*, ***kwargs*)

Implementation of coupled cluster with single- and double excitations ground state solver. Inherits from the **CoupledCluster** abstract base class.

Parameters
- **system**(*QuantumSystem*) A system class from the *quantum_systems* module.
- **include_singles**(*bool, default True*) Includes single excitations if `True`.

7.1.5 Orbital-Adaptive Coupled Cluster

The algorithm applied when computing the ground state in the orbital-adaptive sphere is the nonorthogonal orbital-optimised coupled cluster (NOCC) method, developed by Myhre[54]. The NOCC scheme is shown to converge towards full configuration interaction. Since the `OACCD` class is acutally applying NOCC it can be perceived as a misnomer, but as of yet there exist no ground state equivalent of the time-dependent orbital-adaptive coupled cluster (OACC)

[1] After the labelling from chapter 5 and Shavitt & Bartlett[69]

method. Such a method is in development, and there is strong indication that NOCC would be equivalent to a OACC ground state solver. What is more, NOCC does vary the orbitals as well as iterate over amplitude, and we have therefore opted to call it OACC.

class coupled_cluster.cc.**OACCD** (*system*, ***kwargs*)

Implementation of the orbital-adaptive coupled cluster method with double excitation (OACCD), also called the nonorthogonal orbital-optimized coupled cluster model with double excitations (NOCCD). This algorithm require orthonormal basis functions. Based on work by Rolf H. Myhre[54].
Inherits from the **CoupledClusterDoubles** class.

Parameters
system(*QuantumSystem*) A system class from the *quantum_systems* module.

Methods
compute_ground_state (*max_iterations*=100, *tol*=$1e^{-4}$, *termination_tol*=$1e^{-4}$, *tol_factor*=0.1, *change_system_basis=False*, ***mixer_kwargs*)
Computes ground state of system by iterating over κ equations.
Parameters:
max_iterations (*int, default* 100) Maximum number of iterations.
tol (*float, default* $1e^{-4}$) Tolerance of convergence.
termination_tol (*float, default* $1e^{-4}$) Give up if tolerance is below this.
tol_factor (*float, default* 0.1) Stricter for each κ-iteration.
change_system_basis (*bool, default False*) Changes basis after calculation.
setup_kappa_mixer (**kwargs) Set up mixer for κ vector iterations.
compute_kappa_down_rhs (*f*, *u*, *t_2*, *l_2*, *o*, *v*, *np*)
Parameters:
f (*np.array*) Fock matrix.
u (*np.array*) Two-body operator, Coulomb integrals.
t_2 (*np.array*) τ^{ab}_{ij} amplitudes.
l_2 (*np.array*) λ^{ij}_{ab} amplitudes.
o (*Slice*) Occupied arbitals.
v (*Slice*) Virtual orbitals.
np (*Module*) Linear algebra library.
compute_kappa_up_rhs (*f*, *u*, *t_2*, *l_2*, *o*, *v*, *np*)
Parameters:
f (*np.array*) Fock matrix.
u (*np.array*) Two-body operator, Coulomb integrals.
t_2 (*np.array*) τ^{ab}_{ij} amplitudes.
l_2 (*np.array*) λ^{ij}_{ab} amplitudes.
o (*Slice*) Occupied arbitals.
v (*Slice*) Virtual orbitals.
np (*Module*) Linear algebra library.

Our implementation of the NOCC ground state solver is inherited from code written by Rolf Myhre and adapted to our framework. We supply a brief overview of the algorithm here. The starting point for the NOCC model is the bivariational Lagrangian

$$\mathscr{L} = \langle\tilde{\Psi}|\hat{H}|\Psi\rangle = \langle\tilde{\phi}|(1+\Lambda)e^{-\hat{T}}e^{-\kappa}\hat{H}e^{\kappa}e^{\hat{T}}|\phi\rangle \tag{7.5}$$

which is very similar to the coupled cluster Lagrangian (Equation 5.132), except for a biorthogonal basis and a transformation of the Hamiltonian, defined as follows

$$\begin{aligned} \tilde{c}_p^\dagger &= e^{-\kappa}\hat{c}_p^\dagger e^{\kappa} \\ c_p &= e^{-\kappa}\hat{c}_p^\dagger e^{\kappa} \\ |\phi\rangle &= e^{-\kappa}\,|\hat{\phi}\rangle \end{aligned} \tag{7.6}$$

where the orthogonal reference creation- and annihilation operators marked with a hat (ˆ), as is the reference state function. We require that κ is antihermitian,

$$\kappa = \sum_{pq} \kappa_{pq} c_p^\dagger c_q, \quad \kappa^\dagger = -\kappa. \tag{7.7}$$

Moreover, we split κ into excitations and relaxations (up and down),

$$\kappa = \sum_{ai} \kappa_{ai}^u c_a^\dagger \tilde{a}_i + \kappa_{ia}^d c_i^\dagger \tilde{c}_a = \sum_{ai} \kappa_{ai}^u X_a i + \kappa_{ia}^d \tilde{X}_{ia}^\dagger. \tag{7.8}$$

As in any many-body formulation that includes a Lagrangian, we would like to compute the first-order conditions of the Lagrangian, in order to derive what would be the NOCC equation. The problem with this is that the result would be some extremely lengthy expressions, because κ does not commute with $\hat{T}$ or Λ. Therefore, we express the NOCC equations with an optimized basis where $\kappa = 0$, where a solution would correspond to a stationary point of the Schrödinger equation. This is the same as expanding the exponentials in κ and keeping only zero-order terms. This trick leads to an algorithm which iterates between orbital transformations and amplitudes until self-consistency.

At a particular stationary point the differential of the Lagrangian (Equation 7.5) must be zero with respect to the four sets of parameters $\{\tau\}$, $\{\lambda\}$, $\{\kappa^u\}$ and $\{\kappa^d\}$, giving us four sets of equations,

$$\frac{\partial \mathscr{L}}{\partial \lambda_{\mu_n}} = \langle \tilde{\phi}|\tilde{X}_{\mu_n} e^{-\hat{T}} \hat{H} e^{\hat{T}} |\phi\rangle\,, \tag{7.9}$$

$$\frac{\partial \mathscr{L}}{\partial \tau_{\mu_n}} = \langle \tilde{\phi}|(1+\Lambda) e^{-\hat{T}} [\hat{H}, X_{\mu_n}] e^{\hat{T}} |\phi\rangle\,, \tag{7.10}$$

$$\frac{\partial \mathscr{L}}{\partial \kappa^u_{\mu_1}} = \langle \tilde{\phi}|(1+\Lambda) e^{-\hat{T}} [\hat{H}, X_{\mu_1}] e^{\hat{T}} |\phi\rangle\,, \tag{7.11}$$

$$\frac{\partial \mathscr{L}}{\partial \kappa^d_{\mu_1}} = \langle \tilde{\phi}|(1+\Lambda) e^{-\hat{T}} [\hat{H}, \tilde{X}_{\mu_1}] e^{\hat{T}} |\phi\rangle\,. \tag{7.12}$$

We are now ready to outline the full algorithm of the `compute_ground_state()` in what we have called the `OACCD`. The method is iterating over the the norm of κ^u and κ^d, called the residuals of κ, until consistency compared to a tolerance value is achieved. For each such iteration, iteration over the τ and λ double excitation amplitudes is performed, but at a much less strict tolerance value than under the `CoupledClusterDoubles` scheme. After the iteration over τ and λ is achieved, the values for κ^u and κ^d are recalculated, in order to compute the aggragate κ (Equation 7.8), which in turn can be used to transform the orbitals,

$$\begin{aligned} h^{(k+1)} &= e^{-\kappa} h^{(k)} e^{\kappa}, \\ (u^{pq}_{rs})^{(k+1)} &= (e^{-\kappa})^p_a (e^{-\kappa})^q_b (u^{ab}_{cd})^{(k)} (e^{\kappa})^d_s (e^{\kappa})^c_r, \end{aligned}$$

which (in addition to being written with incomprehensible notation) is used to compute a new Fock operator. The resulting rotation of the orbitals will aid in better convergence towards the ground state.

Specialised Orbital-Adaptive `AmplitudeContainer`

Because of the nature of the orbital-adaptive coupled cluster scheme, it is no longer sufficient to store just the amplitudes as representation of the exact state. Therefore, we have implemented a subclass of the `AmplitudeContainer` data structure which also contains the coefficient matrices necessary to perform the required orbital transformations.

class coupled_cluster.cc_helper.**OACCVector** (*t*, *l*, *C*, *C_tilde np*)

Container for amplitude functions.

Parameters:

- **t**(*list*, *tuple*, *set*) τ amplitudes
- **l**(*list*, *tuple*, *set*) λ amplitudes
- **C**(*np.array*) Right-hand side coefficient matrix
- **C_tilde**(*np.array*) Left-hand side coefficient matrix
- **np**(*module*) Matrix library, e.g. numpy, cupy etc

Attributes:

- **t** τ amplitudes
- **l** λ amplitudes
- **C** Coefficient matrix $\mathbf{C}$
- **C_tilde** Coefficient matrix $\tilde{\mathbf{C}}$

Methods:

- **unpack**()
  - **Returns:** Amplitudes and coefficient matrices
  - **Return type:** *generator*
- **asarray**()
  - **Returns:** Amplitude vector and coefficient matrices
  - **Return type:** *np.array*

Like the `AmplitudeContainer` class, this data structure also implements fuctionality for addition, multiplications and iteration.

7.1.6 Mixing of Amplitude Vectors

Iterative many-body methods are prone to convergence problems for certain configurations. This would be doubly important since we have moved to a variational description of coupled cluster theory, where generalisations of the variational theory dictate inifitesimal variations, which is not always feasible to implement. Moreover, an iterative optimisation scheme may not always converge properly at all. Luckily, there exists numerous techniques both for controlling and acceleration convergence.

Alpha mixer

The simplest way to "massage" convergence out of the coupled cluster ground state methods to use a dampening, where one would include a part of the result from the previous iteration, here applied to the τ amplitudes,

$$\bar{\tau}^{(k+1)} = (1-\theta)\tau^{(k+1)} + \theta\tau^{(k)}, \tag{7.13}$$

where $\tau^{(k+1)}$ is the current result from evaluating the amplitude equations, and $\tau^{(k)}$ is the previous value. Choosing $\theta \in [0, 1]$ will tune how much of the previous amplitude to include in the new state. The idea is to allow for a more gentle transition between the iterations. We have implemented this very simple mixing scheme in the `AlphaMixer` class, which also serves as a base class for further mixer implementations.

class coupled_cluster.mix.**AlphaMixer** (*theta=0.1*, *np=None*)

Class defining the α mixer. Computes a superposition of current and new amplitude vector. Also defines base class and methods the new mixer classes must implement.

Parameters
theta(*float, default 0.1*) Mixing parameter. $\theta \in [0, 1]$
np(*Module*) Matrix library to be used, e.g. numpy, cupy.

Methods
compute_new_vector (*trial_vector*, *direction_vector error_vector*)
Computes new trial vector for mixing with full right hand side of amplitude equation.
Parameters:
trial_vector (*np.array*) Initial vector for mixing
direction_vector (*np.array*) Vector to be added to *trial_vector*.
error_vector (*np.array*) Not used in α mixer. Needed in subclasses.
Returns: New mixed vector
Return type: *np.array*

The Quasi-Newton method with DIIS acceleration

A more sophisticated method to aid in convergence, and perhaps the most popular, is by performing a direct inversion of iterative subspace (DIIS). The DIIS method is built to accelerate the quasi-Newton method, an we will necesarily outline the quasi-Newton before we examine DIIS, which is explained in Helgaker et al.[34].

The commutator of Fock operator with the cluster operator is generally

$$[\hat{f}, \hat{T}] = \sum_{\mu} D_{\mu} \tau_{\mu} X_{\mu}, \tag{7.14}$$

where ϵ_μ is the sum of unoccupied energies minus the sum of all occupied energies, i.e. $D_{ij}^{ab} = \epsilon_a + \epsilon_b - \epsilon_i - \epsilon_j$, τ_μ is the amplitude of a particular excitation, and X_μ is an excitation operator. For CCD Equation 7.14 becomes,

$$[\hat{f}, \hat{T}_2] = D_{ij}^{ab} \tau_{ij}^{ab} c_a^\dagger c_b^\dagger c_i c_j. \tag{7.15}$$

This allows us to write the coupled cluster vector function $\Omega_\mu^{(0)}$, and its Jacobian $\Omega_{\mu\nu}^{(1)}$ of the nth iteration in the form

$$\Omega_\mu^{(0)} = D_\mu \tau_\mu^{(n)} + \langle \Phi_\mu | e^{-\hat{T}^{(n)}} \hat{U} e^{\hat{T}^{(n)}} | \Phi_0 \rangle \tag{7.16}$$

$$\Omega_{\mu\nu}^{(1)} = D_\mu \delta_{\mu\nu} + \langle \Phi_\mu | e^{-\hat{T}^{(n)}} [\hat{U}, X^\nu] e^{\hat{T}^{(n)}} | \Phi_0 \rangle \tag{7.17}$$

which are very similar to the coupled cluster energy and amplitude equations, but the matrix element contains just $\hat{U}$, the fluctuation potential, instead of the entire Hamiltonian $\hat{H} = \hat{F} + \hat{U}$.

The Jacobian constists only of a diagonal part, involving differences of the orbital energies, and a nondiagonal part, containing the fluctuation potential. The trick from *Newton's* method is to expand the vector functions around the set of amplitudes of the current iteration $\tau^{(n)}$,

$$\Omega(\tau^{(n)} + \Delta\tau) = \Omega^{(0)}(\tau^{(n)}) + \Omega^{(1)}(\tau^{(n)})\Delta\tau + \dots, \tag{7.18}$$

which leads to a recursion relation, neglecting terms that are nonlinear in $\Delta\tau$,

$$\Omega^{(1)}(\tau^{(n)})\Delta\tau^{(n)} = -\Omega^{(0)}(\tau^{(n)}). \tag{7.19}$$

By inserting Equation 7.16 and Equation 7.17 we get the *quasi-Newton* equations for the optimisation of the coupled-cluster wavefunction,

$$\Delta\tau_\mu^{(n)} = -\frac{\Omega_\mu^{(0)}(\tau^{(n)})}{D_\mu} \tag{7.20}$$

The quasi-Newton method is fairly robust, but the convergence may be improved significantly by introducing DIIS.

In the DIIS framework[64], the new amplitudes $\tau^{(n+1)}$ are obtained by a linear interpolation among the previous estimates of the amplitudes,

$$\tau^{(n+1)} = \sum_{k+1}^{n} w_k(\tau^{(k)} + \Delta\tau^{(k)}), \tag{7.21}$$

where $\Delta\tau^{(k)}$ are obtained from Equation 7.20, and the interpolations weights sum to unity,

$$\sum_{k=1}^{n} w_k = 1.$$

To determine the DIIS weights, we associate each set of amplitudes $\tau^{(k)}$ with an error vector. We use the scaled vector function $\Delta\tau^{(k)}$ as error vector and determine the interpolation coefficients by minimising the norm of the averaged vector

$$\Delta\tau^{\text{ave}} = \sum_{k=1}^{n} w_k \Delta\tau^{(k)} \tag{7.22}$$

subject to Equation 7.1.6.

We have implemented the DIIS acceleration of the quasi-Newton method in the class `DIIS`. This class inherits from the `AlphaMixer` class and would function in its place. The `DIIS` class allows one to pick how many vectors to store and compute a linear interpolation of, with a default value of 10 vectors.

class coupled_cluster.mix.**DIIS** (*num_vecs*=10, *np*=*None*)

General vector mixing class to accelerate quasi-Newton method using the direct inversion of iterative space (DIIS) scheme. Inherits from *AlphaMixer*.

Parameters

num_vecs(*float, default 10*) Number of vectors to keep in memory.
np(*Module*) Matrix library to be used, e.g. numpy, cupy.

Methods

compute_new_vector (*trial_vector*, *direction_vector error_vector*)

Computes new trial vector for mixing with full right hand side of amplitude equation.

Parameters:

trial_vector (*np.array*) Initial vector for mixing
direction_vector (*np.array*) Vector to be added to *trial_vector*.
error_vector (*np.array*) Error vector associated with QN DIIS.

Returns: New mixed vector

Return type: *np.array*

clear_vectors()

Delete all stored vectors.

7.2 Time Development

We have sought to formulate the time-dependent coupled cluster methods in the abstraction of very general differential equations. By doing this we conform to the mindset of *implement once, apply anywhere*. In any implementation of a time-dependent coupled cluster solver, we consider it as though we are working with a general function $f(u(t), t)$, so that it can be solved by any general solver for a differential equation. The abstract formulation of a differential equation reads

$$u'(t) = f(u(t), t). \tag{7.23}$$

Notice that nearly any equations of motion in physics can be written in this way. Practically, this framework makes it necessary for us to implement the primitive `__call__` method for all coupled cluster solvers, in order to make them into a callable representation of the right-hand side of Equation 7.23.

Similarly to the rest of the `coupled_cluster` module, the portion relating to time development begins with an abstract base class, `TimeDependentCoupledCluster` functioning as an interface for the rest of the classes. At construction, the `TimeDependentCoupledCluster` class is passed an affiliated ground state solver in the form of a `CoupledCluster` object, a `QuantumSystems` object and an `Integrator` object. All these are necessary in order to compute a time-development. The starting point for time development is a system in it's ground state, necessitating the specification of a system and a ground state solver. Inclusion of a `CoupledCluster` object in the `TimeDependentCoupledCluster` class allows one to call the `compute_ground_state()` from this object, and it is included as a wrapper. Several other methods are included from the ground state realm, like the methods for particle density computations. The `__call__` method is implemented in the abstract base class, where the current amplitude in the form as an `AmplitudeContainer` object is passed as an argument together with the current time step. The right hand side of all amplitude equations are evaluated, and new amplitudes are returned. The class is called, i.e. evaluated by an `Intergator`, i.e. the system is developed in time by solving the equations of motion with a numerical integrator. We will consider integrators separately in the next section.

class coupled_cluster.cc.**TimeDependentCoupledCluster**
(*cc*, *np=None*, *system*, *integrator=None **cc_kwargs*)

Abstract base class defining the basic structure for a time-dependent coupled cluster solver.

Parameters

cc(*CoupledCluster*) Class instance defining the ground state solver.
system(*QuantumSystem*) Class instance defining the system to be solved.
np(*module*) Matrix/linear algebra library to be used, e.g. Numpy, Cupy
integrator(*Integrator*) Integrator class instance, e.g. RK4, GaussIntegrator

Methods

compute_ground_state (*t_args=[]*, t_kwargs={}, l_args=[], l_kwargs)
Call on method from *CoupledCLuster* class to compute ground state of system.

compute_particle_density()
Computes one-body density at time t.
Returns: Particle density
Return type: *np.array*

rhs_l_amplitudes()
Abstract function that needs to be implemented as a generator. The generator should return the λ-amplitudes right-hand sides, in order of increasing excitation.

rhs_t_amplitudes()
Abstract function that needs to be implemented as a generator. The generator should return the τ-amplitudes right-hand sides, in order of increasing excitation.

set_initial_conditions(*amplitudes=None*)
Set initial condition of system. It is necessary to make a call to this system before computing time-development. Can be called without argument. Will in that case revert to amplitudes of ground state solver.
Parameters:
amplitudes(*AmplitudeContainer*) Amplitudes for initial system configuration.

solve (*time_points*, *timestep_tol*=$1e^{-8}$)
Develop given system in time, specified by an array of *time_points*. Integrates equations of motion repeatedly, over all time points.
Parameters:
time_points (*list, np.array*) Time points over which to integrate EOM.
timestep_tol (*float, default* $1e^{-8}$) Tolerance in size of steps `dt`.
Returns: Amplitudes **Return type:** *Generator(AmplitudeContainer)*

compute_energy() Abstract function.
compute_one_body_density_matrix() Abstract function.
compute_two_body_density_matrix() Abstract function.
compute_time_dependent_overlap() Abstract function.
compute_particle_density() Calls *compute_one_body_density_matrix*.
update_hamiltonian(*current_time*, *amplitudes*)
Updates Hamiltonian of system in time, constructs new Fock operator.

The bare minimum that a time-dependent coupled cluster scheme needs to implement in order to function is the methods `rhs_t_amplitudes()` and `rhs_l_amplitudes()`, which should return the right-hand side of the amplitude equations. These methods should be integrated as generators, to make it possible to iterate over them, and should yield the amplitudes in order of increasing excitation level. Most of the remaining functionality lies in the superclass `TimeDependentCoupledCluster`.

Arguably the most important method in the `TimeDependentCoupledCluster` abstract base class is the `solve(time_steps)` method. For the array of time steps supplied, this method propagates with the integrator member of the class for all amplitudes. This method remains the same for all time-propagation schemes, and is therefore implemented in the base class for inheritance in sub-classes. This method in full is

```python
def solve(self, time_points, timestep_tol=1e−8):
    n = len(time_points)

    for i in range(n − 1):
        dt = time_points[i + 1] − time_points[i]
        amp_vec = self.integrator.step(
            self._amplitudes.asarray(), time_points[i], dt
        )

        self._amplitudes = type(self._amplitudes).from_array(
            self._amplitudes, amp_vec
        )

        if abs(self.last_timestep − (time_points[i] + dt)) > timestep_tol:
            self.update_hamiltonian(time_points[i] + dt, self._amplitudes)
            self.last_timestep = time_points[i] + dt

        yield self._amplitudes
```

We see that after the integrator is advanced one step in time, returning an amplitude vector. This amplitude object is stored as a member of the class by use of the `from_array()` method from the `AmplitudeContainer` class, after which the Hamiltonian of the system is updated if enough time has passed.

7.2.1 TDCCSD

We have implemented both a time-dependent CCD (TDCCD) solver and a time-dependent CCSD (TDCCSD) solver. For the sake of brevity, we present only the TDCCSD here as their appearance would be nearly identical. The `TDCCSD` class, a sub-class of `TimeDependentCoupledCluster`, inheriting all methods from this super-class. It accepts the same parameter as the super-class, except the parameter that defines the ground state solver to be used - the `CoupledCluster` class implementation. The ground state solver is already decided by the level of excitation for the computation at hand. All parameters are passed to the constructor in the parent class.

The `solve()` method will have the exact same functionality as in the parent class, but since the `TDCCSD` contains amplitudes and everything else needed to solve the equations of motions in a singles and doubles truncation, it will now yield a `Generator` object containing amplitudes that are developed in time. Any observable can be extracted during an iteration over this `Generator` object. We have implemeted several methods that can be useful in extracting information about the state of the time-developed system, for instance `compute_time_dependent_overlap()` which computes the probability of the system being in the ground state, and `compute_energy()` which computes the energy of the system in the current time-dependent state. The ground state probability, i.e. `compute_time_dependent_overlap()`, is given by a general time-dependent auto-correlation function,

$$A(t', t) \equiv \langle S(t')|S(t)\rangle \,. \tag{7.24}$$

Because coupled cluster theory is not variational in the usual sense it is necessary to define a general state vector as combination of both $|\Psi\rangle$ and $\langle\tilde{\Psi}|$,

$$|S\rangle = \frac{1}{\sqrt{2}} \begin{pmatrix} |\Psi\rangle \\ |\tilde{\Psi}\rangle \end{pmatrix} \tag{7.25}$$

which makes the time-dependent auto-correlation function (Equation 7.24),

$$A(t', t) = \frac{1}{2} \Big(\langle\tilde{\Psi}(t')|\Psi(t)\rangle + \langle\Psi(t')|\tilde{\Psi}(t)\rangle \Big) \tag{7.26}$$

according to the definitions of the *indefinite* innerproduct by Pedersen and Kvaal[61]. Here we would set $t' = 0$, because we are interested in the ground state overlap, translating to the state before developement in time.

class coupled_cluster.cc.**TDCCSD** (**args*, ***kwargs*)

Sub-class of **TimeDependentCoupledCluster**. Computes time-development of provided system, employing time-dependent coupled cluster method with single- and double excitations. The orbitals are kept static. This class inherits all methods from the parent class, but includes a few extra.

Parameters

system(*QuantumSystem*) Class instance defining the system to be solved.
np(*module*) Matrix/linear algebra library to be used, e.g. Numpy, Cupy
integrator(*Integrator*) Integrator class instance, e.g. RK4, GaussIntegrator

Methods

rhs_t_0_amplitude (**args*, ***kwargs*)
Evaluates CC energy expression
Returns: CCSD ground state energy.
Return type: *np.array*

rhs_t_amplitudes()
Evaluates τ_i^a and τ_{ij}^{ab} amplitude equations
Returns: τ_i^a, τ_{ij}^{ab}
Return type: *Generator*

rhs_l_amplitudes()
Evaluates λ_a^i and λ_{ab}^{ij} amplitude equations
Returns: λ_a^i, λ_{ab}^{ij}
Return type: *Generator*

compute_energy ()
Computes energy at current time step.
Returns: energy
Return type: *float*

compute_particle_density()
Computes one-body density matrix
Returns: One-body density
Return type: *np.array*

compute_time_dependent_overlap ()
Computes overlap of current time-developed state with the ground state.
Returns: Probability of grond state **Return type:** *np.array*

solve (*time_points*, *timestep_tol*=$1e^{-8}$)
Develop given system in time, specified by an array of *time_points*. Integrates equations of motion repeatedly, over all time points.
Parameters:
time_points (*list, np.array*) Time points over which to integrate EOM.
timestep_tol (*float, default* $1e^{-8}$) Tolerance in size of steps `dt`.
Returns: Amplitudes **Return type:** *AmplitudeContainer*

Within our truncation to include only single- and double excitations, an inner product of two state vectors, in the normal coupled cluster scheme with static orbitals, can be computed in the following manner

$$
\begin{aligned}
\langle\Psi'|\Psi\rangle &= \langle\Phi|(1+\Lambda)e^{-\hat{T}'}e^{\hat{T}}|\Phi\rangle \\
&= \langle\Phi|(1+\Lambda_1+\Lambda_2)(1-\hat{T}_1'-\hat{T}_2'+\frac{1}{2}\hat{T}_1'^2)(1+\hat{T}_1+\hat{T}_2+\frac{1}{2}\hat{T}_1^2)|\Phi\rangle \\
&= \langle\Phi|\Phi\rangle - \langle\Phi|\Lambda_1\hat{T}_1'|\Phi\rangle + \langle\Phi|\Lambda_1\hat{T}_1'|\Phi\rangle - \langle\Phi|\Lambda_2\hat{T}_1'\hat{T}_1|\Phi\rangle - \langle\Phi|\Lambda_2\hat{T}_2'|\Phi\rangle \\
&\quad + \langle\Phi|\Lambda_2\hat{T}_2|\Phi\rangle + \frac{1}{2}\langle\Phi|\Lambda_2\hat{T}_1'\hat{T}_1'|\Phi\rangle + \frac{1}{2}\langle\Phi|\Lambda_2\hat{T}_1\hat{T}_1|\Phi\rangle\,,
\end{aligned}
\tag{7.27}
$$

where we have ignored terms that would give a zero-contribution. Evaluating the remaining terms can be done with your favourite method. Here is an example using Wick's theorem,

$$
\begin{aligned}
\langle\Phi|\Lambda_2\hat{T}_2|\Phi\rangle &= \langle\Phi|\sum_{abij}\frac{1}{4}\lambda^{ij}_{ab}\{\hat{i}^\dagger\hat{a}\hat{j}^\dagger\hat{b}\}\sum_{cdkl}\frac{1}{4}\tau^{cd}_{kl}\{\hat{c}^\dagger\hat{k}\hat{d}^\dagger\hat{l}\}|\Phi\rangle \\
&= \langle\Phi|\sum_{\substack{abcd\\ijkl}}\frac{1}{16}\lambda^{ij}_{ab}\tau^{cd}_{kl}\{\hat{i}^\dagger\hat{a}\hat{j}^\dagger\hat{b}\}\{\hat{c}^\dagger\hat{k}\hat{d}^\dagger\hat{l}\}|\Phi\rangle + \text{three more equivalent contractions} \\
&= \frac{1}{4}\langle\Phi|\sum_{\substack{abcd\\ijkl}}\lambda^{ij}_{ab}\tau^{cd}_{kl}\delta_{ac}\delta_{bd}\delta_{ik}\delta_{jl}|\Phi\rangle = \frac{1}{4}\sum_{abij}\lambda^{ij}_{ab}\tau^{ab}_{ij}.
\end{aligned}
\tag{7.28}
$$

The entirity of the `compute_time_dependent_overlap_method()` consists of similar computations,

```python
def compute_time_dependent_overlap():
    np = self.np
    t_0, t_1, t_2, l_1, l_2 = self._amplitudes.unpack()
    t_1_0, t_2_0 = self.cc.t_1, self.cc.t_2
    l_1_0, l_2_0 = self.cc.l_1, self.cc.l_2

    psi_t_0 = 1
    psi_t_0 += np.einsum("ia, ai ->", l_1, t_1_0)
    psi_t_0 -= np.einsum("ia, ai ->", l_1, t_1)
    psi_t_0 += 0.25 * np.einsum("ijab, abij ->", l_2, t_2_0)
    psi_t_0 -= 0.5 * np.einsum("ijab, aj, bi ->", l_2, t_1_0, t_1_0)
    psi_t_0 -= np.einsum("ijab, ai, bj ->", l_2, t_1, t_1_0)
    psi_t_0 -= 0.5 * np.einsum("ijab, aj, bi ->", l_2, t_1, t_1)
    psi_t_0 -= 0.25 * np.einsum("ijab, abij ->", l_2, t_2)

    psi_0_t = 1
    psi_0_t += np.einsum("ia, ai ->", l_1_0, t_1)
    psi_0_t -= np.einsum("ia, ai ->", l_1_0, t_1_0)
    psi_0_t += 0.25 * np.einsum("ijab, abij ->", l_2_0, t_2)
    psi_0_t -= 0.5 * np.einsum("ijab, aj, bi ->", l_2_0, t_1_0, t_1_0)
    psi_0_t -= np.einsum("ijab, ai, bj ->", l_2_0, t_1, t_1_0)
    psi_0_t -= 0.5 * np.einsum("ijab, aj, bi ->", l_2_0, t_1, t_1)
    psi_0_t -= 0.25 * np.einsum("ijab, abij ->", l_2_0, t_2_0)

    auto_corr = 0.5 * (psi_t_0 * np.exp(-t_0) + (psi_0_t * np.exp(t_0)).conj())

    return np.abs(auto_corr) ** 2
```

The time-dependent energy in `compute_energy()` is found by evaluation of the coupled cluster Lagrangian (Equation 5.132) at the current time-developed amplitudes.

7.2.2 OATDCCD

In order to move to an orbital-adaptive framework, we have implemented a new abstract base class that includes treatment of orbitals. This class has the modified amplitude container `OACCVector` as a memeber. Most important differences from the standard time-dependent coupled cluster framework in the way the `__call__` implementation also returns coefficient matrices, how the Hamiltonian is updated for every time step and the inclusion of functions that compute P- and Q-space equations. As we will get into, the Q-space equations will simplify greatly under the assumption of a complete basis, but the P-space equations will differ depending on the excitation level.

Disappearing RHS of Q-space equations.

A necessary additon to an orbital-adaptive time-dependent coupled cluster framework is the computation of P- and Q-space equations. The Q-space equations can be simplified substatially, because they equate to zero for an infinite basis. We will show this now, starting with Equation 5.195,

$$i\hbar \sum_q \rho_p^q Q \frac{\partial}{\partial t} |\varphi_q\rangle = \sum_q \rho_p^q Q h |\varphi_q\rangle + \sum_{qrs} \rho_{pr}^{qs} Q W_s^r |\varphi_q\rangle . \tag{7.29}$$

Inserting for Q in the second term on the right-hand side gives

$$\sum_{qrs} \rho_{pr}^{qs} Q W_s^r |\varphi_q\rangle = \sum_{qrs} \rho_{pr}^{qs} W_s^r |\varphi_q\rangle - \sum_{qrs} \rho_{pr}^{qs} W_s^r \sum_t |\varphi_t\rangle \langle\tilde{\varphi}_t|\varphi_q\rangle . \tag{7.30}$$

If we assume an infinite orthogonal basis, we have

$$\sum_t |\varphi_t\rangle\langle\tilde{\varphi}_t| \, |\varphi_q\rangle = \hat{1},$$

and the term will disappear. Inserting for Q in the first term on the right hand side of the first Q-space equations also yields zero. This means that the first Q-space equations reduce to

$$\begin{aligned}
i\hbar \sum_q \rho_p^q Q \frac{\partial}{\partial t} &= 0 \\
i\hbar \sum_q \rho_p^q \frac{\partial}{\partial t} |\varphi_p\rangle &= i\hbar \sum_q \rho_p^q \sum_s |\varphi_s\rangle\langle\tilde{\varphi}_s| \frac{\partial}{\partial t} |\varphi_p\rangle \\
\frac{\partial}{\partial t} |\varphi_p(t)\rangle &= \sum_s |\varphi_s(t)\rangle \, \langle\tilde{\varphi}_s(t)| \frac{\partial}{\partial t} |\varphi_p(t)\rangle \\
\frac{\partial}{\partial t} C_p^\alpha(t) |\chi_\alpha\rangle &= \sum_s C_s^\alpha(t) |\chi_\alpha\rangle \, \eta_p^s \\
\dot{C}_p^\alpha &= \sum_s C_s^\alpha \eta_p^s,
\end{aligned} \tag{7.31}$$

which we rewrite more nicely on einsten summation form,

$$\dot{\mathbf{C}} = \mathbf{C}\eta_q^p . \tag{7.32}$$

Similarly for the second Q-space equations (Equation 5.196),

$$\dot{\tilde{\mathbf{C}}} = -\eta^p_q \tilde{\mathbf{C}}. \tag{7.33}$$

We see that the Q space equation has provided us with equations that describe the time propagation of the orbitals through the coefficient matrices $\mathbf{C}$ and $\tilde{\mathbf{C}}$. These equations are valid for all excitations levels of orbital-adaptive time-dependent coupled cluster (OATDCC), and have been implemented in the new abstract class `OATDCC`.

We see that η^p_q is the only thing needed in order to compute the coefficient matrices which dictate the orbital time propagation. We get η^p_q from the P-space equations. Since the P-space equations will be different for each level of sophistication we move onto a treatment of `OATDCCD`.

P-space equations in OATDCCD

The P-space equations for the orbital-adaptive time-dependent coupled cluster doubles (OATDCCD) scheme are nothing more than a series of tensor contractions, given by Equation 5.193 and Equation 5.194, restated here.

$$i\hbar \sum_{bj} A^{ib}_{aj} \eta^j_b = \sum_j \rho^i_j h^j_a - \sum_b \rho^b_a h^i_b + \frac{1}{2}\left[\sum_{prs} \rho^{is}_{pr} u^{pr}_{as} - \sum_{rqs} \rho^{qs}_{ar} U^{ir}_{qs}\right],$$

$$-i\hbar \sum_{bj} A^{ja}_{bi} \eta^b_j = \sum_b \rho^a_b h^b_i - \sum_j \rho^j_i h^a_j + \frac{1}{2}\left[\sum_{prs} \rho^{as}_{pr} u^{pr}_{is} - \sum_{rqs} \rho^{qs}_{ir} U^{ar}_{qs}\right]$$

We apply `numpy.linalg.tensorsolve`, in order to find η^a_i and η^j_b, which is the entirity of η^p_q. Now we have everything we need in order to iterate over the OATDCCD equations of motion.

In the outmost briefness, for each iteration, i.e. for each `Integrator.step()` advance, we compute the right hand side of the OATDCCD equations, Equation 5.191 and Equation 5.175, providing us with new amplitudes λ^{ij}_{ab} and τ^{ab}_{ij}. These can be used to compute density matrices, which in turn can be used to find η^p_q from the P-space equations. These will gives us the time-development or the orbitals in the form of coefficient matrices $\mathbf{C}$ and $\tilde{\mathbf{C}}$, which are used to update the one- and two-body parts of the Hamiltonian $\hat{h}$ and $\hat{u}$, respectively.

class coupled_cluster.cc.**OATDCCD** (**args*, ***kwargs*)

Class for computing time-development of provided system, employing orbital-adaptive time-dependent coupled cluster with double excitations. Subclass of abstract class **OATDCC**, which redefines the essential computations for the orbital-adaptive framework. **OATDCC** inherits all methods from **TimeDependentCoupledCluster**, overwriting those that are necessary to overwrite.

Parameters
- **cc**(*CoupledCluster*) Class instance defining the ground state solver.
- **system**(*QuantumSystem*) Class instance defining the system to be solved.
- **np**(*module*) Matrix/linear algebra library to be used, e.g. Numpy, Cupy
- **integrator**(*Integrator*) Integrator class instance, e.g. RK4, GaussIntegrator

Methods

compute_energy()

Computes energy at current time step.

Returns: energy

Return type: *float*

Problematic Overlap

Notice the absence of a `compute_time_dependent_overlap()` function in the `OATDCCD` class specification. It is unfeasible to compute a time-dependent overlap in an orbital-adaptive scheme, because of the computation increase due to the basis transformations.

Computing the inner product of two state vector at the *same* point in time would be unproblematic, and would result in the same kind of computation as in Equation 7.27. Moreover, in this inner product with static orbitals, many terms evaluate to zero. At two different times, as in a computation of the ground state probability $|\langle\tilde{\Psi}(0)|\Psi(t)\rangle|^2$ this would not be the case, and we need to keep all terms,

$$\begin{aligned}
\langle\tilde{\Psi}|\Psi\rangle &= \langle\tilde{\Phi}|(1+\Lambda)e^{\hat{T}'}e^{\hat{T}}|\Phi\rangle \\
&= \langle\tilde{\Phi}|(1+\Lambda_2)\left(1-\hat{T}_2'+\frac{1}{2}\hat{T}_2'^2\right)\left(1+\hat{T}_2+\frac{1}{2}\hat{T}_2^2\right)|\Phi\rangle \\
&= \langle\tilde{\Phi}|\Phi\rangle - \langle\tilde{\Phi}|\hat{T}_2'|\Phi\rangle + \frac{1}{2}\langle\tilde{\Phi}|\hat{T}_2'^2|\Phi\rangle + \langle\tilde{\Phi}|\Lambda_2|\Phi\rangle - \langle\tilde{\Phi}|\Lambda_2\hat{T}_2'|\Phi\rangle \\
&\quad + \frac{1}{2}\langle\tilde{\Phi}|\Lambda_2\hat{T}_2'^2|\Phi\rangle + \langle\tilde{\Phi}|\hat{T}_2|\Phi\rangle - \langle\tilde{\Phi}|\hat{T}_2'\hat{T}_2|\Phi\rangle + \frac{1}{2}\langle\tilde{\Phi}|\hat{T}_2'^2\hat{T}_2|\Phi\rangle \\
&\quad + \langle\tilde{\Phi}|\Lambda_2\hat{T}_2|\Phi\rangle - \langle\tilde{\Phi}|\Lambda_2\hat{T}_2'\hat{T}_2|\Phi\rangle + \frac{1}{2}\langle\tilde{\Phi}|\Lambda_2\hat{T}_2'^2\hat{T}_2|\Phi\rangle \\
&\quad + \text{six more terms.}
\end{aligned} \tag{7.34}$$

With static orbital, only terms that have the same number of excitations and relaxations would give a contribution to the final result. Now, because the orbitals have evolved in time, we don't have the same orthogonal properties that would cancel the other terms. Because we must include *everything* it becomes unfeasible to compute the time-dependent overlap in the orbital-adaptive scheme. The computation cost would scale at the same level as direct diagonalisation methods does, i.e. full configuration interaction schemes.

7.2.3 Integrators and ODE Solvers

Most, if not all, physical systems that evolve in time can be described as set of equations that we call the equations of motion. These can be usually be formulated as a single- or a set of ordinary differential equations written on the abstract form

$$u'(t) = f(u(t), t). \tag{7.35}$$

To this particular equation there is an infinite number of solutions, so in order to make the solution unique, we must also specify an initial condition

$$u(0) = U_0. \tag{7.36}$$

Given the right hand side of Equation 7.35, $f(u,t)$ and the initial condition U_0, our task would be to compute $u(t)$. The simplest equation of motion in physics is Newton's second law,

$$a(t) = \frac{F(t)}{m}, \tag{7.37}$$

which we have reformulated to be on the standard form as Equation 7.35.

In any numerical scheme, the ODE defining our problem will be discretised, such that the inital value problem Equation 7.35 becomes the following

$$u_{n+1} = u_n + hf(u_n, t_n), \quad u(t_0) = u_0, \tag{7.38}$$

where h is some small time step, $t_{n+1} = t_n + h$. We see that the equation(s) at hand is solve in steps and the most important method of an implementation of any integrator scheme will be the method defining how one would step from one point to the next.

We have already derived the equations of motions for several coupled cluster frameworks[2]. Solving these equations in time is done in the same manner as any other equations of motion. The right hand side of these equations is put into practice by implementing `__call__()` for all the time-dependent classes, and the initial condition of the problem is some configuration defined by the amplitudes of the problem. By formulating the time-dependent many-body problem in this way, we can find solutions to the equations of motion by any numerical integrator scheme. For convenience, we have included two integrator implementations in the `coupled_cluster` module - the common fourth order Runge-Kutta method and the symplectic Gauss-Legendre method. Moreover, we have defined an abstract base class `Integrator`, which defines a general integrator for eventual future additons.

class coupled_cluster.integrators.**Integrator** (*np*)

Abtract integrator parent class. Subclass must implement *step* method **Parameters**

np(*Module*) Matrix library to be used, e.g. numpy, cupy.

Methods

set_rhs (*rhs*)

Setter for right-hand side of problem.

Parameters:

rhs (*callable, int, float*) Right hand side of ODE.

step (*u, t, dt*)

Shell method. Must be implemented by subclass.

The Runge-Kutta Method

The Runge-Kutta methods are a large family of implicit and iterative methods of increasing order. The first-order Runge-Kutta method is the same as the forward Euler method, where a step is defined as follows,

$$u_{n+1} = u_n + hf(u_n, t_n). \tag{7.39}$$

The general step of an explicit n-th order Runge-Kutta method is defined by

$$u_{n+1} = u_n = h\sum_{i=1}^{s} b_i k_i, \tag{7.40}$$

where

$$\begin{aligned}
k_1 =& f(u_n, t_n),\\
k_2 =& f(u_n + h(a_{21}k_1), t_n + c_2h),\\
k_3 =& f(u_n + h(a_{31}k_1 + a_{32}k_2), t_n + c_3h),\\
&\vdots\\
k_s =& f(u_n + h(a_{s1}k_1 + a_{s2}k_2 + \cdots + a_{s,s-1}k_{s-1}), t_n + c_s),
\end{aligned} \tag{7.41}$$

where s is the number of stages, and the coefficients a_{ij} (for $j \in [1, i\rangle$ and $i \in \langle j, s]$), b_i (for $b \in [1, s]$) and c_i (for $i \in [2, s]$) defines the particular method. The matrix a_{ij} is called the

[2]TDCC:Equation 5.176 and Equation 5.177. OATDCC:Equation 5.172, Equation 5.175

Runge-Kutta matrix and b_i and c_i are known as the *weights* and *nodes*, respectively. We call the Runge-Kutta method consistent if

$$\sum_{j=1}^{i-1} a_{ij} = c_i, \quad i \in [2, s].$$

We have implemented the fourth-order Runge-Kutta method in the class `RungeKutta4`. This is the most common of the Runge-Kutta method, and is often sometimes referred to as simply "the Runge-Kutta method".

class coupled_cluster.integrators.**RungeKutte4** (*np*)

Classical fourth-order Runge-Kutta numerical integrator.

Parameters
- **np**(*Module*) Matrix library to be used, e.g. numpy, cupy.

Methods

set_rhs (*rhs*)

Setter for right-hand side of problem.

Parameters:
- **rhs** (*callable, int, float*) Right hand side of ODE.

step(*u, t, dt*)

One itegration step

Parameters:
- **u** (np.array) Array of equations to be integrated.
- **f** (float) Current time step.
- **dt** (float) Time step size.

Returns: RHS advanced one step, u_{n+1}.

Return type: *np.array*

A step of size h in the fourth order Runge-Kutta method is defined by

$$\begin{aligned} u_{n+1} =& u_n + \frac{1}{6}(k_1 + 2k_2 + 2k_3 + k_4), \\ t_{n+1} =& t_n + h, \end{aligned} \tag{7.42}$$

where

$$\begin{aligned} k_1 =& hf(u_n, t_n), \\ k_2 =& hf(u_n + \frac{k_1}{2}, t_n + \frac{h}{2}), \\ k_3 =& hf(u_n + \frac{k_2}{2}, t_n + \frac{h}{2}), \\ k_4 =& hf(u_n + k_3, t_n + h), \end{aligned}$$

This is implemented in the `step(u, t, dt)` method as

```
f = self.rhs
K1 = dt * f(u, t)
K2 = dt * f(u + 0.5 * K1, t + 0.5 * dt)
K3 = dt * f(u + 0.5 * K2, t + 0.5 * dt)
```

```
    K4 = dt * f(u + K3, t + dt)
    u_new = u + (1 / 6.0) * (K1 + 2 * K2 + 2 * K3 + K4
```

Symplectic Gauss Integrator

The Runge-Kutta method, as described above, will be unstable for most systems becuase of its inability to preserve structure and energy of the system. It is necessary to apply an integrator which is both structure-preserving and symplectic. We have inherited code used by Pedersen and Kvaal[61] and have adapted it to our framework. Nevertheless, we give a brief overview of its inner mechanics here.

A quadrature rule is an approximation of the definite integral of a function over an interval $[a, b]$.

The most common family of quadrature rules are derived by defining an equidistant grid of N points on the interval $[a, b]$, where the grid points x_n are given by

$$x_n = a + nh \tag{7.43}$$

where $h = (b - a)/N$, with index $n \in [0, N]$. A quadrature rule is commonly stated as a weighted sum of function values at specified points.

$$\int_a^b f(x)dx \approx \sum_{i=1}^{(N-1)} hf(x_i).$$

The simplest of such schemes of equidistant points is the *trapezoidal* rule given by

$$\int_a^b f(x)dx = h\left(\frac{1}{2}g(x_0) + f(x_1) + f(x_2) + \dots f(x_{N-1}) + \frac{1}{2}f(x_N)\right) + \mathscr{O}(h^2). \tag{7.44}$$

A very efficient method consists of repeating the trapezoidal rule and performing it for successive values of h, each having half the size of the previous one. This yields a sequence of approximations to the integral for various values of h can be fitted to a polynomial, and the value for this polynomial for $h = 0$ will yield a very accurate approximation to the exact value. This is called the *Romberg* method.

The n-point Gaussian quadrature rule functions similarly to the family of methods described above, but instead of equidistant points we use the zeros of orthogonal polynomials for the gripd points x_n. The first pick of orthogonal polynomials are Legendre polynomials, which are orthogonal on the interval $[-1, 1]$, i.e.,

$$\int_{-1}^{1} P_l(x)P_{l'}(x)dx = \delta_{ll'}. \tag{7.45}$$

We also approximate the function f with Legendre polynomials.

The Gauss-Legendre quadrature rule is constructed to yield an exact result for polynomials of degree $2n - 1$ or less. An advantage of the Gauss-Legendre method is that its accuracy is much better than that of other methods using the same number of integration points. In fact, the accuracy of an N-point Gauss-Legendre method is equivalent to that of an equidistiant point method using $2N$ points. The resulting Gauss-Legendre quadrature rule can be stated as

$$\int_{-1}^{1} f(x)dx = \sum_{n=1}^{N} w_n f(x_n) + \mathscr{O}(h^{2N}), \tag{7.46}$$

where x_n are the zeroes of the Legendre polynomial P_n, h is $2/N$ and w_n are appropriately chosen weights for the method.

Orthogonal polynomials p_r of degree r and leading coefficient one, satisfy the following recurrence realtion,

$$P_{r+1}(x) = (x - a_{r,r})p_r(x) - a_{r,r-1}p_{r-1}(x) \cdots - a_{r,0}p_0(x). \tag{7.47}$$

The three-term recurrence relation can be written as a matrix equation

$$J\tilde{P} = x\tilde{P} - p_n(x) \times \mathbf{e}_n, \tag{7.48}$$

where $\tilde{P} = [p_0(x), p_1(x), \dots, p_{n-1}(x)]^T$, $\mathbf{e}_n$ is the nth standard basis vector and J is the Jacobian matrix,

$$J = \begin{pmatrix} a_0 & 1 & 0 & \dots & & \\ b_1 & a_1 & 1 & 0 & \dots & \\ 0 & b_2 & a_2 & 1 & 0 & \dots \\ 0 & \dots & & & \dots & 0 \\ & \dots & 0 & b_{N-2} & a_{N-2} & 1 \\ & & \dots & 0 & n_{N-1} & a_{N-1} \end{pmatrix} \tag{7.49}$$

The eigenvalues of this matrix will be the nodes x_n, i.e. the zeros of the polynomials up to degree N. If $\phi^{(n)}$ is an eigenvector corresponding to an eigenvalue such an eigenvalue x_n, the corresponding weight can be found from the first component of this vector

$$w_n = \mu_0 \left(\phi_1^{(n)}\right)^2, \tag{7.50}$$

where

$$\mu_0 = \int_a^b \omega(x)dx$$

and $\omega(x)$ is the weight function. $\omega(x) = 1$ when Legendre polynomials are used in the Gauss quadrature. This efficient way of arriving at weights and nodes is called the Golub-Welsh algorithm[24].

Generally, a quadrature method is not used to compute the solution to ODEs, but we adapt it to a Runge-Kutta solver in the way explained in Pedersen and Kvaal[61]. A general implicit s-stage Runge-Kutta method is defined by

$$u_{n+1} = u_n + h\sum_{i=1}^{s} x_i f(u_n + Z_{ij}, t_n + w_i h), \tag{7.51}$$

$$Z_{in} h \sum_{j=1}^{s} a_{ij} f(u_n + Z_{jn}, t_n + w_j h). \tag{7.52}$$

This allows us to make an interpolation between each time step t_n and $t_n + h$ by a polynomial of order s and requiring the ODE to be satisfied at the s Gauss-Legendre quadrature points gives a symplectic and reversible integrator of order $2s$. The matrix a_{ij} is computed analytically,

$$a_{ij} = \int_0^{w_j} \ell_j(x)dx, \tag{7.53}$$

where

$$\ell_j(x) = \prod_{k=1,k\neq j}^{s} \frac{x - w_k}{w_j - w_k}, \tag{7.54}$$

is the jth Lagrange interpolation polynomial. The nonlinear equation Equation 7.52 is solved iteratively for each time step, making the method implicit. These fixed-point iterations are defined by

$$Z_{in}^{(k+1)} = h\sum_{j=1}^{s} a_{ij} f(u_n + Z_{jn}^{(k)}, t_n + w_j h). \tag{7.55}$$

The initial guess is crucial to the convergence speed of the method. We have employed guess (A) scheme described in section VIII.6.1 of Ref.[25].

For the user of the Gauss integrator, the experience will be much more pleasant than dealing with the derivations of the method, because its opeartion are the same, as evidenced by the `GaussIntegrator` class specification.

class coupled_cluster.integrators.**GaussIntegrator** (*np*, *s*=2, *maxit*=20, *eps*=$1e^{-14}$)

Simple implementation of symplectic Gauss-Legendre integrator of order 4 and 6 ($s = 2$ and $2 = 3$).

Parameters

- **np** (*Module*) Matrix library to be used, e.g. numpy, cupy.
- **s** (*int*, *default* 2) Order $= 2s$. Scheme only implemented for $s \in \{2, 3\}$.
- **maxit** (*int*) Maximum number of iterations.
- **eps** (*float*, *default* $1e^{-4}$) Convergence tolerance.

Methods

step (*u*, *t*, *dt*)

One itegration step

Parameters:

- **u** (*np.array*) Array of equations to be integrated.
- **f** (*float*) Current time step.
- **dt** (*float*) Time step size.

Returns: RHS advanced one step, u_{n+1}.

Return type: *np.array*

Part IV

Results

Chapter 8

Validation

Here we present a series of reproduced results from the scientific literature as a validation of our computational implementation. We manage to reproduce the instantaneous dipole results from the simulation of the hydrogen molecule in Li et al.[48], the time-dependent ground state probability of a quantum dot from Zanghellini et al.[77] and the spectrum of Helium from Pedersen and Kvaal[61]. The simulation of the ionisation of beryllium from Miyagi and Madsen[52], serves as an illustration of the advantage of adaptive orbitals versus static orbitals in a time-dependent coupled cluster method. For all time-dependent studies in this chapter we have employed the symplectic `GaussIntegrator` integrator class, as it has shown to be most stable in preliminary studies.

8.1 Instantaneous dipole in H_2

Li et al.[48] employ a time-dependent Hartree-Fock apporach in order to study the electronic optical response of molecules in intense fields. To be specific, they model the hydrogen molecule H_2 with a `6-311++G(d,p)` basis set, subject to an oscillating field of 1.72×10^{13} Wcm^{-2} and 456 nm. They find the time-dependent Hartree-Fock method to be nearly indistinguishable from calculations using the full time-dependent Schrödinger equation. We have managed to replicate the instantaneous dipole of this simulation of hydrogen.

A `6-311++G(d,p)` basis set corresponds to a `6-311++Gss` basis set in `PySCF`, and we can extract it from here,

```
molecule = "
    h 0.0 0.0 -0.6948522960236121;
    h 0.0 0.0  0.6948522960236121
    "
basis = "6-311++Gss"
system = construct_pyscf_system_ao(molecule, basis=basis)
```

The bond length of the Hydrogen molecule is approximately 0.7354 Å, converted to multiples of Bohr radii here. As the naming suggests, the basis set is a split-valence triple-zeta basis set, with one added s-type diffuse function and a set of p-type polarisation functions for each Hydrogen atom[1].

In their simulations Li et al. have used a linearly polarised and spatially homogenous external field aligned along the z-axis,

$$\mathbf{e}(t) = \mathbf{E}(t)\sin(\omega t). \tag{8.1}$$

[1]This would be obvious for a quantum chemist, but basis set configurations looks like incantantions from a spellbook to the uninitiated physicist

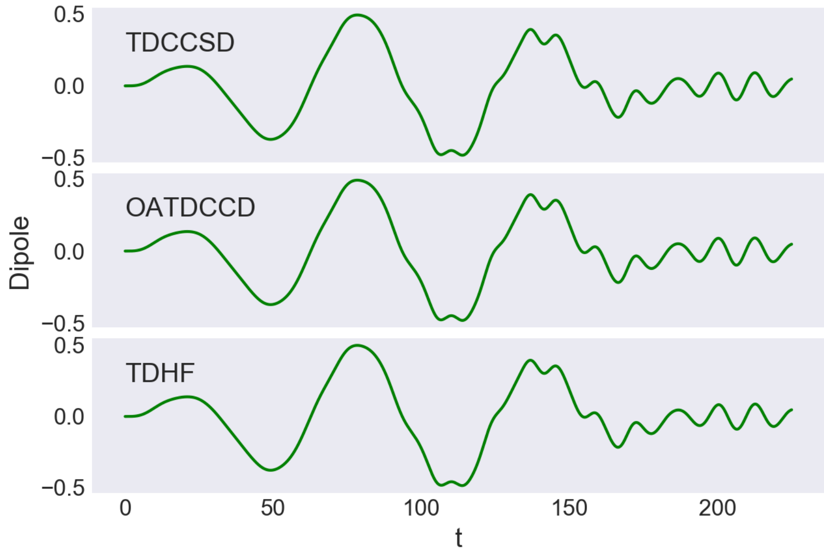

Figure 8.1: Instantaneous dipole for H_2 in an oscillating electric field $E_{\text{max}} = 0.07$ au (1.72×10^14 Wcm^{-2}) and $\omega = 0.1$ au (456 nm) using a `6-311++G(d,p)` basis set.

The field envelope $|\mathbf{E}|$ is linearly increased with time to a maximum value $|\mathbf{E}_{\text{max}}|$ at the end of the first cycle and remains at $|\mathbf{E}_{\text{max}}|$ for one cycle and then decreases linearly to zero by the end of the next cycle,

$$
\begin{aligned}
\mathbf{E}(t) = (\omega t/2\pi)\mathbf{E}_{\text{max}} \quad & \text{for} \quad 0 \leq t \leq 2\pi/\omega \\
\mathbf{E}(t) = \mathbf{E}_{\text{max}} \quad & \text{for} \quad 2\pi/\omega \leq t \leq 4\pi/\omega \\
\mathbf{E}(t) = (3 - \omega t/2\pi)\mathbf{E}_{\text{max}} \quad & \text{for} \quad 4\pi/\omega \leq t \leq 6\pi/\omega \\
\mathbf{E}(t) = 0 \quad & \text{for} \quad t < 0 \text{ and } t > 6\pi/\omega,
\end{aligned}
\tag{8.2}
$$

where the maximum field intensity if 1.72×10^{14} Wcm^{-2} ($E_{\text{max}} = 0.07$ au). Li et al. also run a simulation for a lower intensity, but we are conecerned only with this relatively more intensive pulse. The entire simulation lasts for $T = 225$ au.

The result of our simulation is shown in Figure 8.1, where we have computed the instantaneous dipole over time using three different methods. The time-dependent Hartre-Fock result is shown in the bottom sub-figure, and is expected to be exactly the same as figure 4.a from Li et al.[48], which it appear to be. For comparrison we have computed the result with both of our time-dependent coupled cluster methods. The result of the time-dependent coupled cluster method with single and double excitations are showed in the top subfigure, and the result of the orbital-adaptive coupled cluster method with double excitations are shown in the middle subfigure. We see that there is no perceptible difference between the results of the three methods.

8.2 Ground State Probability in 1D Quantum Dot

Zanghellini et al.[77] calculate the time development of a one-dimensional quantum dot with two electrons using the multi-configurational time-dependent Hartree-Fock method (MCTDHF). This method yields excact results for a very large number of configurations, $\eta \to \infty$. This study would provide a proper benchmark for our implementation because the coupled cluster method with singles and doubles excitations (CCSD) is excact for $n = 2$ particles. The harmonic

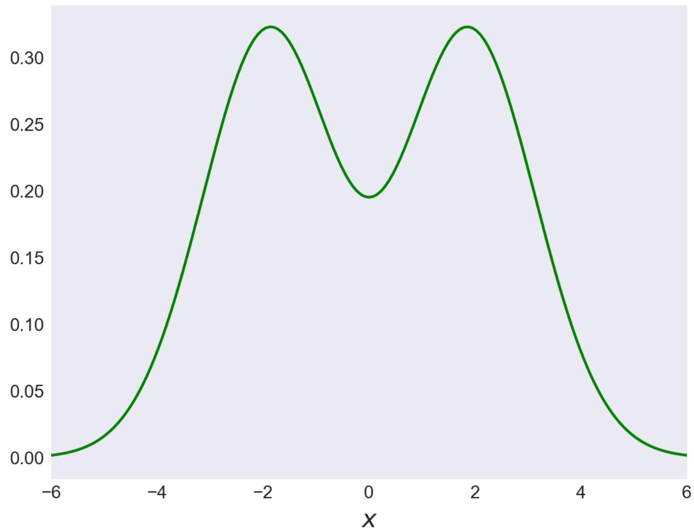

Figure 8.2: Electron density for the ground state wavefunction of a quantum dot with $n = 2$ eletrons and $l = 20$ spin-orbitals in the basis set computed with CCSD. This plot corresponds precisely with figure 1 in Zanghellini et al.[77].

oscillator potential applied in their study had a frequency of $\Omega = 0.25$, used a strong laser-like field with maximum intensity of $\mathbf{E} = 1$ and a laser frequency of $\omega = 8\Omega = 2$. The oscillating field is described much more simply than in Li et al.[48], using a simple sine function,

$$\mathbf{e}(t) = \mathbf{E}\sin(\omega t), \tag{8.3}$$

where the envelope $\mathbf{E}$ does not vary in time.

Zanghellini et al.[77] find that their multi-configurational time-dependent Hartree-Fock scheme convergences as the number of configurations is $\eta \geq 15$, up to the resulotion of their figures. We are able to reproduce this result precisely by employing the time-dependent coupled cluster method with singles and double excitations (TDCCSD). We have used our own one-dimensional quantum dot class, `ODQD`, with a harmonic potential and $l = 20$ spin-orbitals in the basis set for this simulation.

In Figure 8.2 we see the ground state electron density for the ground state wavefunction computed with CCSD. Zanghellini et al. computed the electron density for an increasing number of configurations η using multi-configurational time-dependent Hartree-Fock (MCTDHF). This figure matches the convergent electron density found by Zanghellini et al. as $\eta \to \infty$, in figure 1 from their article.

Figure 8.3 depicts the probability for the system being in the ground state as a function of time. Here we have included both a time-dependent Hartree-Fock computation, corresponding to a multi-configurational time-dependent Hartree-Focke computation with $\eta = 1$ configurations, and a time-depenedent coupled cluster computation with single and double excitations. We see that our coupled cluster scheme corresponds to the multi-configurational Hartree-Fock scheme employed by Zanghellini et al. when $\eta \to \infty$, as Figure 8.3 match figure 2 in Zanghellini et al.[77] precisely.

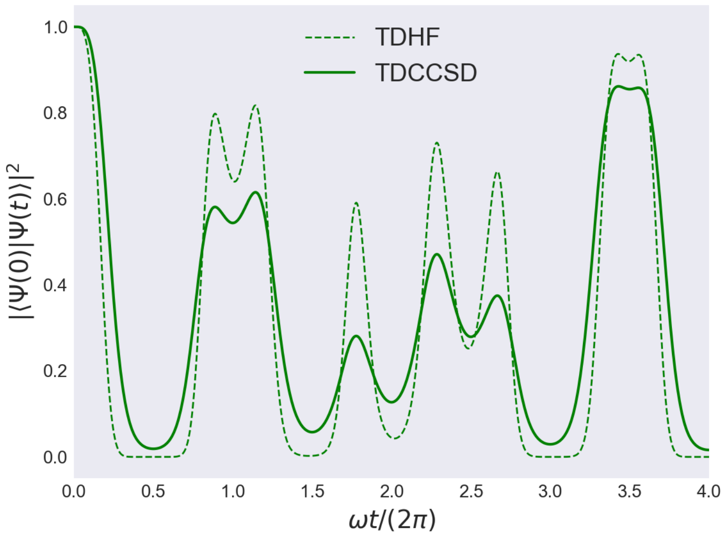

Figure 8.3: Probability of being in the ground state $|\langle\Psi(0)|\Psi(t)\rangle|$ using both TDHF and TDCCSD, for a one-dimensional quantum dot with $n = 2$ particles and $l = 20$ spin-orbitals. This plot corresponds precisely with figure 2 in Zanghellini et al.[77].

8.3 Dipole Spectrum of Helium

In their comparison study of symplectic and regular Runge-Kutta type integrators, Pedersen and Kvaal[61] produce a dipole spectrum of helium.

The basis set employed by Pedersen and Kvaal is a cc-pVDZ basis set which we extract from `Psi4`,

```
He = "
    He 0.0 0.0 0.0
    symmetry c1
"
options = {"basis": "cc-pvdz", "scf_type": "pk", "e_convergence": 1e-8}
system = construct_psi4_system(He, options)
```

The `cc-pVDZ` basis set is a correlation consistent, polarised, valence-only basis set with double zeta-functions. For hydrogen this basis set amounts to five orbitals in total.

In their study Pedersen and Kvaal use an oscillating field with frequency $\omega = 2.8735643$ au and maximum intensity $\mathbf{E}_{\text{max}} = 10$ au. This frequency corresponds to the lowest-lying electric-dipole allowed transition from the ground state of helium. The oscillating field can be described as

$$\mathbf{e}(t) = \mathbf{E}(t)\cos(\omega t), \tag{8.4}$$

with a sinusoidal envelope

$$\mathbf{E}(t) = \mathbf{E}_{\text{max}} \sin^2\left(\frac{\pi t}{t_d}\right) H(t_d - t), \tag{8.5}$$

where H is the Heaviside step function designed to return zero when the field has reached its

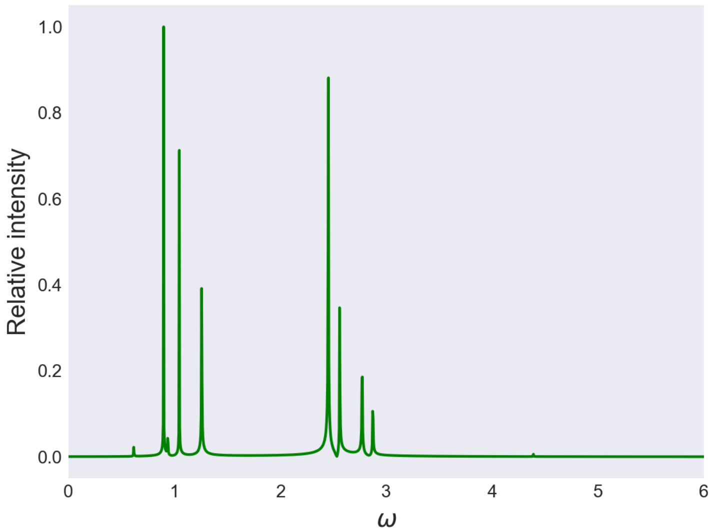

Figure 8.4: Dipole spectrum of He at field strength 10 au using OATDCCD and a `cc-pVDZ` basis set.

designated halting time t_d. This envelope is similar in behaviour to the one in the study by Li et al.[48] - it increaes gradually at first, and then gradually decreases.

The oscillating field is only meant to “disturb” the ground state of the atom, as it is quickly switched off at $t_d = 5$. Then the system is allowed to propagate in time for a long period. In our reproduction of the system, we have let the system evolve for a total time $T = 1500$ au. For each time step we compute the dipole in the same direction as the polarisation of the oscillating field. The fourier transform of this signal will then yield the dipole spectrum of the atom. The time-development is performed with the orbital-adaptive time-dependent coupled cluster method with double excitations. The result from this simulation is depicted in Figure 8.4, which is qualitatively equal to figure 7 in Pedersen and Kvaal[61].

8.4 Ionisation of 1D Beryllium

Miyagi and Madsen[52] implement the time-dependent restricted-active-space self-consistent field singles (TD-RASSCF-S) method and compare it with time-dependent configuration interaction singles (TDCIS) and the multi-configurational time-dependent Hartree-Fock (MCTDHF) method. A simulation they perform in this study is the simulation of the ionisation of beryllium. This simulation is performed by applying an oscillating field defined by the following vector potential,

$$\mathbf{A}(t) = \frac{\mathbf{E}_{\max}}{\omega} \sin\left(\frac{\pi t}{T}\right), \tag{8.6}$$

giving the following field

$$\mathbf{e}(t) = -\mathbf{E}_{\max} \sin\left(\frac{\pi t}{T}\right) \left[\frac{2\pi}{T\omega} \cos\left(\frac{\pi t}{T}\right) \sin(\omega t) + \sin\left(\frac{\pi t}{T}\right) \cos(\omega t)\right]. \tag{8.7}$$

We reproduce the one-dimensional beryllium model with our `AtomicPotential` class, which can be passed as a potential to the `ODQD` (one-dimensional quantum dot) class when setting up

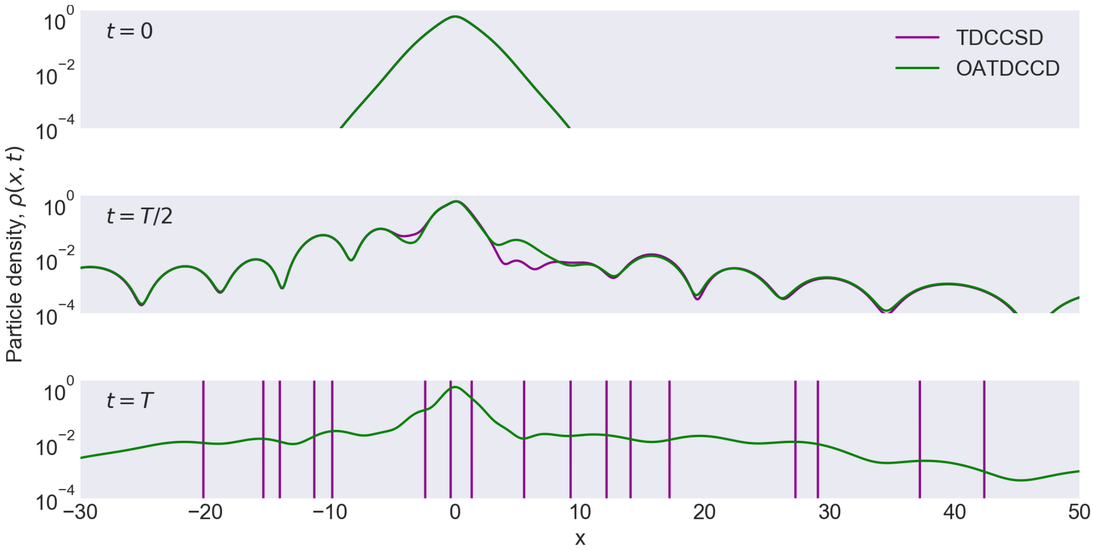

Figure 8.5: Snapshots of the electron density $\rho(x,t)$ in the 1D beryllium atom at $t=0$, $t=T/2$ and T, computed with TDCCSD and OATDCCD.

the system,

```
Z = 4; n = 4; l = 40; c = 1; a = 1; alpha = 1;
potential = AtomicPotential(Z, c)
odbe = ODQD(n, l, grid_length, num_grid_points, a, alpha)
odbe.setup_system(potential=potential)
```

where `Z` are the number of protons, `n` is the number of electrons, `l` is the number of spinorbitals, `c` is the position of the nucleus, `a` is the Coulomb screening parameter and `alpha` is the strength of the Coulomb interaction. We pick a wide grid of 300 au, with 5001 points, and a time step size of $dt = 0.01$.

The idea behind the simulation is to compute the particle density over time, and see if there is more than significantly high probability to see an electron very far away from the nucleus. The total time of the simulation is $T = 331$ au, and the particle density $\rho(x,t)$ is computed at the very beginning of the simulation, halfway through and at the end of the simulation. We do this both with our time-dependent coupled cluster singles doubles (TDCCSD) method with static orbitials and the orbital-adaptive time-dependent coupled cluster doubles method (OATDCCD). The results of the simulations are shown in Figure 8.5.

In the top subfigure in Figure 8.5 we see the electron density before the system is developed in time, and the two methods are in good agreement. In the middle subfigure the simulation is halfway through its course and the two methods both appear to show the same effects, but with slight discrepancies. In the bottom subfigure, we see that the OATDCCD method is doing fine, but the TDCCSD is absolutely non-sensible. We can conclude that the propagating obitals in time enables us to get the same qualitative result as Miyagi and Madsen in figure 4 from their study. Keeping the orbitals static as in the TDCCSD method makes us unable to model the same behaviour. We will delve a bit deeper to try to shed some light on why the TDCCSD method fails.

If we compute the norm of the amplitudes over the course of the simulation for the time-dependent coupled cluster singles doubles (TDCCSD) method, we get the result shown in Figure 8.6. In essence, the amplitudes in any coupled cluster computation provides a linear

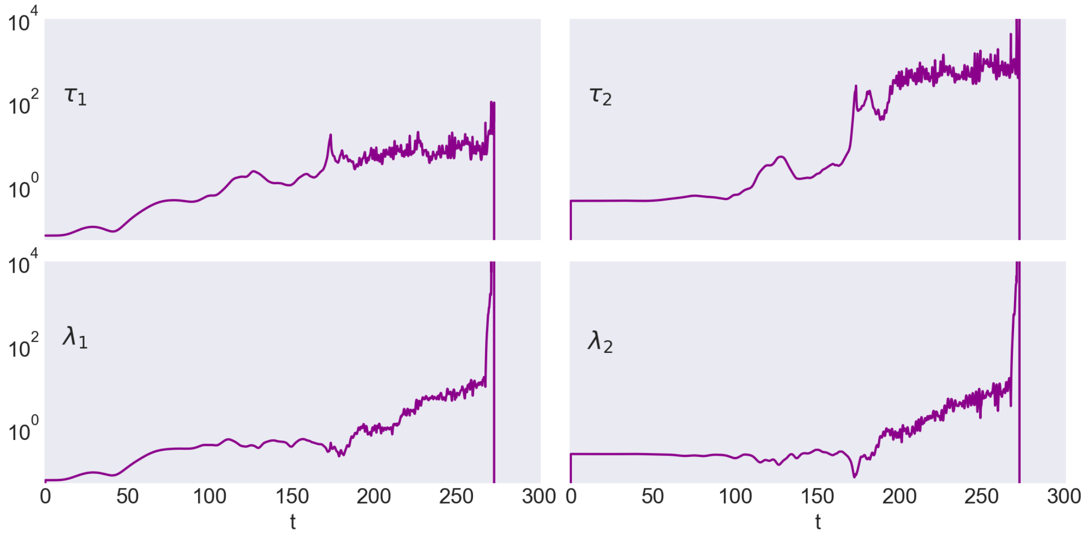

Figure 8.6: Norm of the amplitudes over time in the 1D beryllium atom, computed with TDCCSD. We see unreasonably high amplitude norms.

combination of orbitals from the reference state $|\Phi_0\rangle$, in order to provide the best representation of the exact state $|\Psi\rangle$. For this reason one would not expect the norm of the amplitudes to be realtively low for an exact that is close to the reference state. We encounter problems with the static orbitals because we are dealing with a system that moves very far from its inital state. In Figure 8.6 we see that the amplitudes stay within a reasonable magnitude for up to about halfway through the simulation, after which we see the method is struggling greatly to represent the current state with the basis it has been given. In figure Figure 8.7, a plot of the overlap of the current, time-dependent state with the initial ground state helps to underline this point. The inset figure in Figure 8.7 shows the area of the figure with the highest value for the overlap, at a larger scale. We see that the ground state probability reaches values of more than 300, which is most definitely unreasonable, because a probability like this should always be between 0 and 1.

It is difficult to draw a clear conclusion as to when the time-dependent coupled cluster method with static orbitals breaks down and is unfeasible for use. However, we can draw some broader, qualitative strokes towards a diagnosis of the problem. Any coupled cluster method is supposed to provide the best representation of a system's exact wavefunction by picking fitting parts of the basis set contained in the reference state for that system. If the exact wavefunction exists in a very different basis space than the reference state, it stands to reason that it is very difficult, if not impossible to find a mapping between the two. This problem stems from the foundations of the approximative nature of the coupled cluster method as it has a truncated basis set.

Pedersen and Kvaal[61] provide a similar deduction, highlighting there appears to be system-dependent upper limit for the strength of the external field. They underline the improvement in the computations by using a symplectic integrator instead of a standard fourth-order Runge-Kutta method. We use the exact same integrator as the one Pedersen and Kvaal outline. Pedersen and Kvaal argue that a large amplitude norm should make one question the validity of the result. It is difficult to gauge what constitutes a "large" amplitude norm, however.

Lastly with regards to the ionisation study from Miyagi and Madsen[52], we would like to emphasise how well the orbital-adaptive time-dependent coupled cluster doubles (OATDCCD)

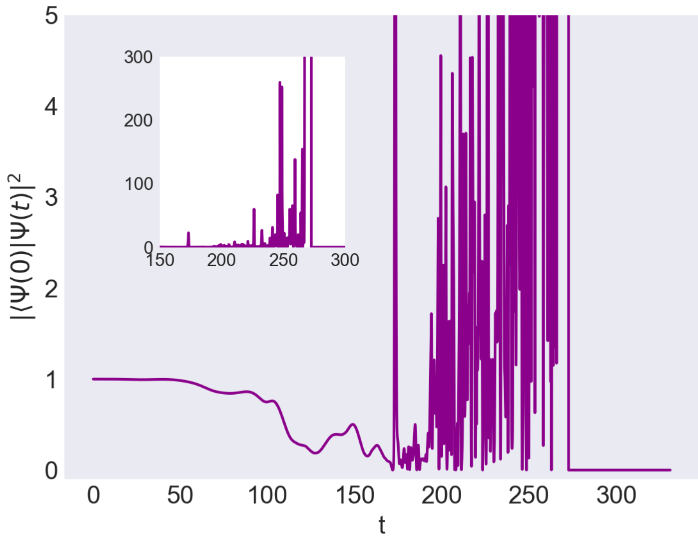

Figure 8.7: Probability of being in the ground state over time $|\langle\Psi(0)|\Psi(t)\rangle|$ in the 1D beryllium atom, computed with TDCCSD. We see impossibly unreasonable probabilities.

method performs. OATDCCD manages to replicate the desired results to a significant degree, giving relatively high values for the entire grid of the particle density represented in Figure 8.7. This is normally interpreted as a free praticle because one would expect the wavefunction of a free particle to spread out in space as time progresses.

Chapter 9

Quantum Dots

Here we present results related to time-dependent simulations of parabolic quantum wells. We have simulated the behaviour of such quantum dots in both one- and two dimensions, producing time dependent energies and ground state probabilities over time as the system is under the influence of oscilalting fields. We also present dipole spectra of the one- and two-dimensional quantum dot as well as the two-dimensional double dot and a two-dimensional double dot under the influence of a homogenous, static magnetic field. We find that the *harmonic potential theorem* holds for all simulations.

The *harmonic potential theorem*[42] states that electrons trapped in a parabolic quantum well shows behaviour as if it was one large quantum oscilaltor, instead of consisting of many smaller parts. This includes exhibiting only one frequency it the dipole spectrum of the system. If one were to compute the Fourier transform of the dipole of an n-electron quantum dot with parabolic potential the result would be one line in the spectrum corresponding to the oscillator frequency of the spectrum. This means that there are no many-body effects in a harmonic quantum dot.

An extension of the theorem to systems under the influence of a magntic field[7]. State that one would expect to see a shift, both up and down, creating two frequencies Ω_+ and Ω_- in the dipole spectrum. The resulting dipole spectrum would show two frequencies with a difference equalling the Larmor frequency $\omega_c = \Omega_+ - \Omega_-$.

9.1 Harmonic Oscillators in One Dimension

For the one-dimensional quantum dot with a harmonic potential we simulate a laser by adding an oscillating field with a sinusoidal envelope, similar to the one in Pedersen and Kvaal[61],

$$\mathbf{e}(t) = \mathbf{E}_{\max} \sin^2\left(\frac{t\pi}{T}\right)\cos(\omega t). \tag{9.1}$$

We set the period of the envelope equal to the duration of the entire simulation, $T = 20$, so that we have a field that at first will gradually increase, then decrease. The oscillator frequency for all simulations are set to $\Omega = 1$, and at first we set the frequency of the oscillating field to twice this, $\omega = 2$. We do this to make sure that we are far from the resonant frequency of the system, and we pick relatively high laser frequency in order to enforce a more dynamic system. We use the more standard time-dependent coupled cluster singles doubles (TDCCSD) method, for these simulations, with the symplectic Gaussian integrator and a time step of $dt = 0.01$. The simulations are performed for an increasing number of electrons $n = \{2, 4, 6, 8, 10, 12\}$. We have computed the energy and the time-dependent overlap, i.e. the time-dependent probability of being in the ground state, for each simulation. We repeat the simulations for a wide range of different number of spin-orbitals to the convergent properties of the simulations as the number of spin-orbitals increase.

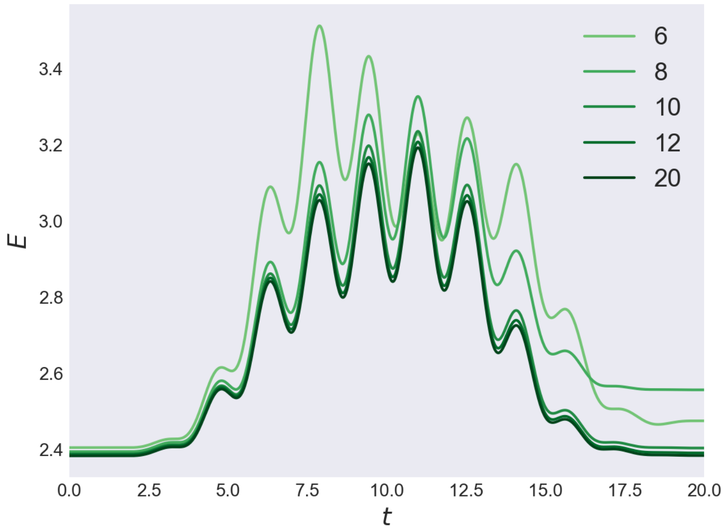

Figure 9.1: Time-dependent energy of a one-dimensional harmonic oscialltor with $n = 2$ electrons under the influence of a laser field for different number of spinorbitals $l \in \{6, 8, 10, 12, 20\}$.

First we study the time-dependent energy of a quantum dot acted upon by an oscillating field. The result for $n = 2$ electrons is shown in Figure 9.1. We have produced comparative results for other number of particles $n = \{4, 6, 8, 10, 12\}$, which can be found in section A.1. We see an apparent convergence in the time-dependent energy as we increase the number of spin-orbitals in the basis set. For larger systems with more electrons it reasonably becomes necessary to also increase the size of the basis set. As is the tendency with ground state coupled cluster computations for quantum dots[41, 49], the time dependent energy of a quantum dot is decreasing until convergence for increasing basis set size.

We see the same general convergent tendency when computing the time-dependent ground state probability $| \langle \Psi(0) | \Psi(t) \rangle |^2$, shown in Figure 9.2 for $n = 2$ electrons. We see that for lower number of spin-orbitals, the computation of overlap with the ground state tends to return a lower value than for a higher number of spin-orbitals.

Since the ground state probability is a number between zero and one, the results for systems of different number of electrons are comparable. We have produced such a comparison in Figure 9.3. In this figure we have chosen the number of spin-orbitals that would produce a convergent plot for the given system size. The general tendency is that a system with more electrons is less likely to be in the ground state over time, than a system with less electrons.

9.1.1 Dipole spectrum

We now turn to a somewhat different kind of simulation. We keep the base system the same, a one-dimensional quantum dot with harmonic potential and oscillator frequency $\Omega = 1$. We also apply an external oscillating field like in Equation 9.1, which will this time be resonant with the frequency of the oscillator $\omega = \Omega = 1$, to ensure population of excited states. In this simuation we set the field to zero at $T_d = 5$ au, by the use of a Heaviside function in a similar manner

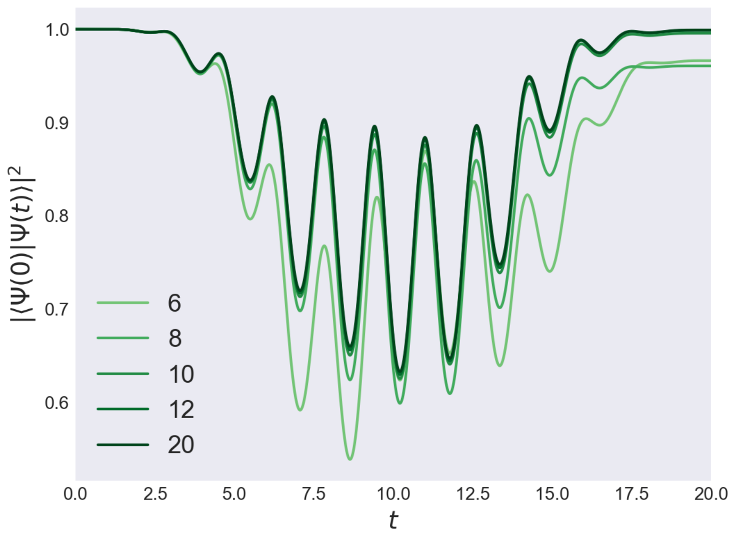

Figure 9.2: Probability of being in the ground state $|\langle\Psi(0)|\Psi(t)\rangle|^2$ for a one-dimensional quantum dot with $n = 2$ electrons under the influence of a laser field for different number of spinorbitals $l \in \{6, 8, 10, 12, 20\}$.

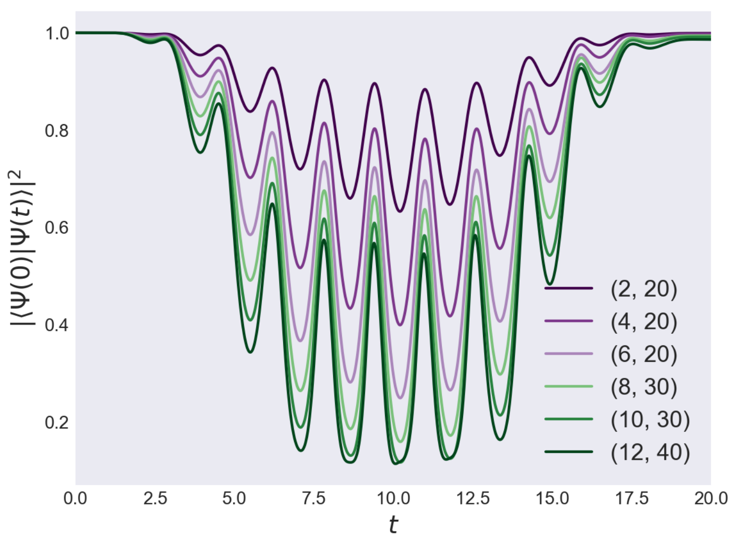

Figure 9.3: Probability of being in the ground state for $|\langle\Psi(0)|\Psi(t)\rangle|^2$ for a one-dimensional quantum dot for different number of electrons $n \in \{2, 4, 6, 8, 10, 12\}$.

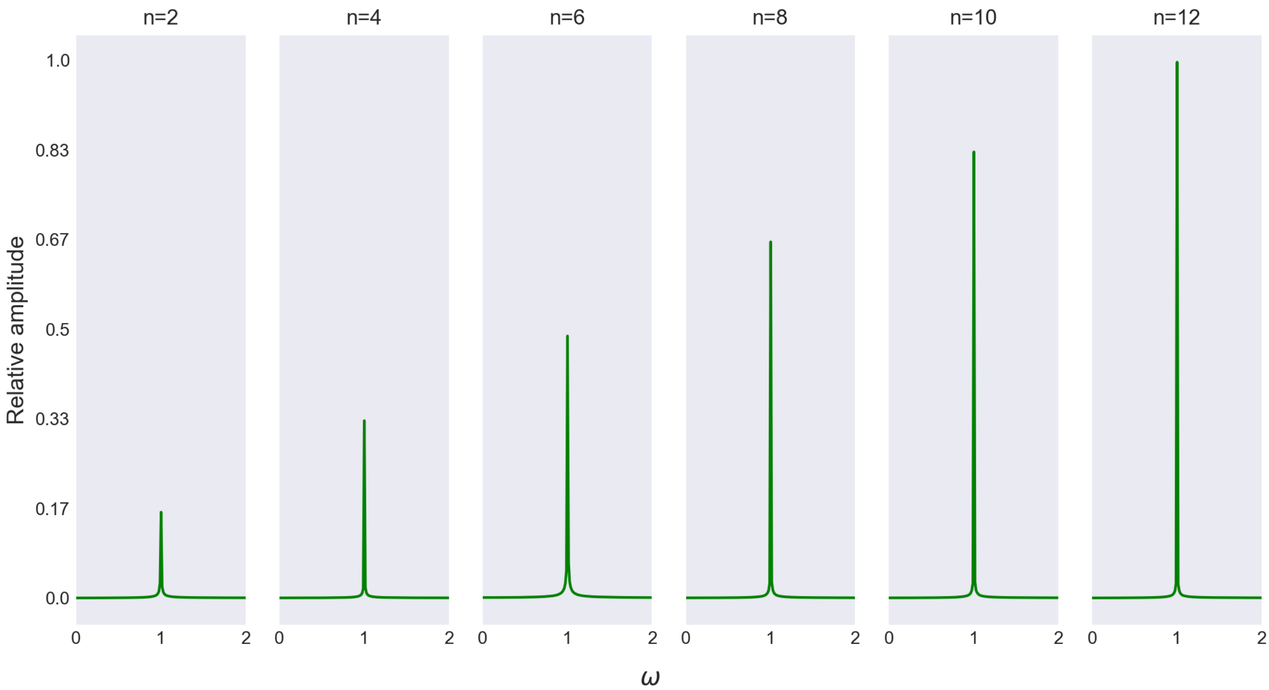

Figure 9.4: Fourier transform of expected value of dipole moment for a one-dimensional quantum dot with different number of electrons $n = \{2, 4, 6, 8, 10\}$ with respective number of spin-orbitals $l = \{20, 20, 20, 30, 30, 40\}$.

as Pedersen and Kvaal[61] in Equation 8.5. After the field has been switched off we propagate the system in time for a total of $T = 500$ au with a time step size of $dt = 0.01$. The same procedure is repeated for systems with $n = \{2, 4, 6, 8, 10, 12\}$ electrons with respective number of spin-orbitals $l = \{20, 20, 20, 30, 30, 40\}$. These system and basis sizes correspond to the ones used in Figure 9.3. For each time step we collect the dipole, i.e. $\langle \hat{x} \rangle = \mathrm{tr}\{\rho x\}$, and compute the Fourier transform of the entire collected array. The results are presented in Figure 9.4.

We see that the result is in accordance with the harmonic potential theorem, as the simulations have produced dipole spectra that show only one line corresponding to the frequency of the confining potential. Morover, we see that the relative intensity of the spectra increases with the number of particles.

9.1.2 Resonance Sensitivity

In order to test the response of a quantum dot as the frequency of the oscillating field apporaches the oscillator frequency, we have run simulations for a selection of laser frequencies ω with the field described by Equation 9.1. We chose frequencies $\omega \in \{1.0, 1.25, 1.5, 1.75, 2.0\}$ and set the oscillator freqcuencies of the quantum dot systems to $\Omega = 1$. The laser pulse had a set period of $T_l = 20$ au, starting from $t = 0$, while time-development of the system was allowed to continue to $T = 30$ au. The results of these simulations are shown for $n = 2$ particles in Figure 9.5 and Figure 9.6, which show the time-dependent energy and the time-dependendent ground state probabilities $|\langle \Psi(0)|\Psi(t)\rangle|^2$ respectively.

The results are as expected, but interesting nonetheless. We see that the quantum dots

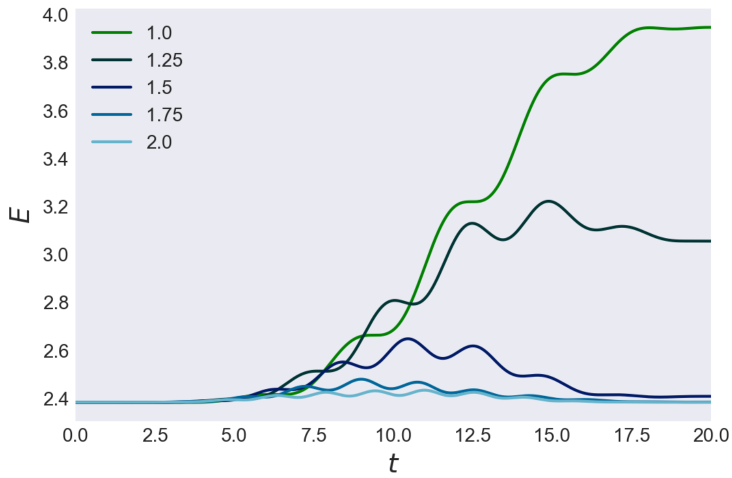

Figure 9.5: Time-dependent energy of a one-dimensional quantum dot with oscillator frequency $\Omega = 1$ and $n = 2$ electrons. The quantum dot is influenced by an oscillating field of different frequencies $\omega \in \{1.0, 1.25, 1.5, 1.75, 2.0\}$ with a maximum intensity of $\mathbf{E}_{\max} = 0.25$.

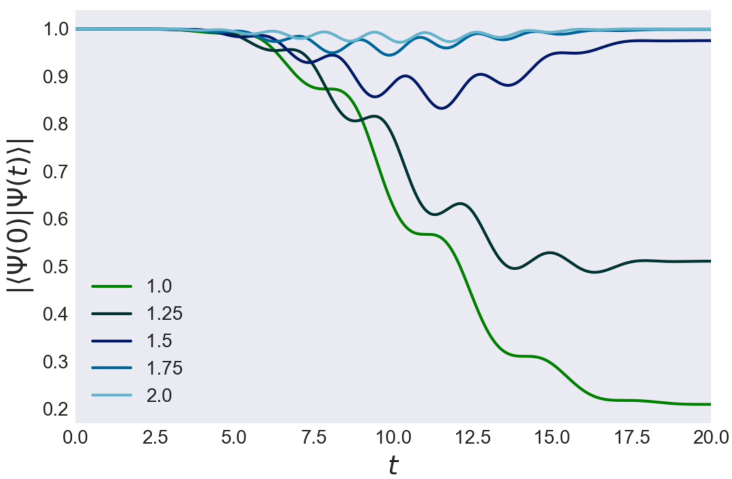

Figure 9.6: Time-dependendent ground state probability $|\langle\Psi(0)|\Psi(t)\rangle|^2$ of a one-dimensional quantum dot with oscillator frequency $\Omega = 1$ and $n = 2$ electrons. The quantum dot is influenced by an oscillating field of different frequencies $\omega \in \{1.0, 1.25, 1.5, 1.75, 2.0\}$ with a maximum intensity of $\mathbf{E}_{\max} = 0.25$.

behave very much as a classical driven harmonic oscillator. If the frequency of the driving force, in this case the oscillating field, is far from the resonant frequency of the system the system falls back to the inital position after the force subsides. Only when we get closer to the resonant system do we see an excitation in energy of the system as a whole after the laser field is switched off (Figure 9.5). In the case for the exact resonant frequency, such that $\omega = \Omega$, we se that the energy of the system is increased even at the very end of the simulation, when the amplitude of the oscillating field is miniscule. The same effects are apparent when studying the overlap of the time-developed system with the initial ground state in Figure 9.6. Closer to the resonant frequency we see a much lower probability of being in the ground state. For frequencies far away from the resonant frequency we see that the system falls back to the exact ground state or a state close to the ground state.

We have run similar simulations to the one described above, in order to study the resonant properties of a quantum dot, for $n = 4, 6, 8, 10$ electrons in a one-dimensional quantum dots. Figures with the results from these simulations can be found in section A.1. In the ground state probability plots for these simulations, one would notice non-sensible probabiliy values $|\langle\Psi(0)|\Psi(t)\rangle|^2 > 1$. This is an issue we have adressed in the following sections, when reviewing the results of the two-dimensional quantum dot results.

9.2 Two-dimensional Quantum Dot

The two-dimensional quantum dot arguably paints a somewhat more interesting picture than the one-dimensional quantum dot, as we shall see. We construct several harmonic potential systems using the `TwoDimensionalharmonicOscillator`. Similarly to the one-dimensional case, we simulate a laser by adding an oscillation field of the kind used by Pedersen and Kvaal[61], shown in Equation 9.1. Because we have added a dimension, we must choose a direction of polarisation. This choice is arbitrary because of the symmertry of the quantum dots. We therefore arbitrarily pick the x-direction. Unlike the one-dimensional dot, we are restricted to only a certan selection of systems, namely systems of $n \in \{2, 6, 12\}$ electrons, that ensure full shells.

Like in our simulations of a one-dimensional harmonic quantum dot we have at first sought to show that convergence in the computations by applying an oscillating field far from the resonant frequency of the system. We set the oscilaltor frequency to $\Omega = 1$ and the frequency of the eletric field to $\omega = 2\Omega = 2$. We perform a simulation over a period $T = 20$ au, for an increasing number of spin-orbitals l. The maximum intensity of the laser field is set to $\mathbf{E}_{\text{max}} = 1$ au. For these initial computations we use the time-dependent coupled cluster singles doubles (TDCCSD) method with static orbitals. The simulations for two and six eletrons show expected results and have therefore been consigned to section A.2, while the results for twelve electrons appear to be on the brink of what the TDCCSD method can handle, within the given basis set size.

The time-dependent energy of a two-dimensional harmonic quantum dot with $n = 12$ electrons under influence of the oscillating field described above is shown in Figure 9.7. In this figure we have run the same simulation for $l \in \{42, 56, 72\}$ spin-orbitals with the time-dependent coupled cluster singles doubles (TDCCSD) method, and we see that only for the very largest of the basis set to we see a behaviour conforming with our expectations. We expect the energy to be close to the ground state energy after the laser-field has died down.

In the same figure (Figure 9.7) we have also included the computed energy over time for the system using the orbital-adaptive time-dependent coupled cluster doubles (OATDCCD) method and the same number if spin-orbitals. We see that the two methods dont't agree completely, and we are prone to trust the OATDCCSD method more than the TDCCSD method in this case, because the energy at the end of the simulations is lower than the initial energy for the TDCCSD method. The reason for the problems the TDCCSD method shows are likely caused

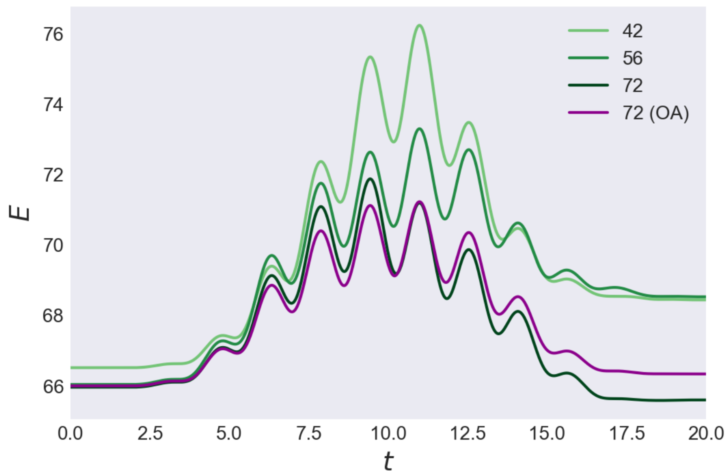

Figure 9.7: Time-dependent energy of a two-dimensional harmonic oscillator with $n = 12$ electrons under the influence of a laser field for different spinorbitals $l \in \{42, 56, 72\}$.

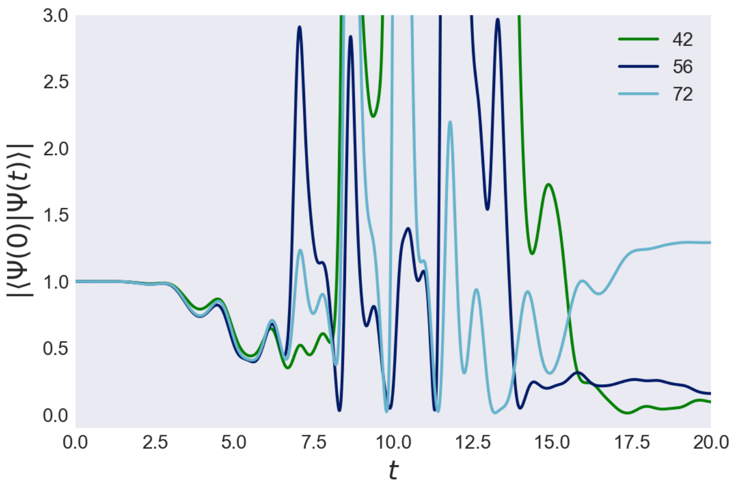

Figure 9.8: Ground state probability $|\langle\Psi(0)|\Psi(t)\rangle|^2$ for two-dimensional quantum dot with $n = 12$ electrons under the influence of a laser field for different number of spinorbitals $l = \{42, 56, 72\}$.

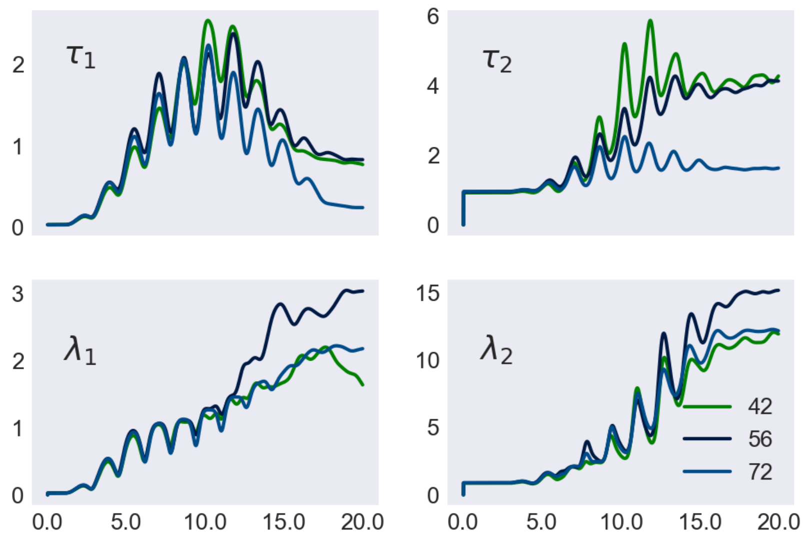

Figure 9.9: Norm of amplitudes in a $n = 12$ electron two-dimensional quantum dot influenced by an oscilalting field, for several number of spin-orbitals $l = \{42, 56, 72\}$.

by our attempt to represent a state with the basis functions contained in the reference, which is very dissimilar to said reference function. We will outline this problem further as we study the time-dependent ground state probability of the simulation.

The ground state probability of the same simulation with the TDDCCSD method is shown in Figure 9.8. We see immediately that the probability becomes non-sensical at some time step after $t = 6$ au. This result is similar to the sort of break-down that occured for the TDCCSD method in the attempt to replicate the results of Miyagi and Madsen[52] in section 8.4.

The probable cause of the non-sensible ground state probability is the need for the amplitudes of the system to acquire relatively high values, in order to compensate for the inadequateness of the reference state to describe the exact time-dependent state. This is underlined by the norm of the amplitudes, displayed in Figure 9.9. As is apparent, the lambda amplitudes shows an upwards trend throughout the simulation. This should be unnecessary because the system would revert back to a state similar to the ground state at the end of the simulation. It appears that some “tipping point” is reached halfway around $t = T/2$ when instabillty increases. The tau amplitudes are more or less well-behaved, at least for the largest basis set, showing some correlation in amplitude with the sinusoidal envelope of the oscillating field.

9.2.1 Dipole Spectrum

We have for the two-dimensional quantum dot computed dipole spectrum for systems of different size, like we did fro the one-dimensiaonal quantum dot. We did this for quantum dots with oscillator frequencies $\Omega = 1$ with $n \in \{2, 6, 12\}$ electrons. We used $l \in \{42, 42, 56\}$ as the number of spinorbitals for the respective systems. In order to excite and disturb the systems from the inial ground state we applied an oscillating field with a resonant frequency $\omega = \Omega = 1$ and a somewhat low maximum intensity $\mathbf{E}_{\max} = 0.1$, with a three-step linear envelope as in Equation 8.2. The systems were allowed to develop in time for $T = 500$ au. The results of

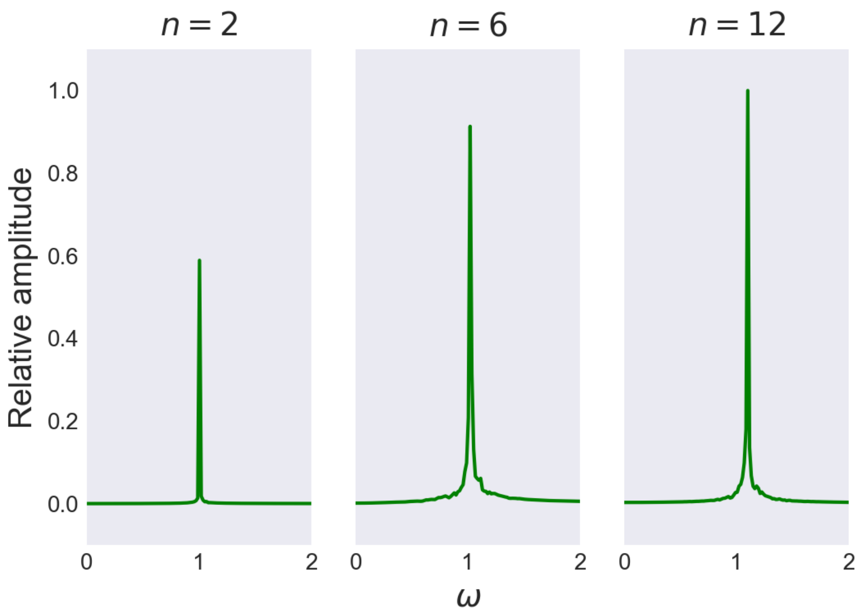

Figure 9.10: Fourier transform of expected value of dipole moment for a two-dimensional quantum dot with different number of electrons $n = \{2, 6, 12\}$ and respective number of spin-orbitals $l = \{40, 40, 56\}$.

computing the Fourier transform of the dipole $\mathbf{x} = \text{tr}\{\rho x\}$ is depicted in Figure 9.10. In this figure we see that the result is qualtitatively in accordance with the harmonic potential theorem - the dipole freqcuencies of all the systems are the same, with an intensity that increases with the number of particles in the system. For the two larger systems with $n = 6$ and $n = 12$ electrons we see some slight inccuracies. These are attributable to the time constraint of this study - a simulation with larger number of spinorbitals would have remedies these inaccuracies, but would have needed more time to complete.

9.2.2 Resonance Sensitivity

9.3 Two-dimensional Double Dot

We have simulated two different two-dimensional double dot systems, one with $n = 2$ electrons and one system with $n = 4$ electrons, using the `TwoDimensionalDoubleWell` class described in subsection 6.2.3. We use $l = 20$ spin-orbitals for the two-electron system and $l = 56$ spin-orbitals for the four-electron system. The class requires two special parameters, `l_ho_factor` and `barrier_strength`, that define the number of regular harmonic oscillator functions to map to and the height of the barrier in the middle of the well, respectively. We set the barrier strength to 2 and the harmonic oscillator factor to 2 for both systems. The oscillator frequency of the double dot is set to $\Omega = 1$. As a visual confirmation of the systems, a one-electron density plot is provided for the $n = 2$ electrons system (left) and the $n = 4$ electron system (right) in Figure 9.13.

The double dot is in essence a perturbation of the regular two-dimensional quantum dot, and we are seeking to uncover any many-body effects that such a perturbation could lead to. In order to do this we would like to compute the dipole spectrum of both systems. The

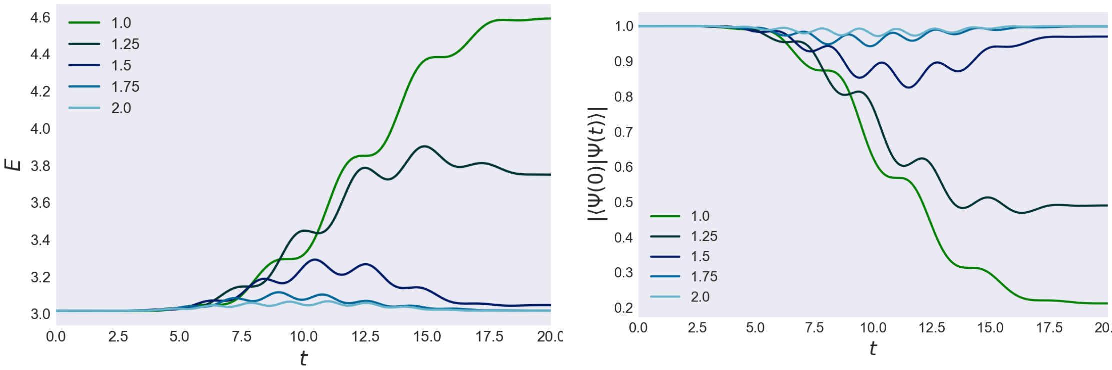

Figure 9.11: Time dependent energy (left) and ground state probability $|\langle\Psi(0)|\Psi(t)\rangle|^2$ (right) for a two-dimensional quantum dot with $n = 2$ electrons. The quantum dot is affected by an oscillating field of different frequencies $\omega \in \{1.0, 1.25, 1.5, 1.75, 2.0\}$ with a maximum inntensity $\mathbf{E}_{\max} = 0.25$.

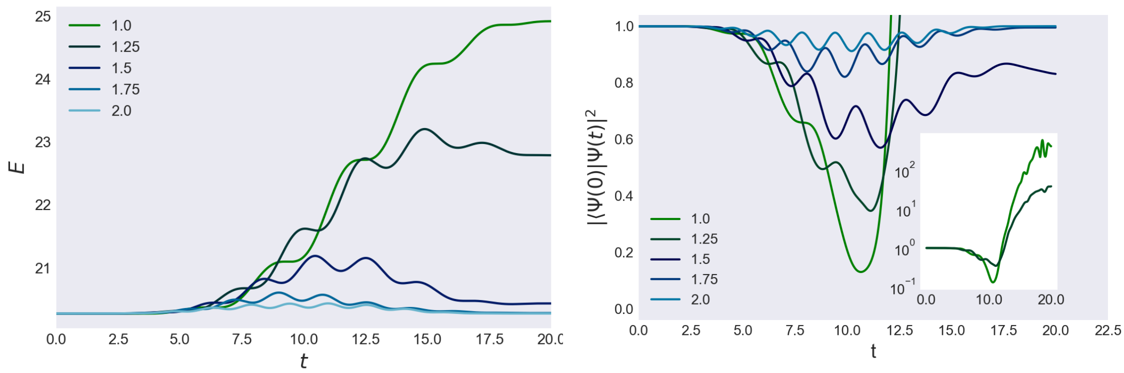

Figure 9.12: Time dependent energy (left) and ground state probability $|\langle\Psi(0)|\Psi(t)\rangle|^2$ (right) for a two-dimensional quantum dot with $n = 6$ electrons. The quantum dot is affected by an oscillating field of different frequencies $\omega \in \{1.0, 1.25, 1.5, 1.75, 2.0\}$ with a maximum inntensity $\mathbf{E}_{\max} = 0.25$.

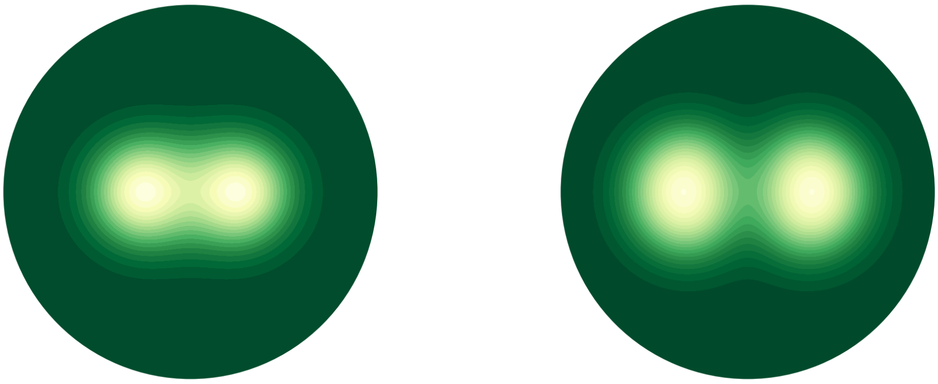

Figure 9.13: Ground state one-electron density for $n = 2$ electrons (left) and $n = 4$ electrons (right) for a double quantum dot.

time-propagation is done using the orbital-adaptive time-dependent coupled cluster doubles (OATDCCD) method, as it has shown the best stability of our time-dependent methods. Both systems are under the influence of an oscillating field with a linearly decreasing- and increasing envelope of the type used by Li et al.[48] (Figure 8.1). We have chosen a frequency of this field that corresponds to the resonant of the first transition energy of the system $\omega = 0.43$ au, and an intensity yielding a maximum amplitude $\mathbf{E}_{\text{max}} = 0.1$ au. The resonant frequency was found by direct diagonalisation of the one-body matrix produced by the system class `TwoDimensionalDoubleWell`.

The system is allowed to develop in time for $T = 100\hat{au}$ and complute the Fourier transform of the dipole moment $\langle x\rangle = \text{tr}\{\rho x\}$, the results of which are shown in Figure 9.14. We immediately see that there is only one frequency apparent in the spectra for each of the systems, meaning that the quantum double dots have a position operators that behaves as if it was the centre of mass of the system. We see that the larger system has a somewhat more rapid movement relative to the smaller system. We also see that the larger system has lower intensity compared with the smaller system. This mya be because there is relatively more mass in the system to move, and the intensity of the laser field is unchanged.

9.4 Two-dimensional Magnetic Quantum Dot

We start the study of two-dimensional quantum dots under the influence of a magnetic field by defining a system of only one particle and solving the time-dependent Schrödinger equation directly. This is a accomplished by using the `TwoDimHarmonicOscB` class to produce a basis set, single-particle functions and transition/intearction matrix (dipole elements), which is everything we need. All of these items are properties of the class and can be easily extracted. A simple periodic function simulates an electric field is constructed, as the product of such a time-dependent operator and the interaction matrix defines the time propagation. We then use a simple integration scheme, in this case the fourth-order Runge-Kutta method, to propagate the ground state single particle function of the system. Taking care to extract the dipole for every time step, we can compute the discrete Fourier transform of the dipole and compute the frequency spectrum of our system. This procedure is applied to a system comletely absent of a magnetic field, and a system under direct influence of a magnetic field.

Before going straight to the results, we study the shell structure and allowed transitions of our two systems. The left part of Figure 9.15 presents the shell structure of a the regular two-dimensional quantum dot. The states have all been assigned a number for easier examination.

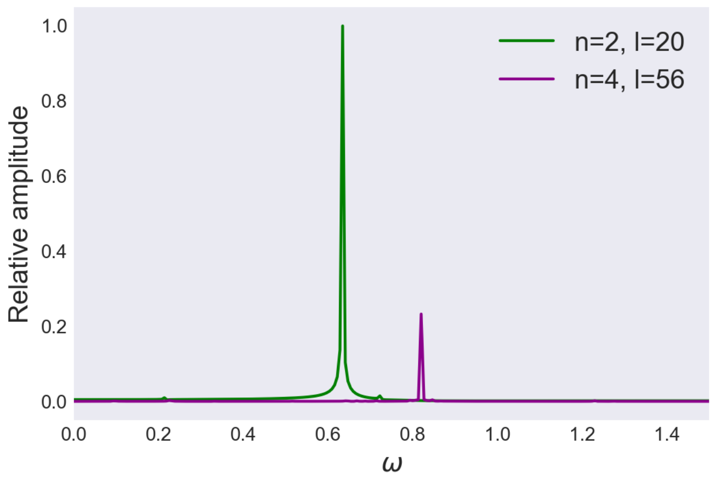

Figure 9.14: Dipole spectrum of two-dimensional double dot system with $n \in \{2, 4\}$ electrons and $l \in \{20, 56\}$ spinorbitals.

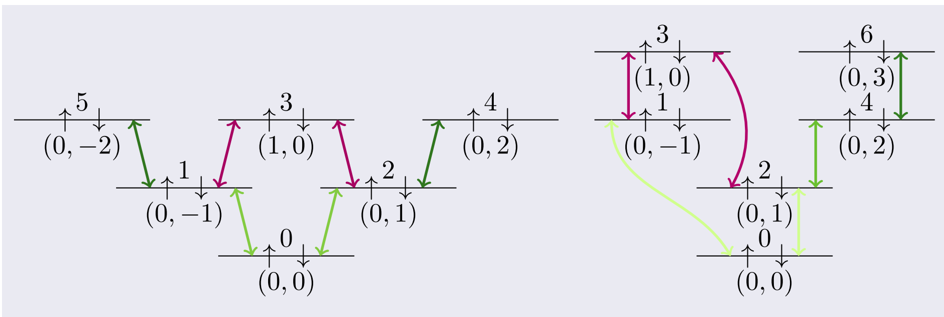

Figure 9.15: Shell structure of six lowest orbitals before (left), and after (right) a magnetic field is applied to a 2D quantum dot.

This shell structure is identical to the one presented in Figure 6.1. Additionally, here we have added coloured double arrows to illustrate the allowed transitions in the quantum dot. These transitions are can be encountered in the transition matrix for the system, which is reproduced in the artistic way in Figure 9.16. Notice that the coloured arrows representing allowed transitions match in colour with the elements of the transition matrix.

When we apply apply a magnetic field of strength $\omega_c/\omega = \sqrt{2}/2$ we obtain the shell structure represented to the right in Figure 9.15, where the allowed transitions correpsond to the transition matrix in Figure 9.17. The chosen magnetic field strength was not chosen arbitrarily, as these accidental degenracies occur only rarely as a function of magnetic field strength[1]. For succinctness we repeat the function for energy eigenvalues for two-dimensional quantum dot influenced by a magnetic field (Equation 6.36),

$$\epsilon_{nm} = \hbar\Omega(2n + |m| + 1) - \frac{\hbar\omega_c}{2}m, \tag{9.2}$$

[1]Hence the term "accidental".

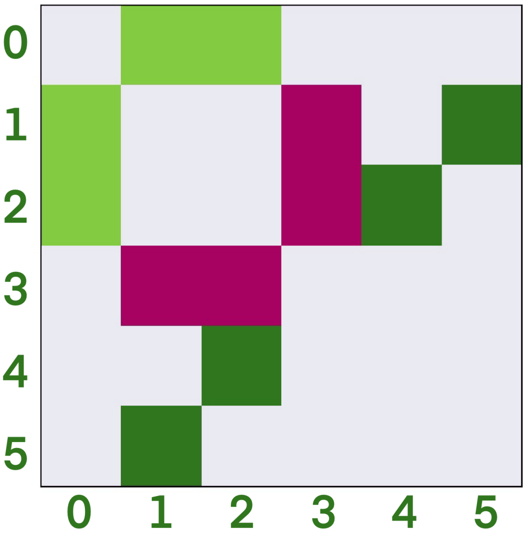

Figure 9.16: Transition matrix dictating the allowed transitions for a 2D quantum dot.

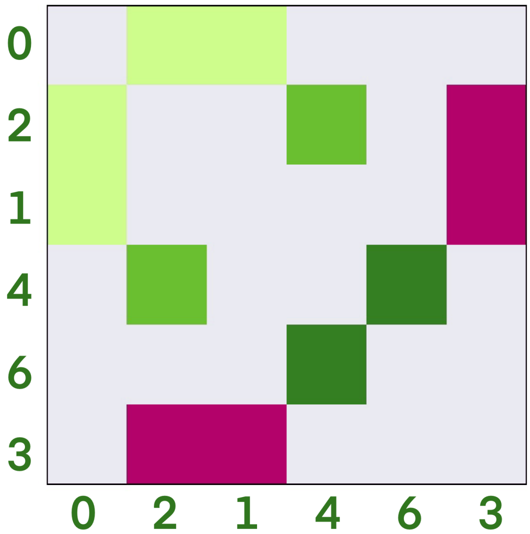

Figure 9.17: transition matrix for a 2D quantum dot when a magnetic field is applied.

where $\Omega = \sqrt{\omega_0^2 + \frac{\omega_c^2}{4}}$. Apart from a general shift up in energy by adding a magnetic field, the states with negative azimuthal quantum number m will experience an increase in energy eigenvalue, and vice versa. We see this effect clearly in the new shell structure in Figure 9.15. The states with negative m have indeed undergone a relative shift upwards, whilst the states with positive m have been shifted downwards, relative to the other states. The ground state, labelled 0, remains relatively stationary, the states labelled 2 ($m = 1$) and 4 ($m = 2$) have been shifted downwards and the states labelled 1 ($m = -1$) and 5 ($m = -2$) have been shifted upwards. State number 5 so much that it has disappeared from the shell structure, with a new state 6 ($= 3$) appearing. This is due to our restriction to include only the six lowest-energy orbitals. We see that the possible remaining allowed transitions remain the same, with the exception of transitioning between state 1 and 5, because state 5 is no more, and the addition of a possible transition between state 4 and 6.

If we compute the frequency spectrum of the two systems (Figure 9.18) we get a single line for the normal quantum dot. This is expected, as the quantum harmonic oscillator has the same energy difference between each level. However, when we apply a magnetic field and shift the energies of the orbitals in the quantum dot, we see that we get two different energy transitions. This is revealed as two lines in the frequency spectrum in Figure 9.18. This is equivalent to a splitting in transmisstion spectra of quantum dot arrays under the effect of a magnetic field in experiments[31, 51].

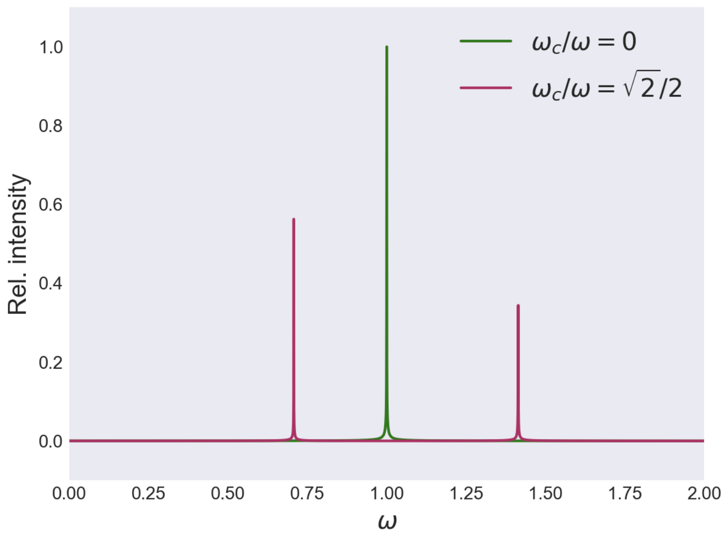

Figure 9.18: Spectrum of a 2D quantum dot both with and without a magnetic field.

Part V

Appendices

Appendix A

Quantum Dot Results

A.1 One Dimension

Four electrons

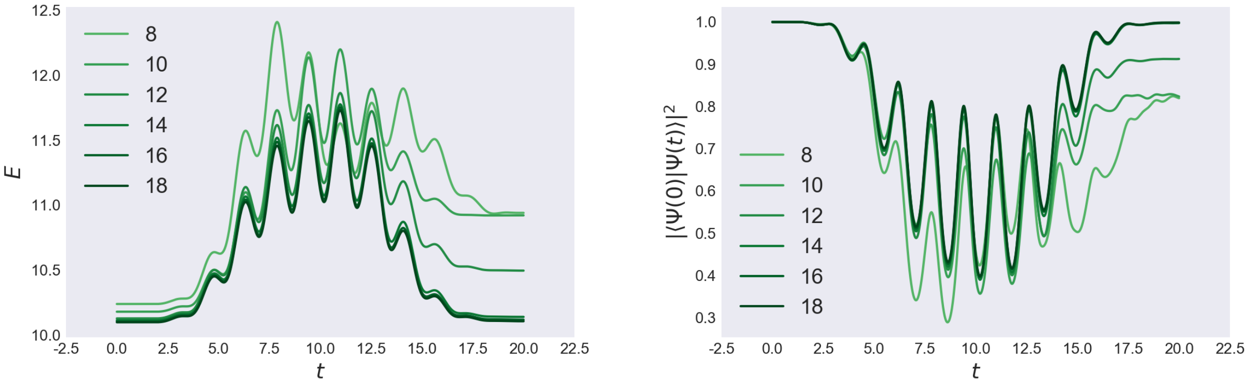

Figure A.1: Time-dependent energy (left) and ground state probability (right) of a one-dimensional harmonic oscillator with $\Omega = 1$ and $n = 4$ electrons under the influence of a oscillating electric field of frequency $\omega = 2\Omega = 2$ and field strength $\mathbf{E}_{\max} = 1$, for different number of spin-orbitals $l = \{8, 10, 12, 14, 16, 18\}$.

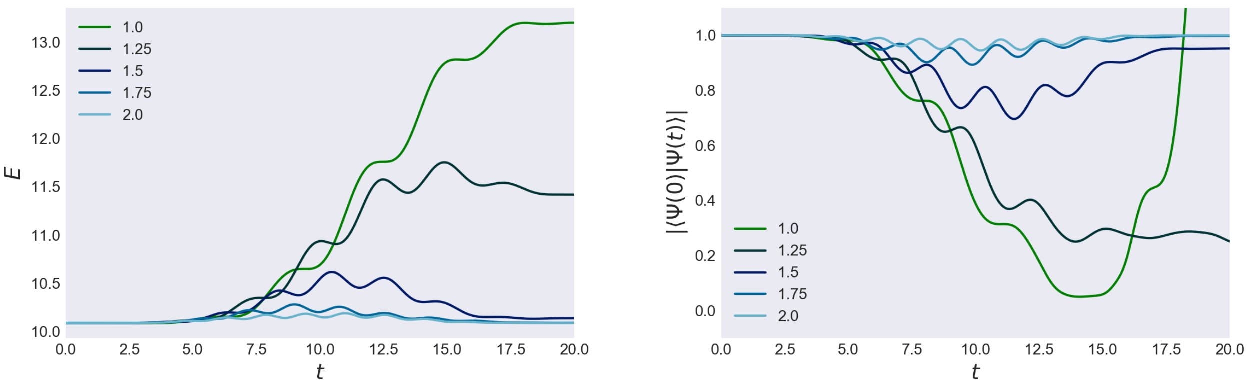

Figure A.2: Time-dependent energy (left) and ground state probability (right) of a one-dimensional harmonic oscillator with $\Omega = 1$ and $n = 4$ electrons under the influence of a oscillating electric field of different frequencies $\omega \in \{1.0, 1.25, 1.5, 1.75, 2.0\}$ with maximum field strength $\mathbf{E}_{\max} = 0.25$ and $l = 30$ spin-orbitals.

Six electrons

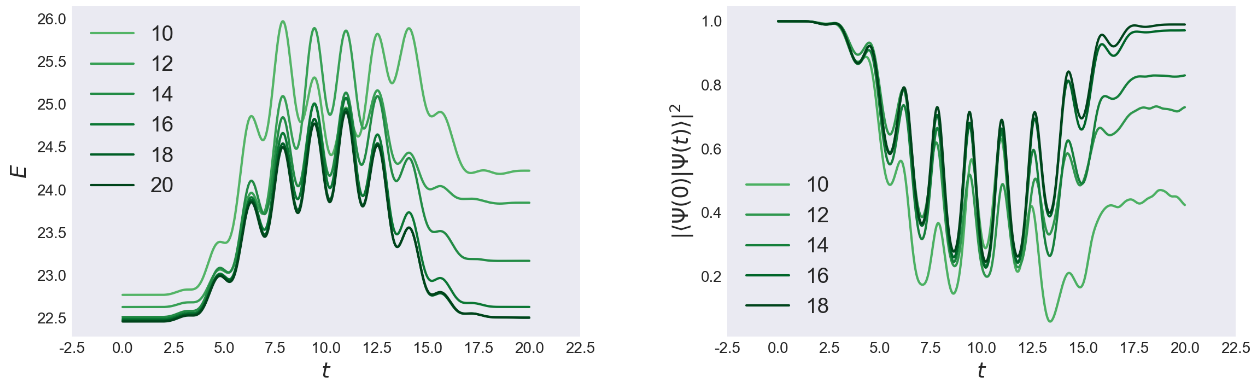

Figure A.3: Time-dependent energy (left) and ground state probability (right) of a one-dimensional harmonic oscillator with $\Omega = 1$ and $n = 6$ electrons under the influence of a oscillating electric field of frequency $\omega = 2\Omega = 2$ and field strength $E_{\max} = 1$, for different number of spin-orbitals $l = \{10, 12, 14, 16, 18, 20\}$.

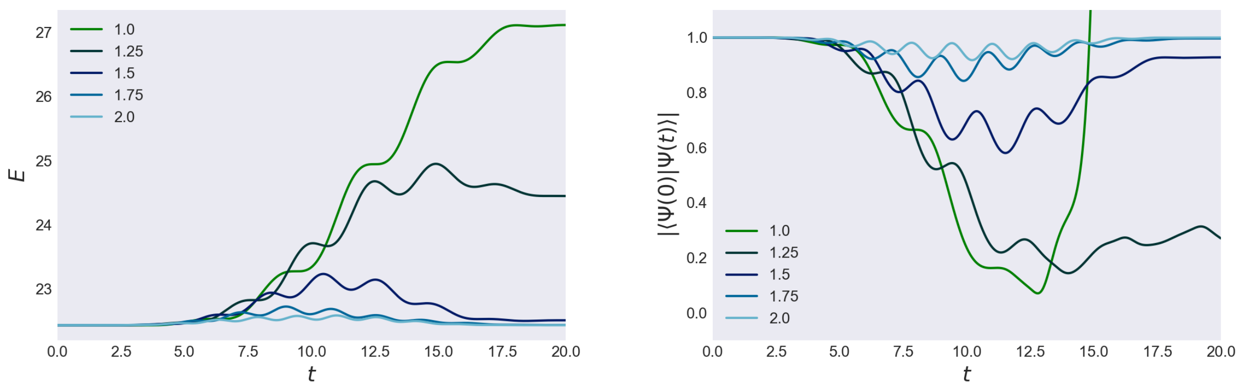

Figure A.4: Time-dependent energy (left) and ground state probability (right) of a one-dimensional harmonic oscillator with $\Omega = 1$ and $n = 6$ electrons under the influence of a oscillating electric field of different frequencies $\omega \in \{1.0, 1.25, 1.5, 1.75, 2.0\}$ with maximum field strength $\mathbf{E}_{\max} = 0.25$ and $l = 30$ spin-orbitals.

Eight electrons

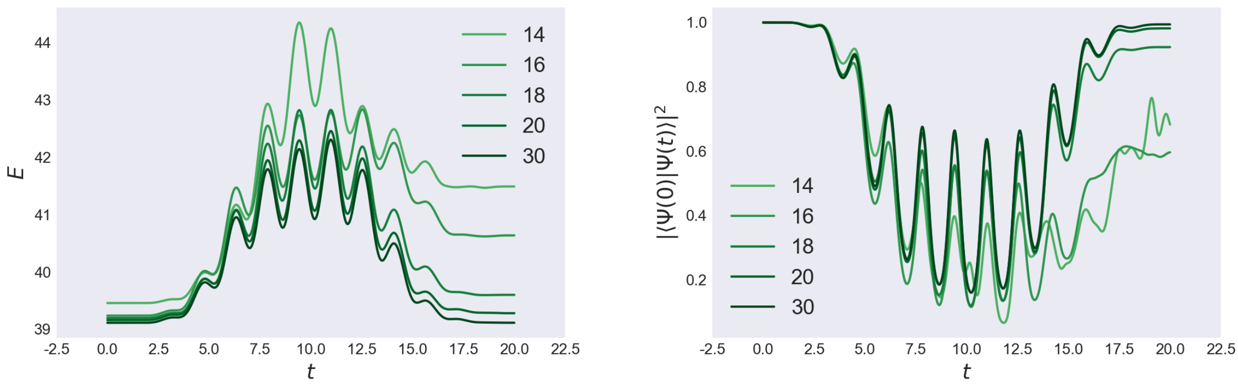

Figure A.5: Time-dependent energy (left) and ground state probability (right) of a one-dimensional harmonic oscillator with $\Omega = 1$ and $n = 8$ electrons under the influence of a oscillating electric field of frequency $\omega = 2\Omega = 2$ and field strength $E_{\text{max}} = 1$, for different number of spin-orbitals $l = \{14, 16, 18, 20, 30\}$.

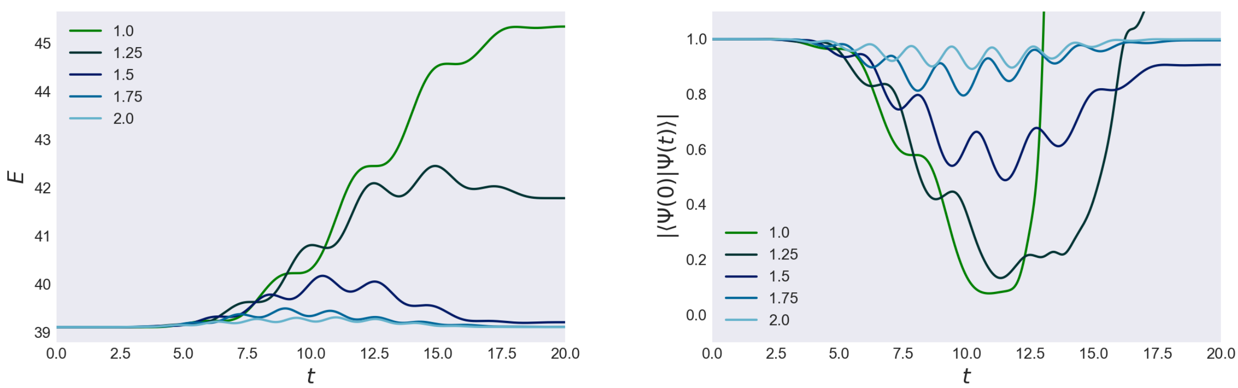

Figure A.6: Time-dependent energy (left) and ground state probability (right) of a one-dimensional harmonic oscillator with $\Omega = 1$ and $n = 8$ electrons under the influence of a oscillating electric field of different frequencies $\omega \in \{1.0, 1.25, 1.5, 1.75, 2.0\}$ with maximum field strength $\mathbf{E}_{\text{max}} = 0.25$ and $l = 36$ spin-orbitals.

Ten electrons

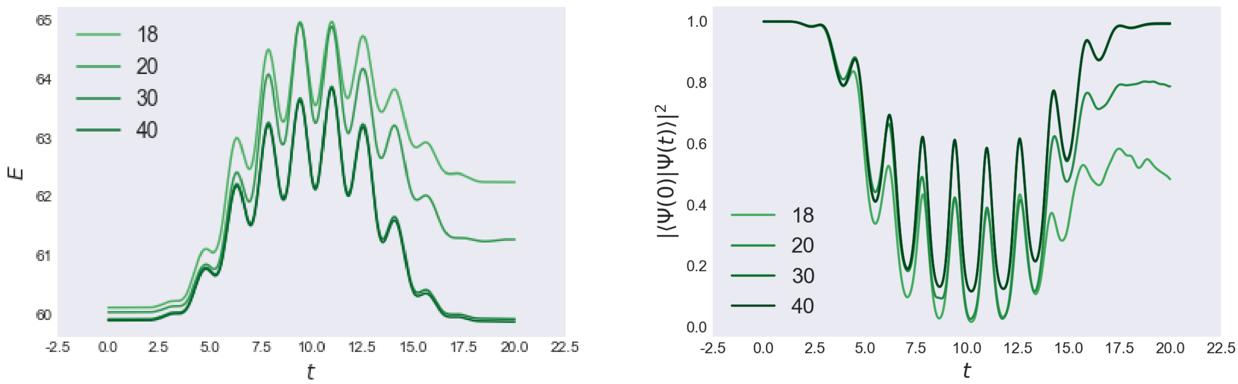

Figure A.7: Time-dependent energy (left) and ground state probability (right) of a one-dimensional harmonic oscillator with $\Omega = 1$ and $n = 10$ electrons under the influence of a oscillating electric field of frequency $\omega = 2\Omega = 2$ and field strength $E_{\max} = 1$, for different number of spin-orbitals $l = \{18, 20, 30, 40\}$.

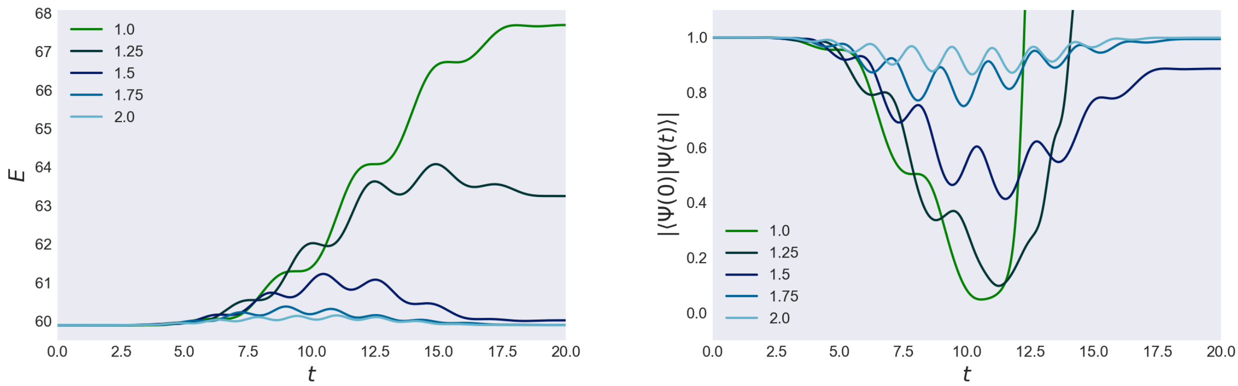

Figure A.8: Time-dependent energy (left) and ground state probability (right) of a one-dimensional harmonic oscillator with $\Omega = 1$ and $n = 8$ electrons under the influence of a oscillating electric field of different frequencies $\omega \in \{1.0, 1.25, 1.5, 1.75, 2.0\}$ with maximum field strength $\mathbf{E}_{\max} = 0.25$ and $l = 40$ spin-orbitals.

Twelve electrons

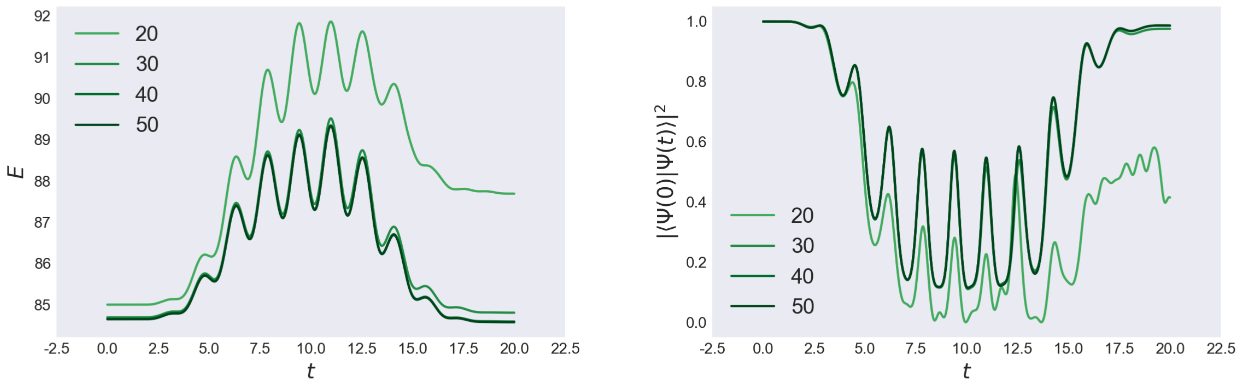

Figure A.9: Time-dependent energy (left) and ground state probability (right) of a one-dimensional harmonic oscillator with $\Omega = 1$ and $n = 12$ electrons under the influence of a oscillating electric field of frequency $\omega = 2\Omega = 2$ and field strength $E_{\max} = 1$, for different number of spin-orbitals $l = \{20, 30, 40, 50\}$.

A.2 Two Dimensions

Two electrons

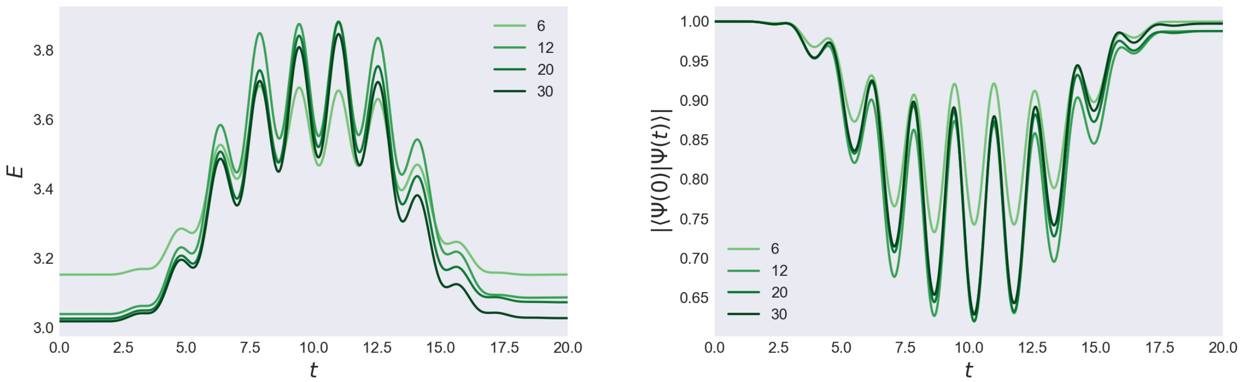

Figure A.10: Time-dependent energy (left) and ground state probability (right) of a two-dimensional harmonic oscillator with $\Omega = 1$ and $n = 2$ electrons under the influence of a oscillating electric field of frequency $\omega = 2\Omega = 2$ and field strength $E_{\text{max}} = 1$, for different number of spin-orbitals $l = \{6, 12, 20, 30\}$.

Six electrons

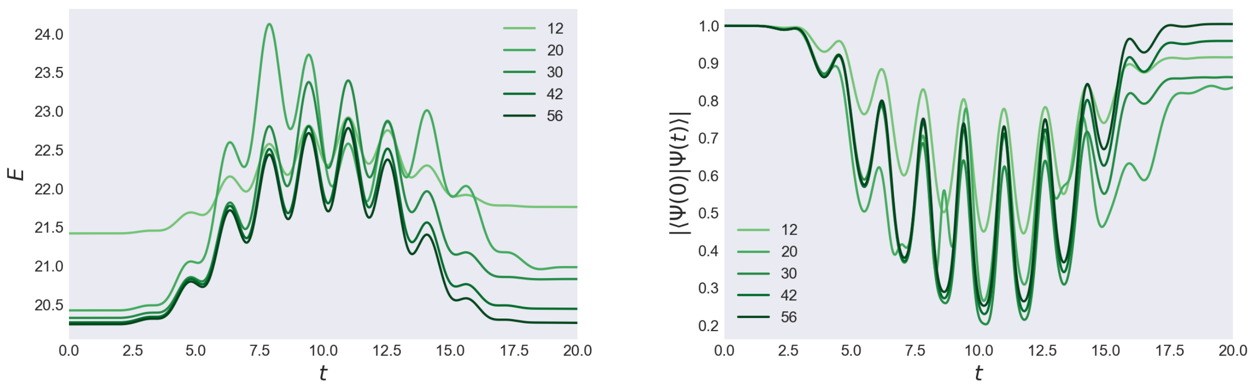

Figure A.11: Time-dependent energy (left) and ground state probability (right) of a two-dimensional harmonic oscillator with $\Omega = 1$ and $n = 6$ electrons under the influence of a oscillating electric field of frequency $\omega = 2\Omega = 2$ and field strength $E_{\text{max}} = 1$, for different number of spin-orbitals $l = \{6, 12, 20, 30\}$.

Appendix B

Slater-Condon Rules

The Slater-Condon rules are ways to express integrals over operators in terms of single-particle orbitals. Here is an outline of a proof for these rules.

Consider first some Slater determinants,

$$|I\rangle = |i_1 i_2 \dots i_N\rangle = \hat{i}_1^\dagger \hat{i}_2^\dagger \dots \hat{i}_N^\dagger \,|\rangle \tag{B.1}$$

$$|J\rangle = |j_1 j_2 \dots j_N\rangle = \hat{j}_1^\dagger \hat{j}_2^\dagger \dots \hat{j}_N^\dagger \,|\rangle \,. \tag{B.2}$$

To get started, we want to compute the inner product $\langle I|J\rangle$ of these two Slater determinants,

$$\langle I|J\rangle = \langle|\, \hat{i}_N \dots \hat{i}_2 \hat{i}_1 \hat{j}_1^\dagger \hat{j}_2^\dagger \dots \hat{j}_N^\dagger \,|\rangle \,. \tag{B.3}$$

In order to evaluate this expression, we move every annihilation operater $\hat{i}_p$ to the right. Starting with $\hat{i}_1$, for instance, we have two possible outcomes. If there is no $\hat{j}_q$ that is the same as $\hat{i}_1$ we get

$$\langle I|J\rangle = \langle|\, \hat{i}_N \dots \hat{i}_2 \hat{j}_1^\dagger \hat{j}_2^\dagger \dots \hat{j}_N^\dagger \hat{i}_1 \,|\rangle\, (-1)^N = 0, \tag{B.4}$$

because $\hat{i}_1 \,|\rangle = 0$. The other possibility that may arise is that $\hat{i}_1 = \hat{j}_q$, so that

$$\hat{i}_1 \hat{j}_q^\dagger = \{\hat{i}_1, \hat{j}_q^\dagger\} - \hat{j}_q^\dagger \hat{i}_1 = \hat{\delta}_{i_1 k_q} - \hat{j}_p^\dagger \hat{i}_1 = \hat{1} - \hat{j}_q^\dagger \hat{i}_1, \tag{B.5}$$

and

$$\langle I|J\rangle = \langle|\, \hat{i}_N \dots \hat{i}_2 \hat{j}_1^\dagger \hat{j}_2^\dagger \dots \hat{j}_{p-1}^\dagger \hat{j}_{p+1}^\dagger \dots \hat{j}_N^\dagger \hat{i}_1 \,|\rangle\, (-1)^{p-1} - 0. \tag{B.6}$$

We continue in this manner, moving all $\hat{i}$ to the right and the final result will be zero if there are any $\hat{i}_p$ without a matching $\hat{j}_q$ or $(-1)^\tau$ if the two operator strings are identical to a permutation τ.

Next, consider a symmetric one-body operator

$$\hat{F} = \sum_{\mu=1}^{N} \hat{f}_\mu, \tag{B.7}$$

where μ is the identity of the electron on which the identical $\hat{f}_\mu$ operate. Computing a matrix element of this one-body operator between two Slater determinants will yield three possible results,

$$
\begin{aligned}
\langle I|\,\hat{F}\,|J\rangle &= \langle i_1 i_2 \dots i_N|\,\hat{F}\,|j_1 j_2 \dots j_N\rangle \\
&= \sum_\mu \langle i_1 i_2 \dots i_N|\,\hat{f}_\mu\,|j_1 j_2 \dots j_N\rangle \\
&= \sum_\mu \langle \phi_{i_1}\phi_{i_2}\dots\phi_{i_N}|\,\hat{f}_\mu \sum_{\hat{P}} (-1)^{\sigma(\hat{P})} \left|\hat{P}\phi_{j_1}\phi_{j_2}\dots\phi_{j_N}\right\rangle = \begin{cases} \sum_k \langle i_k|\,\hat{f}\,|i_k\rangle\,(-1)^{\sigma(\hat{P})} & \mathrm{I} \\ \langle i_k|\,\hat{f}\,|i'_k\rangle\,(-1)^{\sigma(\hat{P})} & \mathrm{II} \\ 0 & \mathrm{III} \end{cases}
\end{aligned} \tag{B.8}
$$

In the last line, the integral is written with spinorbitals instead of Slater determinants. The result will be the first case (I), if the operators needed to construct the Slater determinants are the same, up to a permutation with permutation parity σ associated with the permutation operator $\hat{P}$ needed to permute the product of spinorbitals. If there exists excactly one noncoincidence in the string of operators so that $\hat{P} j_1 j_2 \dots j_N = i_1 i_2 \dots i'_k \dots i_N$ where $i_k \neq i'_k$, we get the result in the second case (II). If there are two or more noncoincidences, the result is zero (III).

With second quantisation we might write a one-electron operators differently,

$$
\sum_{kl} \langle k|\,\hat{f}\,|l\rangle\,\hat{a}_k^\dagger \hat{a}_l = \sum_{kl} f_{kl}\hat{a}_k^\dagger \hat{a}_l. \tag{B.9}
$$

It is possible to show that the results are the same in this representation. First, consider the case where the two Slater determinants are equal,

$$
\begin{aligned}
\langle I| \sum_{kl} f_{kl}\hat{a}_k^\dagger \hat{a}_l\,|I\rangle &= \sum_{kl} f_{kl}\,\langle I|\,\hat{a}_k^\dagger \hat{a}_l\,|I\rangle \\
&= \sum_{kl} f_{kl}\delta_{kl} n_l(I) = \sum_{k\in I} f_{kk} = \sum_{k=1}^{N} \langle i_k|\,\hat{f}\,|i_k\rangle\,.
\end{aligned} \tag{B.10}
$$

Second, we look at the case where we have one noncoincidence, $i_p \neq j_p$,

$$
\begin{aligned}
\langle I| \sum_{kl} f_{kl}\,\langle I|\,\hat{a}_k^\dagger \hat{a}_l\,|J\rangle &= \sum_{kl} f_{kl}\,\langle I|\,\hat{a}_k^\dagger \hat{a}_l\,|J\rangle \\
&= \sum_{kl\neq p} f_{kl}\,\langle I|\,\hat{a}_k^\dagger \hat{a}_l\,|J\rangle + f_{i_p j_p}\,\langle I|\,\hat{i}_p^\dagger \hat{j}_p\,|J\rangle \\
&= 0 + f_{i_p j_p}\,\langle I'|I'\rangle = \left\langle \hat{i}_p\right|\,\hat{f}\,\left|\hat{i}_p\right\rangle .
\end{aligned} \tag{B.11}
$$

Lastly, there is no pair of operators $\hat{a}_k^\dagger \hat{a}_l$ that will give a non-zero result. Consequently, we see that the second-quantised form of the one-body operator gives the same result.

Similarly, consider a symmetric two-body operator,

$$
\hat{G} = \sum_{\mu<\nu}^{N} \hat{g}_{\mu\nu} = \frac{1}{2}\sum_{\mu\neq\nu}^{N} \hat{g}_{\mu\nu} = \frac{1}{2}\sum_{ijkl} \langle ij|\,\hat{g}\,|kl\rangle\,\hat{a}_i^\dagger \hat{a}_j^\dagger \hat{a}_l \hat{a}_k. \tag{B.12}
$$

We would like to show that the second-quantized form is correct, and therefore firstly consider the case where the two Slater determinants are equal, i.e. zero noncoincidences;

$$
\langle I|\,\hat{G}\,|I\rangle = \frac{1}{2}\sum_{ijkl} \langle ij|\,\hat{G}\,|kl\rangle\,\langle I|\,\hat{a}_i^\dagger \hat{a}_j^\dagger \hat{a}_l \hat{a}_k\,|I\rangle\,. \tag{B.13}
$$

We must have $k = i_p$ and $l = i_q$ appear in $|I\rangle$, so that

$$\begin{aligned}\langle I|\,\hat{G}\,|I\rangle =& \frac{1}{2}\sum_{ij}\langle ij|\,\hat{g}\,|i_p i_q\rangle\,\langle I|\,\hat{a}^\dagger\hat{a}^\dagger\hat{a}_{i_p}\hat{a}_{i_q}\,|i_1 i_2\ldots i_p\ldots i_q\ldots\rangle \\ =& \frac{1}{2}\sum_{ij}\langle ij|\,\hat{g}\,|i_p i_q\rangle\,\langle I|\,\hat{a}_i^\dagger\hat{a}_j^\dagger\,|i_1 i_2\ldots\rangle\,(-1)^{(p-1)+(q-2)}.\end{aligned} \tag{B.14}$$

From this point we have two possibilities for the values of i and j, because the creation operators must put the same values back into the ket,

$$\begin{aligned}&\langle i_p i_q|\,\hat{g}\,|i_p i_q\rangle\,\langle I|i_1 i_2\ldots i_p\ldots i_q\ldots\rangle\,(-1)^{(p-1)+(q-2)}(-1)^{(p-1)+(q-2)} \\ &\qquad = \langle i_p i_q|\,\hat{g}\,|i_p i_q\rangle\end{aligned} \qquad (i = i_p,\ j = i_q); \tag{B.15}$$

$$\begin{aligned}&\langle i_q i_p|\,\hat{g}\,|i_p i_q\rangle\,\langle I|i_1 i_2\ldots i_p\ldots i_q\ldots\rangle\,(-1)^{(p-1)+(q-2)}(-1)^{(p-1)+(q-1)} \\ &\qquad = -\,\langle i_q i_p|\,\hat{g}\,|i_p i_q\rangle = -\,\langle i_p i_q|\,\hat{g}\,|i_q i_p\rangle\end{aligned} \qquad (i = i_q,\ j = i_p). \tag{B.16}$$

By starting in the reverse order, we obtain the same contributions. The total matrix element is therefore,

$$\langle I|\,\hat{G}\,|I\rangle = \frac{1}{2}\sum_{i\in I}\sum_{j\in J}(\langle ij|\,\hat{g}\,|ij\rangle - \langle ij|\,\hat{g}\,|ji\rangle) = \sum_{\substack{i<j\\ i,j\in I}}\langle ij|\,\hat{g}\,|ij\rangle_{\mathrm{AS}}\,. \tag{B.17}$$

Next, we consider a single noncoincidence in $|I\rangle$, $i_p \neq i'_p$,

$$|I\rangle = |i_1 i_2\ldots i_p\ldots\rangle\,, \tag{B.18}$$

$$|I'\rangle = \left|i_1 i_2\ldots i'_p\ldots\right\rangle. \tag{B.19}$$

We get contributions to $\langle I|\,\hat{G}\,|I'\rangle$ from the operator string $\hat{a}_i^\dagger\hat{a}_j^\dagger\hat{a}_l\hat{a}_k$ in the following cases,

$$i = i'_p,\ k = i_p,\ j = l = i_q \to \left\langle i'_p i_q\middle|i_p i_q\right\rangle \tag{B.20}$$

$$i = i'_p,\ l = i_p,\ j = k = i_q \to -\left\langle i'_p i_q\middle|i_q i_p\right\rangle \tag{B.21}$$

$$j = i'_p,\ l = i_p,\ i = k = i_q \to \left\langle i_q i'_p\middle|i_q i_q\right\rangle \tag{B.22}$$

$$j = i'_p,\ k = i_p,\ i = l = i_q \to -\left\langle i_q i'_p\middle|i_p i_q\right\rangle, \tag{B.23}$$

where the two first terms are egual to the last terms, respectively. This leaves us with,

$$\langle I'|\,\hat{G}\,|I\rangle = 2\times\frac{1}{2}(\langle i'_p j|\,\hat{g}\,|i_p j\rangle - \langle i'_p j|\,\hat{g}\,|j i_p\rangle) = \sum_{j\in I}\langle i'_p j|\,\hat{g}\,|i_p j\rangle_{\mathrm{AS}}\,. \tag{B.24}$$

After a while we see a pattern emerges. For two noncoincidences ($i_p \neq i'_p$, $i_q \neq i'_q$) we have,

$$\langle I'|\,\hat{G}\,|I\rangle = \left\langle i'_p i'_q\right|\,\hat{g}\,|i_p i_q\rangle\,, \tag{B.25}$$

while for three or more noncoincidences,

$$\langle I'|\,\hat{G}\,|I\rangle = 0. \tag{B.26}$$

Appendix C

2D Coulomb elements

Implementation of two-body matrix elements for the two-dimensional quantum dots[1]. Note that Anisimovas and Matulis uses the chemist's convention $\langle ij | \hat{u} | lk \rangle$ which is $\langle ij | \hat{u} | kl \rangle$ in the physcist's notation. That is, the last two indices are interchanged.

```
def coulomb_ho(n_i, m_i, n_j, m_j, n_l, m_l, n_k, m_k):
    element = 0

    if m_i + m_j != m_k + m_l:
        return 0

    M_i = 0.5 * (abs(m_i) + m_i)
    dm_i = 0.5 * (abs(m_i) - m_i)

    M_j = 0.5 * (abs(m_j) + m_j)
    dm_j = 0.5 * (abs(m_j) - m_j)

    M_k = 0.5 * (abs(m_k) + m_k)
    dm_k = 0.5 * (abs(m_k) - m_k)

    M_l = 0.5 * (abs(m_l) + m_l)
    dm_l = 0.5 * (abs(m_l) - m_l)

    n = np.array([n_i, n_j, n_k, n_l], dtype=np.int64)
    m = np.array([m_i, m_j, m_k, m_l], dtype=np.int64)
    j = np.array([0, 0, 0, 0], dtype=np.int64)
    l = np.array([0, 0, 0, 0], dtype=np.int64)
    g = np.array([0, 0, 0, 0], dtype=np.int64)

    for j_1 in range(n_i + 1):
        j[0] = j_1
        for j_2 in range(n_j + 1):
            j[1] = j_2
            for j_3 in range(n_k + 1):
                j[2] = j_3
                for j_4 in range(n_l + 1):
                    j[3] = j_4
```

```
                g[0] = j_1 + j_4 + M_i + dm_l
                g[1] = j_2 + j_3 + M_j + dm_k
                g[2] = j_3 + j_2 + M_k + dm_j
                g[3] = j_4 + j_1 + M_l + dm_i

                G = np.sum(g)
                ratio_1 = log_ratio_1(j)
                prod_2 = log_product_2(n, m, j)
                ratio_2 = log_ratio_2(G)

                temp = 0
                for l_1 in range(g[0] + 1):
                    l[0] = l_1
                    for l_2 in range(g[1] + 1):
                        l[1] = l_2
                        for l_3 in range(g[2] + 1):
                            l[2] = l_3
                            for l_4 in range(g[3] + 1):
                                l[3] = l_4

                                if l_1 + l_2 != l_3 + l_4:
                                    continue

                                L = np.sum(l)

                                temp += (
                                    -2
                                    * (int(g[1] + g[2] - l[1] - l[2]) & 0x1)
                                    + 1
                                ) * np.exp(
                                    log_product_3(l, g)
                                    + math.lgamma(1.0 + 0.5 * L)
                                    + math.lgamma(0.5 * (G - L + 1.0))
                                )

                element += (
                    (-2 * (int(np.sum(j)) & 0x1) + 1)
                    * np.exp(ratio_1 + prod_2 + ratio_2)
                    * temp
                )

    element *= log_product_1(n, m)

    return element
```

Appendix D

CCSD Equations

Singly excited τ-amplitude equation

$$
\begin{gathered}
f_c^a t_1{}_i^c + f_c^k t_2{}_{ik}^{ac} + t_1{}_k^c u_{ic}^{ak} + \frac{1}{2} t_2{}_{ik}^{cb} u_{cb}^{ak} - f_i^k t_1{}_k^a - \frac{1}{2} t_2{}_{kl}^{ac} u_{ic}^{kl} + t_1{}_k^c t_1{}_l^a u_{ic}^{kl} + t_1{}_k^c t_2{}_{il}^{ab} u_{cb}^{kl} \\
- f_c^k t_1{}_i^c t_1{}_k^a - t_1{}_k^c t_1{}_i^b u_{cb}^{ak} - \frac{1}{2} t_1{}_k^a t_2{}_{il}^{cb} u_{cb}^{kl} - \frac{1}{2} t_1{}_i^c t_2{}_{kl}^{ab} u_{cb}^{kl} - t_1{}_k^c t_1{}_i^b t_1{}_l^a u_{cb}^{kl} + f_i^a = 0
\end{gathered}
$$

Doubly excited τ-amplitude equation

$$
\begin{gathered}
\frac{1}{2} t_2{}_{ij}^{AB} u_{IJ}^{ij} + \frac{1}{2} t_2{}_{IJ}^{ab} u_{ab}^{AB} + f_I^i t_2{}_{Ji}^{AB} P(IJ) + t_1{}_i^A t_1{}_j^B u_{IJ}^{ij} + t_1{}_i^A u_{IJ}^{Bi} P(AB) + t_1{}_I^a t_1{}_J^b u_{ab}^{AB} \\
- f_a^A t_2{}_{IJ}^{Ba} P(AB) - t_1{}_I^a u_{Ja}^{AB} P(IJ) + \frac{1}{4} t_2{}_{IJ}^{ab} t_2{}_{ij}^{AB} u_{ab}^{ij} + f_a^i t_1{}_i^A t_2{}_{IJ}^{Ba} P(AB) + f_a^i t_1{}_I^a t_2{}_{Ji}^{AB} P(IJ) \\
+ t_1{}_i^a t_2{}_{Ij}^{AB} u_{Ja}^{ij} P(IJ) + t_2{}_{Ii}^{Aa} t_2{}_{Jj}^{Bb} u_{ab}^{ij} P(AB) + t_2{}_{Ii}^{Aa} u_{Ja}^{Bi} P(AB) P(IJ) + \frac{1}{2} t_1{}_i^A t_1{}_j^B t_2{}_{IJ}^{ab} u_{ab}^{ij} \\
+ \frac{1}{2} t_1{}_i^A t_2{}_{IJ}^{ab} u_{ab}^{Bi} P(AB) + \frac{1}{2} t_1{}_I^a t_1{}_J^b t_2{}_{ij}^{AB} u_{ab}^{ij} + \frac{1}{2} t_2{}_{Ji}^{ab} t_2{}_{Ij}^{AB} u_{ab}^{ij} P(IJ) - t_1{}_i^a t_2{}_{IJ}^{Ab} u_{ab}^{Bi} P(AB) \\
- \frac{1}{2} t_1{}_I^a t_2{}_{ij}^{AB} u_{Ja}^{ij} P(IJ) - \frac{1}{2} t_2{}_{IJ}^{Aa} t_2{}_{ij}^{Bb} u_{ab}^{ij} P(AB) + t_1{}_I^a t_1{}_J^b t_1{}_i^A t_1{}_j^B u_{ab}^{ij} \\
+ t_1{}_I^a t_1{}_J^b t_1{}_i^A u_{ab}^{Bi} P(AB) + t_1{}_i^A t_2{}_{Ij}^{Ba} u_{Ja}^{ij} P(AB) P(IJ) + t_1{}_i^a t_1{}_j^A t_2{}_{IJ}^{Bb} u_{ab}^{ij} P(AB) \\
+ t_1{}_i^a t_1{}_I^b t_2{}_{Jj}^{AB} u_{ab}^{ij} P(IJ) - t_1{}_I^a t_1{}_i^A t_1{}_j^B u_{Ja}^{ij} P(IJ) - t_1{}_I^a t_1{}_i^A u_{Ja}^{Bi} P(AB) P(IJ) \\
- t_1{}_I^a t_2{}_{Ji}^{Ab} u_{ab}^{Bi} P(AB) P(IJ) - t_1{}_I^a t_1{}_i^A t_2{}_{Jj}^{Bb} u_{ab}^{ij} P(AB) P(IJ) + u_{IJ}^{AB} = 0
\end{gathered}
$$

Single-excited λ-amplitude equation

$$
\begin{gathered}
f_A^a \lambda_1{}_a^I + \lambda_1{}_a^i u_{Ai}^{Ia} + t_1{}_i^a u_{Aa}^{Ii} + \frac{1}{2} \lambda_2{}_{ab}^{Ii} u_{Ai}^{ab} - f_i^I \lambda_1{}_A^i - \frac{1}{2} \lambda_2{}_{Aa}^{ij} u_{ij}^{Ia} \\
+ \lambda_1{}_a^I t_1{}_i^b u_{Ab}^{ai} + \lambda_1{}_A^i t_1{}_j^a u_{ai}^{Ij} + \lambda_1{}_a^i t_1{}_i^b u_{Ab}^{Ia} + \lambda_1{}_a^i t_2{}_{ij}^{ab} u_{Ab}^{Ij} + \lambda_2{}_{ab}^{Ii} t_1{}_j^a u_{Ai}^{bj} \\
+ \frac{1}{2} \lambda_2{}_{ab}^{Ii} t_1{}_i^c u_{Ac}^{ab} + \frac{1}{2} \lambda_2{}_{Aa}^{ij} t_1{}_k^a u_{ij}^{Ik} + \frac{1}{2} \lambda_2{}_{ab}^{ij} t_2{}_{ij}^{ac} u_{Ac}^{Ib} - f_a^I \lambda_1{}_A^i t_1{}_i^a \\
- f_A^i \lambda_1{}_a^I t_1{}_i^a - \lambda_1{}_a^i t_1{}_j^a u_{Ai}^{Ij} - \lambda_2{}_{ab}^{Ii} t_2{}_{ij}^{ac} u_{Ac}^{bj} - \lambda_2{}_{Aa}^{ij} t_1{}_i^b u_{bj}^{Ia} \\
- \lambda_2{}_{Aa}^{ij} t_2{}_{ik}^{ab} u_{bj}^{Ik} - \frac{1}{2} f_a^I \lambda_2{}_{Ab}^{ij} t_2{}_{ij}^{ab} - \frac{1}{2} f_A^i \lambda_2{}_{ab}^{Ij} t_2{}_{ij}^{ab} - \frac{1}{2} \lambda_1{}_a^I t_2{}_{ij}^{ab} u_{Ab}^{ij} \\
- \frac{1}{2} \lambda_1{}_A^i t_2{}_{ij}^{ab} u_{ab}^{Ij} - \frac{1}{2} \lambda_2{}_{ab}^{ij} t_2{}_{ik}^{ab} u_{Aj}^{Ik} - \frac{1}{4} \lambda_2{}_{Aa}^{ij} t_2{}_{ij}^{bc} u_{bc}^{Ia} + \frac{1}{4} \lambda_2{}_{ab}^{Ii} t_2{}_{jk}^{ab} u_{Ai}^{jk} \\
+ \lambda_2{}_{ab}^{Ii} t_1{}_j^a t_1{}_i^c u_{Ac}^{bj} + \lambda_2{}_{Aa}^{ij} t_1{}_k^a t_1{}_i^b u_{bj}^{Ik} + \frac{1}{2} \lambda_2{}_{Aa}^{ij} t_1{}_j^b t_1{}_i^c u_{bc}^{Ia}
\end{gathered}
$$

$$
\begin{gathered}
+\frac{1}{2}\lambda_{2}{}^{ij}_{ab}t_{1}{}^{a}_{k}t_{2}{}^{bc}_{ij}u^{Ik}_{Ac}+\frac{1}{2}\lambda_{2}{}^{ij}_{ab}t_{1}{}^{c}_{i}t_{2}{}^{ab}_{jk}u^{Ik}_{Ac}-\lambda_{1}{}^{I}_{a}t_{1}{}^{a}_{i}t_{1}{}^{b}_{j}u^{ij}_{Ab}\\
-\lambda_{1}{}^{i}_{A}t_{1}{}^{a}_{i}t_{1}{}^{b}_{j}u^{Ij}_{ab}-\lambda_{1}{}^{i}_{a}t_{1}{}^{a}_{j}t_{1}{}^{b}_{i}u^{Ij}_{Ab}-\lambda_{2}{}^{Ii}_{ab}t_{1}{}^{a}_{j}t_{2}{}^{bc}_{ik}u^{jk}_{Ac}\\
-\lambda_{2}{}^{ij}_{Aa}t_{1}{}^{b}_{i}t_{2}{}^{ac}_{jk}u^{Ik}_{bc}-\frac{1}{2}\lambda_{2}{}^{Ii}_{ab}t_{1}{}^{a}_{k}t_{1}{}^{b}_{j}u^{jk}_{Ai}-\frac{1}{2}\lambda_{2}{}^{Ii}_{ab}t_{1}{}^{c}_{j}t_{2}{}^{ab}_{ik}u^{jk}_{Ac}\\
-\frac{1}{2}\lambda_{2}{}^{ij}_{Aa}t_{1}{}^{b}_{k}t_{2}{}^{ac}_{ij}u^{Ik}_{bc}+\frac{1}{4}\lambda_{2}{}^{Ii}_{ab}t_{1}{}^{c}_{i}t_{2}{}^{ab}_{jk}u^{jk}_{Ac}+\frac{1}{4}\lambda_{2}{}^{ij}_{Aa}t_{1}{}^{a}_{k}t_{2}{}^{bc}_{ij}u^{Ik}_{bc}\\
-\frac{1}{2}\lambda_{2}{}^{Ii}_{ab}t_{1}{}^{a}_{k}t_{1}{}^{b}_{j}t_{1}{}^{c}_{i}u^{jk}_{Ac}-\frac{1}{2}\lambda_{2}{}^{ij}_{Aa}t_{1}{}^{a}_{k}t_{1}{}^{b}_{j}t_{1}{}^{c}_{i}u^{Ik}_{bc}+f^{I}_{A}=0
\end{gathered}
$$

Doubly excited λ-amplitude equation

$$
\begin{gathered}
+\frac{1}{2}\lambda_{2}{}^{IJ}_{ab}u^{ab}_{AB}+\frac{1}{2}\lambda_{2}{}^{ij}_{AB}u^{IJ}_{ij}+f^{I}_{i}\lambda_{2}{}^{Ji}_{AB}P(IJ)+\lambda_{1}{}^{i}_{A}u^{IJ}_{Bi}P(AB)+\lambda_{2}{}^{IJ}_{ab}t_{1}{}^{a}_{i}u^{bi}_{AB}+\lambda_{2}{}^{ij}_{AB}t_{1}{}^{a}_{i}u^{IJ}_{aj}\\
-f^{a}_{A}\lambda_{2}{}^{IJ}_{Ba}P(AB)-\lambda_{1}{}^{I}_{a}u^{Ja}_{AB}P(IJ)+\frac{1}{4}\lambda_{2}{}^{IJ}_{ab}t_{2}{}^{ab}_{ij}u^{ij}_{AB}+\frac{1}{4}\lambda_{2}{}^{ij}_{AB}t_{2}{}^{ab}_{ij}u^{IJ}_{ab}+f^{I}_{A}\lambda_{1}{}^{J}_{B}P(AB)P(IJ)\\
+f^{I}_{a}\lambda_{2}{}^{Ji}_{AB}t_{1}{}^{a}_{i}P(IJ)+f^{i}_{A}\lambda_{2}{}^{IJ}_{Ba}t_{1}{}^{a}_{i}P(AB)+\lambda_{1}{}^{I}_{a}t_{1}{}^{a}_{i}u^{Ji}_{AB}P(IJ)+\lambda_{1}{}^{i}_{A}t_{1}{}^{a}_{i}u^{IJ}_{Ba}P(AB)\\
+\lambda_{2}{}^{IJ}_{Aa}t_{1}{}^{b}_{i}u^{ai}_{Bb}P(AB)+\lambda_{2}{}^{Ii}_{AB}t_{1}{}^{a}_{j}u^{Jj}_{ai}P(IJ)+\lambda_{2}{}^{Ii}_{Aa}u^{Ja}_{Bi}P(AB)P(IJ)-\frac{1}{2}\lambda_{2}{}^{IJ}_{Aa}t_{2}{}^{ab}_{ij}u^{ij}_{Bb}P(AB)\\
-\frac{1}{2}\lambda_{2}{}^{IJ}_{ab}t_{1}{}^{a}_{j}t_{1}{}^{b}_{i}u^{ij}_{AB}-\frac{1}{2}\lambda_{2}{}^{Ii}_{AB}t_{2}{}^{ab}_{ij}u^{Jj}_{ab}P(IJ)-\frac{1}{2}\lambda_{2}{}^{Ii}_{ab}t_{2}{}^{ab}_{ij}u^{Jj}_{AB}P(IJ)\\
-\frac{1}{2}\lambda_{2}{}^{ij}_{AB}t_{1}{}^{a}_{j}t_{1}{}^{b}_{i}u^{IJ}_{ab}-\frac{1}{2}\lambda_{2}{}^{ij}_{Aa}t_{2}{}^{ab}_{ij}u^{IJ}_{Bb}P(AB)+\lambda_{1}{}^{I}_{A}t_{1}{}^{a}_{i}u^{Ji}_{Ba}P(AB)P(IJ)\\
+\lambda_{2}{}^{Ii}_{Aa}t_{1}{}^{b}_{i}u^{Ja}_{Bb}P(AB)P(IJ)+\lambda_{2}{}^{Ii}_{Aa}t_{2}{}^{ab}_{ij}u^{Jj}_{Bb}P(AB)P(IJ)-\lambda_{2}{}^{IJ}_{Aa}t_{1}{}^{a}_{i}t_{1}{}^{b}_{j}u^{ij}_{Bb}P(AB)\\
-\lambda_{2}{}^{Ii}_{AB}t_{1}{}^{a}_{i}t_{1}{}^{b}_{j}u^{Jj}_{ab}P(IJ)-\lambda_{2}{}^{Ii}_{Aa}t_{1}{}^{a}_{j}u^{Jj}_{Bi}P(AB)P(IJ)\\
-\lambda_{2}{}^{Ii}_{Aa}t_{1}{}^{a}_{j}t_{1}{}^{b}_{i}u^{Jj}_{Bb}P(AB)P(IJ)+u^{IJ}_{AB}=0
\end{gathered}
$$

Appendix E

Custom Quantum System Functions

E.1 Function for constructing system from Psi4

```python
def construct_psi4_system(
    molecule, options, np=None, add_spin=True, anti_symmetrize=True
):
    import psi4

    if np is None:
        import numpy as np

    psi4.core.be_quiet()
    psi4.set_options(options)

    mol = psi4.geometry(molecule)
    nuclear_repulsion_energy = mol.nuclear_repulsion_energy()

    wavefunction = psi4.core.Wavefunction.build(
        mol, psi4.core.get_global_option("BASIS")
    )

    molecular_integrals = psi4.core.MintsHelper(wavefunction.basisset())

    kinetic = np.asarray(molecular_integrals.ao_kinetic())
    potential = np.asarray(molecular_integrals.ao_potential())
    h = kinetic + potential

    u = np.asarray(molecular_integrals.ao_eri()).transpose(0, 2, 1, 3)
    overlap = np.asarray(molecular_integrals.ao_overlap())

    n_up = wavefunction.nalpha()
    n_down = wavefunction.nbeta()
    n = n_up + n_down
    l = 2 * wavefunction.nmo()

    dipole_integrals = [
        np.asarray(mu) for mu in molecular_integrals.ao_dipole()
```

```
    ]
    dipole_integrals = np.stack(dipole_integrals)

    system = CustomSystem(n, l, n_up=n_up, np=np)
    system.set_h(h, add_spin=add_spin)
    system.set_u(u, add_spin=add_spin, anti_symmetrize=anti_symmetrize)
    system.set_s(overlap, add_spin=add_spin)
    system.set_dipole_moment(dipole_integrals, add_spin=add_spin)
    system.set_nuclear_repulsion_energy(nuclear_repulsion_energy)

    return system
```

E.2 Function for constructing system from PySCF

```
def construct_pyscf_system(molecule, basis="cc-pvdz", np=None, verbose=False):
    import pyscf

    if np is None:
        import numpy as np

    # Build molecule in AO-basis
    mol = pyscf.gto.Mole()
    mol.unit = "bohr"
    mol.build(atom=molecule, basis=basis, symmetry=False)
    mol.set_common_origin(np.array([0.0, 0.0, 0.0]))
    nuclear_repulsion_energy = mol.energy_nuc()

    # Perform UHF-calculations to create the MO-basis
    hf = pyscf.scf.UHF(mol)
    ehf = hf.kernel()

    if not hf.converged:
        warnings.warn("UHF calculation did not converge")

    if verbose:
        print(f"UHF energy: {hf.e_tot}")

    # Build the coefficient matrix from the occupied and virtual integrals. As
    # we have done a UHF-calculation, we stack the two spin-directions on top
    # of each other. That is, instead of using odd or even indices for each spin
    # direction, we set up two separate blocks.
    C_o = np.hstack(
        (
            # Fetch occupied coefficients for both spin-directions
            hf.mo_coeff[0][:, hf.mo_occ[0] > 0],
            hf.mo_coeff[1][:, hf.mo_occ[1] > 0],
        )
    )
```

```
C_v = np.hstack(
    (
        # Fetch virtual coefficients for both spin-directions
        hf.mo_coeff[0][:, hf.mo_occ[0] == 0],
        hf.mo_coeff[1][:, hf.mo_occ[1] == 0],
    )
)

# Build full coefficient matrix.
C = np.hstack((C_o, C_v))

# Get the number of occupied molecular orbitals
n = C_o.shape[1]
# Fetch the number of molecular orbitals
l = C.shape[1]

# Check that the number of occupied molecular orbitals is correct
assert n == sum(hf.mo_occ[0] > 0) + sum(hf.mo_occ[1] > 0)
# Check that the number of molecular orbitals is twice of that of the number
# of atomic orbitals.
assert l == C.shape[0] * 2

# Note: Should the dipole moments have a negative sign?
dipole_moment = [
    -transform_one_body_elements(dm, C, np)
    for dm in mol.intor("int1e_r").reshape(3, mol.nao, mol.nao)
]
dipole_moment = np.asarray(dipole_moment)

# Create a tuple with the shape of the AO two-body elements
u_shape = (mol.nao for i in range(4))

h = transform_one_body_elements(hf.get_hcore(), C, np)
u = transform_two_body_elements(mol.intor("int2e").reshape(*u_shape), C, np)

noa = sum(hf.mo_occ[0] > 0)
nva = sum(hf.mo_occ[0] == 0)
nob = sum(hf.mo_occ[1] > 0)
nvb = sum(hf.mo_occ[1] == 0)
no = noa + nob
nv = nva + nvb

oa = slice(0, noa)
ob = slice(noa, no)
va = slice(no, no + nva)
vb = slice(no + nva, no + nv)

a_slices = [oa, va]
b_slices = [ob, vb]

# Create a combination of slices that should be zero in all matrix elements,
```

```
    # due to unequal spin-direction.
    zero_slices = [(a, b) for a in a_slices for b in b_slices]
    zero_slices += [(b, a) for a in a_slices for b in b_slices]

    # Create a slice object for all indices, i.e., the ":" syntax in NumPy.
    all_slice = slice(None, None)

    # Explicitly set all cross-spin terms to zero
    for s in zero_slices:
        h[s] = 0
        dipole_moment[(all_slice,) + s] = 0
        u[s + (all_slice, all_slice)] = 0
        u[(all_slice, all_slice) + s] = 0

    # Convert to physicist's notation, from Mulliken notation
    u = u.transpose(0, 2, 1, 3)

    # Build a custom system from the integral elements
    system = CustomSystem(n, l, np=np)
    system.set_h(h)
    system.set_u(u, anti_symmetrize=True)
    system.set_dipole_moment(dipole_moment)
    system.set_nuclear_repulsion_energy(nuclear_repulsion_energy)
    system.cast_to_complex()

    return system
```

Bibliography

[1] E Anisimovas and A Matulis. “Energy spectra of few-electron quantum dots”. In: *Journal of Physics: Condensed Matter* 10.3 (1998), p. 601.

[2] Jouko Arponen. “Variational principles and linked-cluster exp S expansions for static and dynamic many-body problems”. In: *Annals of Physics* 151.2 (1983), pp. 311–382.

[3] JS Arponen, RF Bishop, and Erkki Pajanne. “Extended coupled-cluster method. I. Generalized coherent bosonization as a mapping of quantum theory into classical Hamiltonian mechanics”. In: *Physical Review A* 36.6 (1987), p. 2519.

[4] Henry Frederick Baker. “Alternants and continuous groups”. In: *Proceedings of the London Mathematical Society* 2.1 (1905), pp. 24–47.

[5] Rodney J Bartlett and Jozef Noga. “The expectation value coupled-cluster method and analytical energy derivatives”. In: *Chemical physics letters* 150.1-2 (1988), pp. 29–36.

[6] G Berthier. “Extension de la Methode du Champ Meleculaire Self-Consistent a Letude des Etats a Couches Incompletes”. In: *Comptes Rendus Hebdomadaires des Seances de l’Academie des Sciences* 238.1 (1954), pp. 91–93.

[7] L Brey, Neil F Johnson, and BI Halperin. “Optical and magneto-optical absorption in parabolic quantum wells”. In: *Physical Review B* 40.15 (1989), p. 10647.

[8] L Brillouin. “Les problèmes de perturbations et les champs self-consistents”. In: *J. phys. radium* 3.9 (1932), pp. 373–389.

[9] John Edward Campbell. “On a law of combination of operators (second paper)”. In: *Proceedings of the London Mathematical Society* 1.1 (1897), pp. 14–32.

[10] Jiří Čížek. “On the correlation problem in atomic and molecular systems. Calculation of wavefunction components in Ursell-type expansion using quantum-field theoretical methods”. In: *The Journal of Chemical Physics* 45.11 (1966), pp. 4256–4266.

[11] F Coester. “Bound states of a many-particle system”. In: *Nuclear Physics* 7 (1958), pp. 421–424.

[12] Fritz Coester and Hermann Kümmel. “Short-range correlations in nuclear wave functions”. In: *Nuclear Physics* 17 (1960), pp. 477–485.

[13] Charles Galton Darwin. “The diamagnetism of the free electron”. In: *Mathematical Proceedings of the Cambridge Philosophical Society*. Vol. 27. 1. Cambridge University Press. 1931, pp. 86–90.

[14] Paul Adrien Maurice Dirac. *The Principles of Quantum Mechanics*. Oxford University Press, 1930.

[15] Paul Ehrenfest. “Bemerkung über die angenäherte Gültigkeit der klassischen Mechanik innerhalb der Quantenmechanik”. In: *Zeitschrift für Physik A Hadrons and Nuclei* 45.7 (1927), pp. 455–457.

[16] Richard P Feynman. "Nobel lecture: The development of the space-time view of quantum electrodynamics". In: *https://www.nobelprize.org/prizes/physics/1965/feynman/lecture/* (1965).

[17] Richard Phillips Feynman. "Forces in molecules". In: *Physical Review* 56.4 (1939), p. 340.

[18] Markus Fierz. "Über die relativistische Theorie kräftefreier Teilchen mit beliebigem Spin". PhD thesis. Birkhäuser, 1939.

[19] M Fink. "A new method for evaluating the density matrix and its application to the ground state form factors of 4He and 16O". In: *Nuclear Physics A* 221.1 (1974), pp. 163–172.

[20] Vladimir Fock. "Bemerkung zur Quantelung des harmonischen Oszillators im Magnetfeld". In: *Zeitschrift für Physik A Hadrons and Nuclei* 47.5 (1928), pp. 446–448.

[21] Vladimir Aleksandrovich Fock. "Näherungsmethode zur Lösung des quantenmechanischen Mehrkörperproblems". In: *Zeitschrift für Physik* 61.1-2 (1930), pp. 126–148.

[22] John Arthur Gaunt. "A Theory of Hartree's Atomic Fields". In: *Mathematical Proceedings of the Cambridge Philosophical Society*. Vol. 24. 2. Cambridge University Press. 1928, pp. 328–342.

[23] Jeffrey Goldstone. "Derivation of the Brueckner many-body theory". In: *Proceedings of the Royal Society of London. Series A. Mathematical and Physical Sciences* 239.1217 (1957), pp. 267–279.

[24] Gene H Golub and John H Welsch. "Calculation of Gauss quadrature rules". In: *Mathematics of computation* 23.106 (1969), pp. 221–230.

[25] Ernst Hairer, Christian Lubich, and Gerhard Wanner. *Geometric numerical integration: structure-preserving algorithms for ordinary differential equations*. Vol. 31. Springer Science & Business Media, 2006.

[26] Frank E Harris, Hendrik J Monkhorst, and David L Freeman. *Algebraic and diagrammatic methods in many-Fermion theory*. New York, NY (United States); Oxford University Press, 1992.

[27] Douglas Rayner Hartree. "The wave mechanics of an atom with a non-Coulomb central field. Part I. Theory and methods". In: *Mathematical Proceedings of the Cambridge Philosophical Society*. Vol. 24. 1. Cambridge University Press. 1928, pp. 89–110.

[28] Douglas Rayner Hartree and William Hartree. "Self-consistent field, with exchange, for beryllium". In: *Proceedings of the Royal Society of London. Series A-Mathematical and Physical Sciences* 150.869 (1935), pp. 9–33.

[29] Felix Hausdorff. "Die symbolische Exponentialformel in der Gruppentheorie". In: *Ber. Verh. Kgl. Sächs. Ges. Wiss. Leipzig., Math.-phys. Kl.* 58 (1906), pp. 19–48.

[30] Walter Heitler and Fritz London. "Wechselwirkung neutraler Atome und homöopolare Bindung nach der Quantenmechanik". In: *Zeitschrift für Physik* 44.6-7 (1927), pp. 455–472.

[31] Detlef Heitmann and Jörg P Kotthaus. "The spectroscopy of quantum dot arrays". In: *Physics Today* 46 (1993), pp. 56–63.

[32] Trygve Helgaker and Poul Jørgensen. "Analytical calculation of geometrical derivatives in molecular electronic structure theory". In: *Advances in quantum chemistry*. Vol. 19. Elsevier, 1988, pp. 183–245.

[33] Trygve Helgaker and Poul Jørgensen. "Configuration-interaction energy derivatives in a fully variational formulation". In: *Theoretica chimica acta* 75.2 (1989), pp. 111–127.

[34] Trygve Helgaker, Poul Jorgensen, and Jeppe Olsen. *Molecular electronic-structure theory*. John Wiley & Sons, 2014.

[35] Trygve Helgaker et al. "Recent advances in wave function-based methods of molecular-property calculations". In: *Chemical reviews* 112.1 (2012), pp. 543–631.

[36] Robert C Hilborn. "Atoms in orthogonal electric and magnetic fields: A comparison of quantum and classical models". In: *American Journal of Physics* 63.4 (1995), pp. 330–338.

[37] David Hochstuhl, CM Hinz, and Michael Bonitz. "Time-dependent multiconfiguration methods for the numerical simulation of photoionization processes of many-electron atoms". In: *The European Physical Journal Special Topics* 223.2 (2014), pp. 177–336.

[38] John Hubbard. "The description of collective motions in terms of many-body perturbation theory". In: *Proceedings of the Royal Society of London. Series A. Mathematical and Physical Sciences* 240.1223 (1957), pp. 539–560.

[39] NM Hugenholtz. "Perturbation theory of large quantum systems". In: *Physica* 23.1-5 (1957), pp. 481–532.

[40] Charles Jean Joachain, Niels J Kylstra, and Robert M Potvliege. *Atoms in intense laser fields*. Cambridge University Press, 2012.

[41] Marte Hoel Jørgensen. "Many-body approaches to quantum dots". MA thesis. 2011.

[42] Walter Kohn. "Cyclotron resonance and de Haas-van Alphen oscillations of an interacting electron gas". In: *Physical Review* 123.4 (1961), p. 1242.

[43] Anna I Krylov et al. "Size-consistent wave functions for nondynamical correlation energy: The valence active space optimized orbital coupled-cluster doubles model". In: *The Journal of chemical physics* 109.24 (1998), pp. 10669–10678.

[44] Hermann Kümmel. "Origins of the coupled cluster method". In: *Theoretica chimica acta* 80.2-3 (1991), pp. 81–89.

[45] Simen Kvaal. "Ab initio quantum dynamics using coupled-cluster". In: *The Journal of chemical physics* 136.19 (2012), p. 194109.

[46] Simen Kvaal. "Variational formulations of the coupled-cluster method in quantum chemistry". In: *Molecular Physics* 111.9-11 (2013), pp. 1100–1108.

[47] Jon M Leinaas and Jan Myrheim. "On the theory of identical particles". In: *Il Nuovo Cimento B (1971-1996)* 37.1 (1977), pp. 1–23.

[48] Xiaosong Li et al. "A time-dependent Hartree–Fock approach for studying the electronic optical response of molecules in intense fields". In: *Physical Chemistry Chemical Physics* 7.2 (2005), pp. 233–239.

[49] Magnus Pedersen Lohne. "Coupled-cluster studies of quantum dots". MA thesis. 2010.

[50] Daniel Loss and David P DiVincenzo. "Quantum computation with quantum dots". In: *Physical Review A* 57.1 (1998), p. 120.

[51] B Meurer, D Heitmann, and K Ploog. "Single-electron charging of quantum-dot atoms". In: *Physical review letters* 68.9 (1992), p. 1371.

[52] Haruhide Miyagi and Lars Bojer Madsen. "Time-dependent restricted-active-space self-consistent-field theory for laser-driven many-electron dynamics". In: *Physical Review A* 87.6 (2013), p. 062511.

[53] Hendrik J Monkhorst. "Calculation of properties with the coupled-cluster method". In: *International Journal of Quantum Chemistry* 12.S11 (1977), pp. 421–432.

[54] Rolf H Myhre. "Demonstrating that the nonorthogonal orbital optimized coupled cluster model converges to full configuration interaction". In: *The Journal of Chemical Physics* 148.9 (2018), p. 094110.

[55] John von Neumann. *Mathematical Foundations of Quantum Mechanics.* Berlin: Springer, 1932.

[56] J Paldus, J Čížek, and I Shavitt. "Correlation Problems in Atomic and Molecular Systems. IV. Extended Coupled-Pair Many-Electron Theory and Its Application to the B H 3 Molecule". In: *Physical Review A* 5.1 (1972), p. 50.

[57] Robert M Parrish et al. "Psi4 1.1: An open-source electronic structure program emphasizing automation, advanced libraries, and interoperability". In: *Journal of chemical theory and computation* 13.7 (2017), pp. 3185–3197.

[58] Wolfgang Pauli. "The connection between spin and statistics". In: *Physical Review* 58.8 (1940), p. 716.

[59] Wolfgang Pauli. "Über den Zusammenhang des Abschlusses der Elektronengruppen im Atom mit der Komplexstruktur der Spektren". In: *Zeitschrift für Physik A Hadrons and Nuclei* 31.1 (1925), pp. 765–783.

[60] Thomas Bondo Pedersen, Henrik Koch, and Christof Hättig. "Gauge invariant coupled cluster response theory". In: *The Journal of chemical physics* 110.17 (1999), pp. 8318–8327.

[61] Thomas Bondo Pedersen and Simen Kvaal. "Symplectic integration and physical interpretation of time-dependent coupled-cluster theory". In: *The Journal of chemical physics* 150.14 (2019), p. 144106.

[62] JA Pople and R_K Nesbet. "Self-consistent orbitals for radicals". In: *The Journal of Chemical Physics* 22.3 (1954), pp. 571–572.

[63] Heinz Post. "Individuality and physics". In: *The listener* 70.1963 (1963), pp. 534–537.

[64] Péter Pulay. "Convergence acceleration of iterative sequences. The case of SCF iteration". In: *Chemical Physics Letters* 73.2 (1980), pp. 393–398.

[65] George D Purvis III and Rodney J Bartlett. "A full coupled-cluster singles and doubles model: The inclusion of disconnected triples". In: *The Journal of Chemical Physics* 76.4 (1982), pp. 1910–1918.

[66] JWS Rayleigh. "The theory of sound, Article 88, vol. 1". In: *2nd revised edn. New York: Dover (reprint 1945)* (1894), pp. 110–111.

[67] Stephanie M Reimann and Matti Manninen. "Electronic structure of quantum dots". In: *Reviews of modern physics* 74.4 (2002), p. 1283.

[68] Erwin Schrödinger. "Quantisierung als eigenwertproblem". In: *Annalen der physik* 385.13 (1926), pp. 437–490.

[69] Isaiah Shavitt and Rodney J Bartlett. *Many-body methods in chemistry and physics: MBPT and coupled-cluster theory.* Cambridge university press, 2009.

[70] Oktay Sinanoğlu. "Many-Electron Theory of Atoms, Molecules and Their Interactions". In: *Advances in chemical physics* (1964), pp. 315–412.

[71] John Clarke Slater. "Note on Hartree's method". In: *Physical Review* 35.2 (1930), p. 210.

[72] John Clarke Slater. "The self consistent field and the structure of atoms". In: *Physical Review* 32.3 (1928), p. 339.

[73] Qiming Sun et al. *PySCF: the Python-based simulations of chemistry framework.* 2017. DOI: 10.1002/wcms.1340. eprint: https://onlinelibrary.wiley.com/doi/pdf/10.1002/wcms.1340. URL: https://onlinelibrary.wiley.com/doi/abs/10.1002/wcms.1340.

[74] Attila Szabo and Neil S Ostlund. *Modern quantum chemistry: introduction to advanced electronic structure theory.* Courier Corporation, 2012.

[75] David James Thouless. "Stability conditions and nuclear rotations in the Hartree-Fock theory". In: *Nuclear Physics* 21 (1960), pp. 225–232.

[76] EP Wigner. "On a modification of the Rayleigh-Schrödinger perturbation theory". In: *Magyar Tudományos Akadémia Matematikai és Természettudományi Ertesitöje* 53 (1935), pp. 477–482.

[77] Jürgen Zanghellini et al. "Testing the multi-configuration time-dependent Hartree–Fock method". In: *Journal of Physics B: Atomic, Molecular and Optical Physics* 37 (2004), p. 763. URL: %5Chref%7Bhttp://stacks.iop.org/0953-4075/37/i=4/a=004%7D.